

Attosecond physics

Ferenc Krausz

Department für Physik, Ludwig-Maximilians-Universität, Am Coulombwall 1, D-85748 Garching, Germany and Max-Planck-Institut für Quantenoptik, Hans-Kopfermann-Strasse 1, D-85748 Garching, Germany

Misha Ivanov

Steacie Institute for Molecular Sciences, National Research Council of Canada, 100 Sussex Drive, Ottawa, Ontario, Canada K1A 0R6

(Published 2 February 2009)

Intense ultrashort light pulses comprising merely a few wave cycles became routinely available by the turn of the millennium. The technologies underlying their production and measurement as well as relevant theoretical modeling have been reviewed in the pages of *Reviews of Modern Physics* (Brabec and Krausz, 2000). Since then, measurement and control of the subcycle field evolution of few-cycle light have opened the door to a radically new approach to exploring and controlling processes of the microcosm. The hyperfast-varying electric field of visible light permitted manipulation and tracking of the atomic-scale motion of electrons. Striking implications include controlled generation and measurement of single attosecond pulses of extreme ultraviolet light as well as trains of them, and real-time observation of atomic-scale electron dynamics. The tools and techniques for steering and tracing electronic motion in atoms, molecules, and nanostructures are now becoming available, marking the birth of attosecond physics. In this article these advances are reviewed and some of the expected implications are addressed.

DOI: [10.1103/RevModPhys.81.163](https://doi.org/10.1103/RevModPhys.81.163)

PACS number(s): 42.65.Re, 32.80.-t

CONTENTS

I. Introduction	164	C. Single-electron interference within the wave cycle of light	179
A. Time and length scales in the microcosm	165	1. Above-threshold ionization and sub-fs electron pulses	179
B. Concepts for resolving microscopic structure and dynamics	166	2. High-order harmonic emission and sub-fs photon pulses	179
C. Revolutions in time-resolved metrology	166	D. Electron scattering	182
1. Microwave electronics	167	1. Elastic backscattering and high-energy electron emission	182
2. Ultrafast optics	167	2. Inelastic scattering: Multiple electron emission and inner-shell excitation	183
3. Lightwave electronics	167	V. Basic Concepts for Attosecond Control and Metrology	184
D. Evolution of the study of transient phenomena	168	A. Conditions for experimental implementation	184
II. Concepts for Ultrafast Measurements and Control	169	B. Light waveform control	184
A. General connection between measurement and control	169	C. Attosecond metrology using nonlinear XUV optics	185
B. Concepts for ultrafast measurements	169	D. Light-field-controlled attosecond metrology	186
1. Gating, both time and frequency resolved	169	1. Attosecond streak imaging	187
2. Spectral interferometry	170	2. Quantum analysis: The light field as an electron phase modulator	188
C. Evolution of ultrafast control	170	3. Attosecond frequency-resolved optical gating	190
1. Early approaches	170	4. Attosecond spectral shear interferometry	190
2. Advanced control via pulse shaping	171	E. Lightwave electronics at work: From measurement to control of sub-fs pulses	192
D. Principles of attosecond control and measurement of electronic dynamics	172	1. Modulation of recollision electrons: Measuring the creation of a sub-fs pulse	192
III. Intense, Controlled Light Fields	172	2. Modulation of recollision electrons: Controlling the creation of a sub-fs pulse	193
A. Light-wave control: Brief history and current state of the art	172	3. Reproducible generation and measurement of single sub-fs XUV pulses	194
B. Light waveform synthesis	173	4. Breaking the 100-as barrier	196
C. Towards ultrastrong controlled light fields	174		
IV. Lightwave Electronics	174		
A. Significant variations of atomic electron density within the wave cycle of light	175		
B. Semiclassical modeling of strong field-matter interaction	176		

VI. Sub-fs Electron and Photon Pulses: Current Status and Future Prospects	197
A. Atomic electrons interacting with few-cycle fields:	
Atomic HHG	197
B. Relativistic electrons interacting with few-cycle light	198
1. Intense attosecond VUV to soft-x-ray pulses via surface HHG?	198
2. Attosecond electron and hard-x-ray pulses?	200
3. Next-generation accelerators driven by few-cycle light?	201
VII. Real-Time Observation and Control of Atomic-Scale Electron and Nuclear Dynamics	201
A. Electronic motion in atoms: Excitation, relaxation, and correlations	201
1. Electronic excitation and relaxation dynamics: Attosecond streaking and tunneling spectroscopy	202
2. Electronic relaxation and rearrangement: Attosecond absorption spectroscopy	207
3. Electron wave-packet motion: Attosecond photoelectron spectroscopy	207
4. Shedding light on electron-electron interactions: Attosecond coincidence spectroscopy	209
B. Electronic and nuclear motion in complex systems: From simple diatomics to biomolecules and clusters	210
1. Attosecond photoelectron spectroscopy	210
2. Attosecond high harmonic imaging	212
3. Attosecond electron diffraction	213
C. Electronic motion in solids and systems on surfaces	215
1. Extension of attosecond spectroscopy to condensed matter	215
2. Challenges	217
D. Future prospects: Steering and imaging atomic-scale electronic motion	217
1. Steering electrons with the electric field of synthesized light	217
2. 4D imaging of electrons with subatomic resolution in space and time	219
VIII. Conclusions and Outlook	219
Glossary of Abbreviations	220
Acknowledgments	221
References	221

I. INTRODUCTION

Electrons have played a central role in the scientific and technological revolution of the 20th century.¹ It is widely anticipated that in the 21st century their role as a key driver of scientific and technological advances will be increasingly taken over by photons. We disagree with this assessment. Some half a century after the discovery of the transistor and the laser, our insight into and influence upon the atomic-scale motion of electrons in matter is still in its infancy. Consequently, the advance of science and technology by research on electrons is by no means over. On the contrary, it is just beginning, given

the fact that the experimental tools and techniques for real-time observation and steering of electronic dynamics on the atomic scale are now becoming available.

In the microcosm, the borders between biology, chemistry, and physics tend to disappear. The gaps between these apparently so disparate fields are bridged by the microscopic motion of electrons in atoms, molecules, and nanoscale structures. Electronic motion inside atoms is behind the emission of visible, ultraviolet, and x-ray light.² Electronic dynamics on the molecular scale is responsible for the transport of bioinformation and initiates changes in the chemical composition and function of biological systems. The speed of information processing can be increased by ever faster switching of electronic currents in ever smaller nanometer-scale circuitry. Details of these motions often occur on time scales of tens to ten thousands of attoseconds ($1 \text{ as} = 10^{-18} \text{ s}$) and require commensurate measurement and control techniques for their observation and steering, respectively.

What are the most efficient ways of putting atoms into highly excited states that allow x-ray light amplification and thus creation of compact x-ray lasers? Can the function of biomolecules be manipulated and novel molecular structures be formed by steering electrons in chemical bonds? How does charge transfer occur in molecules assembled on surfaces and how can it be optimized for more efficient solar cells or for fighting radiation damage during biological imaging? What are the ultimate size and speed limits of electronic information processing and magnetic information storage, and how can we approach these limits? How can energy be most efficiently transported into high-density matter to ignite nuclear fusion? Answers to these scientific and technological questions will require insight into and possibly control of microscopic electron motion.

We address here (i) the key concepts and experimental tools which provide the means of observing and controlling the atomic-scale motion of electrons in real time, (ii) the theoretical models critical for connecting experimental observables with microscopic variables, and (iii) expected implications of this revolution in technology.³

²The requirement of atomic-scale electronic motion for light emission can be circumvented only by accelerating them to relativistic energies. Only relativistic electrons can radiate visible (or shorter-wavelength) light in the absence of (sub-)atomic-scale interactions.

³To make sure that we draw clear borderlines between facts and conclusions based upon experiments, on the one hand, and our visions, expectations and prediction (necessarily containing a speculative component) on the other hand, comments of the latter type will be systematically introduced by phrases such as “we believe,” “we expect,” “in our opinion,” etc. In this way, we are making an attempt to write not a conventional review, but a review *and* foresight article in combination, with the two components clearly separated. We feel that, at this early stage of its evolution, the advancement of attosecond physics is best served this way.

¹For a general review, see [Huebener \(2005\)](#).

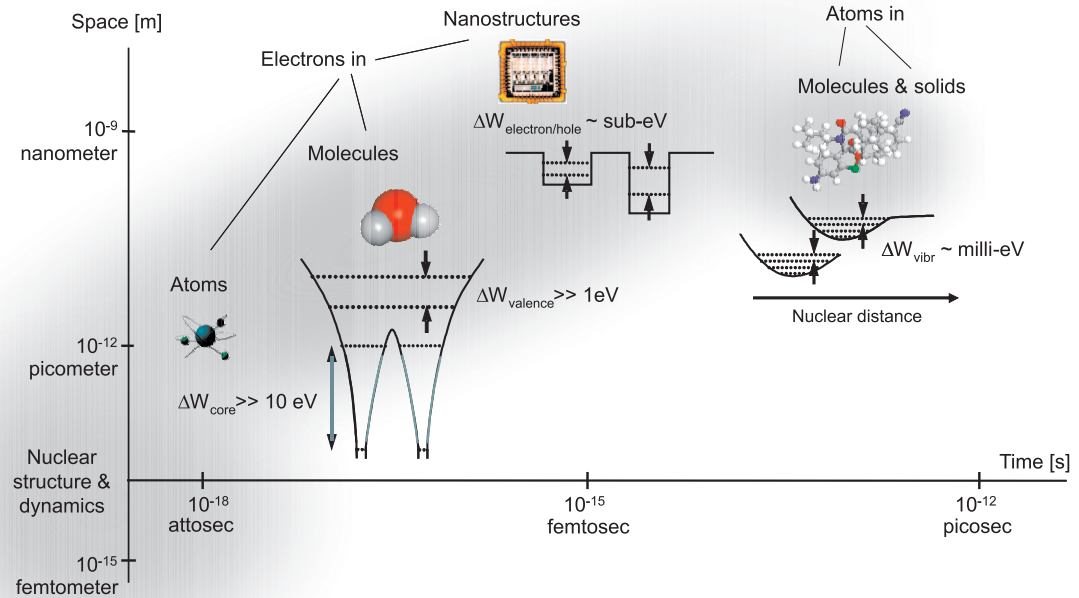


FIG. 1. (Color) Characteristic length and time scales for structure and dynamics in the microcosm, respectively.

A. Time and length scales in the microcosm

Structure and dynamics in the microcosm are inherently connected by the laws of quantum mechanics. Take, for example, a particle put in a superposition of its ground state $\phi_0(x)$ of energy W_0 and the first excited state $\phi_1(x)$ of energy W_1 . Such a superposition state is referred to as a *wave packet*. Change in the position of its center of mass is the closest quantum mechanical analog of classical motion. Solution of the Schrödinger equation for the particle's wave function $\psi(x)$ yields an oscillatory motion with the oscillation period $T_{\text{osc}} = 2\pi(\hbar/\Delta W)$, where $\Delta W = W_1 - W_0$. The larger the energy separation ΔW between the two eigenstates, the faster is the particle's motion in the superposition state. This energy separation is dictated by the spatial extent of the potential confining the motion, in addition to the particle's mass. Quantum mechanics connects the rapidity of dynamics with the extension of structure.

The millielectronvolt-scale energy spacing of vibrational energy levels implies that molecular vibrations occur on a time scale of tens to hundreds of femtoseconds (Fig. 1). This defines the characteristic time scale for the motion of atoms in a molecule, including those resulting in irreversible structural changes during chemical reactions (Zewail, 2000). The motion of individual electrons in semiconductor nanostructures, molecular orbitals, and the inner shells of atoms occurs on progressively shorter intervals of time ranging from tens of femtoseconds to less than an attosecond. Motion within nuclei is predicted to unfold even faster, typically on a zeptosecond time scale.

For a wave packet made of two bound eigenstates, the oscillation period $T_{\text{osc}} = 2\pi(\hbar/\Delta W)$ also determines the response time of the particle to an external perturbation. For example, a two-level atom responds to the radiation field similar to a classical damped electron oscillator of eigenfrequency $\omega_0 = 2\pi/T_{\text{osc}}$ (Siegman, 1986; Boyd, 2003), with $T_0 = 2\pi/\omega_0$ the response time of the atom to an external perturbation. Going from two-level atoms to plasmas, we see similar behavior. The rapidity of collective motion of free electrons is dictated by the plasma oscillation period T_p , which is inversely proportional to the square root of the density of electrons N , $T_p = (2\pi/|e|)\sqrt{\epsilon_0 m_e/N}$ (Kruer, 2003). Here e and m_e are the electron's charge and mass, respectively, and ϵ_0 is the dielectric constant. A characteristic length scale in a free electron gas in the absence of any static structure is the mean distance between adjacent electrons: $\ell_{\text{mean}} \approx N^{-1/3}$. For a mean distance comparable to atomic dimensions, $\ell_{\text{mean}} \approx 0.1 \text{ nm}$, we obtain $T_p \approx 120 \text{ as}$. This is close to the oscillation period of valence electron wave packets in bound atomic or molecular systems. Thus the motion of electrons inside atoms, in molecular orbitals, or confined in nanometer-scale potentials in semiconductors, like the collective dynamics of free electrons in high-density ionized gases, solid-density plasmas, or fusion targets, is naturally measured in attoseconds; see Fig. 2. Attosecond physics is the science of electrons in motion, both collective and individual, on atomic and molecular scales and in high-density mesoscopic systems.

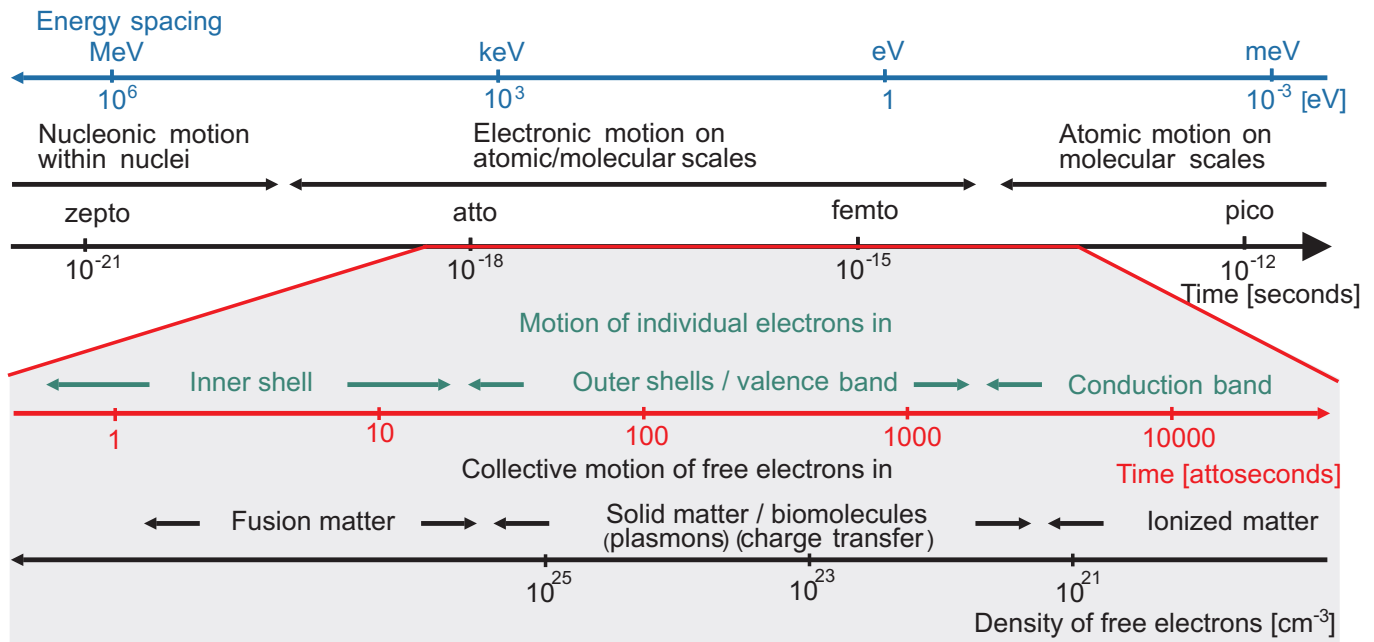


FIG. 2. (Color) Characteristic time scales for microscopic motion and its connection with energy spacing between relevant stationary states (upper panel); characteristic time scales for the motion of one or several electrons and for the collective motion of an electronic ensemble (lower panel).

B. Concepts for resolving microscopic structure and dynamics

Looking into the microcosm with high resolution in space or time requires a physical quantity with a well-controlled spatial or temporal gradient, respectively. Both types of gradients arise in waves, with the wavelength and the oscillation period determining the steepness of the spatial and temporal gradients of the oscillating fields, respectively. In waves these variations are periodic. Periodic spatial or temporal gradients can be efficiently utilized for resolving structures or dynamics (quasi)periodic on the same scale. For example, Angstrom-resolution x-ray crystallography or single-molecule imaging (Neutze *et al.*, 2000) and frequency-domain spectroscopy draw on this concept. Measurement of the frequency-domain response over a sufficiently wide range via x-ray diffraction, absorption, or scattering may, in principle, allow retrieval of the electronic structure and linear temporal response on a subatomic scale in space and time using Kramers-Kronig relationships.⁴

However, uncovering the location of an individual specimen in isolated assemblies (e.g., macromolecular structures on surfaces), or the relative timing of isolated brief events becomes increasingly challenging with increasing distance in space or time. Stationary metrology also fails when it comes to reconstructing a nonlinear response. Under these circumstances, measurements must be performed with an *isolated* temporal or spatial gradient. In general, direct space- or time-domain approaches offer transparent and intuitive measurement

tools.⁵ In space, the technique has become known as *microscopy*. The gradient is introduced by the radial profile of a focused light or electron beam or by a tip. In the temporal domain, a sharp gradient is introduced by a physical quantity rapidly varying in time in a controlled fashion. Its use for measuring brief time intervals and processes taking place within these intervals has been dubbed *chronoscopy*, or time-resolved metrology.

The concept of streak imaging constitutes an instructive example of using a sharp temporal gradient for chronoscopy (Fig. 3). Here the steep gradient is introduced by a voltage ramped within a fraction of a nanosecond but results in subpicosecond resolution. Temporal resolution can be generally much better than the duration Δt of the signal gradient. How much better depends on the signal-to-noise ratio S/N (Fig. 4), yielding the noise-limited resolution $\Delta t_{\text{noise}} \approx \Delta t(N/S)$. Timing jitter Δt_{jitter} also limits the temporal resolution if the measurement requires averaging: $\Delta t_{\text{resolution}} \approx \sqrt{\Delta t_{\text{noise}}^2 + \Delta t_{\text{jitter}}^2}$. The temporal resolution depends on the duration of the measuring transient, the signal-to-noise ratio, and the reproducibility of timing with respect to the process under study.

C. Revolutions in time-resolved metrology

Three radically different technologies have paved the way for advancing time-resolved metrology from the

⁴See, e.g., Abbamonte *et al.* (2004) and Wernet *et al.* (2004).

⁵By advocating direct time- (or space-) domain approaches we do not mean to discard their frequency- and momentum-domain counterparts. When linear response allows their use, they are not only valuable alternatives to direct methods, but also able to complement them to increase their precision.

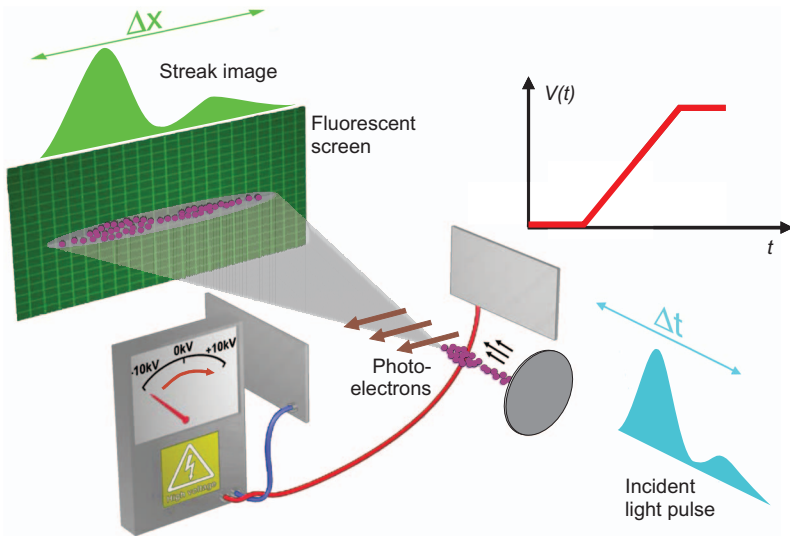


FIG. 3. (Color) Schematic of a microwave-controlled streak camera. Photoelectrons knocked off from a photocathode by a short light pulse (to be measured) are deflected on their way to a screen by a transverse microwave voltage ramp $V(t)$ to an extent depending on their instant of release (Bradley *et al.*, 1971; Schelev *et al.*, 1971). The temporally varying deflection “streaks” the location of the impact of the electrons on the screen, mapping the temporal profile of the light pulse to a spatial distribution, “streak image,” of electrons on a fluorescent screen.

nanosecond to the attosecond regime: microwave electronics→picoseconds, ultrafast optics→femtoseconds, and lightwave electronics→attoseconds (Fig. 5). Technological breakthroughs triggered each of these developments: transistors for fast switching of electric current, lasers and nonlinear optics for ultrashort light pulse generation and measurement, and synthesized light waveforms for steering electrons on the atomic scale.

1. Microwave electronics

For a long time, electrical signals provided the steepest controlled gradients for measuring fast-evolving phenomena. The invention of the transistor triggered rapid evolution of high-speed electrical transients from nanoseconds toward picoseconds (Fig. 5). Their spectrum spans several octaves from radio to microwaves. However, the refractive index of any material varies substantially over this spectral range due to lattice vibrations. As a result, the distortion-free propagation length of few-picosecond electrical signals is as short as a few millimeters. This length scales quadratically with the duration of transients, preventing any substantial further improvement in the speed of practically useful electrical

transients. Advancement of time-domain metrology beyond this frontier called for a new technology.

2. Ultrafast optics

The refractive index of transparent optical materials is nearly constant in the visible or near-infrared spectral range over relative bandwidths of several percent, creating the potential for robust femtosecond transients. This potential was exploited by coherent light amplification in a broadband laser medium and the use of nonlinear optical techniques. The resultant ultrashort laser pulses⁶ approached the 1-fs barrier by the turn of the millennium. As with high-speed electronics, increasing dispersion toward the ultraviolet due to subpetahertz electronic transitions limits the fastest robust optical transients to several femtoseconds. Again, a radically new technology was required for further advance.

3. Lightwave electronics

Controlled variation of the amplitude or frequency of light pushed the frontiers of ultrafast science close the femtosecond frontier. However, light exhibits much steeper gradients than those of the cycle-averaged quantities: the subcycle slopes in the oscillating field. With the advent of controlled few-cycle light waves, a controlled force that is variable on the electronic (i.e., attosecond) time scale and rivals interatomic forces became available and opened the door for versatile attosecond control and metrology.

In nonlinear interactions, electronic motion induced by the controlled light force may exhibit even steeper gradients than the light field itself, giving way to the generation of attosecond electron and photon [extreme

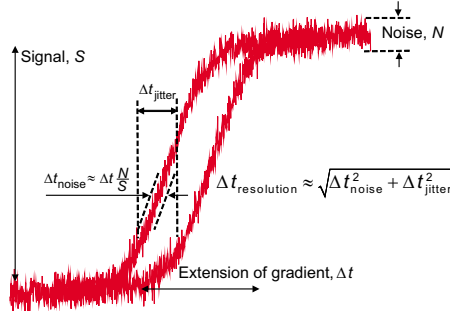


FIG. 4. (Color online) Typical reference (clocking) signal gradients (tainted with noise and jitter) for triggering or probing fast processes.

⁶For recent reviews, see Brabec and Krausz (2000); Keller (2003). Early reviews include DeMaria *et al.* (1969); Bradley and New (1974); Greenhow and Schmidt (1974); Smith *et al.* (1974). Also see Akhmanov *et al.* (1992); Diels and Rudolph (1996).

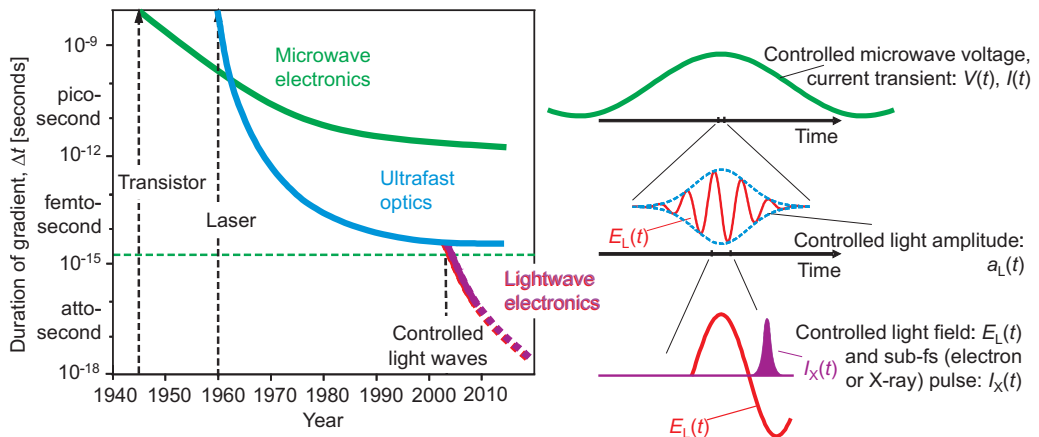


FIG. 5. (Color) Evolution of ultrafast science. The duration of the fastest controlled signal gradients dictates the speed of control and resolution of probing of microscopic processes. Microwave electronics, ultrafast optics, and lightwave electronics offer controlled transient for these purposes on successively shorter time scales, with picosecond, femtosecond, and attosecond gradients.

ultraviolet (XUV) or x-ray] pulses. The resultant pulse (see Fig. 5) is synchronized with the generating light field, allowing the sub-fs pulse to be used either as a “starter gun” (pump) for triggering ultrafast dynamics that can be referenced to the sub-fs laser field transient or as a “photofinish” (probe) taking a snapshot of microscopic motion initiated (and subsequently steered) by the few-cycle light wave or another signal derived from it. The speed of metrology and control is no longer restricted by the femtosecond pulse envelope but can utilize attosecond field oscillations (see Secs. V and VII).

By analogy with microwave electronics, this radically new technology has been dubbed *lightwave electronics* (Goulielmakis *et al.*, 2007). As microwave electronics controls electronic currents in nanoscale circuits on a picosecond time scale, lightwave electronics controls atomic-scale currents on the attosecond scale and constitutes the technological backbone of attosecond science.

As usual, this revolution was also preceded by much research, including proposals for sub-fs pulse generation⁷ and measurement,⁸ and the advancement of femtosecond technology and strong-field interactions, including high-order harmonic generation.⁹ These advances paved the way to the birth of attosecond technology at the turn of the millennium.

⁷Hänsch, 1990; Farkas and Tóth, 1992; Harris *et al.*, 1993; Corkum *et al.*, 1994; Kaplan, 1994; Ivanov *et al.*, 1995; Kaplan and Shkolnikov, 1995; Antoine *et al.*, 1996; Protopapas *et al.*, 1996; Antoine *et al.*, 1997; Christov *et al.*, 1997; Kan *et al.*, 1997; Schafer and Kulander, 1997; de Bohan *et al.*, 1998; Harris and Sokolov, 1998; Lappas and L'Huillier, 1998; Tempea *et al.*, 1999.

⁸Constant *et al.*, 1997; Scrinzi *et al.*, 2001a, 2001b.

⁹Reviewing this early work is beyond the scope of this paper. The reader is referred to Salieres *et al.*, 1999; Joachain *et al.*, 2000; Agostini and DiMauro, 2004; Eden, 2004; Scrinzi *et al.*, 2005; Pfeifer, Spielmann, and Gerber, 2006.

D. Evolution of the study of transient phenomena

Before 1900 it was already known that short flashes of light permit the recording of rapid phenomena by spark photography. In 1864, Toepler extended the technique to study microscopic dynamics (Krehl and Engemann, 1995). He generated sound waves with a short light spark and subsequently photographed them with a second spark that was delayed electronically with respect to the first one initiating the motion. By taking pictures of the sound wave as a function of the delay time, he obtained a complete history of sound-wave phenomena. Pump-probe spectroscopy was created. Abraham and Lemoine (1899) improved the technique by deriving the pump and probe flash from the same spark with a variable optical path length between them. The resultant optical synchronism between the triggering and photographing flash opened the way to improving the resolution of pump-probe spectroscopy to the limit dictated by the flash duration.

With these milestones, the conceptual framework for studying transient microscopic phenomena was complete. Subsequent progress in time-resolved measurements was driven by developing sources of ever shorter light flashes and techniques for their measurement. The resolution of time-resolved spectroscopy was limited by the nanosecond duration of pulses of incoherent light for more than half a century (Fig. 6). Broadband lasers and nonlinear optical techniques for the generation and measurement of ultrashort laser pulses improved the resolving power of pump-probe spectroscopy from several nanoseconds to several femtoseconds, by six orders of magnitude within merely two and a half decades (Fig. 6). The creation of femtosecond technology—four decades after the first observation of intermediates of chemical reactions by Norrish and Porter (1949) and Eigen (1954)—permitted real-time observation of the breakage and formation of chemical bonds, a field triggered by Zewail (1994, 2000).

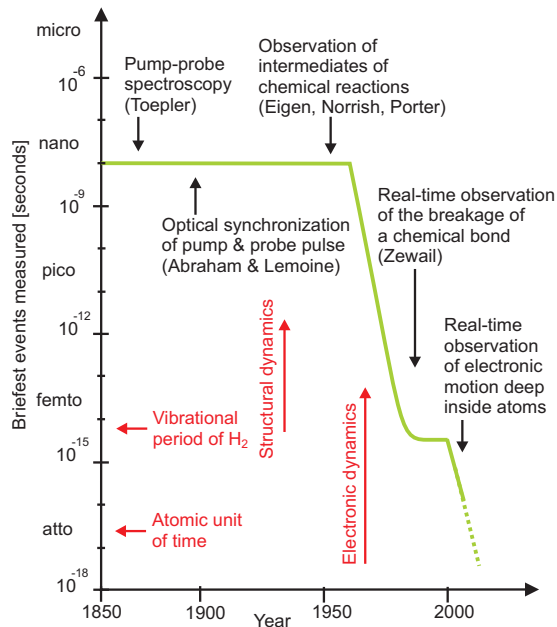


FIG. 6. (Color) Evolution of techniques for real-time observation of microscopic processes. Discontinuities in the slope of briefest measured events vs years indicate revolutions in technology.

Progress in temporal resolution was again halted in the mid-1980s, when the duration of the shortest laser pulses approached the oscillation period of the light wave carrying the pulse. Breaking the femtosecond barrier and providing thereby real-time access to intraatomic electron dynamics came about at the turn of the millennium and permitted the observation of electronic motion deep inside (i.e., in inner shells of) atoms (Drescher *et al.*, 2002) and control of atomic-scale electron motion in real time (Baltuška, Udem, *et al.*, 2003).

II. CONCEPTS FOR ULTRAFAST MEASUREMENTS AND CONTROL

A. General connection between measurement and control

The measurement and control of ultrafast processes are inherently intertwined. In pump-probe spectroscopy, the triggering of a process must be precisely timed with respect to the observing clock: in femtosecond chemistry this capability has been exploited not only for time-resolved measurements¹⁰ but also for control (Rice and Zhao, 2000; Brumer and Shapiro, 2003).

Any measurement process controls the appearance of a certain signal. Insight into the dynamics hinges on understanding the time-dependent changes of this signal.

¹⁰For reviews, see Zewail, 1994; de Boeij *et al.*, 1998; Neumark, 2001; Stolow, 2003a, 2003b; Stolow *et al.*, 2004.

For instance, photoelectron spectra¹¹ may constitute this signal. The fact that these spectra change in a controlled and reproducible way upon varying the time delay between the pump and probe in time-resolved photoelectron spectroscopy is also a manifestation of ultrafast control over the whole process.

Attosecond technology entails the ability to control and shape not only the envelopes of the laser pulses but also the subcycle structure of the field oscillations, extending both measurement and control techniques into the new realm of light-wave engineering and lightwave electronics. Attosecond control and metrology are based on this revolution in technology, but, at the same time, they draw on concepts that have been successfully applied on longer time scales.

B. Concepts for ultrafast measurements

1. Gating, both time and frequency resolved

For sampling the evolution of the electric field $E(t)$ of a light pulse, we need a narrow temporal gate $G(t-\tau)$ with its delay τ scanned across the pulse to be measured:

$$S(\tau) \propto \int_{-\infty}^{\infty} E(t)G(t-\tau)dt. \quad (1)$$

If the gate is much shorter than the process traced, the measured signal $S(\tau)$ yields the temporal evolution of the process,¹² here $E(t)$. The fastest gate femtosecond metrology can offer is the femtosecond laser pulse itself. If we replace $G(t-\tau)$ with $E(t-\tau)$ in Eq. (1), $S(\tau)$ is the linear autocorrelation of the pulse. It allows retrieval of the pulse envelope $a_L(t)$ in Eq. (6) for transform-limited pulses only. In the more general case of chirped pulses, one has to resort to nonlinear autocorrelation. The most powerful and robust version is frequency-resolved optical gating (FROG; Trebino *et al.*, 1997), which acquires the spectrogram of the signal,

$$S(\omega, \tau) = \left| \int_{-\infty}^{\infty} E(t)G(t-\tau)e^{i\omega t} dt \right|^2. \quad (2)$$

It is the set of spectra of all gated chunks of $E(t)$ as the gate $G(t-\tau)$ is scanned across the signal by varying τ .

¹¹Time-resolved photoelectron spectroscopy is key to observing dynamics in real time including structural dynamics in molecules as well as electronic dynamics on surfaces. Some early publications include Seel and Domcke, 1991; Baumert *et al.*, 1993; Assion *et al.*, 1996; Cyr and Hayden, 1996; Greenblatt *et al.*, 1997; Blanchet *et al.*, 1999; Lehr *et al.*, 1999. For reviews, see Haight, 1995; Petek and Ogawa, 1997; Neumark, 2001; Reid, 2003; Stolow, 2003a, 2003b; Stolow *et al.*, 2004; Bauer, 2005; Suzuki, 2006.

¹²Note that the pulse measurement by streak camera in Fig. 3 can also be modeled by a similar equation except that τ must be replaced with x/v_{defl} , where v_{defl} is the speed at which the electron beam's position x is scanned across the screen by the deflecting field, and instead of the field it is the cycle-averaged temporal intensity profile of the pulse, $I(t) \propto |E(t)|^2$, that is sampled.

The gate can generally be complex or even purely imaginary (phase gate). Knowledge of the spectrogram allows one to reconstruct both the gate $G(t)$ (Trebitz, 2000) and the signal's complex pulse envelope $a_L(t)$; see Eq. (6).

2. Spectral interferometry

The temporal evolution of a signal can be inferred from measuring the amplitudes and relative phases of their spectral components. The latter can be accessed by converting spectral phase variations into modulation of signal amplitude. Spectral phase interferometry for direct electric field reconstruction (SPIDER; Iaconis and Walmsley, 1998) implements this concept. Let $E(\omega) = a(\omega)\exp[i\phi(\omega)]$ be the complex Fourier transform of $E(t)$ with the real spectral amplitude $a(\omega)$ and phase $\phi(\omega)$. We generate a second pulse—a “replica” $E_{\text{replica}}(t)$ of the first—delayed in time by τ and shifted (sheared) in frequency by a small amount δ . Its Fourier transform will be

$$a_{\text{replica}}(\omega)\exp[i\phi_{\text{replica}}(\omega)] = a(\omega + \delta)\exp[i\phi(\omega + \delta) - i\omega\tau]. \quad (3)$$

Spectrally resolved interference of the two pulses at the detector yields the SPIDER interferogram

$$\begin{aligned} S_{\text{SPIDER}}(\omega) &\propto |a(\omega)\exp[i\phi(\omega)] \\ &\quad + a_{\text{replica}}(\omega)\exp[i\phi_{\text{replica}}(\omega)]|^2 \\ &= |a(\omega)\exp[i\phi(\omega)] + a(\omega + \delta) \\ &\quad \times \exp[i\phi(\omega + \delta) - i\omega\tau]|^2 \\ &= a^2(\omega) + a^2(\omega + \delta) + 2a(\omega)a(\omega + \delta) \\ &\quad \times \cos\{\omega\tau - [\phi(\omega + \delta) - \phi(\omega)]\}. \end{aligned} \quad (4)$$

It allows one to find the spectral phase $\phi(\omega)$ from the variation of the phase difference $\phi(\omega + \delta) - \phi(\omega)$ across the spectrum: the interferogram maps this phase variation onto modulation of the amplitude. Since $a(\omega)$ can be measured independently, the complex envelope $a_L(t)$ of the pulse [see Eq. (6)], can be completely reconstructed. SPIDER also relies on a well-controlled temporal gradient, to impose the frequency shear. One can think of propagating the original pulse and its time-delayed replica in a medium which shifts the photon energy of the delayed pulse in a controlled way. This implies that some property of the medium must have been changed within the delay interval, requiring the presence of a controlled temporal gradient. By increasing the separation between the two pulses, the steepness of this gradient can be lowered at the expense of increased demands on the spectrometer's resolving power. Thus we conclude that the use of spectral interferometry does not obviate the need for a gradient in time, but may substantially relax the requirements on its steepness. The price to pay is the need for high spectral resolution and shot-to-shot timing stability (in averaging measurements).

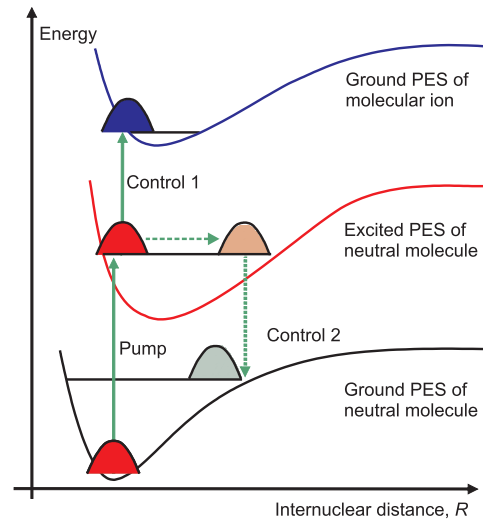


FIG. 7. (Color) Nuclear wave-packet control in a molecule with short pulses; PES, potential energy surface. A pump pulse initiates vibrational motion by exciting the molecule into an excited electronic state. Depending on its time delay with respect to the pump, a control pulse catches the vibrational wave packet at different parts of its trajectory. Control 1 promotes it up to the ground state of the molecular ion. At a different delay (control 2) the molecule will be electronically deexcited, dumping the wave packet back to an excited vibrational manifold of the ground electronic surface.

C. Evolution of ultrafast control

By analyzing ultrafast measurements, we have seen how time- and frequency-domain approaches complement each other. A similar symbiosis comes to light in the evolution of approaches to controlling microscopic dynamics. Here we show that early control approaches may be regarded as two limits of a general approach, which converge on the attosecond time scale.

1. Early approaches

The connection between time-domain measurement and control becomes transparent when considering the time-domain wave-packet control scenario in Fig. 7 (Rice and Zhao, 2000). A pump pulse promotes the molecule into an excited electronic state, initiating nuclear motion. A properly timed control pulse catches the nuclear wave packet at the right place on its trajectory along the excited electronic potential energy surface (PES) to induce a transition toward the desired outcome.

Timing between oscillations of two narrowband optical fields was shown to be an alternative approach to controlling dynamics (Brumer and Shapiro, 2003). In Fig. 8 we show an example of controlling the transition between an initial state $|i\rangle$ and a final state $|f\rangle$ with the superposition of the fields $E_\omega(t) = E_1 \exp(-i\omega_L t) + \text{c.c.}$ (inducing a three-photon transition) and $E_\Omega(t) = E_3 \exp(-i\Omega t + i\phi) + \text{c.c.}$ of frequency $\Omega = 3\omega_L$ (inducing a one-photon transition). Our control knob is the relative phase ϕ between the two colors. In the lowest order

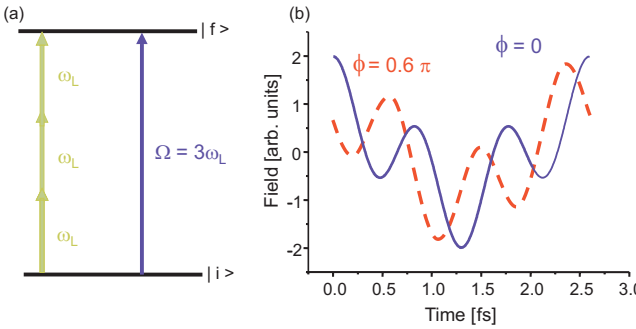


FIG. 8. (Color) Coherent control of quantum transition by changing the relative phase between two waves of different frequency. On the left panel, transition between initial and final states can proceed via two pathways, involving the absorption of one and three photons. Its probability is controlled by the relative phase ϕ between the two colors, ω_L and $3\omega_L$. The right panel shows that changing the relative phase ϕ results in shaping of the electric field oscillations on the subcycle, i.e., sub-fs, time scale, in this example for $\lambda_L=800$ nm. Solid line, $\phi=0$; dashed line, $\phi=0.6\pi$. Although timing is varied on a sub-fs scale the controlled transition usually unfolds over a much longer period.

of perturbation theory, the total transition probability is given by

$$W_{if} \propto |d^{(3)}|^2 E_1^6 + |d^{(1)}|^2 E_3^2 + 2|d^{(3)}d^{(1)}|E_1^3 E_3 \cos(\phi + \theta_{if}), \quad (5)$$

where $d^{(1)}$ and $d^{(3)}$ are the corresponding transition matrix elements and θ_{if} is the relative phase between them.¹³ Changing ϕ controls the transition probability, shifting the outcome between the minima and maxima of the interference pattern. Figure 8(b) shows the total electric field $E_{\Sigma}(t)=E_{\omega}(t)+E_{\Omega}(t)$ for $E_1=E_3$ and for two values of ϕ . Although the approach was conceived in the framework of quantum physics, its functioning can be traced directly to the controlled subcycle modulation of the classical field oscillations in Fig. 8(b) (Franco and Brumer, 2006). Thus the simplest manifestation of light-wave engineering, which uses only two colors, already appears here—even though the evolution of the controlled system towards its final state occurs only on a multicycle (multi-fs) scale due to the perturbative nature of the interaction.

2. Advanced control via pulse shaping

The two control scenarios described above are profoundly connected. The nuclear wave packet created in Fig. 7 is a coherent superposition of many states $|v\rangle$. The transform-limited pump pulse populates these states in phase, while the control pulse generates interference of multiple pathways, the outcome of which depends on

¹³Note that this result is based on the perturbation theory and is not applicable at high light intensities or for transitions between nonstationary (dressed) states, where the phases θ become time dependent.

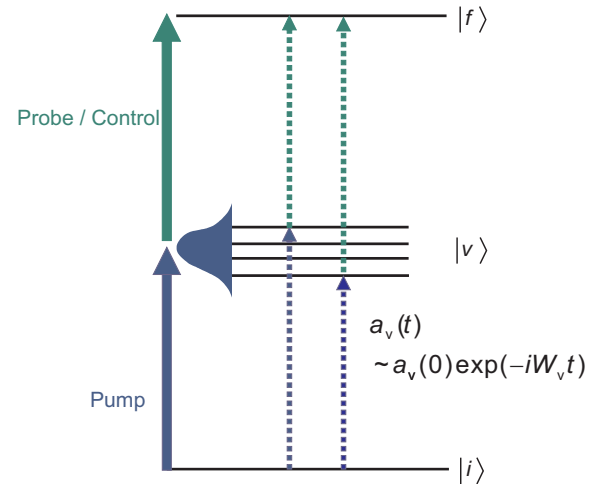


FIG. 9. (Color) Frequency-domain interpretation of wave-packet control with short pulses. Multiple pathways via various intermediate states interfere, with their interference controlled by the relative phases determined by the free wave-packet evolution.

the relative phases between the (complex) amplitudes $a_v(t)=a_v(0)\exp(-iW_v t)$. These phases are controlled via the time delay between the pump and control pulses (Fig. 9).

We do not have to rely on the free evolution of the wave packet to adjust the phases of constituent states for the desired interference in the final state. The same goal can be achieved by changing the relative phases of those colors that populate the intermediate states or complete the transition to the final state. Moreover, using strong laser fields we can also reshape laser-dressed potential energy surfaces¹⁴ and thus alter the wave packet's temporal evolution.

State-of-the-art pulse-shaping technology (Weiner *et al.*, 1988; Weiner, 1995) allows flexible changes of phase, amplitude, and even polarization (Brixner and Gerber, 2001; Brixner *et al.*, 2004) of different spectral components that make up a femtosecond pulse. In the time domain, it controls the evolution of cycle-averaged quantities such as the amplitude vector and the instantaneous frequency of the field oscillations, on a time scale of several tens of femtoseconds. Key ingredients of this technology are feedback loops and learning algo-

¹⁴The idea of Born-Oppenheimer potential energy surfaces (PESSs) shaped by a laser field is quite general. For the effects of resonant fields in creating “light-induced potential energy surfaces” see Bandrauk *et al.* (1994) for an overview. Various applications of this concept for molecular control (Chang *et al.*, 2003; Sola, 2004) include laser catalysis of reactive scattering (Shapiro and Zeiri, 1986). For time-dependent Born-Oppenheimer PESSs shaped by nonresonant fields see Ivanov *et al.*, 1996; Corkum *et al.*, 1997; Niikura, Corkum, and Villeneuve, 2003; Sussman *et al.*, 2005, 2006.

rithms, allowing efficient optimization toward the desired outcome.¹⁵

D. Principles of attosecond control and measurement of electronic dynamics

In the quest for attosecond-scale control and metrology of electron dynamics, the fs-scale gradient of cycle-averaged quantities such as the amplitude and frequency of visible light could be steepened by using shorter-wavelength light. In practice, both the efficiency of coherent light generation and, not independently, the polarizability of matter diminish dramatically toward the XUV and x-ray regimes. With complex, large-scale infrastructures these limitations may be overcome, but a versatile, laboratory-scale technology for implementing control and metrology on the attosecond time scale requires a radically new approach. In our opinion, it will rely on controlled subcycle, i.e., subfemtosecond, variation of strong laser fields in the visible and nearby spectral ranges.

Subcycle light waveform control requires bandwidths of the order of an octave or more, implying “single”-cycle pulses in the Fourier limit (see Sec. III.A). Extending the bandwidth to several octaves will permit on-demand light waveform synthesis (see Sec. III.B), resulting in electric fields with strengths varying from zero to several volts per angstrom within less than 100 as. The resultant tailored force will permit control of electron motion on the atomic scale. We envision that light-wave engineering and lightwave electronics will open a new approach to controlling and exploring the microcosm: rather than controlling transitions between electronic quantum states of definite energy by such cycle-averaged quantities as the amplitude and frequency of light, electron wave packets will be steered with attosecond light forces.

III. INTENSE, CONTROLLED LIGHT FIELDS

Microwave electronics has allowed the temporal evolution of electric current and voltage to be controlled up to microwave frequencies of tens of gigahertz, creating the basis for high-speed data processing and short-distance communication.¹⁶ Ultrafast optics has permitted controlled modulation of light up to terahertz frequencies, revolutionizing long-distance telecommunication as well as exploration and control of the motion of atoms in microscopic systems. Nonlinear optics and ultrafast optics allow one to convert controlled terahertz amplitude modulation of light into controlled terahertz-

frequency electric fields, by means of optical rectification of femtosecond light pulses.¹⁷ However, even these fastest electric fields synthesized are far too slow for controlling and tracing the motion of electrons on atomic scales, which requires an electric force variable at petahertz frequencies. Petahertz-frequency (sub-PHz to few PHz) electric fields are present in near-infrared (NIR), visible (VIS), and ultraviolet (UV) radiation (henceforth, briefly, light). Here we review the recent emergence of light waves with controlled evolution of the field (Sec. III.A) and discuss future prospects for scaling the technology of light field control to bandwidths far beyond an octave (Sec. III.B) and field strengths in the relativistic regime (Sec. III.C).

A. Light-wave control: Brief history and current state of the art

Consider the electric field of a linearly polarized light pulse. For pulses with bandwidths below one octave the light field $E_L(t)$ can be decomposed into a carrier wave and an amplitude envelope,

$$E_L(t) = a_L(t)e^{-i(\omega_L t + \varphi)} + \text{c.c.}, \quad (6)$$

in a physically meaningful manner (Brabec and Krausz, 1997).¹⁸ Here $a_L(t) = |a_L(t)|e^{-i\beta_L(t)}$ is the complex envelope, $|a_L(t)|$ is the time-dependent (real) field amplitude, and $\beta_L(t)$ stands for a possible sweep (chirp) of the carrier frequency ω_L . Last but not least, φ determines the timing of the field oscillations with respect to the pulse peak, $\Delta t_{\text{peak}} = \varphi / \omega_L$ (see Fig. 10) and has been referred to as the carrier-envelope (CE) phase.

In relatively narrowband ($\Delta\omega / \omega_L \ll 1$) pulses, a change of the CE phase has no measurable physical consequence. Measurement of the shape of a light wave and its control (based on this measurement) rely on using pulses with bandwidth $\Delta\omega$ constituting substantial fraction of ω_L . In the absence of spectral phase variation, such pulses comprise merely a few oscillation cycles of the electromagnetic field, henceforth referred to as few-cycle pulses. A change in the CE phase changes significantly their temporal evolution (Fig. 10). In turn, this change affects the atomic-scale motion of electrons driven by these fields, which can be utilized for measuring the CE phase¹⁹ (see Sec. IV). Along with the measurement of the complex envelope $a_L(t)$ (see Sec. II.B) it determines the waveform, opening a route to light waveform control, outlined in Fig. 11(a). With φ known, the desired waveform can be realized by passing the pulse

¹⁵The work of Judson and Rabitz (1992) led to a series of beautiful experiments including Assion *et al.*, 1998, 2001; Bartels *et al.*, 2000, 2004; Brixner, Damrauer, and Gerber, 2001; Brixner, Damrauer, Niklaus, and Gerber, 2001; Levis *et al.*, 2001; Brixner *et al.*, 2003; Daniel *et al.*, 2003; Wohleben *et al.*, 2003, 2004, 2005; Vogt *et al.*, 2005.

¹⁶For a recent review, see Pozar (2004).

¹⁷For a recent review, see Xu and Zhang (2006).

¹⁸Note that we changed the sign convention in defining φ as compared with that used by Brabec and Krausz (2000) to conform with the more customary convention of Eq. (9).

¹⁹Strong-field CE phase effects have been predicted by Haljan *et al.*, 1997; Cormier and Lambropoulos, 1998; de Bohan *et al.*, 1998; Tempea *et al.*, 1999; Dietrich *et al.*, 2000; Nakajima and Watanabe, 2006.

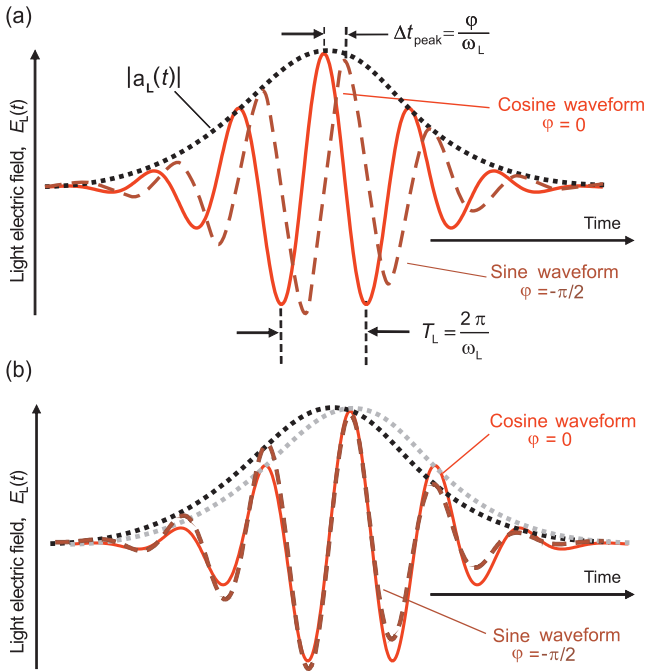


FIG. 10. (Color) Laser pulses containing two oscillation cycles within the full width at half maximum of their intensity profile, with sine- and cosine-shaped waveforms, with their (a) amplitude envelopes and (b) field oscillations coinciding.

through a thin optical medium of length L , shifting the CE phase by

$$\Delta\varphi(L) = 2\pi L(\partial n/\partial\lambda)_{\lambda_L}, \quad (7)$$

where λ_L is the carrier wavelength. The dephasing length which offsets the CE phase by π , $L_{\text{deph}} = 1/2|\partial n/\partial\lambda|_{\lambda_L}^{-1}$, amounts in transparent optical materials to tens of microns, permitting CE phase adjustments by a small translation of thin prisms (Xu *et al.*, 1996).

The above approach to light waveform control requires a single-shot measurement of φ . Stabilizing the frequency comb of femtosecond laser oscillators (Hänsch, 1997; Reichert *et al.*, 1999; Telle *et al.*, 1999) obviated the need for single-shot phase measurement by providing pulse trains with stabilized pulse-to-pulse CE phase shift.²⁰ Selection and amplification of pulses with constant (but unknown) φ from the pulse train yielded intense few-cycle pulses with stabilized and adjustable CE phase.²¹ With these pulses in place, measurement of φ can be performed over many pulses (via signal averaging) to produce intense few-cycle pulses with controlled waveform [see Fig. 11(b)]. Figure 12 shows the

²⁰ Apolonski *et al.*, 2000; Holzwarth *et al.*, 2000; Jones *et al.*, 2000; Kakehata *et al.*, 2001; Ye and Cundiff, 2005; Li *et al.*, 2007; Yu *et al.*, 2007. For detailed discussion, see Cundiff, 2002; Udem *et al.*, 2002; Cundiff and Ye, 2003.

²¹ Baltuška, Udem, *et al.*, 2003; Baltuška, Uiberacker, *et al.*, 2003; Kakehata *et al.*, 2004, 2006; O’Keeffe *et al.*, 2004; Lee *et al.*, 2005; Gagnon *et al.*, 2006; Hong *et al.*, 2006; Li *et al.*, 2006; Imran *et al.*, 2007; Mashiko *et al.*, 2007; Wu *et al.*, 2007.

first controlled and completely characterized light wave. Lightwave engineering is now approaching the single-cycle limit (Cavalieri, Goulielmakis, *et al.*, 2007; Goulielmakis, Schultze, *et al.*, 2008) and being extended to UV (Shverdin *et al.*, 2005) and IR frequencies (Fuji *et al.*, 2006; Manzoni *et al.*, 2006; Hauri *et al.*, 2007).

B. Light waveform synthesis

For atomic-scale electronic motion control we need to control the steering force on a sub-fs time scale. So far, the room for subcycle tailoring of the light waveform has been modest. Indeed, comparison of the cosine- and sine-shaped few-cycle waves in Fig. 10(b) shows merely a few percent difference in the electric field. More flexibility in subcycle shaping of the field requires a spectrum stretching substantially beyond an octave.

Self-phase-modulation (SPM) (Alfano and Shapiro, 1970) and cascaded stimulated Raman scattering (Kaplan, 1994; Harris and Sokolov, 1997; Sokolov *et al.*, 2001, 2005) of intense laser pulses proved most efficient for broadening the spectrum of an optical pulse.²² In a gas-filled, hollow-core fiber (Nishioka *et al.*, 1995; Nisoli *et al.*, 1996, 1997; Sartania *et al.*, 1997; Oishi *et al.*, 2005; Suda *et al.*, 2005) or in a self-induced plasma wave guide (Hauri *et al.*, 2004; Couairon *et al.*, 2006; Guandalini *et al.*, 2006; Chen *et al.*, 2007), SPM permits efficient spectral broadening of powerful femtosecond pulses. These can be compressed to the few-cycle regime using dispersion control with multilayer chirped mirrors (Szipočs *et al.*, 1994; Sting *et al.*, 1995; Jung *et al.*, 1997; Matuschek *et al.*, 1998; Tempea *et al.*, 1998). Recently, the latter approach has led to a supercontinuum stretching from <250 nm to >1000 nm, using 5-fs input pulses (Goulielmakis, Koehler, *et al.*, 2008); see Fig. 13(a). Phase modulation with twin pulses may result in further progress (Yamashita *et al.*, 2006; Matsubara *et al.*, 2007). We believe that covering the wavelength range of ~0.12–1.2 μm (~1–10 eV) with a supercontinuum generated by an intense few-fs pulse is within reach.

Control of the amplitude and phase of the generated spectral components can be realized by separating them in space (Weiner, 1995) and addressing the amplitudes and phases of the individual channels independently. Extending this control over several octaves is a challenge. Figure 13(b) outlines a possible implementation based on the work of Binhammer *et al.* (2005, 2006) using a prism-based system. Another route drawing on several discrete spectral channels separated by dichroic chirped mirrors is also being pursued (Goulielmakis *et al.*, 2007). Figure 14 shows several possible waveforms and demonstrates that superimposing waves of frequencies spanning several octaves permits efficient attosecond shaping of light waveforms. Attosecond sampling of the generated waveform (Sec. V) will allow its measurement and completes the toolbox of lightwave engineering.

²² For a review, see Zheltikov (2006a).

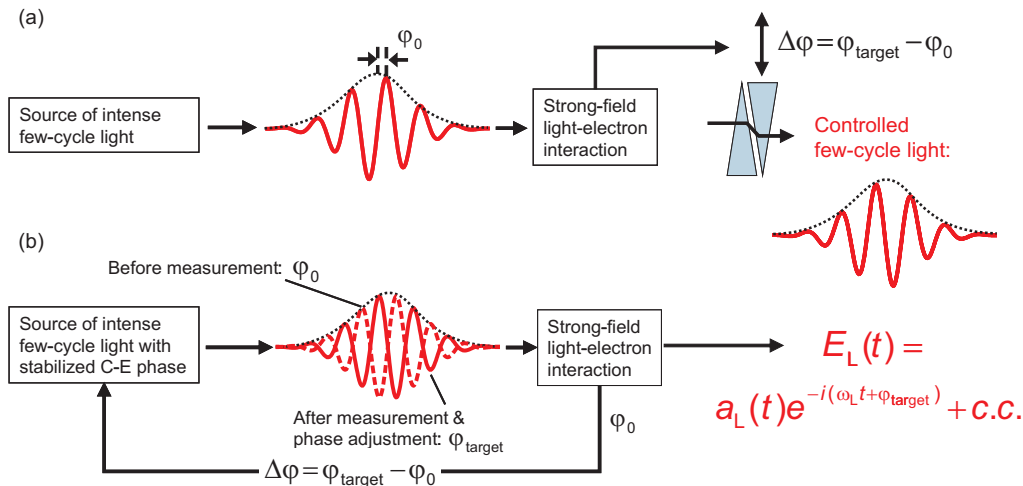


FIG. 11. (Color) Control of the waveform of few-cycle laser pulses relies on measurement of the CE phase by a strong-field light-electron interaction. (a) Once the measurement is performed (yielding ϕ_0), the required CE phase ϕ_{target} can be set by imposing an external phase shift $\Delta\phi = \phi_{target} - \phi_0$, leading to the desired waveform. (b) If the ultrashort-pulse source delivers pulses with a stabilized CE phase, its adjustment to the required value can be performed inside the source via an electronic feedback loop, obviating the need for fast phase measurement.

C. Towards ultrastrong controlled light fields

Today, light waveform control has been realized at power levels where the electric field—upon suitable focusing—can rival the atomic Coulomb field. State-of-the-art attosecond technology draws its tools from the interaction of light fields with electrons, either bound or of low positive energy, at these fields strengths. There exist several proposals for extending lightwave electronics to relativistic interactions, holding promise of enriching attosecond science with high-flux, high-energy electron and photon pulses of subfemtosecond duration (see

Sec. VI). A concept²³ at Max Planck Institute of Quantum Optics draws on three well-established technologies: (i) chirped-pulse amplification (CPA),²⁴ for providing subpicosecond to several-picosecond pulses with high energy; (ii) noncollinear optical parametric amplification (NOPA) over a near-octave-spanning bandwidth,²⁵ which was recently scaled to multiterawatt power levels;²⁶ and (iii) chirped multilayer mirrors (Szipöcs *et al.*, 1994; Steinmeyer *et al.*, 1999) for ultra-wideband, high-throughput dispersion control scalable for handling ultrahigh powers. The emerging source dubbed Petawatt Field Synthesizer may extend attosecond electron steering into the highly relativistic regime.

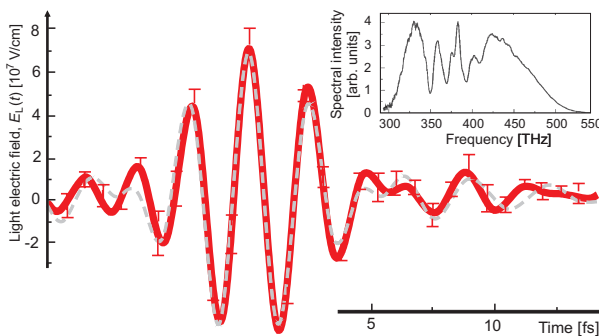


FIG. 12. (Color) Electric field (solid line) of the first completely characterized light wave (Goulielmakis *et al.*, 2004). The measurement has been performed with an attosecond streak camera, described in Sec. V, and yields the temporal evolution, direction, and strength of the field. The pulses are carried at a wavelength of $\lambda_L = 750$ nm with a duration full width at half maximum of 4.3 fs. Dashed line: electric field calculated from the measured spectrum (inset) by Fourier transform, assuming that all spectral components are in phase. Adapted from Goulielmakis *et al.*, 2004.

IV. LIGHTWAVE ELECTRONICS

We use the term lightwave electronics to refer to a microscopically²⁷ significant response of electrons to light oscillations on the time scale of the laser cycle and below. Our discussion begins by assessing the conditions for the appearance of such a response. As shown, it oc-

²³Proposed by Karsch (2004), for more details, see www.attoworld.de/PFS.html.

²⁴Invented by Strickland and Mourou (1985), for a recent review, see Mourou, Tajima, and Bulanov (2006).

²⁵Takeuchi and Kobayashi, 1994; Gale *et al.*, 1995; Cerullo *et al.*, 1997, 1998, 1999; Wilhelm *et al.*, 1997; Shirakawa and Kobayashi, 1998; Shirakawa *et al.*, 1998, 1999; Riedle *et al.*, 2000; Kobayashi *et al.*, 2001; Zavelani-Rossi *et al.*, 2001; Baltuska *et al.*, 2002a, 2002b, 2002c; Dubietis *et al.*, 2006.

²⁶Tavella *et al.*, 2006, 2007; Witte *et al.*, 2006; Renault *et al.*, 2007.

²⁷This attribute is meant to stress that no light propagation over a *macroscopic* distance, which is sensitive to even minuscule changes in the refractive index, is needed to “feel” this response.

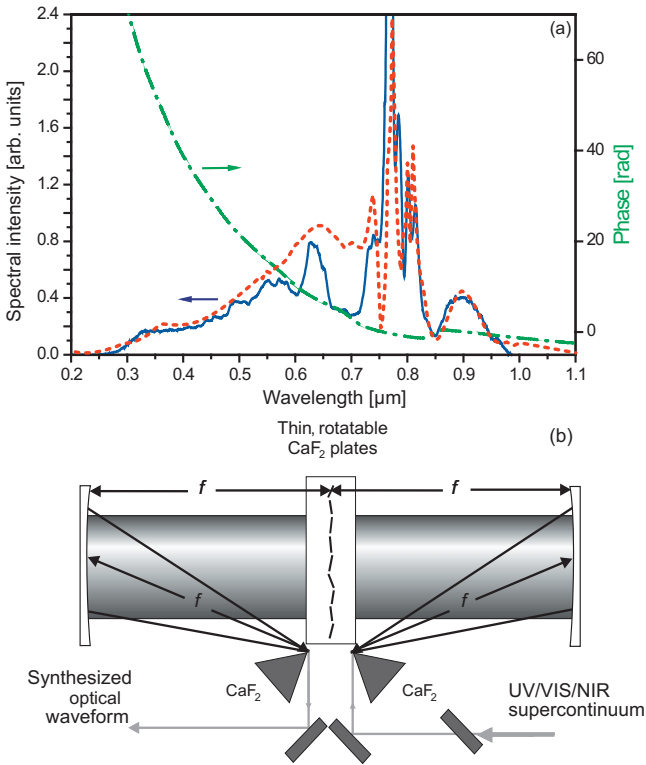


FIG. 13. (Color) Toward ultrawideband optical waveform synthesis. (a) Spectral supercontinuum generated by self-phase modulation of 5-fs, 0.2-mJ, 750-nm laser pulses in a self-induced plasma channel created in a cell filled with helium at a pressure of 25 bars (solid curve). Dotted curve, dashed-dotted curve, spectral intensity and phase, respectively, obtained from numerical simulation. Adapted from Goulielmakis, Koehler, et al., 2008. (b) Possible implementation of arbitrary light waveform synthesis by adjusting the phase and amplitude of spectral components independently in separate channels. The UV-transparent CaF_2 prisms separate the spectral components of the incident continuum, the amplitude and phase of which are then controlled in the Fourier plane of a 4f configuration: rotation of thin CaF_2 plates will result in tuning the phases whereas translation of the plates coated with a thin metal layer of variable thickness will permit amplitude control. Courtesy of E. Goulielmakis.

curs naturally in few-cycle strong-field interactions and plays a key role in developing attosecond technology.

Below, we deal with the atomic response to light fields. Therefore we use the atomic (Hartree) system of units. The corresponding expressions are obtained from the usual CGS units by setting the electron mass m_e , the electron charge $|e|$, and the Planck constant \hbar equal to unity. In these units, the natural scales derive from the physics of the hydrogen atom. The unit of energy is 27.21 eV, twice the ionization potential of hydrogen. The unit of time is 24.2 as, $1/2\pi$ times the electron orbit time around the nucleus in the first Bohr orbit. The unit of length is the radius of this orbit, equal to 0.529 Å. The unit of the electric field strength is that of the nucleus experienced by the electron in this orbit, $5.14 \times 10^9 \text{ V/cm}$. A linearly polarized laser field with such electric field amplitude has the intensity of 3.5

$\times 10^{16} \text{ W/cm}^2$. The speed of light in these units is $c = 137$.

A. Significant variations of atomic electron density within the wave cycle of light

In atoms and small molecules transitions between ground and excited electronic states typically lie in the UV-VUV range. As discussed in Sec. I.A, this implies a near-instantaneous response of the electronic system to NIR and VIS light fields. The scale of the corresponding distortions to the electron density can be estimated from electronic polarizabilities, with the static polarizability α_{st} offering a good estimate for NIR-VIS light. The dipole moment induced by the nonresonant electric field $E_0 \cos \omega_L t$ is $d \approx \alpha_{st} E_0 \cos \omega_L t$. At the same time, $d \approx N_e \Delta R$, where N_e is the number of active electrons (typically electrons in the valence shell) and ΔR is the characteristic displacement per electron. These two equations yield $\Delta R \approx \alpha_{st} E_0 / N_e$. Given that polarizabilities typically do not exceed a few atomic units per participating electron, we see that microscopically significant distortion of the electron density can be induced only with light field strengths approaching typical interatomic field strengths. This implies the onset of ionization, which will dominate modification of the electronic cloud. Then, significant changes within one wave cycle imply ionization rates comparable to the light frequency. This is feasible only with a few-cycle laser pulse (Spielmann et al., 1998); otherwise, ionization will saturate before the desired intensity is reached (Lambropoulos, 1985). The unprecedented ionization rate achievable with few-cycle light benefits the efficient generation of coherent XUV and THz radiation (Gildenburg and Vvedenskii, 2007) likewise.

Thus a microscopically significant change in the electron density of atomic systems within the wave cycle of visible light requires few-cycle light fields. The resultant atomic-scale electronic motion unfolds on the attosecond time scale, is highly sensitive to the subcycle evolution of the light field, and lies at the heart of lightwave electronics. We now examine this motion more closely.

In the dipole approximation, for a linearly polarized laser field the interaction potential energy for an electron at position $\mathbf{r}=(x,y,z)$ is (in atomic units with $|e|=m_e=\hbar=1$)

$$V(\mathbf{r},t) = V_{\text{atom}}(\mathbf{r}) + xE_L(t), \quad (8)$$

where we assume that the laser electric field

$$E_L(t) = E_0 f(t) \cos(\omega_L t + \varphi) \quad (9)$$

is polarized along the x axis and positive when pointing in the direction of increasing x coordinate, see Fig. 15. Here $f(t)$ is a real-valued envelope function, peaked at $t=0$, $f(0)=1$. A snapshot of the total potential at the peak of the field oscillation, $\cos(\omega_L t + \varphi)=-1$, along the direction x of laser polarization, is shown in the elliptical inset of Fig. 15. The strong electric field suppresses the barrier that keeps electrons bound, allowing them to

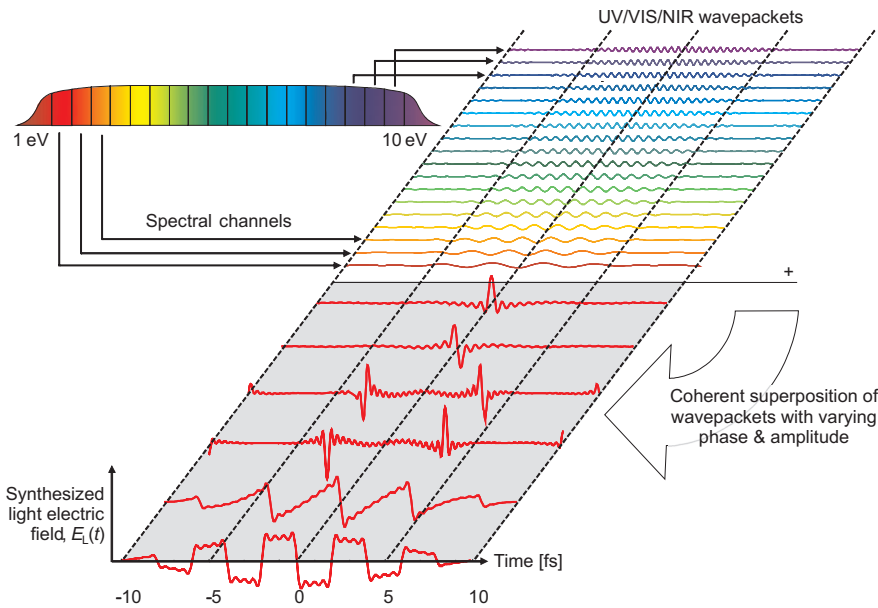


FIG. 14. (Color) Representative optical waveforms (lower panel) that have been numerically synthesized from coherent superposition of quasimono-chromatic wave packets (shown on the right-hand side of the upper panel) delivered in $N = 18$ spectral channels of the supercontinuum stretching over 1–10 eV (left-hand side of the upper panel). Courtesy of E. Goulielmakis.

tunnel out each time the oscillating electric field passes its maxima, twice every laser cycle.²⁸ As a result, the duration of the electron wave packet which emerges on the other side of the barrier is a small fraction of the half oscillation of the driving field, less than 1 fs in a NIR field.²⁹

Once the electron appears at the tunnel exit, it is accelerated away from the parent ion until the field reverses its direction in about a quarter cycle. At field strengths of 10^9 V/cm, the total spatial excursion of the electron driven by a NIR laser field reaches several tens of angstroms, greatly exceeding the size of an atom or a small molecule. If the electron is freed with substantial probability within a single half cycle in a few-cycle field, such an excursion causes a dramatic change in the microscopic electron density distribution.

The electron's motion during these oscillations depends on the phase of the electric field $E_L(t)$ at which ionization has occurred, $\phi_0 = \omega_L t_0 + \varphi$. If the electron is returned, which may happen for the phases ϕ_0 after the peak of the oscillating field, it may recollide with the parent ion; see the inset in Fig. 15. Upon return, the electron wave packet may interact with other electrons left behind in their bound states. Many interactions are confined to a fraction of the optical cycle, giving rise to a wealth of subfemtosecond phenomena. Figure 15 summarizes the most important ones, which will be discussed.

B. Semiclassical modeling of strong field-matter interaction

Our previous discussion of intense laser-atom interaction relied on the semiclassical model introduced by

²⁸Recently, this process was observed in real time; see Uiberacker *et al.*, 2007, and Fig. 49 in Sec. VII.

²⁹A tutorial discussion of this process can be found in Ivanov *et al.* (2005).

Corkum (1993), Kulander *et al.* (1993), and Schafer *et al.* (1993).³⁰ It is based on the single active electron (SAE) approximation,³¹ a key ingredient in our understanding of the interaction between an intense infrared laser field and an atom or a small molecule. This approximation assumes that only one electron actively participates in the ionization of the atom or molecule by the low-frequency laser field. Other electrons are involved only in the screening of the nucleus, creating an effective single-electron potential. The SAE approximation is justified when the energies of multielectron excitations are large compared to the laser frequency and significantly exceed those of single-electron excitations.³²

The first building block of the semiclassical model is tunnel ionization or, more generally, optical field ionization, often modeled using the Keldysh theory or its refined versions.³³ Once the electronic wave packet emerges on the other side of the tunneling barrier at x_0 (see inset in Fig. 15), it is pulled far away within a small

³⁰This model had an important precursor: the so-called “atomic antenna” model (Kuchiev, 1987). Relevant early work also includes Corkum *et al.*, 1989; Krause *et al.*, 1992.

³¹Detailed discussion can be found in Kulander *et al.*, 1993; see also Schafer and Kulander, 1990. Later important work includes Muller and Kooiman, 1998.

³²These conditions are met by noble gases, where the SAE approximation has been extremely successful. For alkaline-metal atoms, nonlocal modifications of the single-electron potential are already required but the SAE approximation still performs well (Sheehy *et al.*, 1999; Gaarde *et al.*, 2000). In small molecules, the SAE approximation is still applicable, but in polyatomic systems, especially when charge-transfer excitations are located within a few electron-volts from the ground electronic state, this approximation fails (see Lezius *et al.*, 2001; Markevitch *et al.*, 2003).

³³For reviews, see Delone and Krainov, 1985; Faisal, 1987; Reiss, 1992; Becker and Faisal, 2005. For earlier references, see Keldysh, 1964; Perelomov *et al.*, 1966a, 1966b; Perelomov and Popov, 1967; Faisal, 1973; Reiss, 1980a, 1980b.

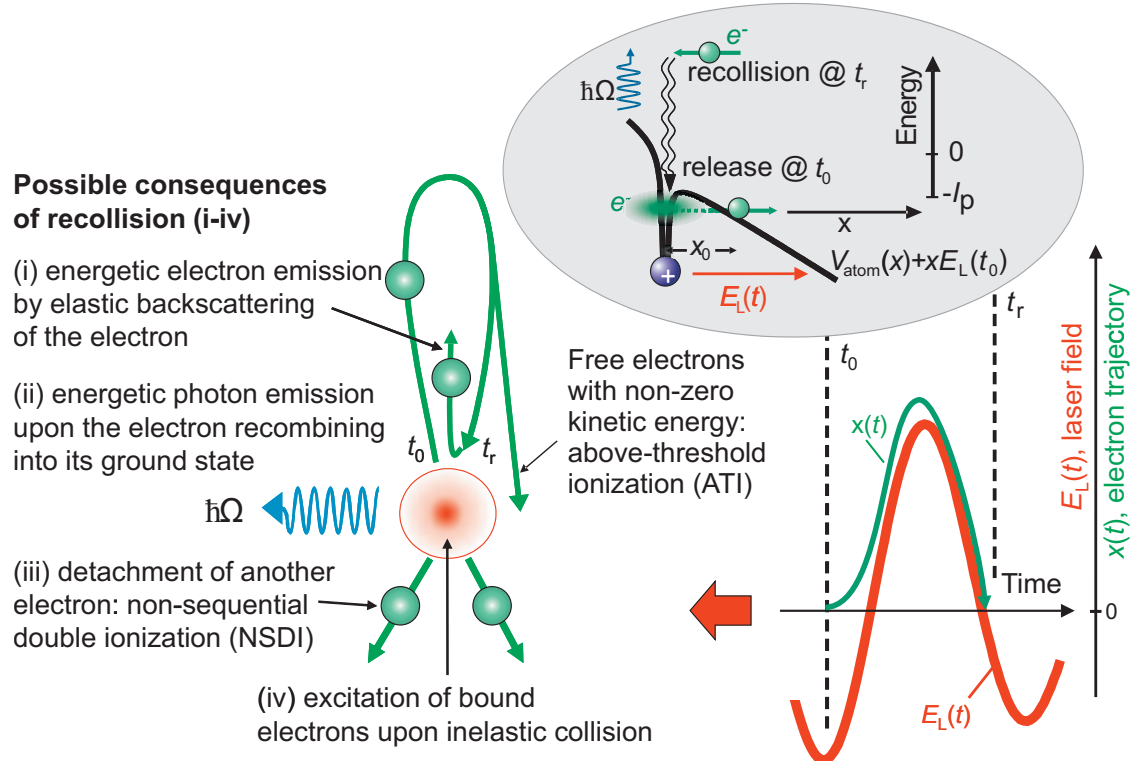


FIG. 15. (Color) Optical field ionization of an atom (at moment t_0) and subsequent recollision of the detached electron (at moment t_r) with the parent ion in a strong, linearly polarized ultrashort-pulsed laser field. (i)–(iv) Possible consequences of recollision. Inset: Release and recollision of electron that returns with highest energy to the parent ion, resulting—via process (ii)—in the highest-energy photons emitted.

fraction of the electric field oscillation cycle. Consequently, the Coulomb attraction to the parent ion quickly becomes a small perturbation compared to the laser field. The simplest approximation is to neglect the Coulomb field after ionization. This is the basis of the quantum strong-field approximation (SFA) (see footnote 32), a theoretical workhorse in strong-field physics. Once $V_{\text{atom}}(\mathbf{r})$ is dropped in Eq. (8), the center-of-mass motion of the quantum wave packet is described by

$$\ddot{x} = -E_L(t). \quad (10)$$

A further essential assumption of the semiclassical model is that the electron appears at the “exit” of the tunneling barrier x_0 with zero velocity $v(t_0)=0$. Then Eq. (10) yields for the electron’s velocity [equal to its (kinetic) momentum in atomic units]

$$v(t) = v(t_0) + A_L(t) - A_L(t_0) = A_L(t) - A_L(t_0). \quad (11)$$

Here the vector potential $A_L(t)$ is defined by $E_L(t) = -dA_L/dt$. In the limit of a slowly varying envelope, $df/dt \ll \omega_L f$, we have

$$A_L(t) \approx -(E_0/\omega_L)f(t)\sin(\omega_L t + \varphi), \quad (12)$$

which is valid down to the few-cycle regime. In this limit, Eq. (11) yields

$$v(t) = A_L(t) - A_L(t_0) \approx \frac{E_0}{\omega_L}f(t_0)\sin\phi_0 - \frac{E_0}{\omega_L}f(t)\sin(\omega_L t + \varphi), \quad (13)$$

where $\phi_0 = \omega_L t_0 + \varphi$ is the phase of the laser field at the instant of ionization. Figure 16 shows $v(t)$ for different instants of release. The final momentum is

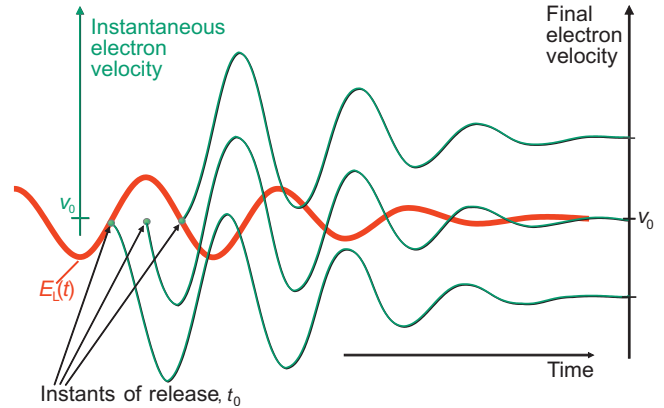


FIG. 16. (Color) Temporal variation of the electron velocity component parallel to the electric field of a linearly polarized light wave for different moments of release. The electron’s final velocity v_f shown on the right-hand side sensitively depends on the instant of release.

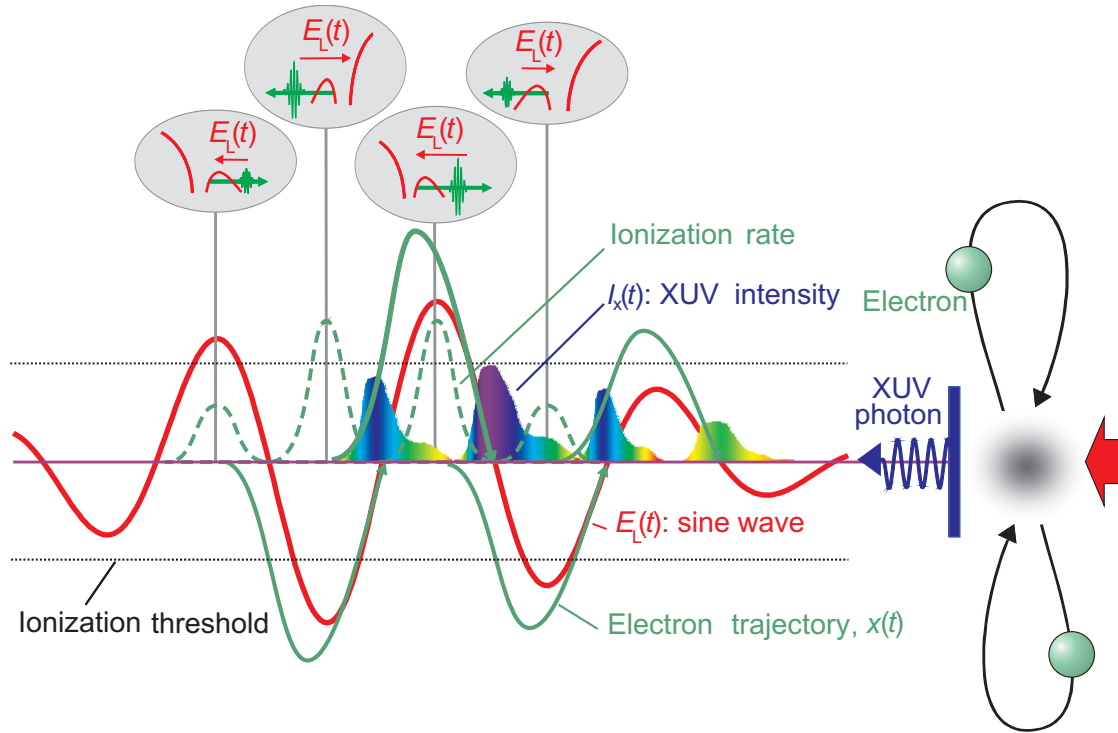


FIG. 17. (Color) Trajectories of electrons returning to the vicinity of the core with maximum kinetic energy (solid green lines) for a laser pulse consisting of two oscillation cycles within the full width at half maximum of its cycle-averaged intensity profile (e.g., a 5-fs pulse at a carrier wavelength of $\lambda_L=750$ nm). We have set $\varphi=-\pi/2$, i.e., used a “sine-shaped” electric field waveform. Dashed line sketches time dependence of ionization rate.

$$\begin{aligned} v_f &= A_L(t \rightarrow \infty) - A_L(t_0) \\ &= -A_L(t_0) \\ &\approx (E_0/\omega_L)f(t_0)\sin \phi_0. \end{aligned} \quad (14)$$

Further integration yields the electron trajectory

$$\begin{aligned} x(t) &\approx x_0 + \frac{E_0}{\omega_L^2}[f(t)\cos(\omega_L t + \varphi) - f(t_0)\cos(\omega_L t_0 + \varphi)] \\ &+ \frac{E_0}{\omega_L}f(t_0)\sin(\omega_L t_0 + \varphi)(t - t_0). \end{aligned} \quad (15)$$

For an instant of release shortly after the field oscillation peak, $x(t)$ is sketched in Fig. 15. In a few-cycle, linearly polarized laser field, ionization is significant only a few times near the strongest field oscillation peaks. Figure 17 illustrates trajectories launched shortly after the oscillation peak and returning to the core with maximum kinetic energy, which are responsible for emission of the highest-energy photons (upon recombination) and electrons (upon elastic backscattering). Predictions of this simple classical model including the assumption $v(t_0)=0$ have been checked against full quantum mechanical simulations, with good agreement in the strong-field limit (de Bohan *et al.*, 2002).

Is this classical analysis useful if the final step of the strong-field interaction has to be handled quantum mechanically? For example, high-order harmonic generation (HHG; see Sec. IV.C.2) is governed by the interference of the “continuum” electron wave packet ψ_c

revisiting the core with the portion of the wave function left behind in the ground atomic state ψ_g . Classical analysis enters via the quantum-classical correspondence. The wave packet ψ_c evolves as

$$\psi_c(\mathbf{r},t) \propto \sqrt{w_i(t_0)} \exp[iS(\mathbf{r},t,t_0)]. \quad (16)$$

Here S is the action along the classical trajectory that starts at the moment t_0 with zero initial velocity and arrives at the point \mathbf{r} at the moment t and $w_i(t_0)$ is the ionization rate. The moment t_0 is uniquely defined by the \mathbf{r} and t , i.e., $t_0=t_0(\mathbf{r},t)$. In general, the action and trajectories are quite complicated. However, in the SFA the result is relatively simple:

$$S(\mathbf{r},t,t_0) = [\mathbf{p} + \mathbf{A}_L(t)]\mathbf{r} - \frac{1}{2} \int_{t_0}^t [\mathbf{p} + \mathbf{A}_L(t')]^2 dt', \quad (17)$$

where $\mathbf{A}_L(t)$ is the vector potential of the laser field, \mathbf{p} is the electron’s drift (canonical) momentum, and $\mathbf{v}(t)=\mathbf{p} + \mathbf{A}_L(t)$ is the instantaneous (kinetic) momentum. The relevant canonical momentum \mathbf{p} is defined by the assumption that, at the moment of ionization t_0 , $\mathbf{v}(t_0)=\mathbf{p} + \mathbf{A}_L(t_0)=0$. The first term in Eq. (17) gives the spatial dependence of the wave function, which in the SFA is a plane wave. The second term describes the energy-dependent contribution to its phase—the integral of the instantaneous kinetic energy of the electron along the trajectory. Equations (16) and (17) imply that the wave packet’s instantaneous wavelength and instantaneous carrier frequency are determined by the instantaneous

values of the electron's momentum and kinetic energy, respectively. Equations (16) and (17) establish the link between the quantum wave function and the underlying classical evolution.³⁴

Another key aspect of ψ_c is the dynamics in the plane perpendicular to the x direction. The wave packet launched by tunnel ionization is confined laterally during tunneling. The Heisenberg uncertainty relationship implies transverse velocity distribution, which has a width [see, for example, Ivanov *et al.* (2005)]

$$v_{\perp,\text{spr}} \approx E_L^{1/2}/(2I_p)^{1/4} \quad (18)$$

in each transverse direction.³⁵ This reduces the probability of recollision as

$$|\psi_c|^2 \propto w_i[v_{\perp,\text{spr}}(t_r - t_0)]^{-2}, \quad (19)$$

where t_r is the moment of return (recollision). A further reduction factor of $1/(t_r - t_0)$ in the recollision probability at the moment t_r arises due to the longitudinal spreading of the wave packet.

C. Single-electron interference within the wave cycle of light

The interaction of atoms with strong fields provides textbook examples for one manifestation of quantum physics: the interference of a particle with itself. Electron wave packets released from the same valence electronic state (ground state) near subsequent wave crests and moving in the same direction will interfere with each other, resulting in the appearance of electrons at discrete energies spaced by the laser photon energy [above-threshold ionization (ATI)]; see Fig. 18(a) (Agostini *et al.*, 1979). Similarly, interference of the photon wavepackets emitted upon each recollision (twice per laser cycle) gives rise to periodic modulations of the emitted energetic photon spectrum, leading to HHG (McPherson *et al.*, 1987; Ferray *et al.*, 1988); see Fig. 18(b). The discrete ATI and HHG emission structure results from single-electron interference and the temporal coherence of the driving light wave.

The probability of tunnel ionization decreases exponentially with decreasing field strength. Consequently, atoms driven by a few-cycle wave eject only a few electron wave packets with significantly differing energy distributions due to significant differences between the field amplitudes in the subsequent half cycles of the pulse. This has two major implications: the emission of the

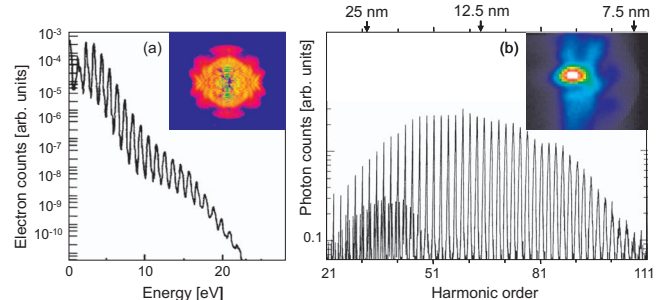


FIG. 18. (Color) Implications of single-electron interference in a strongly driven atom. (a) Energy distribution of above-threshold ionized (ATI) electrons produced by a multicycle femtosecond laser pulse. Courtesy of G. Paulus. Inset: Angular interference pattern of ATI electrons. Courtesy of M. Vrakking. (b) Spectral distribution of high order harmonic emission. Adapted from Macklin *et al.*, 1993. Inset: Spatial intensity profile of few-cycle driven harmonics at a photon energy of ~ 100 eV, implying a coherent near-diffraction-limited laser-like beam. Courtesy of M. Uiberacker.

most energetic electrons (i) can be confined to a single wave cycle at the peak of the pulse, and (ii) its temporal profile is most sensitive to the CE phase of the pulse. This opens the door to controlling electron dynamics in the sub-fs domain (lightwave electronics) and—by allowing measurement of the CE phase—control of light waveforms (light-wave engineering).

1. Above-threshold ionization and sub-fs electron pulses

An easily accessible physical quantity is the final velocity v_f of electrons ejected from strongly driven atoms. According to Eq. (14), it is given by the vector potential of the field $A_L(t)$ at the instant of release t_0 . Figure 19(a) plots the laser-induced change of electron velocity, $\Delta v = -A_L(t_0)$, for the “sine-shaped” electric field waveform of Fig. 17. The dashed line sketches the ionization probability, i.e., the initial temporal profile of the released electron wave packets. As indicated in Fig. 17, the four central half cycles of $E_L(t)$ have sufficiently large amplitude to open a window—a “slit” in the time domain—for releasing the wave packet. The electron's final momentum is dictated by $A_L(t_0)$, which—for the sine-shaped electric field waveform—opens either one or two slits for high-energy electron emission toward the left and right detectors,³⁶ respectively. Figure 19(b) reveals that emission of the highest-energy ATI electrons indeed occurs in a twin or in a single sub-fs pulse, depending on the few-cycle waveform driving the interaction (Lindner *et al.*, 2005).

2. High-order harmonic emission and sub-fs photon pulses

In the previous section, we dealt with electrons whose motion toward the detector is undisturbed by the parent

³⁴Lewenstein *et al.*, 1995; Salieres *et al.*, 2001; Corsi *et al.*, 2006; Kanai *et al.*, 2007 For an earlier reference, see Volkov, 1935.

³⁵Spreading is reduced if part of the electron's ground-state wave function is driven into excited bound states; see Hu *et al.* (2001). This effect, which is ignored in the SFA, might play an important role in generating low-order harmonics, typically up to I_p .

³⁶We use this terminology by assuming the laser fields to be polarized horizontally.

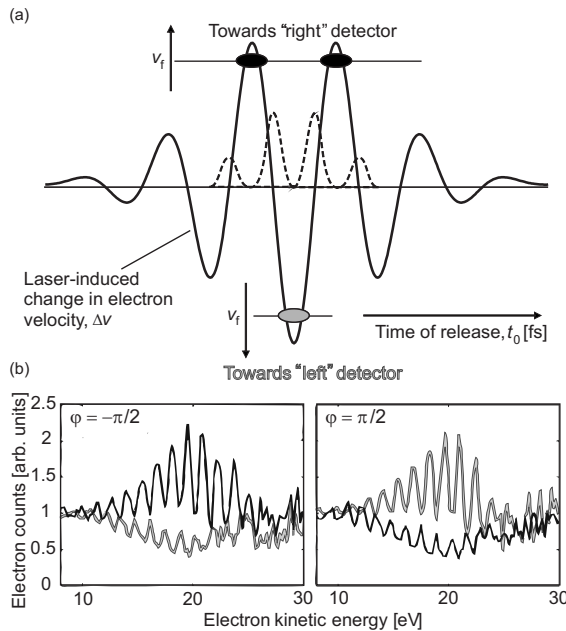


FIG. 19. Attosecond ‘double-slit’ experiment (Lindner *et al.*, 2005). (a) A sine-shaped few-cycle pulse (not shown) ionizes atoms via optical-field ionization. Electrons are created with zero velocity at the instant of ionization, hence the change imposed by the laser field (solid line) is equal to their final velocity. ‘Slits’ corresponding to a particular final velocity are shown by black and gray ellipses. The dashed line sketches the ionization rate. (b) Kinetic energy distributions of electrons arriving at the right and left detectors, depicted in black and gray, respectively. Adapted from Lindner *et al.*, 2005. The left panel shows spectra for the case shown in (a): the modulation of the spectrum on the right detector indicates interference between electrons released at two instants separated by the oscillation cycle, whereas the absence of pronounced modulation on the left detector reveals that electron emission in this direction is confined to a single ionization event, in accordance with the model shown in (a). By reversing the laser field (right panel), the situation is reversed. The measured spectra set an upper limit of 500 as for the duration of emitted electron wave packets. The experiment demonstrates attosecond control of electron emission from atoms using waveform-controlled few-cycle light.

atomic or molecular³⁷ ion. However, depending on the phase at the instant of ionization, ϕ_0 , oscillations in the laser field may bring the electron back to its parent ion. In Eq. (13), the first term describes the drift velocity of the electron, which changes the sign near the maximum of the electric field, at $\phi_0=0$. Electrons released after the peak of the field, $\phi_0>0$, return to the core (see the shaded part of the electron emission probability in Fig. 20). The respective trajectories as a function of the instant of release t_0 or the phase ϕ_0 are given by Eq. (15). The return time t_r can be obtained by setting $x(t_r)=0$ in Eq. (15) for $t_r>t_0$. Figure 20 shows recolliding electron

³⁷High-order harmonic generation in molecules has been reviewed by Bandrauk *et al.* (2007).

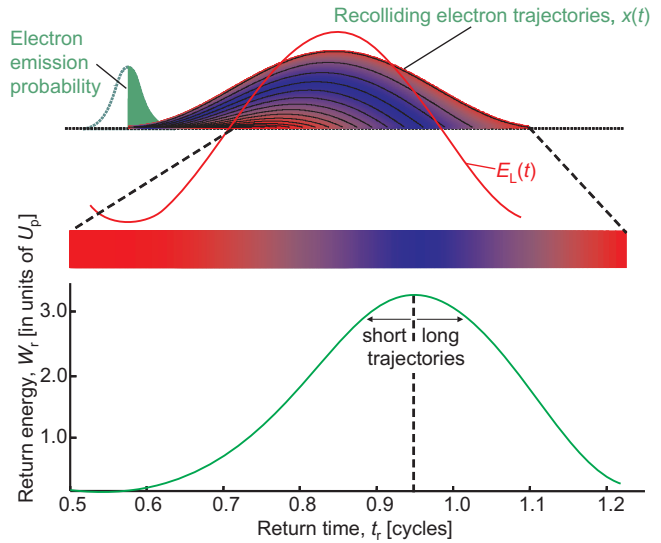


FIG. 20. (Color) Recolliding electron trajectories in atoms ionized with linearly polarized light. Top panel sketches electron trajectories—distance from the ion (vertical coordinate) vs time (horizontal coordinate). Depending on the moment of ionization, electrons return at different times with different energies, shown with changing color. Bottom panel shows energy of the returning electron vs return time $W_r(t_r)$ in units of U_p , see Eq. (20), for the selected laser cycle. This dependence indicates that electron wave packets returning along short and long trajectories carry positive and negative chirp, respectively. Courtesy of A. L’Huillier. (See also Varjú, Johnsson, *et al.*, 2005.)

trajectories³⁸ obtained with this procedure (upper panel) along with the energy of the electrons at t_r , in units of U_p , where (in atomic units)

$$U_p(t) = E_0^2 f^2(t)/4\omega_L^2 \quad (20)$$

is the cycle-averaged wiggle energy of the electron in the laser field given by Eq. (9), also known as the ponderomotive potential.

Figure 20 conveys several important messages. First, it shows that the moment of return is uniquely determined by the moment of ionization. Second, the maximum energy of the returning electron W_{\max} , reaches about $3.2U_p$, yielding for the maximum photon energy emitted during recollision (Kulander *et al.*, 1992; Corkum, 1993)³⁹

$$\Omega_{\max} \approx 3.2U_p + I_p, \quad (21)$$

where I_p is the ionization potential. For few-cycle laser fields, valence electrons in rare gas atoms with high I_p , such as neon or helium, may survive in the ground state

³⁸For strong IR and visible fields the electron oscillation amplitude during its first excursion exceeds the Bohr radius by two orders of magnitude. Hence the initial offset of the electron’s place of creation from the origin in Eq. (15) can be neglected on this scale, $x_0 \approx 0$.

³⁹ Ω_{\max} can be enhanced with chirped few-cycle pulses (Carrera and Chu, 2007).

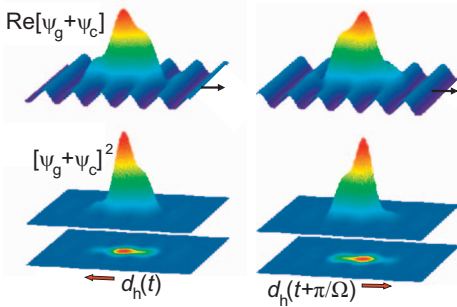


FIG. 21. (Color) Interference of recolliding wave packet with the ground state part of the same electron wave function, at two adjacent moments of time (left and right set of panels). Top and bottom panels show real part of the total wave function and the electron density, respectively. Interference leads to oscillations of electron density and hence of the induced dipole moment. Courtesy of D. Villeneuve.

up to intensities of several times 10^{15} W/cm². For NIR and IR light, W_{\max} can reach hundreds and thousands of eV, respectively. Third, for each recollision energy, except for the maximum, there are two trajectories along which the electron can acquire the same energy by the time it returns to the core. These two sets of trajectories have been termed *short* and *long* trajectories. Last but not least, the electron wave packet returning to the core is heavily chirped. As a consequence, its duration is substantially longer (~ 1 fs) than the duration of the original wave packet released by optical field ionization [see, e.g., Niikura *et al.* (2005)].

This classical picture is reflected in the quantum analysis based on Eqs. (16) and (17).⁴⁰ As the returning electron reencounters its parent ion, the unbound (continuum) part of its wave function ψ_c , with its fast-oscillating phase, can interfere with the bound part of the electron wave function ψ_g . This interference creates fast-moving volumes of constructive and destructive interference, resulting in hyperfast oscillations of the electron density, as illustrated in Fig. 21. The one-active-electron dipole moment of our atom induced by the laser field, $d(t) = \langle \psi | d | \psi \rangle$, includes these fast oscillations via the term⁴¹

$$d_h(t) = \langle \psi_g | d | \psi_c \rangle + \text{c.c.}, \quad (22)$$

resulting in the harmonic emission intensity

$$I_h(t) \propto |\ddot{d}_h(t)|^2. \quad (23)$$

To assess the emission spectrum, we write the bound part of the wave function as $\psi_g = \phi_g(\mathbf{r}) \exp(-iW_g t)$. After

⁴⁰ Lewenstein *et al.*, 1994; Kopold *et al.*, 2000; Salieres *et al.*, 2001; Becker *et al.*, 2002; Milošević and Becker, 2002; Frolov *et al.*, 2007a, 2007b; Mineo *et al.*, 2007; Pérez-Hernández and Plaja, 2007.

⁴¹ Equation (22) is also a matrix element describing the recombination of the returning electron back to its original ground state, a process observed recently via particle detection (Williams *et al.*, 2007).

spatial integration in the expression of the matrix element given by Eq. (22), $d_h(t)$ will beat with the frequency $\Omega(t)$ given by the time derivative of the phase of ψ_c minus the time derivative of the phase of ψ_g . These derivatives are the energies of bound and returning wave packets $W_g = -I_p$, and, from Eq. (17), $W_r(t_r) = \mathbf{v}(t_r)^2/2$, respectively, so that $\Omega(t_r) = W_r(t_r) + I_p$. The beat frequency follows the curve $W_r(t_r)$ in Fig. 20, obtained from classical trajectories. The harmonic emission spectrum will contain all these frequencies up to the maximum frequency Ω_{\max} given by Eq. (21), determined by the maximum energy of the returning electron. Analysis of the spectrogram

$$H(\Omega, \tau) = \left| \int \ddot{d}_h(t) G(t - \tau) \exp(i\Omega t) dt \right|^2, \quad (24)$$

where $G(t - \tau)$ is a gating function (e.g., Gaussian), allows us to study when different frequencies are emitted (Yakovlev and Scrinzi, 2003).⁴² Figure 22 shows the spectrogram of the harmonic emission from a macroscopic volume of gas exposed to a few-cycle NIR laser pulse. The time-frequency distribution of emission consists of branches resembling their classical counterpart, $W_r(t_r)$ in Fig. 20.

Figure 22(a) reveals a crucial correction to the simple classical approach. Quantum mechanically, the emission extends beyond the classical cutoff Ω_{\max} with exponentially decreasing spectral intensities for $\Omega > \Omega_{\max}$, as revealed in Fig. 22(b). In this range the temporal chirp of emission is almost negligible. This is of great practical importance to attosecond technology: filtering highest-energy emission around Ω_{\max} with a bandpass filter yields isolated [for a cosine-shaped pulse, Figs. 22(a) and 22(b)] or twin [for a sine-shaped pulse, Figs. 22(c) and 22(d)] emission bursts. These bursts are predicted to be near-Fourier-limited XUV pulses with sub-fs duration.

The disappearance of periodic modulation of the cutoff emission in the first HHG experiments with waveform-stabilized, few-cycle pulses [Fig. 23(a)] provided the first indication of the emergence of a single, isolated pulse of sub-fs duration from a few-cycle strong-field interaction (Baltuška, Udem, *et al.*, 2003). A shift of the CE phase of the few-cycle driver by $\pi/2$ introduced quasiperiodic modulation in the cutoff range with a maximum modulation depth, see Fig. 23(b), in accordance with the prediction of Fig. 22(d). These experiments have demonstrated the feasibility of controlling sub-fs coherent XUV emission with waveform-reproducible few-cycle light. Complete temporal characterization of the emitted radiation will be addressed in Sec. V.

⁴² See also Kim *et al.*, 2001, 2006; Pukhov *et al.*, 2003; Chipperfield *et al.*, 2005; Carrera *et al.*, 2006.

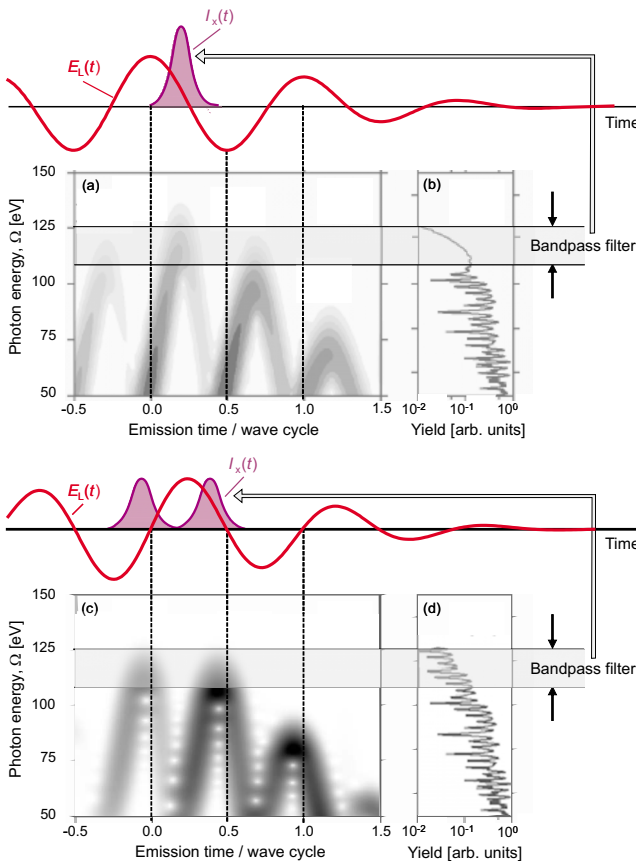


FIG. 22. (Color online) (a), (c) The spectrogram $H(\Omega, \tau)$ of the atomic high-harmonic emission from a gas of neon atoms exposed to a few-cycle NIR laser pulse ($\tau_L=5$ fs, $\lambda_L=750$ nm); for further parameters used for the calculation, see [Yakovlev and Scrinzi, 2003](#). (b), (d) Emission spectra. (a), (b) are calculated for a cosine-shaped driving pulse. From [Yakovlev and Scrinzi, 2003](#). (c), (d) are for a sine-shaped driving pulse calculated for the same parameter set ([Yakovlev, 2007](#)). Propagation tends to eliminate the contribution of multiple returns. Filtering out high-energy emission yields a (a) single or (c) twin sub-fs XUV pulse. Courtesy of V. Yakovlev.

D. Electron scattering

1. Elastic backscattering and high-energy electron emission

We now turn our attention to the elastic scattering of the recolliding electron (Fig. 15). The scattering breaks the phase of the electron's wiggling motion and abruptly changes the direction of the electron velocity. Equation (13) yields for the instant just before the recollision (denoted by $t_r=0$)

$$v(t_r=0) = A_L(t_r) - A_L(t_0). \quad (25)$$

As before, we assume that the laser field is linearly polarized and the electron is moving along the direction of the laser polarization for $t < t_r$. Upon elastic scattering, the electron changes the direction of its velocity while keeping its absolute value the same:

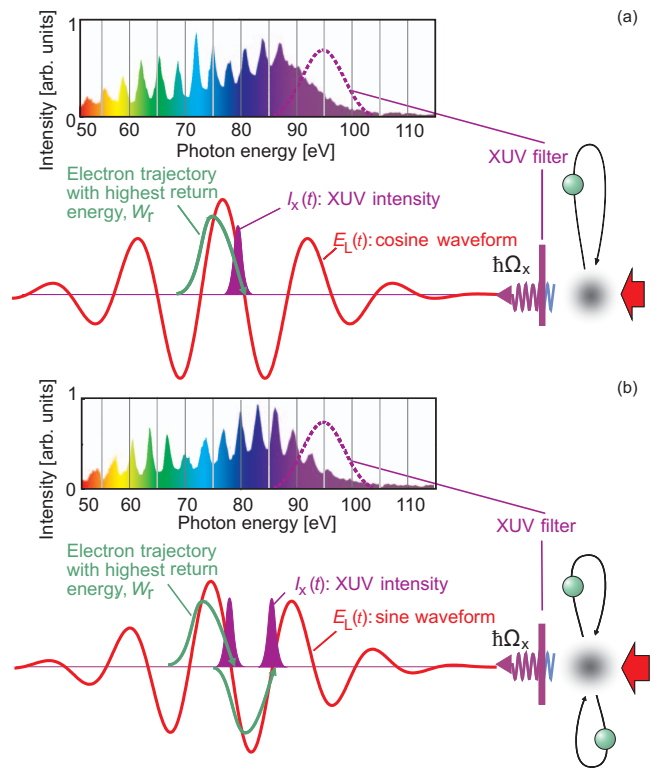


FIG. 23. (Color) High-order harmonic spectra obtained experimentally with a few-cycle NIR pulse ($\tau_L=5$ fs, $\lambda_L=750$ nm) with (a) cosine-shaped and (b) sine-shaped waveforms ([Baltuška, Udem, et al., 2003](#)). The cosine wave leads to a smooth spectrum in the cutoff range, indicating emission in a single burst of potentially sub-fs duration, whereas the appearance of modulation for the sine wave is in accordance with the prediction of Fig. 22(d) and suggests that emission is delivered in two bursts half a cycle apart.

$$v_{\parallel}^2(t_r+0) + v_{\perp}^2(t_r+0) = [A_L(t_r) - A_L(t_0)]^2, \quad (26)$$

where v_{\parallel} and v_{\perp} stand for the momentum vector components parallel and perpendicular to the laser polarization. At the end of the laser pulse, these two components become

$$v_{\parallel,f} = v_{\parallel}(t_r+0) - A_L(t_r), \quad v_{\perp,f} = v_{\perp}(t_r+0). \quad (27)$$

As an example, take a closer look at backscattering. Then $v_{\perp}=0$ and the relationship between the momenta before and after the collision is

$$v_{\parallel}(t_r+0) = -v_{\parallel}(t_r-0) = -A_L(t_r) + A_L(t_0). \quad (28)$$

At the end of the pulse we then have

$$v_{\parallel,f} = v_{\parallel}(t_r+0) - A_L(t_r) = -2A_L(t_r) + A_L(t_0). \quad (29)$$

This result is different from the final momentum $-A_L(t_0)$ for the case when no collision was present. The back-scattered electron's final momentum is sensitive to the

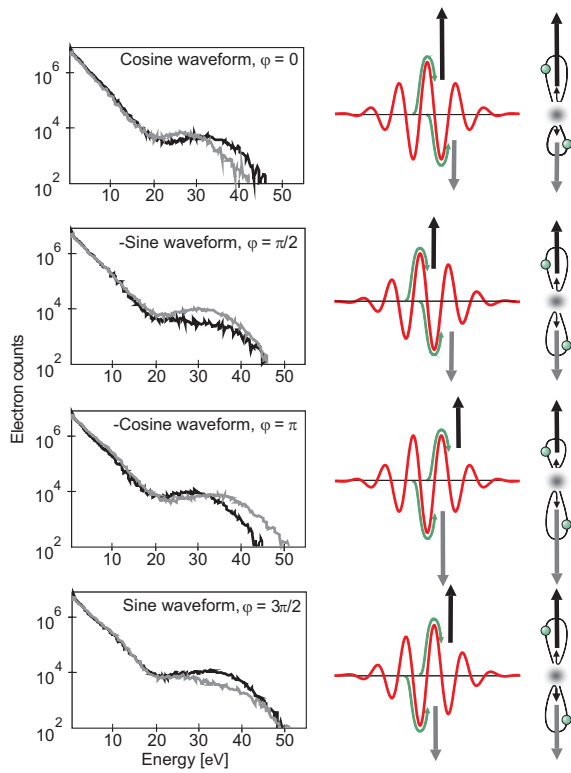


FIG. 24. (Color) Sensitivity of backscattered electrons to the CE phase. Left panels, energy distribution of ATI electrons emitted parallel to the electric field vector of the few-cycle ionizing field ($\tau_L=5$ fs, $\lambda_L=750$ nm) towards the right and left detectors of Fig. 19, shown in black and gray colors, respectively. Adapted from Paulus *et al.*, 2003. The high energy shoulders originate from backscattering upon recollision. The highest-energy electrons are emitted for a “cosine-shaped” light waveform. Note that while the maximum electron energy is the same in both directions for a “sine-shaped” wave, the yield of electrons scattered to opposite directions (with energies above 20 eV) differ significantly (by a factor of more than 2) owing to the difference in the field strengths at the moment of ionization. As a result, the method also permits single-shot determination of the CE phase even for the symmetric case of a sine waveform, which was demonstrated experimentally (Wittmann *et al.*, 2008). The calibration of the stereo-ATI “phase meter” can be subjected to a self-consistency check by shifting the CE phase in a known way, by simply changing the path length in a thin glass plate; see Eq. (7).

values of the vector potential at the moment of ionization and the moment of recollision.⁴³

In a few-cycle laser field the final energy and the number of the highest-energy backscattered electrons is a sensitive probe of the subcycle field evolution. Owing to this sensitivity and the intuitive insight provided by a

⁴³If the recollision occurs near the zero of the electric field, i.e., when $|A_L(t_r)| \approx E_0/\omega_L$ see [Eq. (12)], the final energy after backscattering may reach values of up to $10U_p$. Detailed analysis can be found in Walker *et al.*, 1996 and Goreslavski and Popruzhenko, 1999. For earlier references, see, Corkum, 1993; Schafer *et al.*, 1993; Yang *et al.*, 1993.

simple “billiard-ball” model⁴⁴ into the underlying physical process, backscattered electrons constitute a reliable tool for determining the CE phase. Simultaneous detection of electrons ejected in both directions along the laser polarization offers robustness against laser amplitude noise. This “stereo-ATI” detection scheme was invented by Paulus (Paulus *et al.*, 2001) and subsequently used for the first unambiguous determination of the CE phase of few-cycle light (Paulus *et al.*, 2003; Milošević *et al.*, 2006); see Fig. 24. Recently, it also permitted single-shot measurement of the CE phase (Wittmann *et al.*, 2008). The stereo-ATI technique is about to become a standard diagnostic tool in attosecond laboratories—an elegant example of how fundamental physics provides a practical tool for laser engineers.⁴⁵

2. Inelastic scattering: Multiple electron emission and inner-shell excitation

Electron recollision does not have to be elastic. The recollision electron acts like an antenna (Kuchiev, 1987), which an atom extends into the laser field to absorb energy. The energy of the recolliding electron can (sometimes dramatically) exceed the binding energy of valence electrons. As a consequence, the recolliding electron may knock off a second electron from the electronic shell of the parent ion.

Efficient double ionization of noble gas atoms in infrared laser fields was first observed by L’Huillier *et al.* (1983). Recent experiments, in particular those using elliptically polarized light or correlated detection of both electrons, have established recollision as the origin of this process, now referred to as nonsequential double ionization (NSDI; Fittinghoff *et al.*, 1992; Walker *et al.*, 1993, 1994).⁴⁶ The elliptical field tends to deflect the returning electron wave packet from its target. The transverse velocity, induced by the transverse component of the field, is, in the limit of a slowly varying envelope, see Eq. (12),

$$v_{\perp}(t) = A_{\perp}(t) - A_{\perp}(t_0) \approx \frac{E_{\perp}}{\omega_L} f(t) \cos(\omega_L t + \varphi) - \frac{E_{\perp}}{\omega_L} f(t_0) \cos \phi_0, \quad (30)$$

where $E_{\perp} = \epsilon E_0$ and ϵ is the field ellipticity. When the resultant transverse drift exceeds $v_{\perp,\text{spr}}$ given by Eq.

⁴⁴This is a reasonable approximation for energetic backscattered electrons, which spend little time near the core.

⁴⁵Solid-state phase meters are also being developed: Apolonski *et al.*, 2004; Fortier *et al.*, 2004; Mücke *et al.*, 2004; Irvine *et al.*, 2006; Van Vlack and Hughes, 2007.

⁴⁶Correlated measurement for the spectra of both electrons yields insight into the collision dynamics. See Becker and Faisal, 2005; furthermore, Moshammer *et al.*, 2000; Weber *et al.*, 2000a, 2000b; Rottke *et al.*, 2002; Weckenbrock *et al.*, 2003, 2004; Eremina *et al.*, 2003, 2004; Alnaser, Tong, *et al.*, 2004; Alnaser, Voss, *et al.*, 2004; de Jesus *et al.*, 2004; Rudenko *et al.*, 2004; Zeidler *et al.*, 2005; Zrost *et al.*, 2006. Recent work includes Figueira de Morisson Faria *et al.*, 2006; Ruiz *et al.*, 2006; Ho and Eberly, 2007.

(18), the returning electron misses the parent ion. Dietrich *et al.* (1994) demonstrated that increasing ellipticity gradually suppressed both HHG and NSDI in the same way, providing conclusive evidence for electron recollision being responsible for both phenomena. Recently, NSDI was also found to be controllable with the waveform of a few-cycle pulse.

Attosecond control over the recollision (Zeidler *et al.*, 2005) provides a unique opportunity for unraveling multielectron interactions and dynamics triggered by collisions (Rudenko *et al.*, 2004; Zrost *et al.*, 2006). Inelastic recollision in a molecule may induce structural dynamics in the molecular ion (see, e.g., Niikura *et al.*, 2002; Niikura, Légaré, *et al.*, 2003; Liu *et al.*, 2004; Kling *et al.*, 2006; Gräfe and Ivanov, 2007; Tong and Lin, 2007a, 2007b), for further discussion, see Sec. VII.

V. BASIC CONCEPTS FOR ATTOSECOND CONTROL AND METROLOGY

A. Conditions for experimental implementation

The atomic-scale electron dynamics discussed in the previous section unfold within the wave cycle. They are extraordinarily sensitive to the subcycle evolution of the field. Relatively small changes in the driving light waveform [see Fig. 10(b)] affect the energy distribution of high-energy photons (Fig. 23) and electrons (Fig. 24) originating from the strong-field interaction. This indicates two possible approaches to precision attosecond metrology.

For multicycle waves of laser light and attosecond pulse trains, one has to make sure that the subcycle electron-light interaction is repeated over several or many oscillation cycles under precisely the same conditions. Then, and only then, no information is lost due to the accumulation of attosecond signals originating from individual cycles during the multicycle interaction period. Multicycle attosecond metrology can draw either on periodically repeated recollisions or on sub-fs photon pulse trains emerging from them. In the former case, the multicycle light wave generates the recollision electron and triggers the process under study in a correlated fashion in one and the same interaction within each wave cycle. Then one of the two correlated processes can serve as a clock for the other. The concept, first demonstrated by Niikura *et al.* (2002) and Niikura, Legaré, *et al.* (2003) for a diatomic molecule, relies on exploiting such correlations in the time domain.⁴⁷

Ideally, this technique would require a light pulse with a constant amplitude (i.e., flat-top intensity profile) to make sure that both the processes under study as well as the reference process used as a clock unfold in the same

way in each wave cycle.⁴⁸ Similar requirements hold when a train of sub-fs pulses, with adjacent bursts spaced by a half (or a full) cycle of the generating laser field, are used in conjunction with its multicycle driver. Ideally, a constant-amplitude light wave would be required to produce a PHz train of *identical* sub-fs pulses. Even with this in place, metrology would have to be restricted to processes terminating within the laser wave cycle to avoid multiple start and exposure while the process is under way. Realistic multicycle drivers have bell-shaped envelopes; consequently, the attosecond pulse trains produced by them have burst parameters varying significantly across the train. Complicated temporal profiles resulting even from simple processes triggered by these trains are rather difficult to retrieve, making high demand on the S/N ratio.⁴⁹

These shortcomings can be overcome using few-cycle attosecond technology, which draws on a light wave consisting of easily distinguishable⁵⁰ oscillation cycles with well-controlled temporal evolution. This permits triggering of a microscopic process within any selected wave cycle with subcycle precision. Thus the process can be initiated with attosecond timing precision with respect to an entire light wave, rather than only to one of many possible cycles. An excellent example is a single sub-fs photon or electron pulse that can be generated with attosecond timing with respect to the generating few-cycle light wave. Subsequently it can be used either (i) for initiating motion with attosecond timing with respect to an extended light wave or (ii) for probing the motion that was triggered and steered by waveform-controlled light on subcycle as well as multicycle time scales.

In both scenarios, timing relative to the whole light waveform is critical for controlling and observing atomic-scale electronic motion. From the control perspective, it allows one to trigger the motion with attosecond accuracy with respect to the steering light force. From the measurement perspective, it enables a few-cycle light pulse to probe the triggered motion on both attosecond and, if needed, longer time scales.

B. Light waveform control

Energetic photon and electron emission from few-cycle-ionized atoms (Figs. 23 and 24, respectively) as

⁴⁷Essentially the same concept underlies the core-hole-clock technique used for studying ultrafast (sub-fs to several femtoseconds) dynamics with the core hole decay serving as a clock. See Brühwiler *et al.*, 2002; Brena *et al.*, 2004; Föhlisch *et al.*, 2005; Nordlund *et al.*, 2007.

⁴⁸It is challenging to produce a light wave with a rectangular temporal intensity profile (it would require the same bandwidth as that of a few-cycle pulse). Instead of using such a pulse, Niikura *et al.* (2002) were able to fulfill this condition by exploiting high-order nonlinearity involved in triggering the process: it confined the interaction to the central portion of the multicycle pulse, where the amplitude was nearly constant.

⁴⁹Other than CRAB, see Sec. V.D.4, adiabatic phase expansion (Varjú *et al.*, 2005) and two-color probing (Huo, Zeng, Leng, *et al.*, 2005) have been proposed for this purpose.

⁵⁰The cycles may be distinguished due to significant differences in either their period or their amplitude. Both options require a superposition of light frequencies covering about an octave or more.

well as terahertz emission from the emerging plasma (Kress, 2006; Gildenburg and Vvedenskii, 2007) carries direct information about the CE phase. With this parameter, the waveform is uniquely determined. Controlling of the shape of light waveforms is a first manifestation of attosecond control and metrology.

The stereo-ATI technique offers the highest control precision: it allows the CE phase to be determined with an accuracy of 100 mrad for a 6-fs, 750-nm laser pulse, implying a timing accuracy of the field oscillations cycles with respect to the pulse peak of approximately 40 as (Paulus *et al.*, 2005).⁵¹ Forty attoseconds before or after the pulse peak the (cycle-averaged) intensity is reduced by merely $\approx 0.01\%$ with respect to its value on the pulse peak in a 6 fs pulse. This extraordinary sensitivity is a direct consequence of the highly nonlinear atomic response to the field. Recently, this sensitivity could be further improved by single-shot measurements (Wittmann *et al.*, 2008). Few-cycle-driven HHG opened another route to on-line monitoring of the CE phase (Cavalieri, Goulielmakis, *et al.*, 2007; Haworth *et al.*, 2007).⁵²

Measurements often require signal accumulation over many laser shots. This prompts an important question regarding the robustness of the few-cycle waveforms generated. The degree of stabilization of the CE phase in the laser oscillator meanwhile reached the level of accuracy of its measurement (Fuji *et al.*, 2005). Delivery of few-cycle pulses with undistorted shape requires control of optical delay to within 1–2 fs over a spectral band of several hundred terahertz. Dispersion in optical components introduces delay differences of several or more picoseconds over this band. The required dispersion control with an accuracy of 10^{-3} or better over more than 100 THz of optical bandwidth can be afforded by chirped multilayer mirrors (Szipöcs *et al.*, 1994; Stingl *et al.*, 1995; Jung *et al.*, 1997), with their programmable counterparts: acousto-optic filters (Tournois, 1997; Kaplan and Tournois, 2004), with frequency-domain modulators (Zeek *et al.*, 1999; Yamane *et al.*, 2003; Yamashita *et al.*, 2006), or with their combinations (Baltuška *et al.*, 2002a, 2002b, 2002c). Preserving a selected waveform on target is even more challenging, given that a path length change by several microns through optical components shifts the CE phase considerably. Active compensation of CE phase drifts is therefore indispensable (Baltuška, Udem, *et al.*, 2003). The standard f - $2f$ interference technique, which was used for stabilizing the frequency comb of oscillators (Apolonski *et al.*, 2000; Holzwarth *et al.*, 2000; Jones *et al.*, 2000), is unable to accurately monitor extracavity CE phase drifts⁵³ (Dombi *et al.*, 2004; Paulus *et al.*, 2005). Precision high-field waveform syn-

thesis relies on CE phase metrology based on strong-field interactions discussed above.

There is yet another effect that requires attention: the wave front of a continuous-wave laser beam delivered in the fundamental (Gaussian) mode of a stable laser resonator (Siegmans, 1986) advances by a phase $\phi(z) = -\arctan(z/z_R)$ with respect to a plane wave carried at the same wavelength (Gouy, 1890) as the wave propagates through the focal region. Here $z_R = \pi w_0^2/\lambda_L$ denotes the Rayleigh distance and w_0 the beam radius in the focal plane. In a pulse, the Gouy effect shifts the CE phase as it propagates through the focal region. Within the Rayleigh range, the resultant shift was found to be a linear function of distance from the position ($z=0$) of the beam waist, $\Delta\varphi_{\text{Gouy}}(z) \approx (\pi/2)z/z_R$ (Fig. 25, Lindner *et al.*, 2004).⁵⁴ Within an interaction length of L , the CE phase gets shifted by $\Delta\varphi_{\text{Gouy}}(z=L)$ in addition to the dispersion-induced shift $\Delta\varphi(L)$, given by Eq. (7); hence constant waveform requires

$$|\Delta\varphi(L) + \Delta\varphi_{\text{Gouy}}(L)| \ll 1. \quad (31)$$

C. Attosecond metrology using nonlinear XUV optics

Conceptually, the most straightforward approach to characterizing a short pulse is to use the pulse to measure itself, e.g., using autocorrelation as discussed in Sec. II.B.1. In the case of an XUV pulse, this would require a suitable XUV nonlinearity (Kobayashi *et al.*, 2007). In the XUV or soft x-ray regime, multiphoton resonant absorption or ionization provides options for implementing nonlinear autocorrelation. For XUV photon energies less than the atomic ionization potential, measurement of the two-photon ionization yield as a function of delay between two replicas of the XUV pulse resulted in the second-order autocorrelation of this pulse (Kobayashi *et al.*, 1998; Sekikawa *et al.*, 2002). Recently this technique has been used to measure trains of sub-fs pulses via cycle-averaged (intensity) autocorrelation (Tzallas *et al.*, 2003, 2005; Nikolopoulos *et al.*, 2005) as well as the fringe-resolved (interferometric) autocorrelation (Nabekawa *et al.*, 2006). Detecting doubly charged (instead of singly charged) helium extended the photon energy range of the technique to ~ 79 eV (Nabekawa *et al.*, 2005).

Watanabe and co-workers recently succeeded in overcoming this limitation by realizing two-photon above-threshold ionization (ATI) and detecting photoelectrons instead of ions (Miyamoto *et al.*, 2004; Hasegawa *et al.*, 2005). They demonstrated the first autocorrelation and FROG measurement of a single, sub-fs pulse (Sekikawa *et al.*, 2004; Kosuge *et al.*, 2006). Unfortunately, the relevant two-photon cross sections become prohibitively low toward shorter wavelengths (Nikolopoulos and

⁵¹For a theoretical analysis, see Zhang *et al.*, 2007.

⁵²Recently, Wu and Yang (2007) pointed out that bound-state dynamics at weak fields may be affected by the C-E phase and hence can possibly be used for its measurement.

⁵³Even though it is currently widely used for this purpose.

⁵⁴Note that $\Delta\varphi_{\text{Gouy}}(z)$ is different from $\phi(z)$ both in sign and slightly in magnitude, owing to the broad bandwidth and non-Gaussian beam profile of the few-cycle wave used (Lindner *et al.*, 2004).

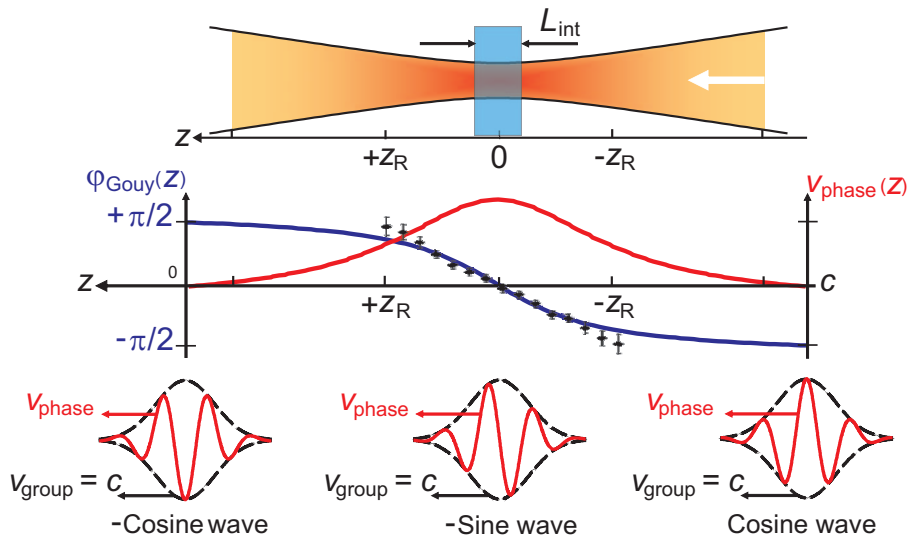


FIG. 25. (Color) Few-cycle pulse propagation through the beam focus. The pulse envelope propagates at the group velocity, which in vacuum equals the speed of light, $v_{\text{group}} = c$. The carrier wave suffers a phase advance due to the Gouy effect. As a consequence, it rushes on ahead of the envelope as the pulse propagates through the beam focus. Propagation from the far field to the focus and from the focus to the far field causes a Gouy phase shift of $\pi/2$ each, turning a “cosine”-shaped waveform into a “–sine”-shaped one at the beam waist and to a “–cosine”-shaped waveform in the far field behind focus. Courtesy of G. Paulus.

Lambropoulos, 2001), preventing straightforward extension of this metrology toward SXR frequencies.⁵⁵

D. Light-field-controlled attosecond metrology

Two ways were found out of this corner. In one class of experiments a train of attosecond pulses was characterized by measuring the relative phase between the high-order harmonics comprising the train (Paul *et al.*, 2001; Aseyev *et al.*, 2003; Mairesse *et al.*, 2003; López-Martens *et al.*, 2005). The technique was dubbed RABBITT.⁵⁶ In the other class, a single sub-fs pulse was measured by attosecond streaking (Drescher *et al.*, 2001; Hentschel *et al.*, 2001; Kienberger *et al.*, 2004). These two apparently different approaches have common roots, as we show in this section.

From an experimental point of view, both techniques draw on cross correlation between the sub-fs pulse (or pulse train; henceforth, briefly, pulse) and a femtosecond laser pulse. The interaction medium is a gas of atoms from which the XUV pulse ejects photoelectrons (Fig.

⁵⁵Novel techniques based on relativistic interactions addressed in Sec. VI.B may lead to femto- and attosecond x-ray pulses intense enough for nonlinear x-ray optics and x-ray-pump or x-ray-probe spectroscopy (Schweigert and Mukamel, 2007).

⁵⁶The reconstruction of attosecond beating by interference of two-photon transitions. Together with its more advanced versions, developed by Salieres and co-workers and L’Huillier and co-workers, this technique has been used for characterizing and optimizing attosecond pulse trains in a number of experiments, e.g., Aseyev *et al.*, 2003; Dinu *et al.*, 2003; Mairesse *et al.*, 2003, 2004; López-Martens *et al.*, 2005; for recent reviews, see Agostini and DiMauro, 2004; Corkum and Krausz, 2007; Goulielmakis *et al.*, 2007.

26) in the presence of the strong laser field. Because the same laser field was previously used for generation of the sub-fs XUV pulse, the two fields are inherently synchronized. In the absence of resonances, the temporal profile of the XUV-induced photoemission rate follows the intensity profile $|\alpha_X(t)|^2$ of the incident XUV pulse. The laser field modulates the final electron momentum and energy distribution. Measuring the modulated electron spectra as a function of the time delay between the XUV pulse and the laser pulse contains all information required for complete retrieval of both the laser field and the XUV pulse (Mairesse and Quéré, 2005; Quéré *et al.*, 2005). In contrast to autocorrelation, the technique

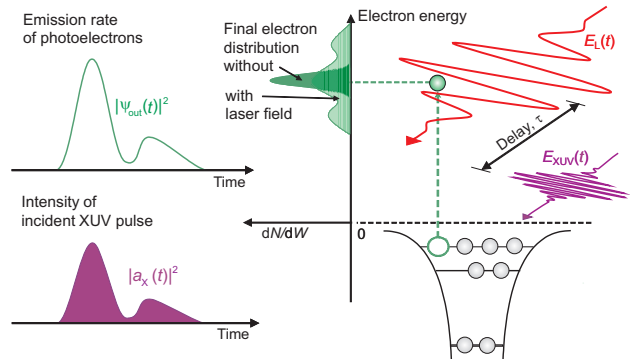


FIG. 26. (Color) Concept of light-field-controlled attosecond metrology. An ultrashort XUV pulse creates—in the presence of a strong laser field—a photoelectron, the temporal emission profile of which replicates that of the XUV pulse. The laser field modifies the final energy distribution of ejected photoelectrons. Measurement of this modification, as a function of delay between the XUV pulse and the laser field, offers the potential for sampling both processes (the XUV intensity and the laser field) with attosecond resolution.

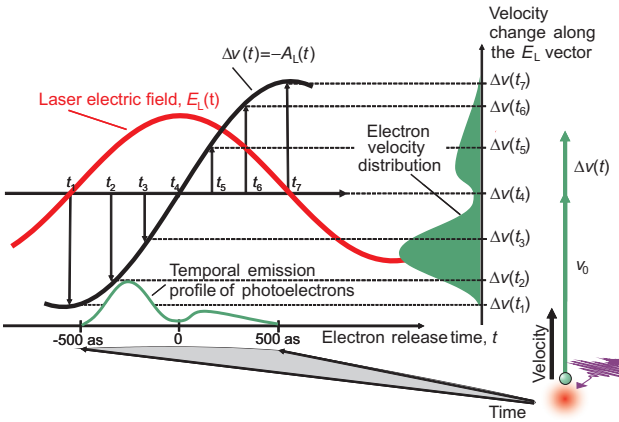


FIG. 27. (Color) Concept of optical-field-driven attosecond streaking. Photoelectrons released in a laser field parallel to the direction of electric field (red line) suffer a change of their initial velocities that is proportional to the vector potential of the field (black line) at the instant of release. This function is monotonic within a half wave cycle of the field, mapping the intensity profile of a sub-fs XUV pulse into a corresponding final velocity (or energy) distribution of photoelectrons.

can easily be scaled to shorter wavelengths, because the strong laser field obviates the need for an intense short-wavelength pulse.

A quantum analysis of XUV photoionization in the presence of the laser field reveals common grounds of this versatile attosecond metrology: the oscillating field of the laser acts as an attosecond phase gate, or phase modulator, on the electron wave packet released by the sub-fs pulse.⁵⁷ We show in this section how the generic concept of electron phase modulation, in specific circumstances, allows streaking, shearing, and spectral interferometry of the sub-fs electron wave packet and thereby leads (in a natural way) to the extension of streak imaging (Bradley *et al.*, 1971; Schelev *et al.*, 1971), FROG (Kane and Trebino, 1993; Trebino and Kane, 1993), SPIDER (Iaconis and Walmsley, 1998), and tomographic methods (Beck *et al.*, 1993; Walmsley and Wong, 1996) into the attosecond regime. The ultimate light-based ultrafast metrology, drawing on the oscillating light field as a gate, therefore naturally unifies apparently very different measurement concepts of time-resolved science.

1. Attosecond streak imaging

We time the strong laser field such that the XUV pulse fits within the time window of the central half cycle of the laser electric field, as shown in Fig. 27. The laser field is supposed to be weak enough not to ionize atoms, but strong enough to impart substantial momentum to the photoelectrons liberated by the XUV pulse (what is meant by “substantial” is discussed at the end of

this section). We assume that the photoelectron is released with large initial kinetic energy,

$$W_0 = v_0^2/2 = \Omega_X - I_p \gg I_p, \quad (32)$$

where Ω_X is the carrier frequency of the incident XUV pulse

$$E_X(t) = a_X(t)e^{-i\Omega_X t} + \text{c.c.} \quad (33)$$

As a consequence, the electron quickly leaves the atom; therefore neglect of the Coulomb potential after the absorption of the energetic XUV photon is a reasonable approximation. The final velocity of an electron ejected at the moment t with initial velocity v_0 is $v_f = v_0 - \mathbf{e}_x A_L(t)$ [see Eq. (11)], where the laser field is linearly polarized along the x direction, with \mathbf{e}_x the corresponding unit vector. The change in the electron’s velocity along the x direction is

$$\Delta v(t) = -A_L(t). \quad (34)$$

Within any half cycle between negative and positive maxima, $A_L(t)$ is a monotonic function of time (see Fig. 27). Consequently, the temporal distribution of the outgoing electron wave packet, which traces the temporal profile of the sub-fs XUV pulse, is mapped one to one onto a corresponding final velocity distribution of photoelectrons (Fig. 27). The resultant streak image provides direct time-domain information on the electron wave packet’s emission time and hence the duration of the XUV pulse (Drescher *et al.*, 2001; Itatani *et al.*, 2002; Kitzler *et al.*, 2002).⁵⁸

When contrasting this optical-field-driven “streak camera” with its microwave-driven predecessor (Fig. 3), the vastly increased streaking speed is most striking. However, there is a more profound difference. In contrast with its predecessor, here the streaking field is virtually jitter-free and acts directly at the location and instant of electron emission, preventing the initial velocity spread from impeding resolution as it does in conventional streak cameras. Moreover, the initial velocity (momentum) distribution can be measured together with the temporal emission profile, yielding information on the duration and chirp of the XUV pulse, as explained with the example of a linearly chirped XUV pulse in Fig. 28.

The optical-field-driven streak camera offers more degrees of freedom. One may observe electrons at an angle to the laser polarization. Assuming $|v_0| > |A_L|$, one obtains

$$\begin{aligned} \frac{v_f^2}{2} &= \frac{v_0^2}{2} + \frac{A_L^2(t)}{2} \cos 2\theta - A_L(t) \cos \theta \sqrt{v_0^2 - A_L^2(t) \sin^2 \theta} \\ &\approx W_0 + 2U_p(t) \cos 2\theta \sin^2(\omega_L t + \varphi) \\ &\quad + \alpha \sqrt{8W_0 U_p(t)} \cos \theta \sin(\omega_L t + \varphi), \end{aligned}$$

⁵⁷Here the field acts upon a freed electron. Zheltikov (2006b) showed that it can also probe bound-state dynamics.

⁵⁸For recent theoretical advances, see Kazansky and Kabachnik, 2006, 2007a; and Yudin *et al.*, 2007.

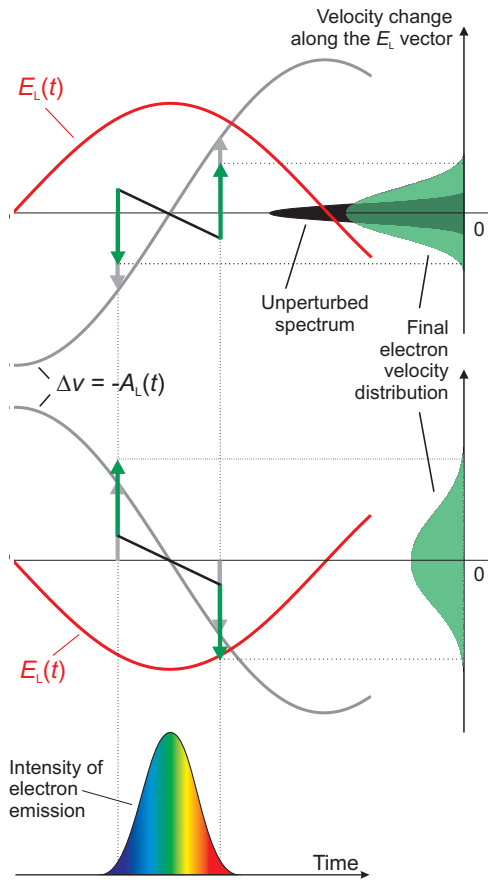


FIG. 28. (Color) Attosecond streak imaging of sub-fs pulses carrying lowest-order (linear) chirp. The linear chirp causes a linear sweep of initial photoelectron velocities. The laser field also sweeps the electron velocity, the sign and strength of which depends on the timing of the streaking field. During the positive half cycle of $E_L(t)$, see top panel, the two sweeps counteract each other, reducing the final width of the streaked spectrum as compared to the one expected for a Fourier-limited XUV pulse of identical bandwidth. In an adjacent half cycle [$E_L(t) < 0$] the sweeps add, enhancing the broadening of the “streak image,” as shown in the lower panel. Thus comparison of streak images recorded with vector potentials of different slopes at the instant of release yields not only the duration but also the chirp of a sub-fs pulse.

$$\alpha = \sqrt{1 - [2U_p(t)/W_0]\sin^2 \theta \sin^2(\omega_L t + \varphi)} \quad (35)$$

(Drescher *et al.*, 2001; Itatani *et al.*, 2002; Quéré *et al.*, 2005). The observation angle θ is the angle the final velocity makes with the x direction and the approximate expression is valid in the limit of a slowly varying envelope; see Eq. (12). This expression allows us to select the optimum detection geometry for various applications.

Observation of electrons along the laser polarization direction is referred to as *parallel detection geometry*, $\theta \approx 0$; see Fig. 29(a). In the case of $W_0 \gg U_p$, this geometry offers the largest streaking owing to the third term in Eq. (35) and the advantage of direct correspondence of the streak image with the wave packet’s temporal profile for a near-transform-limited pulse; see Fig. 27. These benefits come in combination with the possibility of a

large collection angle. In fact, $\cos \theta$ does not change much within a detection cone as large as $\pm 30^\circ$. The disadvantage of this geometry is that the laser-induced energy shift ΔW depends on the initial electron energy. This dependence becomes significant if the bandwidth of the electron wave packet is comparable to its mean energy. For this case, the *perpendicular detection geometry*, $\theta \approx \pi/2$, shown in Fig. 29(b) may be more advantageous, because the third term in Eq. (35) vanishes, and with it the dependence of streaking on the initial energy.

Attosecond streaking maps the temporal profile of a sub-fs pulse to a distribution of final electron energies. Hence the resolution limit Δt , indicating the duration of the shortest pulse that can be measured, is dictated by the condition that the laser-field-induced change in the electron energy should be comparable to the initial energy spread of the wave packet given by the ionizing XUV pulse. For the most favorable conditions, in the parallel detection geometry near the peak of the laser field, these considerations yield

$$\Delta t \sim 1/\sqrt{\omega_L \Delta W_{\max}}, \quad (36)$$

where $\Delta W_{\max} = v_0 E_0 / \omega_L$ is the maximum energy shift induced by the streaking field at t_1 and t_3 in Fig. 29(a) (Kienberger *et al.*, 2004). This is an order-of-magnitude estimate. As always, with good S/N this resolution limit can be improved (Smirnova *et al.*, 2005; Yakovlev *et al.*, 2005; Goulielmakis *et al.*, 2008).

2. Quantum analysis: The light field as an electron phase modulator

We now address the quantum treatment of photoionization in the presence of an intense laser field (Itatani *et al.*, 2002; Kitzler *et al.*, 2002). This will allow us to look at laser-affected photoelectron spectra from various perspectives, unifying all advanced measurement and reconstruction approaches of modern ultrafast metrology: streak imaging, frequency-resolved optical gating, spectral shearing interferometry, and tomographic techniques.

Consider the bound wave function of our atom $\psi_g = \phi_g(\mathbf{r}) \exp(-iW_g t) = \phi_g(\mathbf{r}) \exp(iI_p t)$. In the absence of the laser field, first-order perturbation theory in terms of the XUV field defined by Eq. (33) yields the amplitude of populating the state with final velocity v ,

$$a(v) = -i \int_{-T}^T \exp\left(-i \frac{1}{2} \int_t^T v^2 dt'\right) a_X(t) \times e^{-i\Omega t} d(v) \exp\left(i \int_{-T}^t I_p dt'\right) dt. \quad (37)$$

Here $d(v)$ is the transition matrix element between the ground state and the free state with momentum v (we detect only electrons ejected parallel to the laser polarization direction; thus the electron momentum can be described by a scalar variable). T is some distant moment in time, so that the XUV pulse begins past $t = -T$ and ends before $t = +T$. Performing the integrals in the

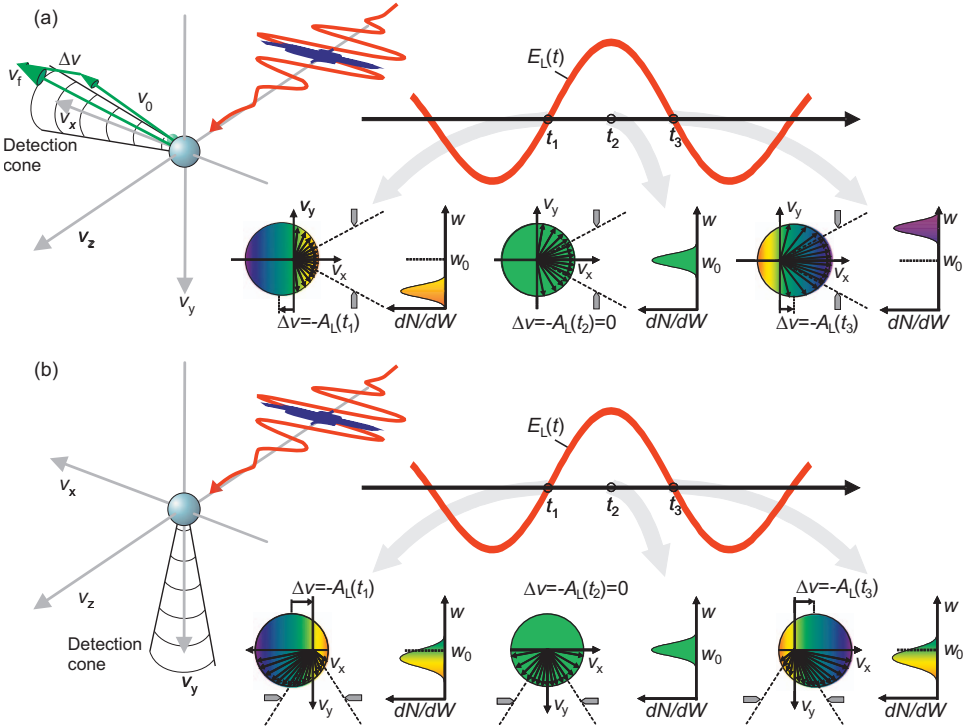


FIG. 29. (Color) Attosecond streaking: (a) parallel and (b) perpendicular detection geometries. Distribution of final electron velocities and corresponding energy distribution of electrons collected within the detection cone for three representative instants of electron release within the central half oscillations cycle of the few-cycle streaking light field. The laser-streaked electron spectra are illustrated for the hypothetical case of an XUV pulse duration much shorter than the half period of the streaking field.

exponents, using Eq. (32), dropping a constant phase factor, and letting $T \rightarrow \infty$, we obtain

$$a(v) = -i \int_{-\infty}^{\infty} \chi(v, t) e^{i(v^2/2)t} dt, \quad (38)$$

where we have introduced

$$\chi(v, t) = a_X(t) d(v) e^{-i(v_0^2/2)t}, \quad (39)$$

which plays the role of a quantum-mechanical distribution released by the XUV pulse (Yakovlev *et al.*, 2005);⁵⁹ here $v_0^2/2 = \Omega - I_p$. In Eq. (38) we recognize the Fourier transform of $\chi(v, t)$. In the absence of resonances within the band of transition energies (determined by the spectral width of the XUV pulse), $d(v)$ is a smooth function with nearly constant phase [and $|d(v)|$ is known from experiment]. Hence the complex envelope of the XUV pulse $a_X(t)$ could be determined by a simple inverse Fourier transform of $a(v)$. Unfortunately, a simple photoelectron experiment measures $|a(v)|^2$ and not $a(v)$, with the phase of the transition amplitude remaining unknown.

To retrieve the unknown phase, we switch on the streaking field. In the framework of the SFA, the ampli-

tude of populating the state with the final velocity v becomes

$$a(v) = -i \int_{-T}^T \exp\left(-i \frac{1}{2} \int_t^T [v + A_L(t')]^2 dt'\right) \times a_X(t) e^{-i\Omega_X t} d[v + A_L(t)] \times \exp\left(i \int_{-T}^t I_p dt'\right) dt, \quad (40)$$

where the first exponent in the integrand comes from the second term in Eq. (17). Assuming that the dipole matrix element is not affected much by the laser field, $d(v + A_L(t)) \approx d(v)$, and with $T \rightarrow \infty$, we can rewrite Eq. (40) in the form

$$a_A(v) = -i \int_{-\infty}^{\infty} \chi(v, t) \exp\left(-i \frac{1}{2} \int_t^T [v + A_L(t')]^2 dt'\right) dt = -i \int_{-\infty}^{\infty} \chi(v, t) e^{i\Theta(t)} e^{i(v^2/2)t} dt, \quad (41)$$

where

⁵⁹A release distribution was also derived for the Auger decay (Smirnova *et al.*, 2003), forming the basis of attosecond Auger spectroscopy (Sec. VII.C).

$$\begin{aligned}\Theta(t) &= -v \int_t^\infty A_L(t') dt' - \frac{1}{2} \int_t^\infty A_L^2(t') dt' \\ &\approx \frac{vE_0}{\omega_L^2} f(t) \cos(\omega_L t + \varphi) + \frac{E_0^2 t}{4\omega_L^2} f^2(t) \\ &\quad + \frac{E_0^2}{8\omega_L^3} f^2(t) \sin 2(\omega_L t + \varphi)\end{aligned}\quad (42)$$

with the approximation applicable if Eq. (12) is valid. According to Eq. (41), quantum mechanically the streaking laser field works as an attosecond electron phase modulator (Kosik *et al.*, 2005; Quéré *et al.*, 2005). As we show in the following sections, this fact allows us to benefit from well-established femtosecond pulse retrieval techniques in reconstructing both the XUV pulse and the streaking laser field from the measurement of a set of laser-streaked photoelectron spectra,

$$\sigma_A(v, t_0) = |a_A(v, t_0)|^2, \quad (43)$$

recorded for different values of t_0 , where t_0 is the moment of arrival of the sub-fs pulse.

We now relate this quantum treatment to the classical approach of the previous section. If the XUV pulse and hence the released electron wave packet are short compared with the laser oscillation half cycle, the phase $\Theta(t)$ can be Taylor expanded about the moment of release t_0 . If we restrict expansion to the linear term $\Theta(t) \approx \Theta_0 + (\partial\Theta/\partial t)_{t_0}(t-t_0)$ in Eq. (41), the resultant linear phase modulation shifts the spectrum of the electron wave packet and hence its mean energy by $\Delta W = W_f - W_0 = v_f^2/2 - v_0^2/2 = -\partial\Theta/\partial t$. Calculating the first derivative of $\Theta(t)$ given by Eq. (42) using the approximation $\Delta W \ll W_0 \Rightarrow v \approx v_0$ in Eq. (41) leads us back to the classical expression for the laser-induced electron energy shift as given by Eq. (35). If the XUV pulse is longer than the laser wave cycle, the electron wave packet experiences several periodic modulations of its phase, leading to energy shifts in multiples of the laser photon energy ω_L . The final photoelectron spectrum is then composed of a series of sidebands separated by multiples of ω_L from the unperturbed spectrum.⁶⁰ This spectral structure is the result of quantum-mechanical interference and cannot be accounted for by our classical model. Only sub-fs confinement of the released electron wave packet, i.e., attosecond technology, enables classical physics to account for the main features of intense light-electron interaction (Drescher and Krausz, 2005).

3. Attosecond frequency-resolved optical gating

We rewrite Eq. (41) to explicitly include the adjustable delay τ between the phase-modulating laser pulse and the XUV pulse:

⁶⁰They can be used for measuring the duration of femtosecond XUV pulses, see Schins *et al.*, 1994, 1996; Glover *et al.*, 1996; Bouhal *et al.*, 1997; Toma, *et al.*, 2000; Ge, 2006.

$$\begin{aligned}\sigma_A(v, \tau) &= |a_A(v, \tau)|^2 = \left| \int_{-\infty}^{\infty} \chi(v, t) G(t - \tau) e^{i(v^2/2)t} dt \right|^2, \\ G(t - \tau) &= e^{i\Theta(t - \tau)}.\end{aligned}\quad (44)$$

The analogy with Eq. (2) is evident. The streaked photoelectron spectrum is the gated Fourier transform of the electron release distribution $\chi(v, t)$. Here the gate is not an amplitude gate as in standard FROG techniques, but a phase gate. Due to its sub-fs gradients, it is well suited to resolving sub-fs transients. Hence $\sigma_A(v, \tau)$ can be viewed as an attosecond spectrogram and the iterative algorithms developed for complete retrieval of femtosecond pulses from FROG measurements⁶¹ can be used to extract both $\chi(v, t)$ and the phase gate $\Theta(t)$. From them, the complex amplitude of the sub-fs XUV pulse $a_X(t)$, as well as the complete evolution of the streaking electric field $E_L(t)$, can be reconstructed. The method was dubbed CRAB-FROG (briefly, CRAB).⁶² At least, in principle, it is applicable to retrieving arbitrarily complex and extended attosecond pulse structures (including trains of pulses) and femtosecond laser fields (including multicycle fields). CRAB generalizes RABBITT in that it is, in principle, capable of reconstructing not only the average characteristics of sub-fs pulses in the train, but also each individual pulse, although such a retrieval imposes increasing demands on S/N with increasing complexity of the spectrogram (see Fig. 30 for the case of a sequence of merely four XUV bursts). When implemented with a few-cycle NIR field and sub-optical-period XUV emission durations, CRAB constitutes an extremely powerful method of attosecond metrology. Due to a large redundancy of information in the spectrogram, it can, with good S/N, substantially improve the resolution given by Eq. (36).

4. Attosecond spectral shear interferometry

The attosecond FROG described in the previous section naturally leads us to the attosecond version of SPIDER. This becomes obvious by a closer glance at Figs. 30(c) and 30(d), showing streaking spectrograms of sub-fs XUV radiation composed of two identical bursts of 150 as duration spaced by the half period $T_L/2$ of the streaking field. The spectral fringes spaced by $2\omega_L \approx 3$ eV appear to be due to spectral interference between the two electron wave packets released by the two XUV replicas, which is caused by the difference in phase shift $\Delta\Theta = \Theta(t + T_L/2 - \tau) - \Theta(t - \tau)$ imposed by the streaking field upon the wave packets. At selected delays τ , the two released wave packets coincide with adjacent zero

⁶¹Such as, e.g., the principal component generalized projections algorithm, PCGPA (Kane, 1999).

⁶²Complete reconstruction of attosecond bursts via FROG (Mairesse and Quéré, 2005; Quéré *et al.*, 2005).

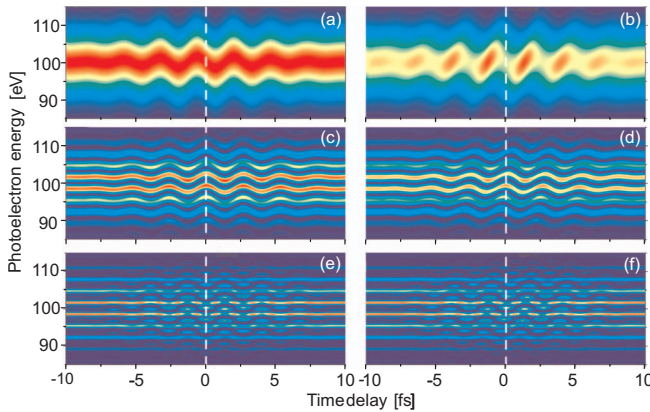


FIG. 30. (Color) Calculated attosecond streaking spectrograms. Top panels show spectrograms for (a) a single transform-limited 150-as pulse and (b) the same pulse dispersively stretched to a duration of 620 as. Middle panels show the same for two pulses separated by half the oscillation cycle of the streaking field. Bottom panels show corresponding traces for four pulses. The traces have been calculated for parallel detection geometry, see Fig. 29(a), and for a laser peak intensity of $I=5\times 10^{10}$ W/cm² at a wavelength of $\lambda_L=800$ nm. Adapted from Quere *et al.*, 2005.

transitions of the streaking field $E_L(t-\tau)$, when the vector potential passes its maximum and minimum. Recalling the relationship between the initial and final electron velocities $v_f=v_0-A_L(t_{\text{release}})$, we realize that one wave packet is shifted up in the final energy while the other is shifted down; see Fig. 31(a). Note that the streaking field strength is adjusted here to be much weaker than in the case of streak imaging (Fig. 27). Since the two replicas are also time delayed with respect to each other, SPIDER is, in principle, only a small step from here: one merely has to generate two XUV replicas from one and the same XUV pulse that we want to characterize (Cormier *et al.*, 2005). The modulated spectrum in Fig. 31(a) then becomes the perfect attosecond version of a SPIDER interferogram (Quéré *et al.*, 2003; Remetter *et al.*, 2006).

In attosecond metrology, there is a regime (Sekikawa *et al.*, 2003) where SPIDER- (Cormier *et al.*, 2005; Kosik *et al.*, 2005; Quéré *et al.*, 2005) and FROG-type characterization methods almost merge (Smirnova *et al.*, 2005; Yakovlev *et al.*, 2005). Let the original sub-fs pulse (without splitting it into two) interact with a weak streaking field. Without the streaking field, absorption of the XUV photon generates a photoelectron spectrum but the measurement is blind to the spectral phase of the photoelectron wave packet. With a perturbative streaking field present, the liberated electron can still absorb one photon from the IR field, creating an upshifted “replica” of the original photoelectron spectrum. Stimulated emission of a laser photon will create a downshifted replica. Interference of these replicas with the original spectrum transforms the spectral phase into amplitude modulation, just as in SPIDER, except that here one has to deal

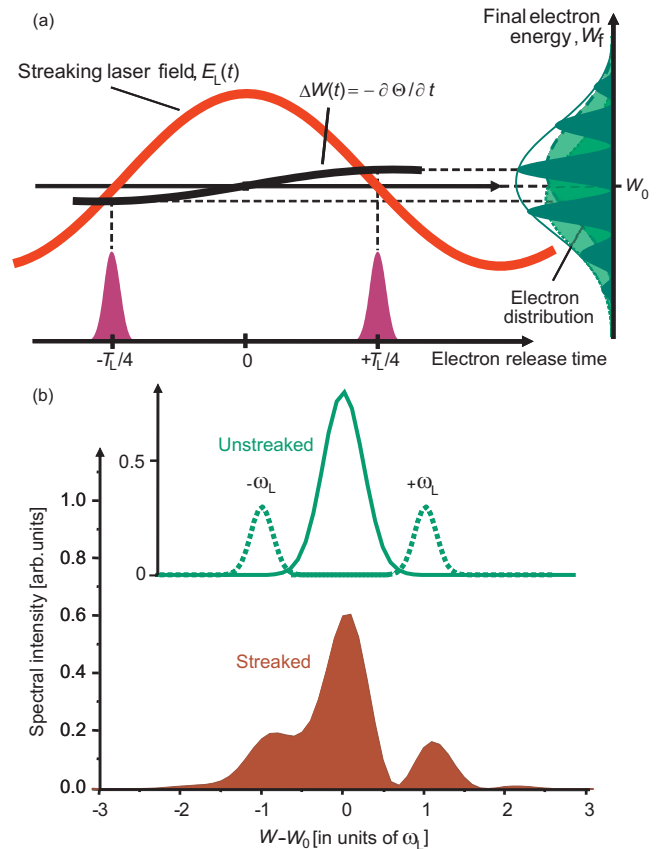


FIG. 31. (Color) SPIDER for attosecond XUV pulses. (a) SPIDER interferogram (in the form of a photoelectron energy distribution; see green area) for two delayed replicas of the XUV pulse, slightly sheared by a weak IR field (red line shows electric field of the shearing IR field). The amount of spectral shear between the two electron wave packets released by the two sub-fs XUV bursts can be adjusted by the strength of the streaking field. It is preferable that the spectral shear is small as compared to the width of the unperturbed electron energy spectrum, a demand precisely opposite to that required for the best possible resolution in streak imaging. (b) In the presence of a weak IR field, two spectral replicas of the same sub-fs XUV pulse corresponding to stimulated absorption or emission of a single photon (green dashed lines on the inset) may—together with the main (unperturbed) photoelectron spectrum—combine to SPIDER-like interferogram in the total spectrum.

with three interfering spectral shapes and not two; see Fig. 31(b).

Despite complications in experimental implementation or numerical reconstruction, attosecond SPIDER may become the method of choice for pulses approaching the atomic unit of time (24 as), because SPIDER has no fundamental resolution limit. In practice, the time resolution will be limited by the precision of controlling the energy shear, which in turn is dictated by the quality of controlling the timing of the attosecond pulse with respect to the streaking field. Beyond attosecond pulse metrology, attosecond spectral shearing interferometry may also find intriguing applications in exploring correlated multielectron processes (Smirnova *et al.*, 2005); see Sec. VII.

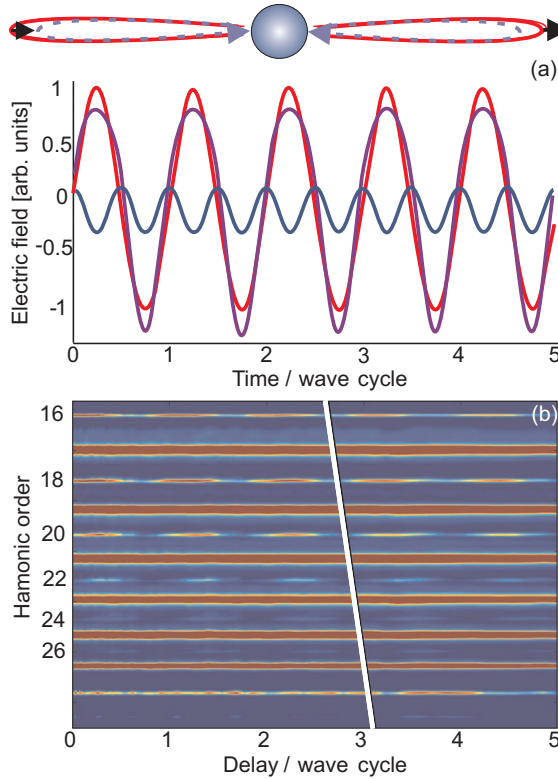


FIG. 32. (Color) Gating and control of electron recollision. (a) Adding weak second harmonic (blue solid line) to the fundamental field (red line) driving ionization and subsequent recollision breaks the symmetry between two electron trajectories starting at adjacent half cycles of the fundamental field (illustration on the top) due to a corresponding asymmetry in the total field (dashed line). This symmetry breaking yields even high-order harmonics. (b) Harmonic spectral intensity (in false-color representation) vs delay between the fundamental wave and the weak second harmonic modulating field. The white line indicates the variation of the delay which maximizes even harmonics of different order. From Dudovich, Smirnova, *et al.*, 2006.

E. Lightwave electronics at work: From measurement to control of sub-fs pulses

The quantum-mechanical description of a strong light field interacting with an electron ejected from an atom revealed that the light field modulates the phase of the outgoing electron's wave function. It is this sub-fs phase gate that light-field-controlled attosecond metrology is based upon. The electron can be released by either photoexcitation or collisional excitation. It must be timed, with sub-fs precision, to the streaking laser field, which modulates the electron's quantum phase. This requirement can be met only by optical synchronization. Therefore the “starter gun” must be derived from the streaking field. Photoemission can be linear, induced by an XUV photon pulse via single-photon absorption, or nonlinear, induced by a strong light field. Our observable can be a characteristic of the modulated electrons themselves, such as their final energy and momentum distributions (as considered in the previous section), or

the energy and momentum distributions of the photons they produce upon recollision. The observables are measured as a function of the delay of the streaking field with respect to electron release. Using a waveform-controlled few-cycle streaking field, the complete history of the motion—including attosecond-scale dynamics and (possible) slower femtosecond-scale evolution—can be retrieved.

On the basis of different combinations of triggering of the electron release and observation of their modulated quantum phase, many variations of attosecond control and metrology are conceivable. Two combinations have been demonstrated so far. One of them provides a profound insight into the atomic process responsible for sub-fs XUV pulse generation. The other one permits complete temporal characterization of the sub-fs pulse at the location where it can be used for attosecond spectroscopy. We review them in this section.

1. Modulation of recollision electrons: Measuring the creation of a sub-fs pulse

Consider the electron liberated by a strong, linearly polarized laser field and its subsequent recollision with its parent ion (Fig. 15). Light-field-controlled attosecond metrology offers a simple recipe for gaining time-domain insight into recollision: (i) modulate the electron's phase or amplitude with a weak auxiliary light field and (ii) monitor the response of the products of recollision (e.g., photon emission) to this modulation. Measuring this response versus delay of the modulating field with respect to the electron's release provides in-depth time-domain information on the dynamics of recollision and concomitant sub-fs XUV emission (Dudovich, Levesque, *et al.*, 2006; Dudovich, Smirnova, *et al.*, 2006).

In the example sketched in Fig. 32(a), a weak light field oscillating at $2\omega_L$ is added to the fundamental light of frequency ω_L that drives ionization and recollision. This introduces a small additional phase shift Θ_2 to the quantum phase Θ_1 that the electron accumulates in the fundamental field from ionization at t_0 until recollision at t_r :

$$\Theta_{1+2}(t_r, \tau) \approx \Theta_1(t_r) + \Theta_2(t_r, \tau),$$

$$\Theta_2(t_r, \tau) \approx - \int_{t_r(t_0)}^{t_0} v(t', t_r) A_2(t' - \tau) dt', \quad (45)$$

where $A_2(t - \tau) = A_2 \sin[2\omega_L(t - \tau)]$ is the vector potential of the second field and $v(t, t_r)$ is the velocity of the electron returning to the core at t_r .⁶³ Although Θ_2 is much smaller than Θ_1 , it has a large effect. Because $\Theta_2(t_r - \pi/\omega_L, \tau) = -\Theta_2(t_r, \tau)$, the weak field breaks the symme-

⁶³The total phase is given by the second term in the classical action in Eq. (17), with the vector potential $A_L(t) = A_1(t) + A_2(t)$. Expanding the square in Eq. (17) and keeping terms linear in weak second harmonic field, we obtain Eq. (45).

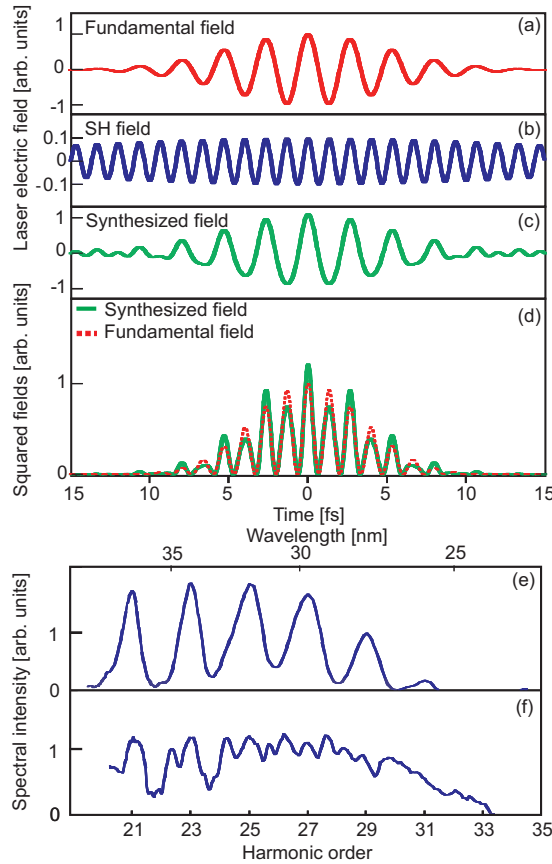


FIG. 33. (Color) A few-cycle field (c) and (d), synthesized, (a) from a fundamental wave, and (b) its second harmonic, is used to produce high-harmonic radiation with (f) a broad unmodulated continuum, for isolated sub-fs XUV pulse generation. For comparison, (e) shows the harmonic spectrum obtained with the fundamental driver field alone. From Oishi *et al.*, 2006.

try between the left and the right trajectories⁶⁴ of electrons returning to the core; see Fig. 32(a). As a result, even harmonics of ω_L appear in the harmonic spectrum, which can be measured as a function of the delay τ or equivalently of the relative phase $\phi=2\omega_L\tau$ of the modulating light with respect to the fundamental field releasing the electron wave packet; see Fig. 32(b). The measurement reveals the relative phase of the modulating field that maximizes the yield in any even harmonic: $\phi_{\max}(2N)$, see white line in Fig. 32(b). At the same time, for weak $2\omega_L$ field the relative phase $\phi_{\max}(t_r)$ maximizing Θ_2 in Eq. (45) and hence even harmonic emission at a given t_r can be reliably calculated using the SFA. Equating these (measured and calculated) quantities with each other, $\phi_{\max}(2N)=\phi_{\max}(t_r)$, maps emission frequency to emission time within the time interval of recollision, yielding the group delay versus frequency of the emitted sub-fs pulse (Dudovich, Smirnova, *et al.*, 2006).

⁶⁴We use this terminology by assuming the laser fields to be polarized horizontally.

2. Modulation of recollision electrons: Controlling the creation of a sub-fs pulse

A simple increase of the modulating field amplitude turns the previous measurement into control. By varying ϕ , the emission can be switched completely between odd and even harmonics (Dudovich, Smirnova, *et al.*, 2006). Adjusting the modulating field so that even and odd harmonics are similar in strength implies that the sub-fs pulses repeat every cycle rather than the half cycle of the fundamental (Mauritsson *et al.*, 2006).⁶⁵

If atoms are driven by a cosine-shaped few-cycle field [Fig. 33(a)], adding its second harmonic with appropriate phase [Fig. 33(b)] suppresses the half cycles neighboring the central one [Figs. 33(c) and 33(d)], confining highest-order harmonic emission to the recollision following the most intense, central half cycle. The result is a broad continuum near the cutoff, as shown in Fig. 33(f) (Oishi *et al.*, 2006).⁶⁶ Adding a weak sub-fs pulse or pulse train to the fundamental field provides yet another way of controlling HHG.⁶⁷

The trajectory of recolliding electrons can also be manipulated by adding an orthogonally polarized moderate deflecting field to the fundamental field. By creating a pulse with temporally varying ellipticity of its polarization, linear polarization can be confined to the central wave cycle of the strong driving field, confining emission from a broad range of harmonics to a single recollision at the pulse peak.⁶⁸ The technique was dubbed polarization gating. Its recent implementation with waveform-controlled few-cycle light resulted in a continuum extending over some 25 eV at photon energies near 40 eV (Sola, Mével, *et al.*, 2006; Sola, Zair, *et al.*, 2006).

Ultrafast depletion of the ground state by ionization on the leading edge of a few-cycle laser pulse (Sekikawa *et al.*, 2004)⁶⁹ and propagation effects in wave guides (Christov *et al.*, 2000) as well as in gas jets (Gaarde *et al.*, 2006) can also select a single pulse.

⁶⁵One attosecond burst per cycle may also emerge from HHG in asymmetric molecules (Lan, Lu, Cao, Li, and Wang, 2007).

⁶⁶Related work includes Watanabe *et al.*, 1994; Kim, Kim, Kim, *et al.*, 2004; Taranukhin, 2004; Zamith *et al.*, 2004; Pfeifer *et al.*, 2006a, 2006b; Fleischer and Moiseyev, 2006; Cao, Lu, Lan, Hong, and Wang *et al.*, 2007; Lan, Lu, Cao, Li, and Wang, 2007; Zeng *et al.*, 2007.

⁶⁷Bandrauk and Shon, 2002; Schafer *et al.*, 2004; Biegert *et al.*, 2006; Figueira de Morisson Faria *et al.*, 2006; Heinrich *et al.*, 2006; Chen, Li, Chi, and Yang, 2007; Figueira de Morisson Faria and Salieres, 2007.

⁶⁸Budil *et al.*, 1993; Corkum *et al.*, 1994; Ivanov *et al.*, 1995; Altucci *et al.*, 1998; Platonenko and Strelkov, 1999; Kovacev *et al.*, 2003; Tcherbakoff *et al.*, 2003; Chang, 2004; López-Martens *et al.*, 2004; Strelkov *et al.*, 2004; Zair *et al.*, 2004; Huo, Zeng, Li, and Xu, 2005; Kim *et al.*, 2005; Shan *et al.*, 2005; Strelkov *et al.*, 2005; Strelkov, 2006; Altucci *et al.*, 2007.

⁶⁹See also Bouhal *et al.*, 1997, 1998; Cao *et al.*, 2006; and Pfeifer *et al.*, 2007.

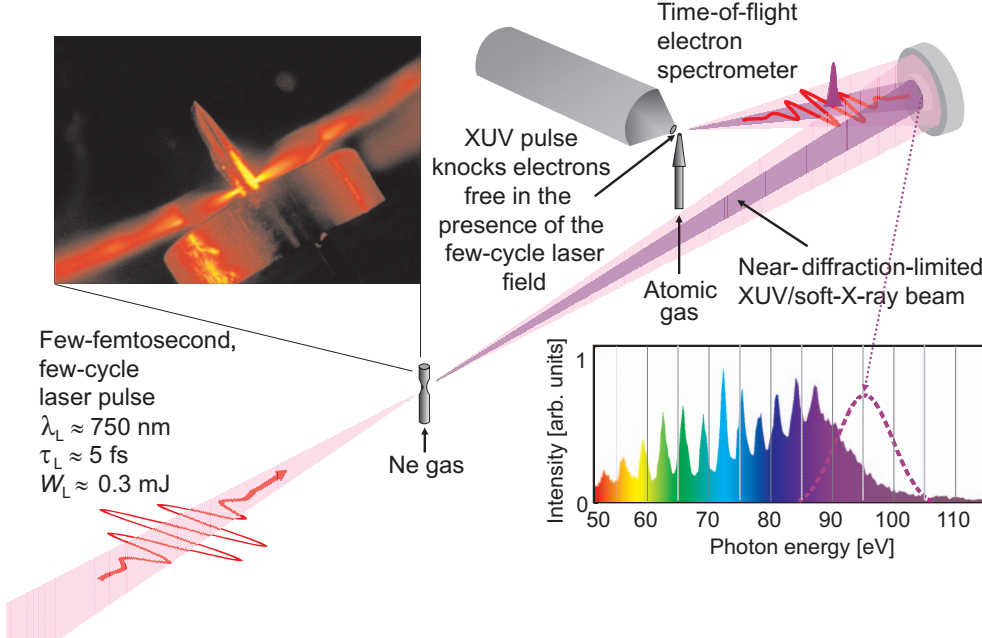


FIG. 34. (Color) Schematic of the first attosecond metrology beamline using waveform-controlled few-cycle light and isolated sub-fs XUV pulses (Vienna University of Technology).

3. Reproducible generation and measurement of single sub-fs XUV pulses

In this section we review the first experiments demonstrating the ability of controlled few-cycle light waves to control and measure subfemtosecond electronic transients. The laser pulse first generates the sub-fs pulse in a reproducible fashion (attosecond control) and subsequently samples it with sub-100-as resolution (attosec-

ond measurement). Employing the same light wave for generation and measurement ensures sub-fs synchronism between the XUV pulse and the sampling field.

Figure 34 illustrates the apparatus developed for sub-fs pulse generation and measurement at Vienna University of Technology. Figure 35 provides information on the diagnostics required for making attosecond metrology work in a second-generation beamline. In

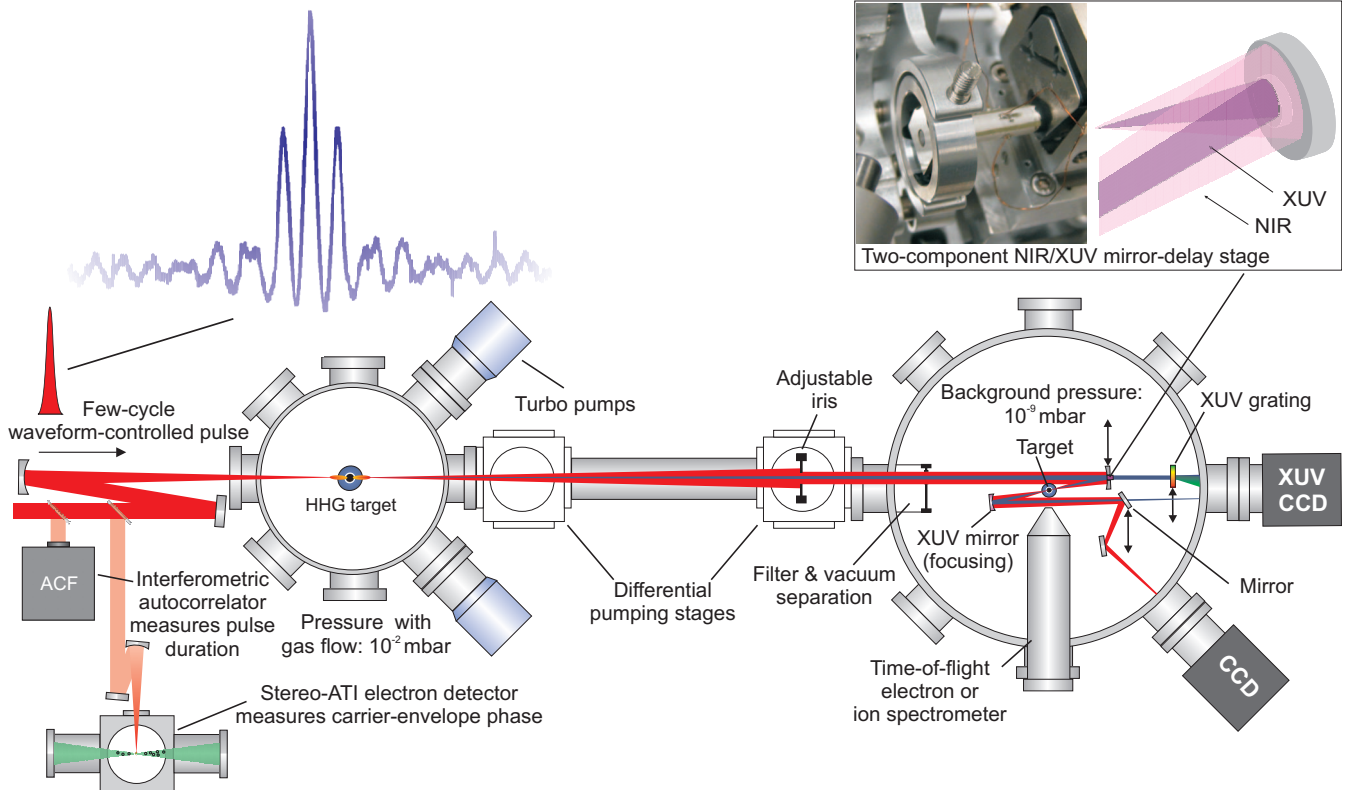


FIG. 35. (Color) Schematic of the AS-1 attosecond metrology beamline at Max Planck Institute of Quantum Optics.

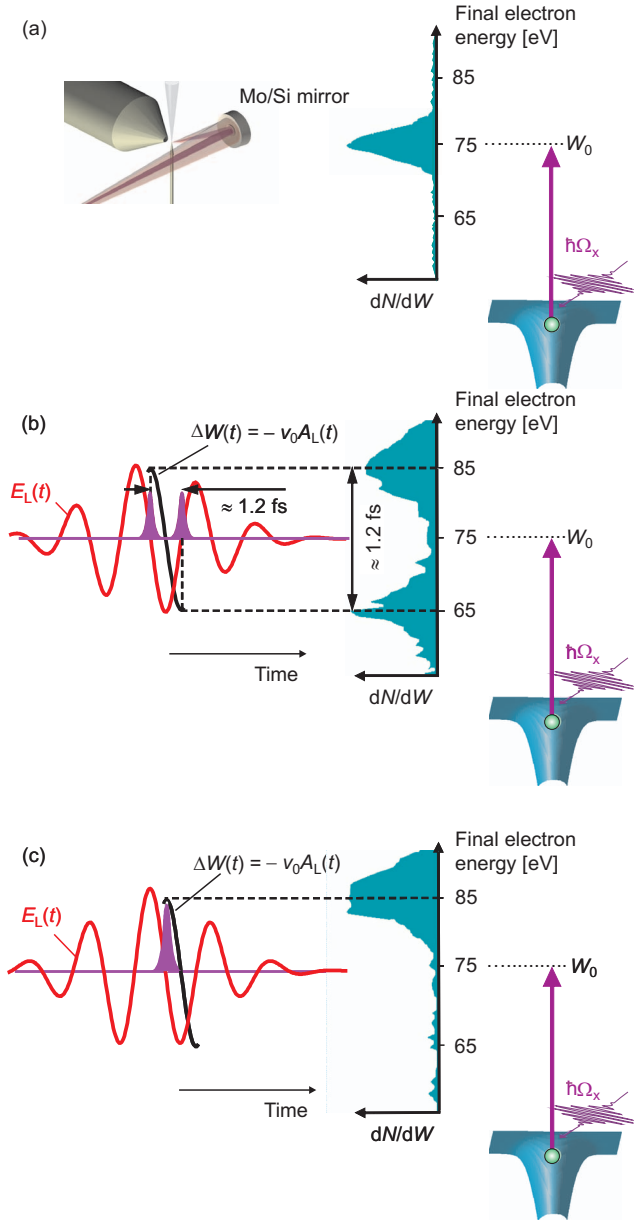


FIG. 36. (Color) Attosecond streak images of single and twin sub-fs XUV pulses. (a) In the absence of the streaking field $E_L(t)$, photoelectrons arrive at the detector with a kinetic energy equal to the XUV photon energy (~ 95 eV) minus their binding energy (~ 21.5 eV in neon). The width of their energy spread is determined by the bandwidth of the incident XUV pulse (~ 9 eV), which in turn is controlled by that of the Mo/Si mirror (dotted line in Fig. 34). (b) The streak image of twin pulses generated by a near-sinusoidal waveform allows calibration of the attosecond streak camera: 20-eV energy shift corresponds to a time interval of $T_L/2 \approx 1.2$ fs. (c) Streak image of a single sub-fs XUV pulse generated with a near-cosine waveform. No delay between the XUV pulse and its generating few-cycle wave has been introduced. The measurement yields an upper limit of 0.5 fs for the duration of the 95-eV XUV pulse and its absolute timing with respect to the generating wave: the sub-fs XUV pulse emerges near the zero transition of the laser field following the pulse peak. The laser-induced change in the electron's final energy, $\Delta W(t)$, is derived from the momentum change, $\Delta\nu(t) = -A_L(t)$, see Eq. (34) and Fig. 27, as $\Delta W(t) \approx \nu_0\Delta\nu(t) = -\nu_0A_L(t)$, by utilizing $\Delta\nu \ll \nu_0$.

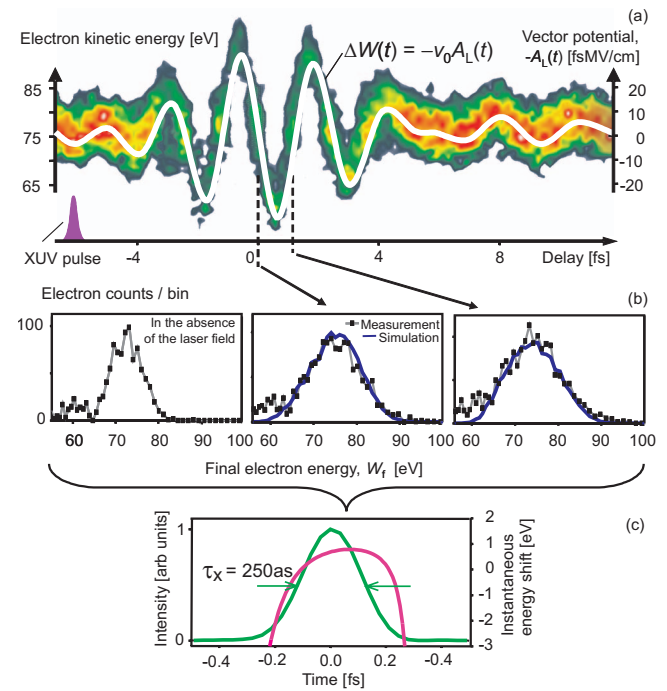


FIG. 37. (Color) Attosecond streaking spectrogram of an XUV pulse, recorded with a few-cycle streaking field. The streak images exhibit little broadening at any timing, indicating that the XUV pulse is near Fourier limited and is much shorter than $T_L/2$. As a consequence, one does not need to know its detailed structure to determine $E_L(t)$. The shift of the first moment ("center of mass") of the streaked spectra is proportional to $A_L(t)$. From the vector potential (white line) the electric field can be determined by differentiation. The result is plotted in Fig. 12. Since the XUV pulse appears to be near Fourier limited, its characteristics can be determined from a couple of streak images recorded at delays for which streaking is strongest, indicated with dashed lines in (a). As analyzed in Fig. 28, these streaked spectra (b) are very sensitive to lowest-order (linear) chirp. The absence of any measurable difference between the two streak images, see central and right panels of (b), indicate that the pulse is indeed close to its Fourier limit. Together with the unstreaked photoelectron spectrum shown on the left of (b), these images allow for complete reconstruction of the intensity profile (green line) and temporal chirp (violet line) of the sub-fs XUV pulse, as shown in (c).

these systems, few-cycle-driven high-order harmonics are generated in neon, with the peak intensity of the few-cycle driver adjusted to result in cutoff emission near 100 eV; see inset in Fig. 34. The XUV radiation, emitted in a collimated laserlike beam with a divergence much smaller than that of the focused laser beam, is passed through a metal filter blocking the laser light. The two collinear beams are reflected by a two-component Mo/Si multilayer mirror, which serves several purposes. It filters XUV photons in the ~ 90 –100 eV energy band, allows an adjustable delay to be introduced between the laser field and the XUV pulse, and focuses both beams into a second target of atoms where the XUV pulse liberates electrons in the presence of the laser field. The photoelectrons' final en-

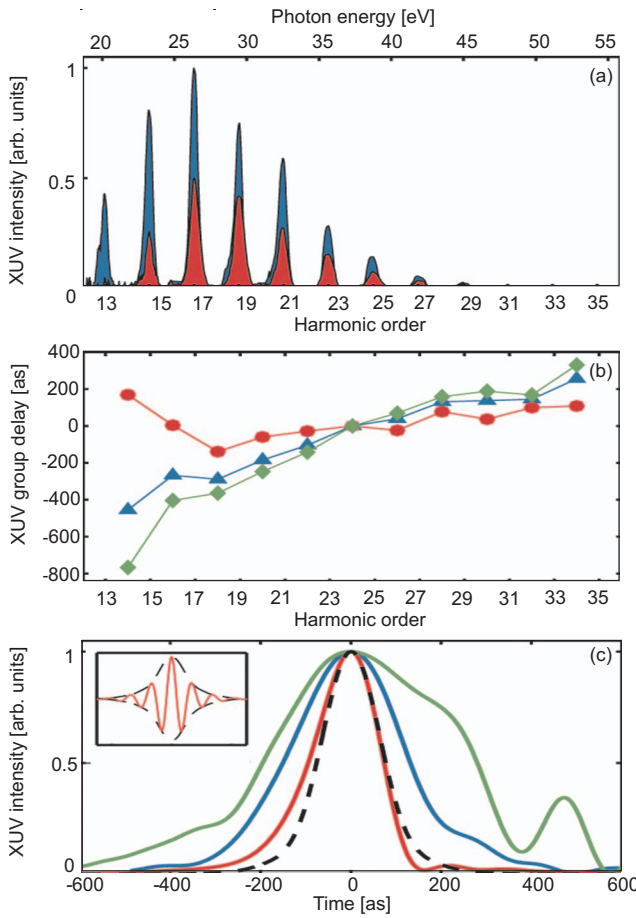


FIG. 38. (Color) Generation of trains of near-single-cycle 170-as pulses by trajectory and dispersion control (López-Martens *et al.*, 2005). (a) Emission from short trajectories, see Fig. 20, was selected by spatial filtering with an iris. (b) Measured group delay vs XUV frequency (harmonic order). The green curve was obtained without any dispersion added, indicating a positive frequency sweep, in accordance with the theoretical predictions for short trajectories; see Figs. 20 and 22. The blue and red curves were obtained with dispersion compensation via one and three 200-nm-thick aluminum filters placed in the XUV beam, respectively. (c) Corresponding temporal profiles of the transmitted XUV pulses. Courtesy of A. L’Huillier.

ergy distribution is analyzed in a time-of-flight spectrometer.

The first attosecond streaking experiment (Hentschel *et al.*, 2001) was performed using orthogonal detection geometry [Fig. 29(b)]. Although the CE phase of the few-cycle driver pulse was not stabilized, single sub-fs XUV pulses were observed in the experiment. Recently, Gaarde and co-workers have indeed found numerically that propagation effects and far-field spatial filtering can effectively isolate a single attosecond burst for a broad range of the CE phase values (Garde *et al.*, 2006; Garde and Schafer, 2006).

Figure 36 reviews the follow-up experiments, performed with phase-stabilized pulses in the parallel geometry in Fig. 29(a) (Kienberger *et al.*, 2004). The results

reveal controlled emission of a single or double sub-fs XUV pulse⁷⁰ and corroborate predictions of the semi-classical theory summarized in Fig. 22. For an accurate measurement of the XUV pulse as well as the few-cycle laser wave, the XUV pulse has been delayed in steps of 150 as to scan its arrival time in the second target across the laser wave. Figure 37(a) shows the result of this measurement (Goulielmakis *et al.*, 2004), a particularly simple attosecond streaking spectrogram. As discussed in Sec. V.D.3, FROG-type algorithms allow complete reconstruction of the complex amplitude envelope $a_X(t)$ of the sub-fs XUV pulse [see Eq. (33)], and the few-cycle laser field $E_L(t)$.⁷¹ Given the shortness and simplicity of the XUV pulse profile, from the measurements summarized in Fig. 37, reconstruction of $A_L(t)$ and $a_X(t)$ was straightforward and did not require iterative steps, yielding the laser field $E_L(t)$ shown in Fig. 12 and a near-transform-limited XUV pulse duration of 0.25 fs (full width at half maximum) as shown in Fig. 37(c) (Kienberger *et al.*, 2004).

4. Breaking the 100-as barrier

Chirp-free harmonic emission is restricted to a relatively narrow bandwidth of about 10–15 % of the cutoff energy. Below-cutoff harmonics result from electrons returning to the core along short and long trajectories (see Figs. 20 and 22). They produce emission at increasingly different moments, requiring trajectory selection⁷² and dispersion control (Kim, Kim, Baik, *et al.*, 2004; López-Martens *et al.*, 2005); see Fig. 38. Along with few-cycle polarization gating, they permitted the production of isolated 36-eV pulses of 130 as in duration (Sansone *et al.*, 2006),⁷³ see the low-energy spectrogram in Fig. 39.

Using waveform-controlled sub-1.5-cycle NIR laser pulses and chirped XUV multilayers for spectral filtering and dispersion control (Wonisch *et al.*, 2004, 2006; Morlens *et al.*, 2005), isolated sub-100-as pulses at \sim 85 eV photon energy have also been demonstrated (Goulielmakis, Schultze, *et al.*, 2008); see the high-energy spectrogram in Fig. 39. These pulses are delivered with a flux of $\sim 10^{11}$ photons/s, allowing for time-resolved measurements of electron processes with a resolution approaching the atomic unit of time (~ 24 as).

⁷⁰While the single pulse is needed for pump-probe studies, the double pulse is ideal for time-domain interferometry (Ishikawa, 2006; Remetter *et al.*, 2006).

⁷¹By detecting electrons ejected in opposite directions, the method can be generalized to measuring the field evolution in arbitrarily polarized laser pulses (Popruzhenko *et al.*, 2007; Shvetsov-Shilovski *et al.*, 2007).

⁷²Antoine *et al.*, 1996, 1997; Lee *et al.*, 2001; López-Martens *et al.*, 2005; Merdji *et al.*, 2006; Cao, Lu, Lan, Wang, and Yang, 2007; Cao, Lu, Lao, Wang, and Li, 2007.

⁷³There is an extensive literature on the optimization of single sub-fs pulse generation, see, e.g., Cao *et al.*, 2006; Chakraborty *et al.*, 2006; Lan *et al.*, 2006; Lan, Lu, Cao, Wang, and Hong, 2007; Ishikawa *et al.*, 2007; Popov *et al.*, 2007.

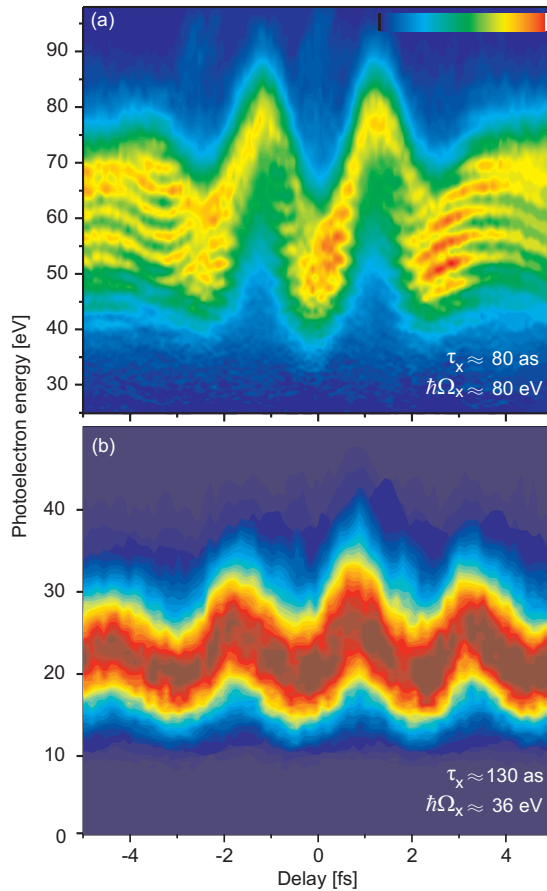


FIG. 39. (Color) Current frontiers of attosecond technology. (a) Attosecond streaking spectrograms of isolated XUV pulses generated and recorded with few-cycle, (a) ~ 3.5 fs and (b) ~ 5 fs ~ 750 -nm pulses. Low-energy spectrogram: carrier photon energy ≈ 36 eV; target atoms: argon (Sansone *et al.*, 2006). High-energy spectrogram: carrier photon energy ~ 80 eV; target atoms: neon (Goulielmakis, Schultze, *et al.*, 2008). Measurements yielded XUV pulse durations of 78 and 130 as, respectively.

VI. SUB-fs ELECTRON AND PHOTON PULSES: CURRENT STATUS AND FUTURE PROSPECTS

High-order harmonic generation (HHG) from atoms and molecules has so far been the only source of sub-fs pulses suitable for spectroscopic use. The technique has played a central role in establishing attosecond technology, but the limited photon energy and photon flux currently available may stall its dynamic expansion. Promising routes to higher photon energy and yield include atomic HHG driven at longer wavelengths and exploitation of the interaction of relativistic electrons with intense laser light. They are discussed below.

A. Atomic electrons interacting with few-cycle fields: Atomic HHG

The physics of atomic HHG has been reviewed in Sec. IV.C.2. Here we address possible ways of scaling the

technique to higher photon energies at experimentally useful flux levels. Such an advance will require us to overcome current limitations. The most fundamental is reabsorption of the harmonics by the generation medium itself. Absorption-limited HHG has been demonstrated up to photon energies of ~ 100 eV with conversion efficiencies ranging from 10^{-4} to 10^{-6} over the spectral range of 10–100 eV, respectively.⁷⁴ Absorption rapidly decreases for increasing harmonic photon energies above 100 eV. Here another limiting effect becomes dominant: dephasing between the driving wave and the harmonic wave due to free-electron-induced dispersion, limiting the coherent growth of the harmonic wave. However, unlike absorption, dephasing does not constitute an ultimate limitation. It can be overcome by periodic readjustment of the phase difference between the driving and the harmonic wave, a technique called quasi-phase-matching (QPM).⁷⁵

If we can maintain phasing of the driving wave with the growing harmonic wave (by a suitable QPM scheme, see, e.g., Seres *et al.*, 2007) and prevent self-defocusing from occurring (by some guiding structure or beam shaping), dispersion-induced destruction of the driving pulse will become a major limitation. For ionizing fields, free electrons lead to two dispersion-related processes: temporal broadening and blueshift of the carrier frequency. Both effects lower the maximum ponderomotive potential [see Eq. (20)] and hence decrease Ω_{\max} [see Eq. (21)] during propagation, limiting the growth of the near-cutoff harmonics. We denote the dispersion-induced pulse destruction length as L_{disp} .

How can plasma-induced dispersion be minimized? By lowering ionization. This, however, lowers the maximum harmonic photon energy. Use of a longer, i.e., infrared (IR) driver wavelength may offer a way out. Then, according to Eq. (21), any selected Ω_{\max} achievable at λ_{NIR} can be produced at reduced intensity $|E_{\text{IR}}|^2 = |E_{\text{NIR}}|^2 (\lambda_{\text{NIR}}/\lambda_{\text{IR}})^2$ as compared to the intensity $|E_{\text{NIR}}|^2$ required at λ_{NIR} , and consequently at an exponentially reduced ionization rate w_i . This weakens the radiating atomic dipole, $d_h \propto \sqrt{w_i}$ [Eqs. (16) and (22)], but the enhanced coherent buildup may overcompensate this detrimental effect (Yakovlev *et al.*, 2007; Ivanov *et al.*, 2008).

Indeed, the harmonic photon yield F_h at Ω_{\max} is proportional to $|N_h d_h|^2$, with N_h denoting the number of

⁷⁴Constant *et al.*, 1999; Schnürer *et al.*, 1999; Hergott *et al.*, 2002; Takahashi *et al.*, 2002, 2004; Goulielmakis, Schultze, *et al.*, 2008.

⁷⁵Phase-matched and quasi-phase-matched (QPM) HHG in the VUV-XUV-SXR spectral range has been experimentally demonstrated by Kapteyn, Murnane, and co-workers, see, e.g., Rundquist *et al.*, 1998; Durfee *et al.*, 1999; Gibson *et al.*, 2003, 2004; Paul *et al.*, 2003; Zhang *et al.*, 2004, 2005 (for a review, see, Paul *et al.*, 2006), and Zepf *et al.*, 2007. Rapid destruction of the driver pulse due to strong ionization prevented the potential of QPM HHG from being fully exploited.

dipoles radiating Ω_{\max} in phase. Ultimately, N_h is proportional to L_{disp} . The difference in refractive index between the fundamental and high-order harmonic waves induced by free electrons of density N_e scales as $\Delta n(\omega_L) \propto N_e \propto \omega_i$. As a consequence, $L_{\text{disp}} \propto 1/\Delta n \propto 1/N_e \propto 1/\omega_i$. The maximum achievable photon yield at frequency Ω_{\max} therefore scales as

$$F_h \propto |N_h d_h|^2 \propto 1/w_i(E_L). \quad (46)$$

This result predicts favorable scaling with wavelength, given that a moderate increase of λ_L allows dramatic reduction of $w_i(E_L)$ owing to the extremely nonlinear dependence of the tunnelling rate on the laser field strength E_L , which scales as $1/\lambda_L$. Equation (46) is valid as long as dispersion is dominated by free electrons. A more elaborate analysis of [Yakovlev et al. \(2007\)](#) corroborates the above conclusions.

IR-driven HHG was pioneered by L'Huillier and co-workers ([Balcou et al., 1992](#)) and DiMauro and co-workers ([Sheehy et al., 1999](#)), followed by studies of [Bellini \(2000\)](#) and [Shan and Chang \(2001\)](#). As pointed out by DiMauro, a long driver wavelength benefits HHG and strong-field interaction in many ways ([Schultz et al., 2007; Tate et al., 2007](#)) and may result in keV attosecond pulses ([Seres et al., 2005](#)).

B. Relativistic electrons interacting with few-cycle light

1. Intense attosecond VUV to soft-x-ray pulses via surface HHG?

So far, we have been concerned with light-matter interactions at intensities where the electric field is strong enough to ionize atoms, but too weak to accelerate the freed electrons to speeds approaching the speed of light in vacuum, c . The electron's quiver energy in the light field becomes comparable to its rest energy when the normalized amplitude of the vector potential

$$a_0 = |e|A_0/m_e c \quad (47)$$

becomes comparable to or larger than unity, defining the regime of relativistic light-electron interactions. In terms of laser intensity I_L and laser wavelength λ_L , it can be expressed as $a_0^2 = I_L \lambda_L^2 / (1.37 \times 10^{18} \text{ W } \mu\text{m}^2/\text{cm}^2)$. Present-day femtosecond laser technology allows a_0 to approach 100 ([Mourou et al., 2006](#)). As ionization occurs at much lower intensities, bound-electron nonlinear optics is virtually “switched off” for $a_0 \gg 1$. That is, nonlinear response of matter associated with the motion of electrons near the atomic core is relevant only at the leading edge of ultraintense laser pulses, with only a tiny fraction of the laser pulse “feeling” this response. However, in this regime, free electrons respond in a nonlinear fashion. Indeed, the magnetic component of the Lorentz force $\mathbf{v} \times \mathbf{B}_L$ becomes comparable to that of the electric component \mathbf{E}_L . As the electron's velocity \mathbf{v} is initially acquired from \mathbf{E}_L , modification of this velocity by \mathbf{B}_L implies a nonlinear response of the electron to the field.

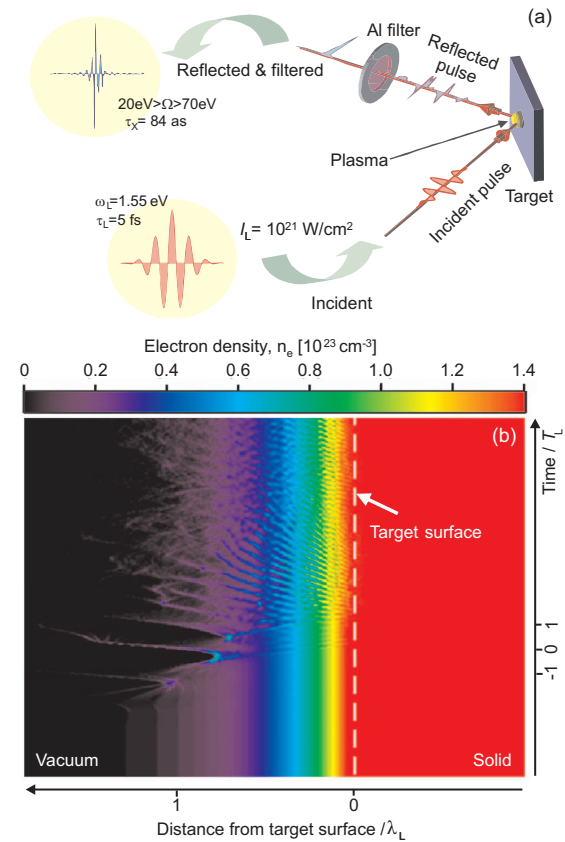


FIG. 40. (Color) High-order harmonic generation on a surface exposed to ultrashort-pulsed laser radiation at relativistic intensities. (a) Incident and reflected few-cycle laser wave, with the latter containing high-frequency components. Their isolation by a band-pass filter (in this example between 20 eV and 70 eV) is predicted to result in a single burst of attosecond duration. (b) Temporal evolution of the electron density of a preformed plasma with scale length $L_p = \lambda_L/4$ upon exposure to a p -polarized, cosine-shaped few-cycle NIR pulse ($\tau_L = 5$ fs, $\lambda_L = 750$ nm) incident at 45° at the surface with its peak at moment $t=0$ and a peak amplitude of the normalized vector potential of $a_0=3$. The relativistic motion of the plasma surface (excursions on the order of $\lambda_L/4$ over periods of $T_L/4$) is evident in the evolution of the electron density distribution (shown in false-color representation). Sharpening the oscillation peaks of the reflected pulse are conspicuous, indicative of a highly efficient conversion ($\sim 10\%$) of the incident IR light into UV or VUV light with sub-fs temporal structure. From [Tsakiris et al., 2006](#).

The main advantage of free-electron (or relativistic) nonlinear optics over its counterpart based on bound electrons is that the field strength can be increased virtually without limitation. Higher intensities tend to induce a more pronounced nonlinear response, offering the potential for more efficient conversion of (low-energy) laser photons into high-energy photons and electrons. Striking examples of this potential include the predicted conversion of more than 10% of the laser pulse energy into that of a relativistic electron bunch accelerated in a broken plasma wave (“bubble”) in the

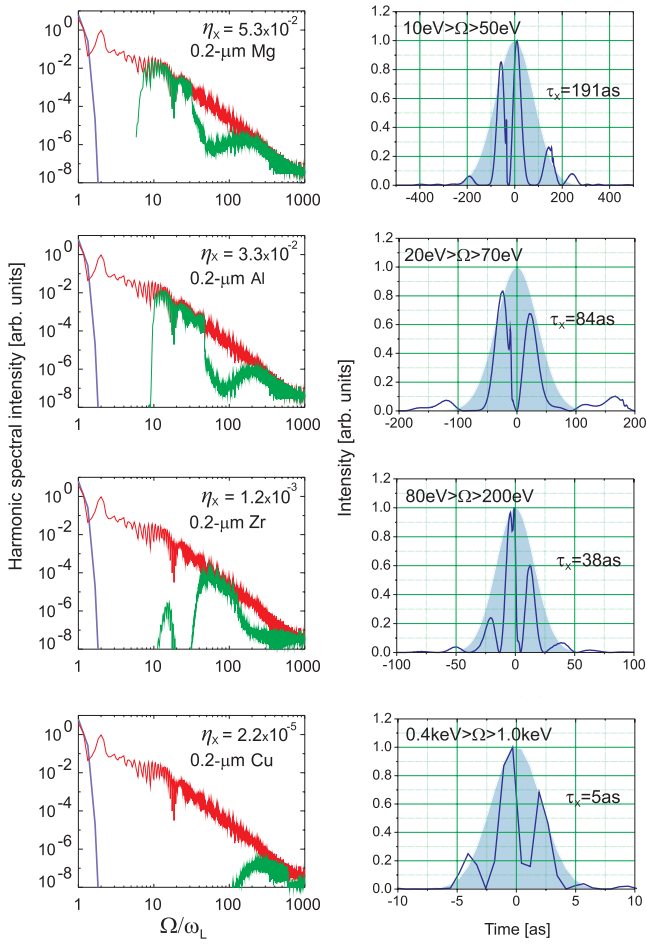


FIG. 41. (Color) Attosecond pulses from surface HHG, predicted by numerical simulations. Left panels, high-order harmonic spectra generated by a Gaussian-shaped few-cycle NIR laser pulse ($\tau_L=5$ fs, $\lambda_L=0.8$ μm , $a_0=20$) impinging at a 45° angle of incidence on a planar target with a step-like density profile (red lines) and as transmitted through different spectral filters (green lines). Right panels, corresponding temporal profile of the reflected radiation transmitted through the filters. The simulations predict *isolated* attosecond pulses in different spectral ranges. From Tsakiris *et al.*, 2006.

forward direction⁷⁶ (Pukhov and Meyer-ter-Vehn, 2002) or into sub-fs and as VUV and XUV emission upon reflection from or transmission through a solid surface.⁷⁷

In particular, the relativistic interaction of a few-cycle pulse with a solid surface (Fig. 40) has been predicted to result in attosecond pulses with unprecedented power

⁷⁶Invented by Pukhov and Meyer-ter-Vehn (2002) in numerical studies and first demonstrated experimentally by Faure *et al.*, 2004; Geddes *et al.*, 2004; Mangles *et al.*, 2004. For a review, see Pukhov and Gordienko, 2006. Geissler and Meyer-ter-Vehn (2006) were the first to point out the benefits of few-cycle driver pulses.

⁷⁷Reflection: Naumova, Sokolov, *et al.*, 2004; Pirozhkov *et al.*, 2006; Tsakiris *et al.*, 2006; Geissler *et al.*, 2007. Transmission: Mikhailova *et al.*, 2005. For a discussion of relativistic nonlinear optical phenomena, see Bulanov *et al.*, 1994; Lichters *et al.*, 1996; Gordienko *et al.*, 2004; Mourou *et al.*, 2006.

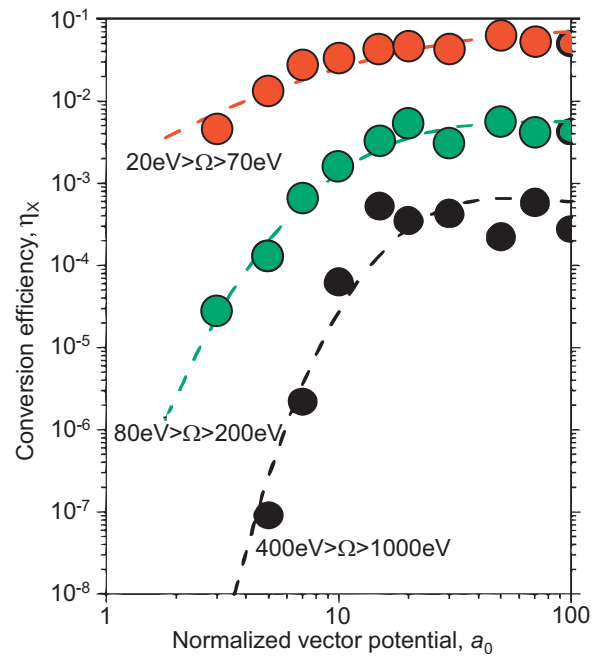


FIG. 42. (Color) Production efficiency of filtered attosecond pulses emerging from few-cycle-driven surface harmonic generation for three different spectral ranges (isolated by the filters specified in Fig. 41), as a function of the normalized vector potential. Simulation parameters other than the vector potential are the same as in Fig. 41. From Tsakiris *et al.*, 2006.

(Naumova, Nees, *et al.*, 2004; Gordienko *et al.*, 2005; Baeva *et al.*, 2006a, 2006b; Tsakiris *et al.*, 2006). The theoretically predicted slow roll-off of the harmonic intensity according to the power law $I_h \propto \omega^{-5/2}$ (Gordienko *et al.*, 2004), later corrected to $I_h \propto \omega^{-8/3}$ in Baeva *et al.* (2006a) was recently corroborated experimentally to keV photon energies (Dromey *et al.*, 2006, 2007).⁷⁸ Theoretical analysis also indicates that (i) reflected light from the oscillating plasma mirror suffers a Doppler up-shift up to

$$\Omega_{\max} \approx 4\gamma_{\max}^2\omega_L = 4(1 + a_0^2)\omega_L \quad (48)$$

and the emission of these photons is confined to small fractions of the laser period, of the order of

$$\tau_{\text{cutoff}} \approx T_L/4\gamma_{\max}^2, \quad (49)$$

resulting in a periodic train of high-energy photon bursts. Recently Baeva *et al.* (2006a) have refined this simple model for the super-relativistic regime, $a_0 \gg 1$. Driving the interaction with a few-cycle laser field and suitable spectral filtering (Tsakiris *et al.*, 2006) or longer pulses with time-dependent ellipticity of their polarization (Baeva *et al.*, 2006b) may lead to single attosecond pulse generation;⁷⁹ see Fig. 41 (Tsakiris *et al.*, 2006; Geissler *et al.*, 2007). A train of sub-fs pulses was recently

⁷⁸Different contributions to the process are discussed in Tarasevitsch *et al.*, 2007, and Thaury *et al.*, 2007.

⁷⁹Spatial filtering can also isolate a single pulse in case of λ_L -sized interaction volume (Naumova, Nees, *et al.*, 2004).

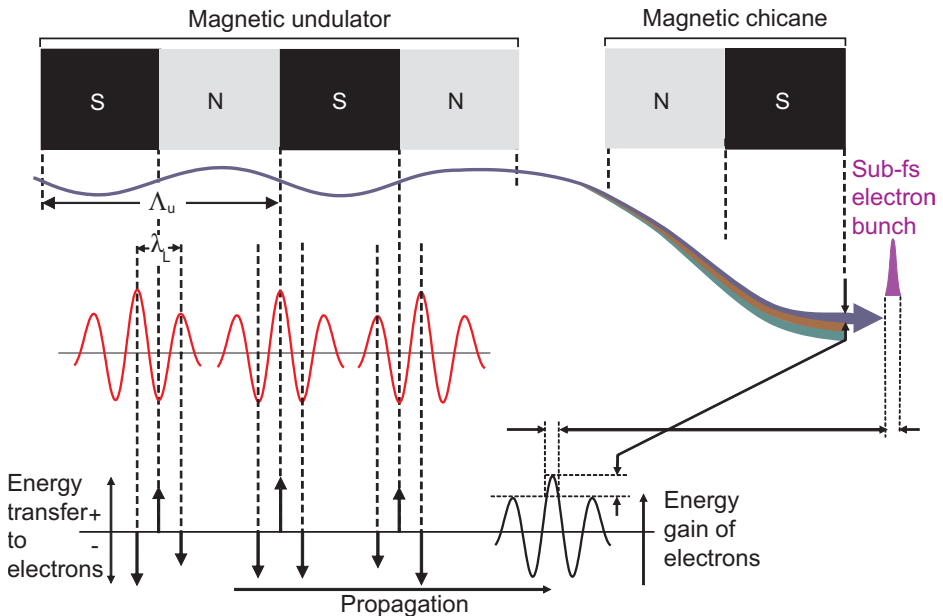


FIG. 43. (Color) Principle of sub-fs electron bunch slicing, by light-field-induced energy modulation of a relativistic electron beam. Energy transfer between the wiggling electron beam and the copropagating laser beam $E_L(t)$ polarized along the direction of the wiggling motion can take place owing to the transverse component $v_x(t)$ of the electron's velocity: $dW/dt = -v_x(t)E_L(t)$. The direction of energy transfer at the interface of bending magnets, where $v_x(t)$ is maximum, is depicted by arrows in the bottom panel. The undulator period Λ_u is chosen such that the electron beam is delayed by the laser wavelength λ_L with respect to the laser wave upon traveling one undulator period. As a consequence, those sub-laser-wavelength, sub-fs portions of the electron bunch that gain energy in one undulator period will also gain energy in the next one. In between, electrons will lose energy, repeatedly, from one undulator period to the next. This inverse free-electron laser (IFEL) effect results in an electron beam carrying an energy spectrum modulated following the oscillating electric field of the laser field at the output of the undulator. If IFEL is implemented with a cosine-shaped few-cycle laser field, maximum energy shift will be confined to a fraction of the half laser cycle at the pulse peak. This sub-fs portion of the electron bunch can be sliced out with a magnetic chicane and an aperture.

observed from the interaction driven by a multicycle laser pulse (Nomura *et al.*, 2009).

Figure 41 reveals several striking differences when compared with atomic HHG. First, isolated sub-fs pulse generation appears to be feasible for a wide range of frequencies including bands far below Ω_{\max} . Second, increase of the filter bandwidth does not compromise the quality of single-pulse isolation up to bandwidths of more than an octave, implying isolated soft-x-ray pulses of a few attoseconds in duration. Last but not least, the efficiency of few-cycle-driven surface HHG is predicted to surpass that of atomic HHG by several orders of magnitude (Fig. 42). If these predictions can be verified, few-cycle-driven surface HHG will open up a new chapter in attosecond science.

2. Attosecond electron and hard-x-ray pulses?

Several theoretical studies suggest that the interaction of ultraintense few-cycle light with relativistic electrons may result in the production of isolated attosecond relativistic electron (Naumova, Sokolov, *et al.*, 2004; Ma *et al.*, 2006; Sakai *et al.*, 2006; Varin and Piché, 2006) and hard-x-ray (Zhang *et al.*, 2006) pulses. As an example, here we review a scheme proposed by Saldin *et al.* (2004) and Zholtens and Fawley (2004), in which a few-cycle pulse acts as a sub-fs electron energy modulator, permitting sub-fs bunch slicing. The concept draws on the in-

teraction of a strong, but nonrelativistic, few-cycle light field with an ultrashort (femtosecond) bunch of ultrarelativistic electrons ($W \gg 1$ MeV), in the static, periodic magnetic field of an undulator⁸⁰ and explained in Fig. 43. A several-millijoule energy, cosine-shaped, few-cycle near-infrared pulse ($\tau_L=5$ fs at $\lambda_L=800$ nm) is capable—within merely two magnet periods—of introducing a sub-fs, central peak energy offset of some 40–50 MeV, which exceeds by a factor of 2 the energy shift induced in any other portion of the bunch. If the initial energy spread of the electron bunch is a small fraction of this light-induced energy shift, selecting the upshifted energy band at the output of a magnetic chicane (Fig. 43) results in a sub-fs ultrarelativistic electron bunch. Injection of this sub-fs electron bunch into a second undulator with a much shorter magnet period may allow generation of sub-fs hard-x-ray pulses up to peak powers at the 100-GW level (Saldin *et al.*, 2004) by free-electron lasing (Kroll *et al.*, 1981; Feldhaus *et al.*, 2005).

⁸⁰The utility of this interaction, known as the inverse free-electron laser (Palmer, 1972; Courant *et al.*, 1985; Sears *et al.*, 2005), has been demonstrated for manipulating relativistic electron bunches, including microbunching (Liu *et al.*, 1998; Sung *et al.*, 2006), phase locking to a laser wave (Kimura *et al.*, 2001, 2004) as well as acceleration (Musumeci *et al.*, 2005).

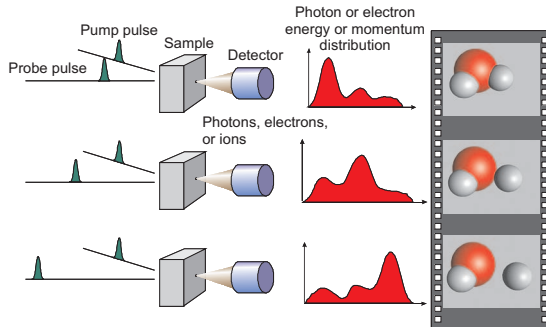


FIG. 44. (Color) Principle of pump-probe (time-resolved) spectroscopy.

3. Next-generation accelerators driven by few-cycle light?

Byer and his co-workers recognized that the peak acceleration gradient of ~ 50 MeV/m of conventional radio-frequency (rf) accelerators can potentially be increased to GeV/m by using laser (instead of rf) fields in dielectric (instead of metal) structures for acceleration.⁸¹ Efficient operation of such a laser-driven vacuum accelerator relies on few-cycle driver pulses with a controlled CE phase.⁸² The use of intense waveform-controlled few-cycle light in future linear electron accelerators will naturally lead to high-energy attosecond electron bunches and thereby extend the frontier of attosecond science into high-energy physics.

VII. REAL-TIME OBSERVATION AND CONTROL OF ATOMIC-SCALE ELECTRON AND NUCLEAR DYNAMICS

Real-time observation of microscopic motion requires the ability to trigger and subsequently probe the process under scrutiny.⁸³ The instants of triggering and probing must be defined with an accuracy sufficient to resolve details of the motion. This accuracy is dictated by the duration of the triggering and probing events, the accuracy of controlling the delay between them, and the S/N ratio, see Fig. 4. Dynamical information is provided by an observable varying as a function of the delay between triggering and probing events in a pump-probe measurement (Fig. 44). This quantity varies on the time scale at which the motion occurs, affording the observer *real-time access* to the process. If the observable also yields information on the location of the moving particles, a series of freeze-frame pump-probe images allows retrieval of the microscopic motion. We refer to this as four-dimensional (4D) imaging.

Microscopic dynamics outside the atomic core fall into

⁸¹Huang *et al.*, 1996; Salamin and Keitel, 2000; Wang *et al.*, 2001, 2007; Plettner *et al.*, 2005.

⁸²Plettner *et al.*, 2006.

⁸³Kinematically complete collision experiments also provide insight into attosecond dynamics, but a delayed probe for real-time observation is not available in these experiments. See, e.g., Moshammer *et al.*, 1997; Chatzidimitriou-Dreismann *et al.*, 2003.

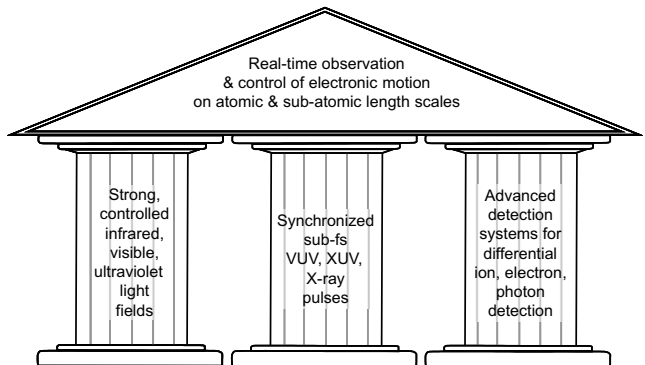


FIG. 45. Major technological pillars of attosecond science.

two major categories: (i) motion of atoms as a whole leading to structural rearrangements in molecules and condensed matter and (ii) motion of electrons inside and between atoms. The natural time scales for these particles to travel atomic distances extend from several femtoseconds to several picoseconds and from several attoseconds to tens of femtoseconds, respectively (Figs. 1 and 2). Real-time observation and control of atomic motion relies on femtosecond laser techniques, using cycle-averaged quantities such as field amplitude and carrier frequency for initiating, probing, and controlling dynamics. Attosecond technology constitutes a radical shift: the oscillatory laser field along with a sub-fs XUV pulse takes over this job, potentially improving the resolution of probing and the precision of control by orders of magnitude.

The main technological pillars for attosecond science are shown in Fig. 45. Depending on the type of microscopic process to be studied and the questions to be asked, these tools are to be used in different combinations. Tables I–III provide an overview of the toolbox within attosecond technology, summarizing the different options of how to trigger, steer, probe, and image electronic and nuclear dynamics. Many of the tools listed are already available, other will hopefully emerge in the near future. In this section we review the status and address some prospects of attosecond spectroscopy and control. In doing so, we first consider the simplest case of isolated atoms (Sec. VII.A) and then move towards ever more complex systems, from simple diatomic molecules, through large biomolecules and supramolecular assemblies, to mesoscopic systems and condensed matter. We show how tools from our attosecond toolbox (Tables I–III), referred to using the code (I–III/A–E/1–2), are to be combined to address a wealth of questions in a wide range of different systems.

A. Electronic motion in atoms: Excitation, relaxation, and correlations

Electronic motion inside or around atoms can be triggered with sub-fs precision either by optical-field ionization or by a sub-fs VUV, XUV, or x-ray pulse. In this section we address schemes for attosecond spectroscopy based on these scenarios and review experiments.

TABLE I. Toolbox of attosecond technology: triggering and steering the motion of electrons.

Ultrashort-pulsed tools for electronic and concomitant atomic motion with sub-femtosecond or attosecond precision		1	2
		triggering	steering
A	Strong, multicycle, envelope-controlled IR/NIR light	periodic launching of positive-energy electron wave packets, periodic recollision, and recollision-induced dynamics, generation of a train of sub-fs XUV pulses via optical field ionization intensity requirement: ¹ $\gamma < 1$ or $\gamma \approx 1$ timing precision: ² $\sim T_L/20$	periodic subcycle control of strong-field atomic processes (ionization, recollision, recollision-induced dynamics); shaping sub-fs pulse trains by superimposing harmonic fields intensity requirement: $\gamma < 1$ or $\gamma \approx 1$ steering precision: ³ $\sim T_{\min}/4$
B	Train of sub-fs VUV/XUV pulses	affecting and controlling periodic strong-field electron dynamics induced by a synchronous, multicycle laser field, e.g., by seeding desired electron trajectories via single-photon (possibly two-photon) bound-bound or bound-free transition timing precision: ⁴ $\sim \tau_X/5$	
C	Strong, few-cycle, waveform-controlled IR/NIR/VIS/UV light	initiation of electronic and possibly nuclear rearrangements in ionized systems with “absolute” timing precision, generation of a single sub-fs XUV/SXR pulse via optical field ionization requirement: definite waveform, $\gamma \ll 1$ or $\gamma \approx 1$ timing precision: $\sim T_L/20$	steering the motion of valence-band electrons in atomic and molecular systems with synthesized waveforms requirements: bandwidth > 1 octave and/or intensity: ⁵ $\Delta W_{\text{Stark}} \approx \Delta W_{\text{valence}}$ steering precision: $\sim T_{\min}/4$
D	High-flux, sub-fs VUV/ XUV/ SXR pulse	triggering electronic motion in matter, especially localized, site-selective electronic excitation in molecular and condensed systems via single-photon bound-bound or bound-free transition flux requirement: ⁶ $F \approx 1/\sigma$ timing precision: $\sim \tau_X/5$	(possibly) coherent control of electronic excitation in atoms, molecules, and solids via two-photon transition induced by a sub-fs pulse with shaped amplitude and swept frequency intensity requirement: ⁷ $I\sigma^{(2)}\tau_X \approx 1$ steering precision: $\sim \tau_X/5$
E	Low-flux ($F \ll 1/\sigma$) sub-femtosecond XUV/X-ray pulse	time-resolved inner-shell spectroscopy via single-photon bound-bound or bound-free transition timing precision: $\sim \tau_X/5$ to be implemented in conjunction with (IIC1)	

¹ γ : Keldysh parameter, for definition, see, e.g., Brabec and Krausz, 2000.² T_L : oscillation period of carrier wave.³ T_{\min} : oscillation period of shortest wavelength spectral component of the wave.⁴ τ_X : pulse duration (FWHM) of XUV/SXR/X-ray pulse.⁵ $\Delta W_{\text{Stark}} \approx \Delta W_{\text{valence}}$: Stark shift of valence-band energy levels comparable to level spacing.⁶ $F \approx 1/\sigma$: Photon flux (number of photons/beam cross-sectional area) comparable to the inverse single-photon transition cross section. If, for example, $\sigma \approx 1 \text{ Mbarn}$ (10^{-18} cm^2) and the beam cross section $\sim 1 \mu\text{m}^2$, this condition requires $\sim 10^{10}$ photons to be carried by the pulse.⁷ I : intensity (number of photons/beam cross-sectional area/time); $\sigma^{(2)}$: two-photon cross section of the transition one is attempting to control, which depends very sensitively on frequency and system. Some feeling for the required intensity can be gained from requiring that one-photon absorption is saturated.

1. Electronic excitation and relaxation dynamics: Attosecond streaking and tunneling spectroscopy

Core excitation of atoms causes a wealth of multielectron processes. Figure 46 presents a few examples. They

unfold on a time scale ranging from tens of attoseconds to tens of femtoseconds. Direct time-domain access promises to yield deeper insight into these processes and to identify ways of affecting them. This, in turn, may

TABLE II. Toolbox of attosecond technology: probing and imaging the motion of electrons.

Ultrashort-pulsed tools for		1	2
		probing	imaging
electronic and concomitant atomic motion with sub-femtosecond or attosecond precision			
A	Strong, multicycle, envelope-controlled IR/NIR light	probing periodic electron emission induced by a synchronized train of sub-fs XUV pulses (IB1) by measuring side-band intensity versus delay between IR pulse and sub-fs pulse train via single-photon free-free transition: RABBITT, CRAB intensity requirement: ⁸ $I_L \approx 10^{11} \text{ W/cm}^2$ resolution $\sim T_L / 20$ electronic response restricted to shorter than the period of the sub-fs train	imaging dynamic change in molecular structure induced by optical-field ionization (IA1) via analyzing high-order harmonics and/or rescattered ATI electrons intensity requirement: $\gamma < 1$ or $\gamma \approx 1$ resolution: sub- $T_L / 2$, sub-Angström delay of imaging with respect to the start of the dynamics restricted to less than T_L
B	Train of sub-fs VUV/XUV pulses	probing periodic strong-field electron dynamics induced (IA1) and possibly steered (IA2) by a synchronous, multicycle laser field via single-photon bound-free transition resolution $\sim \tau_X / 5$	seeding desired electron trajectories for probing electronic and nuclear dynamics via single-photon bound-free transition resolution $\sim \tau_X / 5$
C	Strong, few-cycle, waveform-controlled IR/NIR/VIS/UV light	probing multielectron excitation (shake-up) and relaxation (Auger, Coster-Kronig) processes following core excitation with a (low-flux) sub-fs XUV/X-ray pulse (see IE1) via one-photon or multiphoton free-free transition: attosecond streaking spectroscopy (AST) via multiphoton bound-free transition: attosecond tunneling spectroscopy (ATS) intensity requirement: $I_L \approx 10^{11} \text{ W/cm}^2$ or higher for free-free transitions ⁹ , $\gamma \approx 1$ for bound-free transitions resolution $\sim T_L / 20 - T_L / 10$	imaging dynamic change in molecular structure induced by optical field ionization with a preceding cosine-shaped waveform-controlled few-cycle light (see IC1) or by a synchronized single high-flux, sub-fs VUV/XUV pulse (see ID1) via ATI and HHG resolution: sub- $T_L / 2$, sub-Angström 4D imaging of electron and structural dynamics on surfaces via tunneling from a tip induced by a cosine waveform resolution $\sim T_L / 20$, potentially sub-Å
D	Low-flux ($F \ll 1/\sigma$) sub-femtosecond XUV/SXR/hard-X-ray or electron pulse	probing (i) inner-atomic electron-electron interactions initiated and possibly steered via ID1-2 (ii) valence-band electron dynamics and simultaneous nuclear dynamics in molecular systems, initiated and possibly steered via (IC1-2) by observing dynamic changes in valence-band and inner-shell photoelectron spectra, respectively, via single-photon bound-free transition (photoionization) resolution $\sim T_L / 5$	4D imaging of electron and structural dynamics atoms, molecules, solids initiated by either IC1 or ID1 with XUV/SXR pulse in combination with photoelectron emission microscopy: attosecond PEEM resolution $\sim \tau_{\text{XUV}} / 5$, $\sim 10 \text{ nm}$ with hard-x-ray or electron pulse: by recording freeze-frame diffraction pattern: attosecond diffraction imaging resolution $\sim \tau_{\text{XUV}} / 5$, \sim sub-Angström

⁸Critical parameter for free-free transitions is $vA_L \approx \omega_L$ where v is the electron momentum after ionization and A_L is the vector potential of the IR field. For $v \approx 1$ a.u. and 800 nm one obtains $I_L \approx 4 \times 10^{11} \text{ W/cm}^2$.

⁹As in the previous footnote, the critical parameter for free-free transitions is $vA_L \approx \omega_L$.

pave the way toward the development of compact, efficient XUV and x-ray lasers.

We assume that the atoms are hit by a sub-fs XUV or x-ray (henceforth, briefly, XUV) pulse. Depending on the XUV photon energy, atoms may be ionized or excited in several ways, as shown in Fig. 46. Core-level excitation typically triggers numerous intra-atomic and molecular processes including shakeup of one or more

electrons and a number of subsequent relaxation processes, such as Auger decay, Coster-Kronig decay, or cascaded decay phenomena. Inner-valence ionization, on the other hand, usually does not open a channel for double ionization, but can—if the ion is in close proximity to other atoms (e.g., in a cluster or in an endohedral fullerene)—result in energy transfer to its neighbor via

TABLE III. Toolbox of attosecond technology: detecting observables in attosecond time-resolved experiments.

Detectors for	1	2	
	probing	imaging	
by observing and analyzing final products of a pump-probe excitation			
A	Ion detectors	study of electron excitation & relaxation processes, multielectron dynamics in highly excited (core-excited) atoms by charge-state detection observation of molecular fragments during chemical and biochemical reactions by mass spectrometry	measurement of 3D momentum distribution of ionic fragments by velocity map imaging (for emission possessing cylindrical symmetry)
B	Electron detectors	measuring the energy distribution of ejected electrons [both primary (photo) and secondary (Auger) electrons] by time-of-flight analysis /magnetic-bottle spectrometers or by hemispherical detection	measurement of 3D momentum distribution of ejected electrons by velocity map imaging (for emission possessing cylindrical symmetry) measurement of 2D momentum distribution of scattered electrons by position-sensitive (e.g., multichannel-plate detector)
C	Electron-ion detectors	coincidence detection of electrons and ions along with measurement of the electron energy distribution and charge state detection and ion mass spectrometry by some combination of IIIA1 and IIIB1	Coincidence measurement of momenta of all products (electrons and ionic fragments) of a reaction: reaction microscope by COLTRIMS: cold-target recoil-ion-momentum spectroscopy
D	Photon detectors	measurement of transmitted (absorption spectroscopy) or ejected (fluorescence spectroscopy) photon energy distribution by wavelength-dispersive spectrometry (WDS) drawing on grating or crystal spectrometers and CCD or channel plate detectors or by energy-dispersive spectrometry (EDS) drawing on single-photon counting semiconductor detectors	measurement of 2D momentum distribution of scattered photons: time-resolved x-ray diffraction with CCD or channel plate detectors

interatomic and molecular Coulombic decay.⁸⁴

Two approaches to accessing sub-fs electron dynamics in the time domain have been demonstrated so far: attosecond streaking spectroscopy (AST) is an extension of streaking to positive-energy electrons containing atom-specific dynamic information such as Auger electrons, whereas in attosecond tunneling spectroscopy (ATS) electrons shaken up to the valence band are released from negative-energy (bound) states by tunnel ionization; see Fig. 46. Both approaches have in common that the sub-fs electric field transients of VIS and NIR light sample the process under study. As the probability of laser-field-induced transitions in these techniques may approach or even reach 100%, the sub-fs

XUV pulse initiating the dynamics is allowed to have a low flux (type IE1-IIC1 spectroscopy; see Tables I and II), leading to a weak-pump-strong-probe scenario.

Energetic excitation of atoms or molecules usually leads to ejection of one or more electrons. Their temporal evolution often carries information about inner-atomic dynamic processes. For instance, the emission of Auger electrons mirrors the decay of a core hole. Therefore resolving the emission process in time by AST provides direct information on the temporal evolution of inner-shell dynamics. Figure 47 shows simulated streak images of Auger electron spectra versus delay between the sub-fs triggering XUV pulse and the few-cycle probing laser field (Drescher *et al.*, 2002). These spectrograms, if recorded with satisfactory S/N ratio, allow retrieval of the temporal evolution of the electron emission and hence of the core-hole decay, as discussed in Sec. V.D.3. Drawing on this concept, AST resulted in the first real-time observation of the decay of

⁸⁴Cederbaum *et al.*, 1997; Marburger *et al.*, 2003; Averbukh *et al.*, 2004; Jahnke *et al.*, 2004; Averbukh and Cederbaum, 2006; Morishita *et al.*, 2006; Öhrwall *et al.*, 2004; Barth *et al.*, 2006; Kuleff and Cederbaum, 2007; Vaval and Cederbaum, 2007.

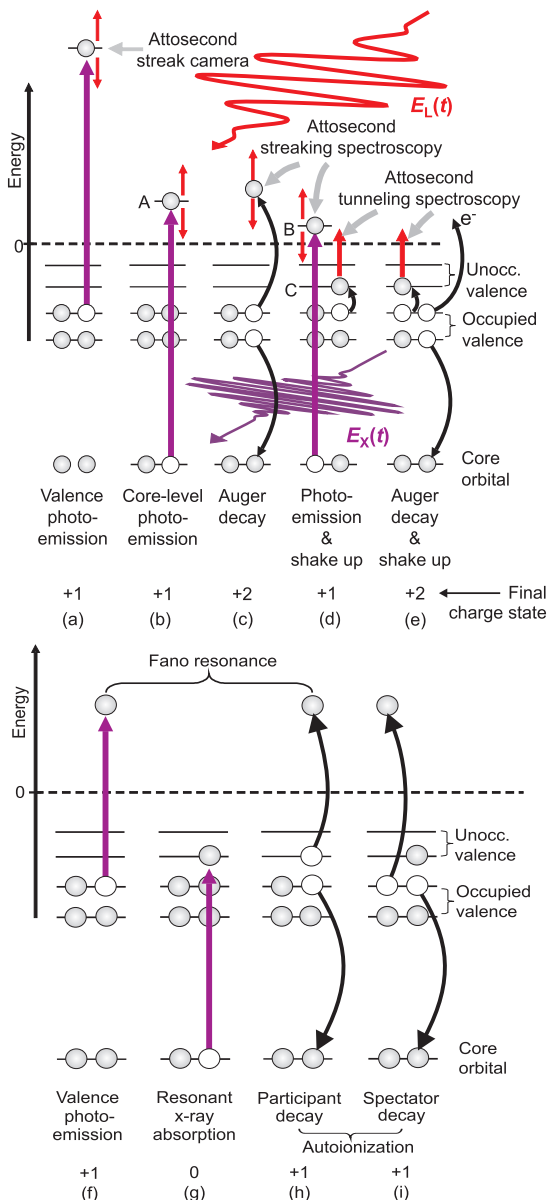


FIG. 46. (Color) Electronic excitation via XUV and x-ray photons followed by relaxation, which can be probed in real time via attosecond streaking spectroscopy and attosecond tunneling spectroscopy. The new spectroscopies draw on nonlinear free-free and bound-free electronic transitions, respectively, induced by waveform-controlled few-cycle light. (a), (f) Valence-electron emission, (b) core-electron emission, accompanied by (c) Auger decay or (d) valence-band excitation (shakeup), or both (e). (g) Resonant core-level excitation and subsequent (h) participant and (i) spectator decay. The basic idea for the graphical representation is borrowed from Brühwiler *et al.*, 2002.

an inner-shell vacancy (Drescher *et al.*, 2002).⁸⁵

The lifetime of the inner-shell vacancy acquired in the above time-resolved measurement can also be inferred

⁸⁵Short-pulse-induced Auger decay was realized before (Schins *et al.*, 1994, 1996), nevertheless with the decay remaining unresolved because of the long (sub-ps) duration of the x-ray excitation.

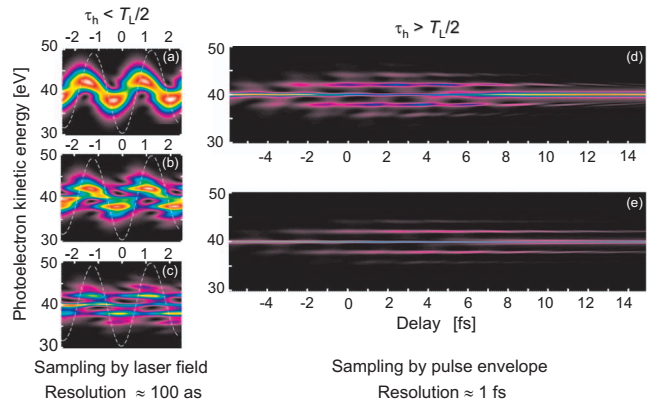


FIG. 47. (Color) Streaking spectrograms of Auger electron emission, simulated by V. Yakovlev and A. Scrinzi for different core-hole decay times, (a) $\tau_h=0.2$ fs, (b) $\tau_h=0.5$ fs, (c) $\tau_h=1$ fs, (d) $\tau_h=2$ fs, (e) $\tau_h=5$ fs, using a few-cycle NIR streaking laser field ($\tau_L=5$ fs, $\lambda_L=0.75 \mu\text{m}$) and a sub-fs ($\tau_X=0.5$ fs) XUV excitation pulse. Depending on whether the electron emission time τ_h is shorter or longer than the half wave cycle $T_L/2$, the spectrograms look different. For $\tau_h < T_L/2$, we see variations of the streaked spectra within the laser cycle (left panels). This subcycle variation in the streaked spectra tends to disappear as the emission time becomes longer than $T_L/2$. Instead, sidebands spaced by the laser photon energy appear for a delay range dictated by the duration of emission and the laser pulse. Variation of the sideband amplitude vs delay is the convolution of the emission process and the amplitude envelope of the laser field. If the laser pulse is short enough, the duration of electron emission can be determined by deconvolution. In the sub-fs domain, the process is sampled by the oscillating field, whereas in the femtosecond domain, the pulse envelope takes over the role of the “sampling function.” It has to offer a resolution on the order of $T_L/2$, if all details of the motion, possibly ranging from the sub-fs to multi-fs regime, are to be uncovered. This is ensured only by a few-cycle streaking field. From Drescher *et al.*, 2003.

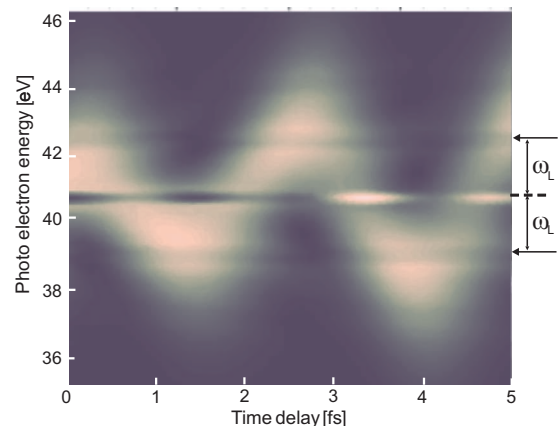


FIG. 48. (Color) Attosecond streaking spectrogram of two coalescent Lorentz resonances decaying over disparate time scales: $\tau_{h,1}=0.4$ fs and $\tau_{h,2}=40$ fs. Simultaneous launching of Auger electrons with different emission times manifests itself in the appearance of a broad oscillating feature displaying the short-lived emission and sidebands spaced by ω_L from the peak of the main lines (indicated by arrows) with their (long) temporal extension reflecting the duration of the long-lived emission. From Wickenhauser *et al.*, 2006.

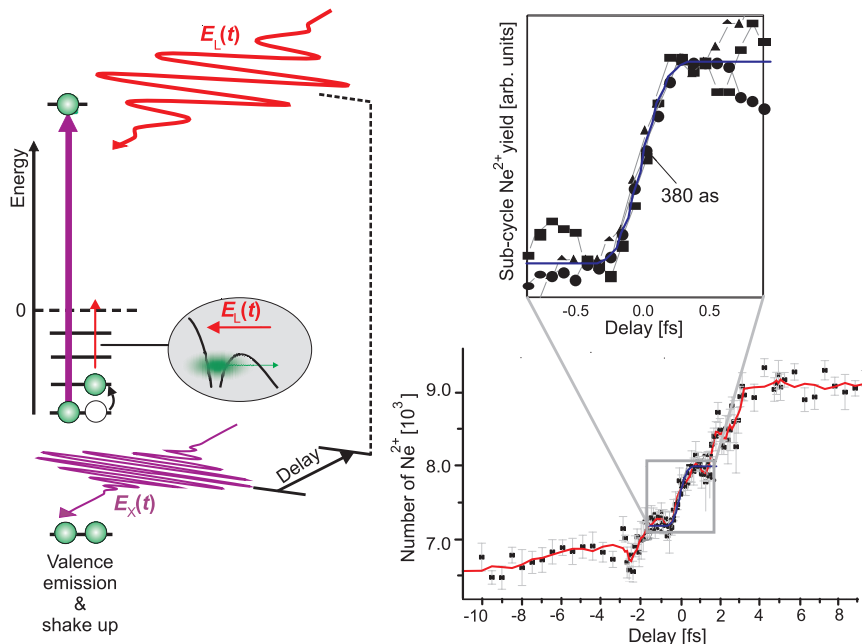


FIG. 49. (Color) Attosecond real-time observation of light-field-induced electron tunneling (Uiberacker *et al.*, 2007). A 250-as, 95-eV XUV pulse sets a valence electron free from neon atoms. The excess photon energy gives way to shakeup, promoting an electron to an excited state in the valence band. A time-delayed, waveform-controlled, few-cycle pulse ($\tau_L=5$ fs, $\lambda_L=0.75$ μm) probes the transient population of the shakeup states by field ionization, resulting in doubly charged neon ions, Ne^{2+} . The squares and the line (five-point average) depict the number of Ne^{2+} ions measured as a function of delay between the XUV excitation and the probing NIR laser field. The steplike increase in Ne^{2+} yield with the steps approximately separated by half the laser period provides conclusive evidence for optical field ionization responsible for the depletion of excited valence states, in accordance with the theory of nonadiabatic tunneling by Yudin and Ivanov (2001a). The inset zooms in onto the central subcycle ionization step, plotting data (dots, squares, triangles) obtained from different measurements, which reproducibly indicate that shakeup and tunneling occur within less than 400 attoseconds. Kazansky and Kabachnik (2007c) proposed a modification of the above scheme for studying tunneling in the absence of shakeup.

from time-integral, spectrally resolved (briefly, frequency-domain) measurements (Jurvansuu *et al.*, 2001). However, retrieval of dynamics from frequency-domain spectroscopy becomes challenging when the final state of the dynamical evolution can be reached via several channels, resulting in complex spectral structures due to resonances between competing quantum transitions. A prominent example is the Fano resonance, which emerges whenever a positive-energy state can be accessed by more than one quantum pathways; see Figs. 46(f)–46(i). Fano resonances have been ubiquitous in time-integral studies.⁸⁶ AST was found to be capable of exploring details of complex temporal dynamics related to coherent excitation of several nearby Fano resonances, which are only partially accessible by frequency-domain spectroscopy (Wickenhauser *et al.*, 2005, 2006; Zhao and Lin, 2005), see Fig. 48, and to be sensitive to off-diagonal elements of the excitation density matrix, opening the way to monitor decoherence.

⁸⁶ Examples include photoabsorption (Beutler, 1935; Fano, 1935, 1961), electron, neutron, and Raman scattering (Adair *et al.*, 1949; Simpson and Fano, 1963; Cerdeira *et al.*, 1973), and show up in such disparate systems as atoms (Lambropoulos and Zoller, 1981; Rzazewski and Eberly, 1981), quantum-well structures and quantum dots (Göres *et al.*, 2000), and scanning tunneling microscopes (Madhavan *et al.*, 1998).

AST can probe not only relaxation but also excitation of the electronic shell. Indeed, detailed comparison of the temporal history of the electron emission processes populating states *A* and *B* in Figs. 46(b) and 46(d) may shed light on how part of the absorbed photon energy ends up promoting another electron into an excited state (shakeup) in Fig. 46(d).

AST probes positive-energy (freed) electrons; see Figs. 46(b)–46(d). Alternatively, intra-atomic or intramolecular processes can also be interrogated by probing intermediate states of negative-energy (bound) electrons. This is exactly what ATS does by probing the population of valence-band energy levels that are unoccupied before excitation; see Figs. 46(d) and 46(e). In this way, ATS is capable of tracing how valence states are being populated and subsequently depleted, following a core-level excitation, allowing real-time observation of both excitation and subsequent relaxation of the electronic shell of a core-excited atom (Uiberacker *et al.*, 2007), or, e.g., the dynamics of excited electronic states in a dissociating molecule (Gagnon *et al.*, 2007).

While AST relies on electron energy analysis (IIIB1), ATS draws on counting ions of different charge states (IIIA1). Again, as a first step, a core electron is ejected by a sub-fs XUV pulse [Fig. 46(b)]. The first question that arises is how the electronic shell of the ion gets excited, i.e., how does “shakeup” occur? Is it instanta-

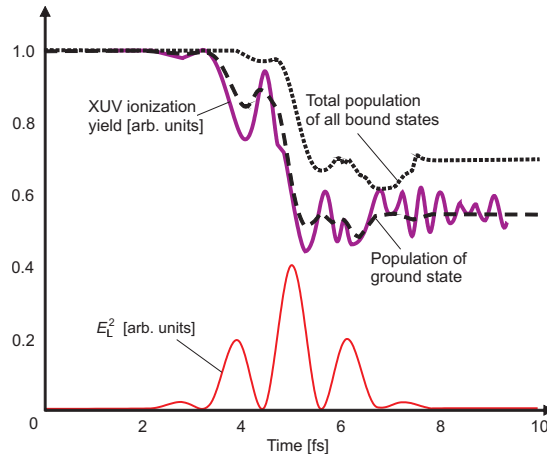


FIG. 50. (Color) Attosecond XUV probing of strong-field dynamics of a bound electron. Solid curve shows how the yield of ions created by XUV-induced ionization depends on the arrival time of the XUV pulse, relative to oscillations of the two-cycle, NIR driving field. As the bound electron wave packet $\psi_b(x,t)$ is stretched away from the core near the NIR field oscillation peaks, the high-momentum components decrease, because stretching the wave packet in coordinate space implies compression in momentum space. This reduces the bound-free transition matrix element and accounts for dips in the XUV yield near the maxima of the NIR field. Oscillations of the total yield at the end of the laser pulse suggest that nonadiabatic excitation during the laser pulse results in bound-state dynamics following the laser pulse. From Smirnova *et al.*, 2006.

neous (as it is currently understood) or is it possibly delayed? In principle, ATS may provide the answer by sampling the buildup of population in previously unoccupied valence states, such as state *C* in Fig. 46(d). But how can this population be probed with attosecond resolution using a femtosecond laser?

Theory⁸⁷ (Yudin and Ivanov, 2001b) predicts that not only in the conventional tunneling regime of $W_b \ll 2U_p$, but also in the intermediate regime of $W_b \approx U_p$ liberation of electrons with binding energies of $W_b \geq 10$ eV,⁸⁸ by intense several-cycle NIR or IR pulses occurs via nonadiabatic tunneling, with subcycle yield localized within small fractions of the half oscillation cycles near the wave crests. Proof-of-principle ATS experiments (Uiberacker *et al.*, 2007) corroborated this prediction (see Fig. 49). The observed 400-as rise time of the Ne^{2+} yield indicates that shakeup occurs too fast to be resolved with the current tools. Nevertheless, this sub-fs probe is sufficiently fast to sample a wide range of inner-shell relaxation processes. This potential was proven by

⁸⁷For a review of strong-field ionization, see Popov, 2004. For earlier papers, see Keldysh, 1964; Perelomov *et al.*, 1966a, 1966b; Perelomov and Popov, 1967; Reiss, 1980a, 1980b, and Faisal, 1987.

⁸⁸For pulses approaching the single-cycle limit, which may become available in the foreseeable future, this condition may be further relaxed toward a few electron-volts.

tracing multielectron relaxation in xenon (Penent *et al.*, 2005) following a 95 eV as excitation (Uiberacker *et al.*, 2007). With recently improved tools, sub-1.5-cycle NIR waveforms (Schultze *et al.*, 2007) and sub-100-as XUV pulses (Goulielmakis *et al.*, 2008), details of shakeup and nonadiabatic tunneling may also come to light.

With the increase of the excitation photon energy towards the keV frontier and possibly beyond, AST and ATS will provide direct, time-domain access to a vast range of electronic dynamics, including those in magnetic materials. With their time resolution approaching the atomic unit, comparative ATS and AST studies may shed light on how energy absorbed by an atom is distributed among its electrons and how the electronic shell of the atom is re-arranged following the loss of one or more electrons (Breidbach and Cederbaum, 2005) and thereby on the fundamental question of electron correlations.

2. Electronic relaxation and rearrangement: Attosecond absorption spectroscopy

In the previous section we discussed how attosecond electron dynamics can be probed with strong, controlled light fields. Alternatively, sub-fs XUV pulses can also be used as probe pulses. Transient absorption spectroscopy (Loh *et al.*, 2007, 2008) with isolated attosecond XUV and x-ray pulses (IID1–IID1; see Tables II and III) will also provide unprecedented insight into the relaxation dynamics and rearrangement of the electronic system of atoms or molecules following controlled excitation by a waveform-controlled few-cycle IR or VIS pulse (IC1-2; see Table I) or by an intense (possibly shaped) sub-fs XUV or x-ray pulse (ID1-2; see Table I). Isolated attosecond XUV pulses with a spectral width of several 10 eV (Schultze *et al.*, 2007; Goulielmakis *et al.*, 2008) provide ideal prerequisites for implementing attosecond absorption spectroscopy (AAS) by extending the experiments of Loh *et al.* (2007, 2008) into the time domain of the electronic response of matter (Breidbach and Cederbaum, 2005). This spectroscopy may give an answer to a long-standing question in atomic and molecular physics: How does the electronic system rearrange after the sudden removal or excitation of an electron?

3. Electron wave-packet motion: Attosecond photoelectron spectroscopy

Consider the simplest case when a single-electron bound wave packet is formed in an atom. Angle-resolved sub-fs XUV photoelectron spectra have been predicted to be sensitive to the instantaneous intraatomic or intramolecular electron density near the core, enabling us to trace its dynamic changes with attosecond resolution (Yudin *et al.*, 2005, 2006). As an example, consider the electron wave-packet dynamics induced by a strong linearly polarized IR field during optical field ionization (Smirnova, Spanner, and Ivanov, 2006). The laser field depletes the ground state stepwise, every half cycle, via tunneling. While doing so, it also “shakes up” the electron, populating several excited states; see Fig. 50.

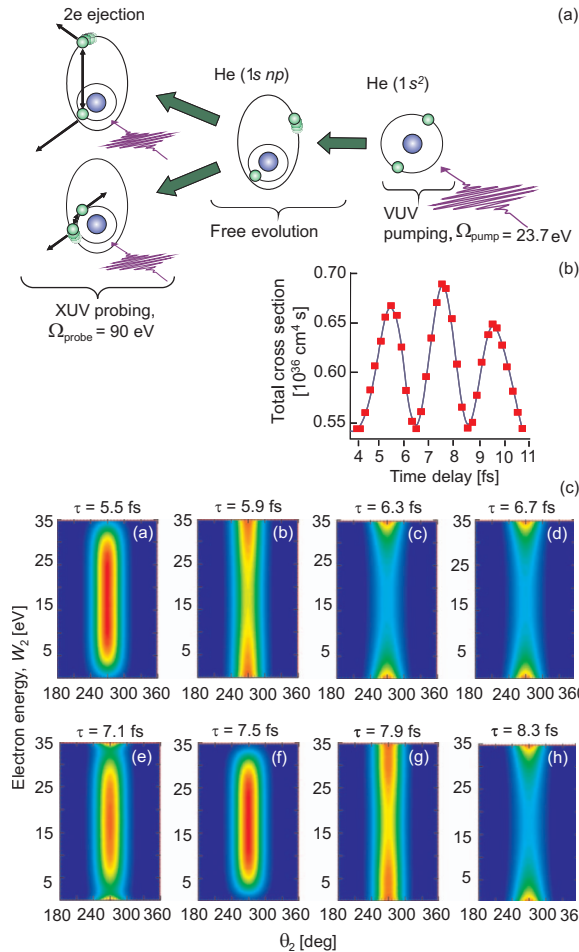


FIG. 51. (Color) Tracing intra-atomic electron motion and electron-electron interactions in helium (Hu and Collins, 2006). (a) Relevant interactions with the VUV pump ($\Omega_{\text{pump}} = 23.7 \text{ eV}$, $\tau_{\text{pump}} = 1.5 \text{ fs}$) and XUV probe pulse ($\Omega_{\text{probe}} = 90 \text{ eV}$, $\tau_{\text{probe}} = 250 \text{ as}$). (b) Calculated probability of XUV-induced double ionization vs pump-probe delay. (c) Contour plots showing the angular and energy distribution of the second electron for the first electron emitted along the XUV field polarization ($\theta_1 = 90 \text{ deg}$) vs delay τ . The second electron is ejected with the largest probability in the opposite direction ($\theta_2 = 270 \text{ deg}$). The total energy the two electrons carry is $\approx 35 \text{ eV}$. If ionization occurs when the excited electron wave packet is at its outer turning point (around $\tau = 6.5$ and 8.5 fs), the inner electron benefits from the vicinity of the core and picks up almost all of the incoming XUV photon energy. The outer electron is set free by the sudden change of the potential as the inner electron leaves the atom (shakeoff). 1 fs sooner or later, when the outer electron arrives at the core, the two electrons share the available excess energy, leaving the atom with comparable energy. Adapted from Hu and Collins, 2006.

This implies the formation and subsequent dynamics of an electronic wave packet bound to the core. The step-like decrease of the bound state population due to field ionization is, not surprisingly, also reflected in the XUV ionization yield (Fig. 50), which, however, shows much richer dynamics. Its origin becomes transparent when we realize that XUV absorption occurs near the core, from the high-momentum components of the wave func-

tion. Consequently, attosecond photoelectron spectroscopy (APS) uncovers the dynamics of these components in the bound electron wave packet $\psi_b(x, t)$.⁸⁹ Extended with spin-sensitive detection, spin-orbit wave-packet dynamics (Santra *et al.*, 2006) can also be studied in real time. Experimental implementation will draw on techniques IC1-IIID1-IIIB1/2 for triggering, probing, and detection, respectively; see Tables I–III.

In the above example, a sub-fs XUV pulse was used to explore the motion of a bound-electron wave packet inside an atom. Smirnova, Patchkovskii, and Spanner (2007) proposed that—along with some control over the ionizing IR field—it can also be used for determining the spatiotemporal characteristics of the detached electron wave packet, as it recollides with its parent ion. In this case, the atom works like the tip of a STM microscope—XUV photons can only be absorbed by free electrons in its vicinity.

Attosecond atomic (molecular) electron dynamics can also be initiated via resonant single-photon excitation for tracing intra-atomic electron motion and electron-electron interaction in real time. Consider the prototypical case of a helium atom (Hu and Collins, 2006, 2007) exposed to a broadband VUV pulse which promotes one of the two electrons from the ground state (1s) into the superposition state np with $n=2, 3, 4, \dots$. In this way, an electron wave packet is launched into an atomic orbit; see Fig. 51(a). This electron wave packet oscillates between the core and its outer turning point, while the other electron resides close to the nucleus in its ground state. The strength of interaction between these two electrons is therefore varying in time. The simulations of Hu and Collins (2006) predict that the probability of double ionization induced by a time-delayed sub-fs XUV probe pulse significantly varies with the center of gravity position of the outer electron. If the attosecond probe arrives when the outer electron is closest to the inner one, i.e., correlation between the two electrons is strongest, e.g., at a delay of $\tau = 5.5 \text{ fs}$ in Fig. 51(b), double ionization is most probable. On the other hand, it is least likely when the electron reaches its outer turning point, e.g., at $\tau = 6.5 \text{ fs}$ in Fig. 51(b). The double ionization yield can be measured by collecting He^{2+} as a function of delay τ between the UV pump and the XUV probe pulse. Implementation therefore relies on techniques ID1-IIID1-IIIA1 for pumping, probing, and detection, respectively; see Tables I–III. The variation of the pump-probe-induced double ionization yield versus τ , once measured, will display the motion of the excited electron wave packet in real time. Detection of ejected electrons in coincidence, discussed in the next section, will yield

⁸⁹This dynamics is even richer in multielectron systems; see Eichmann *et al.*, 2000; Zon, 2000; Lezius *et al.*, 2001; Markevitch *et al.*, 2003; Bryan *et al.*, 2006. These studies can also be extended to situations when the electron wave packet is promoted into the continuum and may provide access to effects such as Rabi flopping from continuum states (Dimitrovski *et al.*, 2004).

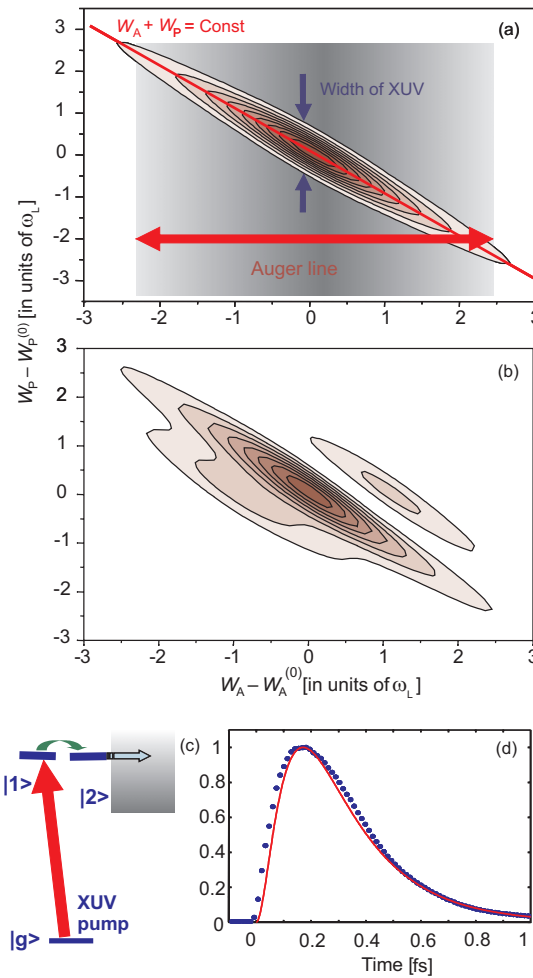


FIG. 52. (Color) Tracing sub-fs Auger decay triggered with a 1.2-fs XUV pulse and probed with a weak ($I_{\text{peak}} \approx 10^{10} \text{ W/cm}^2$) NIR ($\lambda_L = 800 \text{ nm}$) few-cycle streaking field via coincidence detection (Smirnova *et al.*, 2005). (a) Correlated spectrum of the liberated photoelectron and Auger electron. (b) Correlated electron spectrum recorded in the presence of a weak IR field, which creates sidebands of the original spectrum. (c) Model Auger decay. (d) Reconstruction of the decay dynamics: solid line is the exact decay, dots represent numerical reconstruction from a simulated spectrum containing 10^5 coincidence counts and recorded with a 160-meV energy resolution with 100-as jitter between the pump and probe pulses. The result indicates that a temporal resolution below the atomic unit of time (24 as) may be feasible using a ~ 1 fs XUV pump pulse. From Smirnova *et al.*, 2005.

further insight into interaction between the two electrons and the way they share the energy of the absorbed XUV photon.

4. Shedding light on electron-electron interactions: Attosecond coincidence spectroscopy

Measurement of the final momenta of all correlated particles produced in a pump-probe exposure in

⁹⁰Coincidence⁹⁰ offers unprecedented insight into correlated electron dynamics.⁹¹ In what follows, three prototypical interactions will exemplify the concept: (i) simultaneous two-electron ejection induced by a single XUV photon, (ii) photoelectron and Auger electron emission following absorption of a single XUV photon, and (iii) XUV-pulse-triggered, strong-IR-field-controlled electron-electron collision.

Simultaneous two-electron photoemission. The intriguing questions of how the energy of the absorbed XUV photon is shared between the two ejected electrons and how this energy sharing depends on the distance between electrons in the intra-atomic dynamics discussed in the previous section can be answered by combining the attosecond pump-probe experiments (ID1-IIID1; see Tables I and II) outlined in Fig. 51(a) with coincidence detection (IIIB2 or IIIC2; see Table III). The results of Hu and Collins (2006) summarized in Fig. 51(c) predict pronounced variations of the energy sharing between the two electrons as the moment of ionization is varied. Correlation between two free electrons released by an attosecond XUV pump pulse can also be resolved in time by the same method (Hu and Collins, 2007).

Auger decay. Inner shell XUV photoionization often results in the ejection of two electrons, one via photoemission [Fig. 46(b)], with energy W_P , the other via Auger decay [Fig. 46(c)], with energy W_A . When probing Auger decay via standard AST, the XUV pump pulse should be shorter than the process resolved. Smirnova *et al.* (2005) showed how coincidence detection allows one to abandon this stringent requirement. Consider a sub-fs Auger decay initiated by a substantially longer, few-fs XUV pulse. The total energy of the two electrons liberated in the correlated process is fixed by the relatively well-defined energy of the absorbed XUV photon: $W_P + W_A = \Omega_X - I_p^{++}$. The large uncertainty in W_A (caused by the ultrafast decay) translates into an equally large uncertainty in W_P ; see Fig. 52(a). Correlated spectra of such shape appear whenever a two-particle energy conservation law is present.⁹²

The correlated process can be completely characterized by attosecond streaking of the two-electron spectra in a weak IR laser field. The field creates energy-shifted “replicas” of the original spectrum via one-photon absorption and emission, with the spectral phase encoded in the interference of these replicas with the original spectrum [Fig. 52(b)]. Just as in SPIDER (Fig. 31), the time resolution is not limited by the XUV pulse duration, but rather by the jitter between the XUV and IR pulses and by noise.

⁹⁰Cold-target recoil-ion-momentum spectroscopy (COLTRIMS) enables one to perform kinematically complete experiments. See, e.g., Cocke and Olson (1991), Ullrich *et al.* (1997), and Dörner *et al.* (2000).

⁹¹Nicolaides *et al.*, 2002; Mercouris *et al.*, 2004, 2007a, 2007b; Emmanouilidou and Rost, 2007; Morishita, Watanabe, and Lin, 2007.

⁹²See, e.g., Chan *et al.*, 2002, 2003, 2004; and Fedorov *et al.*, 2004, 2005.

This approach can be used for any process resulting in the emission of two charged particles with fixed total energy, such as two-electron single-photon ionization. Processes of particular interest include shakeoff, Zeno and anti-Zeno stages of decay (Kofman and Kurzik, 2000), electron rearrangements in the core, and nonexponential decay due to a structured continuum.

Nonsequential double ionization. With coincidence detection, strong-field-controlled recollision provides time-domain access to the process of nonsequential double ionization. If the temporal evolution of the strong laser field is well controlled and known, the vector potential connects the moments of liberation of the two electrons after recollision with their final momenta. The SFA along with a few additional assumptions⁹³ offers a simple means of tagging the moments of liberation by the vector potential $\mathbf{A}_L(t)$, which induces changes in the final velocities of the ejected electrons that depends on their moments of creation. Coincidence measurement of the final electron velocities then allows retrieval of the history of their liberation. This approach provided insight⁹⁴ into NSDI and inneratomic electron thermalization following the recollision (Liu *et al.*, 2006).

If the recolliding electron is previously freed by the strong laser field, there is a direct connection between its energy W_r and the instant of recollision t_r , as shown by Fig. 20. Recent theoretical studies backed by experiments suggest that liberation of the electron with a sub-fs XUV pulse and its subsequent control with a polarization-shaped laser pulse will allow one to manipulate t_r and W_r of the recolliding electron independently.⁹⁵ Along with advances in theory⁹⁶ required for reliable retrieval of the moments at which the two electrons appear in the continuum after collision, this attosecond control may provide insight into the dynamics of electron-electron collision, as well as into more complex multielectron collision phenomena.

B. Electronic and nuclear motion in complex systems: From simple diatomics to biomolecules and clusters

The fundamental theory for molecules is that of the electronic structure. In the Born-Oppenheimer approxi-

⁹³Supported by extensive classical simulations of double ionization in strong laser field performed by Haan, Eberly, and co-workers: Haan *et al.*, 2002, 2006; Panfili *et al.*, 2002; Ho *et al.*, 2005.

⁹⁴See, e.g., Weckenbrock *et al.*, 2004, and Zeidler *et al.*, 2005.

⁹⁵Bandrauk and Shon, 2002; Schafer *et al.*, 2004; Johnsson *et al.*, 2005, 2006; Kitzler and Lezius, 2005; Biegert *et al.*, 2006; Figueira de Morisson Faria *et al.*, 2006; Kitzler *et al.*, 2006.

⁹⁶See, e.g., Becker *et al.*, 1994, 2000, 2001; Brabec *et al.*, 1996; Becker *et al.*, 1997, 2002; Lohr *et al.*, 1997; Becker and Faisal, 2000, 2002; Maeda *et al.*, 2000; Goreslavskii *et al.*, 2001; Yudin and Ivanov, 2001b; Figueira de Morisson Faria *et al.*, 2002; Haan *et al.*, 2002; Panfili *et al.*, 2002; Popruzhenko *et al.*, 2002; Figueira de Morisson Faria, Liu, *et al.*, 2004; Figueira de Morisson Faria, Schomerus, *et al.*, 2004; Jaron-Becker *et al.*, 2004, 2006; Ho *et al.*, 2005; Prauzner-Bechcicki *et al.*, 2005; Haan *et al.*, 2006, 2007; Haan and Smith, 2007.

mation electrons are considered to instantly adjust to the current position of the nuclei. The equilibrium molecular structure is determined by the minimum of the electron energy. Change in this energy with nuclear position creates the force setting the atoms in motion. The resultant rearrangement of atoms is responsible for a change of chemical composition and biological function. Consequently, the fundamental time scale of chemistry and biochemistry is defined by the atomic motion in molecules. It unfolds on a femtosecond scale (Fig. 1) and has been traced by femtosecond laser pulses in real time.⁹⁷

Recent work suggests that attosecond-scale electronic dynamics in molecules may affect chemical changes.⁹⁸ Insight into electronic wave-packet motion in molecules (Breidbach and Cederbaum, 2003; Krause *et al.*, 2005; Remacle and Levine, 2006a) may also shed light on the microscopic mechanisms behind many chemical and biological phenomena such as electron delocalization in aromatic molecules (Poater *et al.*, 2005), biological energy conversion processes (Mirkin and Ratner, 1992; Miyashita *et al.*, 2005), DNA damage and repair (Yavin *et al.*, 2005), long-range electron transfer in biomolecules (Szent-Györgyi, 1941; Gray and Winkler, 2005), and its role in biological signal transduction. Transferring electrons efficiently inside and between molecules (Goldsmith *et al.*, 2005) is also a prerequisite for molecular electronics⁹⁹ and molecular photovoltaics. Molecule-substrate electron transfer, on the other hand, may be relevant to fighting radiation damage in biological imaging with atomic resolution (Fill *et al.*, 2008). Insight into the interplay between collective and collisional processes is of key importance to explore and possibly utilize collective phenomena in many-body systems; clusters offer an ideal test bed for addressing these phenomena (Fennel *et al.*, 2007).

Motivated by a number of questions, we review approaches to accessing electron dynamics in ever more complex atomic assemblies directly in the time domain.

1. Attosecond photoelectron spectroscopy

Just as in atoms, electronic motion in molecules can be triggered by creating a coherent superposition of two or more electronic states. Here we review how this motion can be tracked by APS, by measuring the angular momentum distribution of photoelectrons produced by

⁹⁷For a comprehensive review of femtochemistry, see Zewail, 2000. The state of the art of this evolving field is well represented by Gessner *et al.*, 2006.

⁹⁸The theoretical literature on coupled electronic and nuclear dynamics in molecules is expanding towards the sub-fs domain. Relevant work include Martinez *et al.*, 1996, 1997; Kawata *et al.*, 1999; Harumiya *et al.*, 2002; Kono *et al.*, 2004, 2006; Zhu *et al.*, 2004; Amano and Takatsuka, 2005; Awasthi *et al.*, 2005; Hu *et al.*, 2005; Nguyen and Bandrauk, 2006; Takahashi and Takatsuka, 2006; Takatsuka, 2006, 2007; Nest *et al.*, 2007. For a review, see Levine, 2005.

⁹⁹For recent reviews, see, e.g., Jortner and Ratner, 1997; Ferlinga, 2001; Nitzan, 2001.

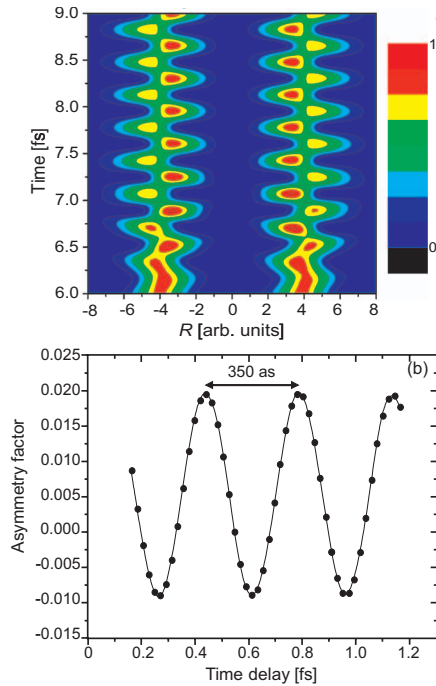


FIG. 53. (Color) Proposal for inducing attosecond electron wave-packet dynamics by a 0.8-fs, 115-nm VUV pump pulse in H_2^+ and probing it with a time-delayed 0.1-fs, 20-nm XUV pulse (Bandrauk *et al.*, 2004). Both pulses are polarized parallel to the molecular axis. (a) Contour plot of the electron probability distribution along the molecular axis for an internuclear distance of eight atomic units vs pump-probe delay. (b) Asymmetry factor $(P_- - P_+)/P_+ + P_-)$ vs delay, where P_+ and P_- represent the probability of observing the electron liberated by the XUV probe in the positive or negative direction (along the molecular axis), respectively. Adapted from Bandrauk *et al.*, 2004.

a time-delayed sub-fs XUV pulse (probing, IID1; detection, IIIB2; see Tables II and III).¹⁰⁰ Consider the simplest case: a coherent superposition of the two lowest-energy states of the H_2^+ molecular ion,

$$\psi(\mathbf{r}, t) = c_1 \phi_1(\mathbf{r}) e^{-iW_1 t} + c_2 \phi_2(\mathbf{r}) e^{-iW_2 t}, \quad (50)$$

where indices 1 and 2 represent the $1\sigma_g$ (ground) electronic state and $2\sigma_u$ (the lowest excited) electronic state, respectively. In their simulations, Bandrauk *et al.* (2004) created this state with a sub-fs VUV pulse and probed the unfolding wave-packet dynamics with a 100 as XUV probe via photoionization. They found that the unfolding intramolecular electronic motion [Fig. 53(a)] can be

¹⁰⁰Scrinzi *et al.*, 2001a, 2001b; Bandrauk *et al.*, 2004; Yudin *et al.*, 2005, 2006; Chelkowski *et al.*, 2006. In the femtosecond regime, the technique was demonstrated by Strasser *et al.*, 2007.

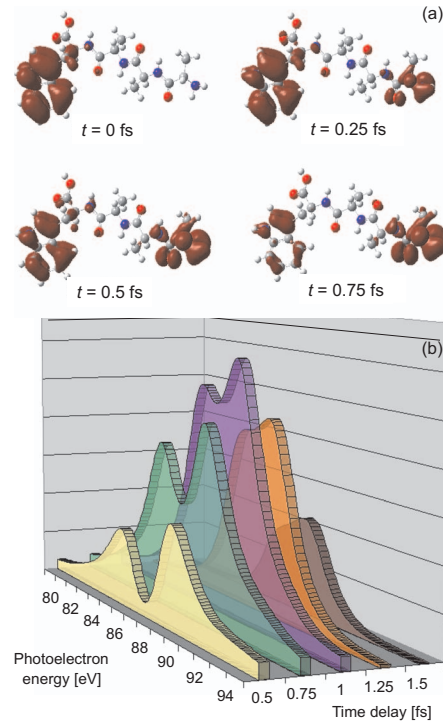


FIG. 54. (Color) Computed ultrafast positive charge (hole) migration in a tryptophane-terminated tetrapeptide (Remacle and Levine, 2006a, 2007). (a) The hole density shown in red indicates that the charge swings across the entire peptide from the aromatic amino acid on the left to the N end on the right within less than one femtosecond, following excitation of the electronic wave packet on an attosecond time scale. This hyperfast charge migration is proposed to be probed by measuring the kinetic energy distribution of photoelectrons released by a time-delayed sub-fs XUV pulse. (b) A series of such freeze-frame spectra calculated for a 250-as, 95-eV probe pulse at different pump-probe delays. From Remacle and Levine, 2007.

traced by collecting photoelectrons in two opposite directions along the molecular axis aligned with the light fields [Fig. 53(b)].¹⁰¹¹⁰²

Inspired by the experiments of Weinkauf *et al.* (1995, 1996, 1997), theoretical studies of electronic wave-packet dynamics have been extended for the charge (hole or electron) transport in large, biologically relevant systems.¹⁰³ Complexity arises here in several ways: the initially localized wave packet (created by photoexcitation) is composed of a large number of stationary electronic states and electron correlation must be considered during charge transport. Beyond its relevance to molecular electronics, photovoltaics, and biology, elec-

¹⁰¹The measurement also reveals the spectral phase of the attosecond probing pulse (Itakura, 2007).

¹⁰²Studies were extended to asymmetric molecules (Remacle *et al.*, 2007).

¹⁰³Martinez *et al.*, 1996, 1997; Remacle and Levine, 1997, 1999, 2006a; Cederbaum and Zobeley, 1999; Remacle *et al.*, 1999; Breidbach and Cederbaum, 2003, 2005; Hennig *et al.*, 2005; Kuleff *et al.*, 2005.

tron charge transfer in extended molecular systems may also play a key role in the fragmentation of large molecules observed by Weinkauf, Schlag, and co-workers (1995, 1996). The concept of “charge-directed reactivity” (Weinkauf *et al.*, 1997; Remacle *et al.*, 1998) may offer a new route to chemical reaction control.

APS, possibly combined with coincidence detection of the reaction products (IIC2; see Table III), lends itself to unraveling the mysteries and implications of charge transfer in molecular systems. Viability of this approach depends on the sensitivity of this probing in *large systems*. Results of Levine and Remacle (2006) give us grounds to be optimistic. Figure 54(a) depicts hole migration in a tryptophane-terminated tetrapeptide following sub-fs photoionization (implemented either with a cosine-shaped few-cycle wave: IC1, or with an intense VUV pulse: ID1; see Table I). Figure 54(b) reveals that the sub-fs photoelectron probe is highly sensitive to the unfolding charge migration (Remacle and Levine, 2007), offering a means of monitoring it with attosecond resolution.¹⁰⁴ In our view, real-time observation (and possibly control) of electron transfer in large molecular systems, such as DNA (Kato *et al.*, 2004), is among the most exciting challenges attosecond technology faces today.

APS was proposed for observing ultrafast electron and structural motion in clusters (Georgescu *et al.*, 2007). Experiments of this kind may address fundamental questions about the way collisions destroy collective dynamics in many-body systems (Fennel *et al.*, 2007) and offer information that no conventional (time-integrated) measurement can provide due to dissipation (Georgescu *et al.*, 2007).

2. Attosecond high harmonic imaging

HHG from laser-atom or laser-molecule interaction carries information on the structure (Lein, Hay, *et al.*, 2002) and dynamics (Averbukh, 2004) of the bound electronic wave function interfering with the returning wave packet.¹⁰⁵

Look at the component of the dipole moment responsible for high-frequency emission during recollision,

¹⁰⁴The sub-fs photoelectron probe is also sensitive to structural changes (which did not occur in this example), due to dynamic shifts of core levels following rearrangement. In case of fragmentation, coincidence detection of photoelectrons and fragments may help in retrieving the complex electron-nuclear dynamics. Another option is to map out the kinetic energy release of the molecular ion fragments following a Coulomb explosion after the probe pulse (Stapelfeldt *et al.*, 1998; Lin *et al.*, 2006; Tong and Lin, 2006).

¹⁰⁵Lein, Hay, *et al.*, 2002; Niikura *et al.*, 2002; Lein *et al.*, 2003; Averbukh, 2004; Itatani *et al.*, 2004; Kanai *et al.*, 2005; Lein, 2005; Niikura *et al.*, 2005; Vozzi *et al.*, 2005; Zimmerman *et al.*, 2005; Baker *et al.*, 2006; Chirila and Lein, 2006a, 2006b; Le, Morishita, and Lin, 2008; Morishita *et al.*, 2008; for a review, see Lein, 2007.

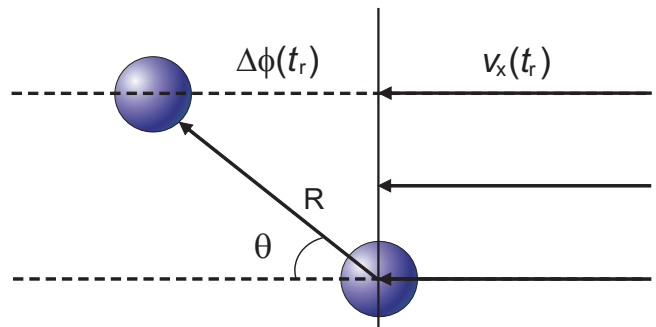


FIG. 55. (Color) Origin of interference in harmonic emission from a diatomic molecule. Returning electron with velocity v_x interferes with the ground state wave function—a superposition of atomic orbitals centered around the two nuclei spaced by R . The phase delay accumulated by the returning electron between the two nuclei is $\Delta\phi(t_r)=v_x(t_r)R \cos \theta$. From Lein, Hay, *et al.*, 2002.

$d_h(t)=\langle\psi_b|d|\psi_c\rangle+c.c.$ As compared with Eq. (22), we replaced $|\psi_g\rangle$ with $|\psi_b\rangle$ to allow the bound portion of the wave function to be different from the ground state $|\psi_g\rangle$. In the framework of the SFA, stationary phase analysis of $d_h(t)$ (Ivanov *et al.*, 1996) implies that, in good approximation, at every moment t the transition matrix element is proportional to the matrix element between the bound wave packet and a *single* continuum state corresponding to the instantaneous velocity $v_x(t_r)$ of the classical electron recolliding with the parent ion at this moment in time. This velocity $v_x(t_r)$ of the recolliding electron determines the frequency of the emitted radiation:

$$\Omega(t_r)=v_x^2(t_r)/2 + I_p. \quad (51)$$

Now consider harmonic generation by a diatomic molecule (see Fig. 55), and approximate the electronic ground state as a linear superposition of two atomic orbitals $|\psi^{(A)}\rangle$ centered at each of the two nuclei:

$$\psi_b=\frac{1}{\sqrt{2}}[\psi^{(A)}(\mathbf{r}-\mathbf{R}/2)+\Lambda\psi^{(A)}(\mathbf{r}+\mathbf{R}/2)], \quad (52)$$

where $\Lambda=1$ and $\Lambda=-1$ correspond to even and odd superposition, respectively, and \mathbf{R} is the vector connecting the two nuclei; see Fig. 55. The recombination matrix element becomes a sum of two identical contributions from each atomic orbital (each of the two nuclei). These two amplitudes interfere with each other much as in Young’s double-slit experiment:

$$d_h(t_r) \propto d_h^{(A)}(t_r)\{1+\Lambda \exp[i\Delta\phi(t_r)]\}, \quad (53)$$

where $d_h^{(A)}(t_r)$ is the contribution from a single atom and $\Delta\phi(t_r)=v_x(t_r)R \cos \theta$. For more complex molecules, the induced dipole will contain interference of several amplitudes with relative phases determined by the scattering centers’ positions. The resultant interference in the

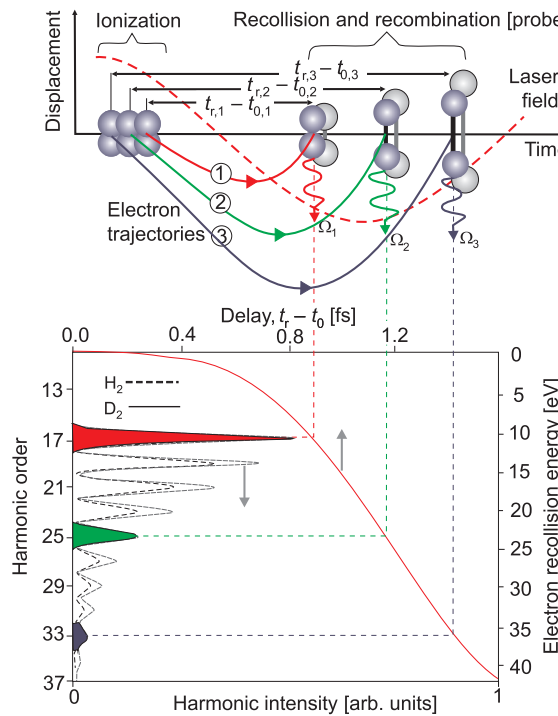


FIG. 56. (Color) Probing initial temporal evolution of nuclear coordinates in a molecule, following sudden excitation by ionization. The nuclear motion is mapped onto the spectral intensity distribution of high-order harmonics via the energy chirp of the recolliding electron responsible for the harmonic emission (Baker *et al.*, 2006). For the simplest case of a diatomic molecule, such as H_2 or D_2 , the internuclear separation starts increasing at the moment of ionization. For increasing recollision instants $t_{r,1}$, $t_{r,2}$, and $t_{r,3}$ it increasingly deviates from the initial value (upper panel). The induced dipole responsible for the harmonic emission includes the overlap between vibrational wave functions in the neutral molecule and its ion. This overlap decreases with increasing internuclear separation in the ion, reducing the harmonic intensity. The monotonic dependence of the recollision energy W_r on the recollision time t_r for either short or long trajectories (Fig. 20) gives a one-to-one map between harmonic energy $\Omega(t_r) = W_r(t_r) + I_p$ and the recollision time t_r . The red line in the lower panel connects $\Omega(t_r)$ with t_r for short trajectories. From the decrease of the harmonic signal and knowledge of $W_r(t_r)$, the different internuclear separations at different moments of time following ionization can be determined. The technique is called PACER: probing attosecond dynamics by chirp encoded recollisions. Adapted from Baker *et al.*, 2007.

harmonic emission spectrum therefore reflects the structure of the molecule. This theoretical prediction (Lein, Hay, *et al.*, 2002) has stimulated further theoretical activity.¹⁰⁶ Experiments for diatomic and triatomic molecules (Itatani *et al.*, 2004; Kanai *et al.*, 2005; Vozzi *et al.*, 2005) have demonstrated clear minima in the harmonic spectra, even though their exact origin is currently un-

¹⁰⁶See, e.g., Zhou *et al.*, 2005a, 2005b; Chirila and Lein, 2006a, 2006b; Gordon *et al.*, 2006; Le *et al.*, 2006; Santra and Gordon, 2006; Patchkovskii *et al.*, 2006; and, for a review, Lein, 2007.

clear (the minima appear to shift with the intensity of the driving field). With molecular alignment (Torres *et al.*, 2007) and/or elliptic polarization of the driving field (Kitzler *et al.*, 2007), attosecond high harmonic imaging (AHI) hold promise for imaging molecular structures and multielectron dynamics. However, theory will have to meet a formidable challenge, especially for polyatomic molecules: quantitative description of rich laser-driven multielectron dynamics.¹⁰⁷

AHI also provides access to nuclear motion (Lein, 2005; Baker *et al.*, 2006, 2008; Wagner *et al.*, 2006). For example, one can excite vibrations in a neutral molecule and probe them via a high-order harmonic generation signal, which shows modulations as a function of the vibrational motion (Wagner *et al.*, 2006). Alternatively, one can probe the dynamics in the ion. As soon as the electron is liberated from the molecule, a molecular ion is formed. The equilibrium configuration of the molecular ion is usually different from that of the neutral molecule. As a consequence, the nuclei are set in motion at the same instant t_0 as the electron is liberated. This correlation along with the chirped nature of the recolliding electron wave packet, see Fig. 20, permits one to map the nuclear motion onto the frequency spectrum of the harmonic emission. Drawing on the theoretical analysis of Lein (2005), Baker *et al.* (2006, 2008) put this concept into practice. This pioneering experiment is reviewed in Fig. 56. Implemented with a few-cycle (ideally single-cycle) IR laser pulse, AHI may allow one to capture both electronic and nuclear rearrangement in molecules within the first few femtoseconds following excitation.

3. Attosecond electron diffraction

Observation of short-lived transient structures calls for the combination of ultrafast probing techniques with those of conventional diffraction: following excitation by an ultrashort pump pulse the sample is exposed to a delayed electron or x-ray probe pulse. Time-resolved x-ray and electron diffraction as well as microscopy have recently attained sub-ps resolution with x-ray pulses emitted from laser-driven plasma sources¹⁰⁸ and with electron bunches (with energies ranging from ~ 30 to ~ 300 keV, corresponding to de Broglie wavelengths of ~ 0.06 to 0.02 Å) that are produced by femtosecond

¹⁰⁷In atoms and diatomic molecules, correlated multielectron (mostly two-electron) dynamics has been extensively studied; see, e.g., Watson *et al.*, 1997; Tong and Chu, 1998; Chu and Chu, 2001; Lein, Engel, *et al.*, 2001; Lein, Gross, *et al.*, 2001, 2002; Lein, Kreibich, *et al.*, 2002; Becker and Faisal, 2005; Caillet *et al.*, 2005; Krause *et al.*, 2005; Klamroth, 2006; Gordon *et al.*, 2006; Jordan *et al.*, 2006; Patchkovskii *et al.*, 2006; Rohringer *et al.*, 2006; Santra and Gordon, 2006; Gräfe and Ivanov, 2007; Volkova *et al.*, 2007; Walters *et al.*, 2007; Xie *et al.*, 2007.

¹⁰⁸For reviews, see Rousse *et al.*, 2001; Bressler and Chergui, 2004; Pfeifer, Spielmann, and Gerber, 2006.

photoemission followed by acceleration via a dc field.¹⁰⁹

Electron scattering cross sections exceed those of x-ray scattering typically by five to six orders of magnitude, but this comes at the expense of rapid pulse broadening due to Coulomb repulsion and/or velocity dispersion, which has so far limited resolution to a few hundred femtoseconds. In this section we discuss possible ways of improving the temporal resolution of ultrafast electron diffraction to the few-fs and sub-fs regime using the recolliding electron in an ionizing molecule or a microwave-accelerated, phase-focused single-electron pulse for recording diffraction images of transient molecular structure.

Electron diffraction upon recollision can be used to record and retrieve information on molecular structure (Lein, Marangos, *et al.*, 2002; Spanner *et al.*, 2004; Yurchenko *et al.*, 2004; Morishita *et al.*, 2008; Murray and Ivanov, 2008; Okunishi *et al.*, 2008; Ray *et al.*, 2008; Zhou *et al.*, 2008) and was recently demonstrated experimentally (Meckel *et al.*, 2008). When the electron returns to the parent ion, “elastic” scattering takes a diffraction image of the parent molecule.¹¹⁰ In laser-induced electron diffraction, temporal confinement of the recolliding electron wave packet adds sub-fs temporal resolution to the spatial resolution dictated by the de Broglie wavelength of the returning electron. With NIR ($\lambda_L \approx 0.8 \mu\text{m}$) and IR ($\lambda_L \approx 2 \mu\text{m}$) light one may achieve recollision energies W_r in excess of 0.1 and 1 keV, respectively (see Fig. 20), implying a de Broglie wavelength of $\approx 1 \text{ \AA}$ and well below 1 \AA , respectively. Few-cycle (ideally single-cycle) laser pulses will benefit the technique by maximizing W_r and suppressing multiple recollision and related undesirable interference effects (Spanner *et al.*, 2004; Yurchenko *et al.*, 2004; Hu and Collins, 2005).

Figure 57 shows results of the calculations of Spanner *et al.* (2004) for a diatomic molecule aligned perpendicularly to laser polarization. The diffraction image is clear when proper directions and energies corresponding to a fixed moment of recollision are selected; see Fig. 57(b). When implemented with a sub-two-cycle IR laser pulse,

¹⁰⁹Since first demonstrations in the 10–100-ps range (Mourou and Williamson, 1982; Williamson *et al.*, 1984; Elsayed-Ali and Mourou, 1988) the technique evolved to sub-ps resolution owing to developments by Ahmed Zewail and Dwayne Miller (Williamson and Zewail, 1991; Williamson *et al.*, 1992, 1997; Ihee *et al.*, 2001; Siwick *et al.*, 2003; Dwyer *et al.*, 2007a, 2007b; Shorokov and Zewail, 2008). For reviews, see Srinivasan *et al.*, 2003; Zewail, 2006.

¹¹⁰Laser-induced electron diffraction is related to a well-established imaging technique, in which an electron freed by a picosecond synchrotron pulse takes an image of the core potential of the parent ion on its way out of the molecule in what is often referred to as a “half collision.” Angle-resolved photoelectron spectra then reveal structural dynamics with picosecond resolution; see, e.g., Becker and Shirley, 1996; Gessner *et al.*, 2002; Kugeler *et al.*, 2004; Weber *et al.*, 2004; Rolles *et al.*, 2005.

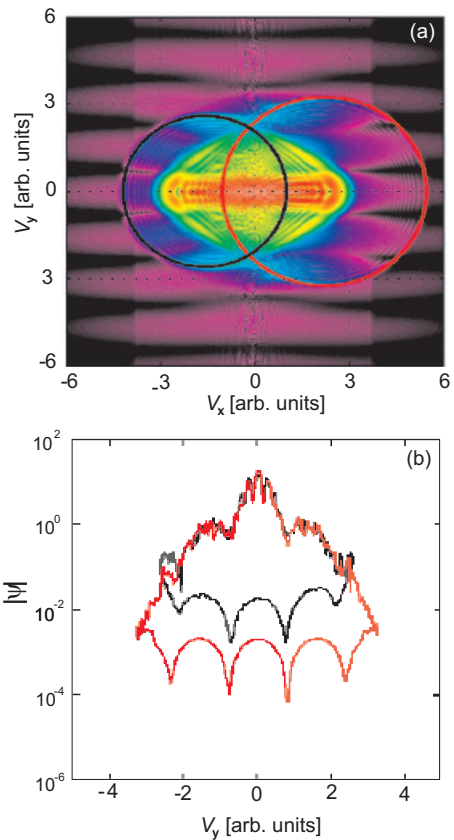


FIG. 57. (Color) Laser-induced recollision imaging of molecular structure by diffraction of strong-field-driven recollision electron (Spanner *et al.*, 2004). Driving field: $\tau_L=5 \text{ fs}$, $\lambda_L=0.8 \mu\text{m}$. (a) Transverse momentum distribution of the recolliding electron diffracted off its parent diatomic molecule. The molecule is aligned parallel to the y axis and the driving laser field is polarized parallel to the x axis. Different colors in (a) correspond to different orders of magnitude, from red to green to blue to violet to black. (b) Selected cuts of the spectrum, which correspond to the fixed (maximum) electron energy during recollision, show clear diffraction pattern. The pattern is particularly clear for electrons scattered at large angles (left part of the black circle, right part of the red circle in panel (a)). Adapted from Spanner *et al.*, 2004.

this technique offers subfemtosecond resolution combined with subangstrom resolution.

Both AHI and laser-induced diffraction imaging rely on ionization. However, in many cases ionization is an invasive probe, inducing significant atomic rearrangements between the instants of release and recollision; see Fig. 56. The following proposal aims at overcoming these restrictions.

Microwave-accelerated sub-fs single-electron pulses. The electron bunches used by conventional ultrafast electron diffraction typically contain several thousand electrons. Repulsion (space charge) between them limits the pulse duration to several hundred femtoseconds on target. Zewail and co-workers were the first to propose the use of single-electron pulses produced at megahertz repetition rates with femtosecond laser oscillators (Lobastov *et al.*, 2005). In order to advance the state of the

art of ultrafast electron diffraction by this approach, two conditions must be met. First, sufficiently intense few-fs pump pulses at megahertz rate must be available. Recent advances in scaling the pulse energy from femtosecond Ti:sapphire oscillators afford promise of fulfilling this condition (Naumov *et al.*, 2005). Second, broadening of the electron pulse on its way from the photocathode to the target due to a spread of the initial electron velocity must be minimized. In the nonrelativistic limit this spread limits the duration of a dc-field-accelerated electron bunch on target to¹¹¹

$$\tau_e = 2.34\sqrt{\Delta W_i}/E_{\text{acc}} \text{ ps}, \quad (54)$$

where ΔW_i is the initial energy spread of electrons in eV and E_{acc} is the acceleration field in MV/m (Schelev *et al.*, 1971). Note that the temporal spread due to velocity dispersion is independent of the distance of the target from the photocathode. Vacuum breakdown limits E_{acc} to less than 10 MV/m (Kinoshita *et al.*, 1987), whereas ΔW_i typically ranges between 0.25 and 1 eV, preventing the delivery of electron pulses on target with a duration substantially less than 0.2 ps by applying a dc accelerating field.

Fill *et al.* (2006) proposed to accelerate single electrons released from a photocathode by a femtosecond laser pulse in a microwave cavity to overcome this limitation (Fig. 58). The microwave acceleration permits applying higher fields due to increased breakdown threshold and, more importantly, time dependence of the accelerating field, $E_{\text{acc}}(t) = E_0 \sin(\omega t + \phi)$, results in different energy gain for particles with different initial energies or release moments. With proper choice of ϕ different initial energies and release instants can be simultaneously corrected (Monastyrskiy *et al.*, 2005).

Figure 58(b) depicts the simulated single-electron wave-packet duration on target along with the corresponding optimum phase as a function of target distance from the accelerating cavity for a 10 fs spread (full width at half maximum) of the instants of release (achievable with a 10-fs laser pulse). For a target distance of $L \approx 1$ cm, a 40-kV electron pulse can have a duration of less than 1 fs on target, demonstrating the power of microwave phase focusing. However, this pulse will be locked to the microwave field rather than to the fs laser pulse (Weisz *et al.*, 2007). Therefore the resolution of a laser-pump–electron-probe experiment will be limited by the jitter between the fs laser and the microwave field. They could already be synchronized to better than 10 fs (Ma *et al.*, 2001). Further progress along with techniques for measurement (Baum and Zewail, 2006; Reckenthaler *et al.*, 2008) may allow single-electron diffraction to access transient electronic structures with atomic resolution in space and time.

¹¹¹From an experimental perspective, Eq. (54) gives the arrival time jitter on target of single electrons with respect to the femtosecond pulse that released them. In quantum mechanics, it is the duration of the electron wave packet on target.

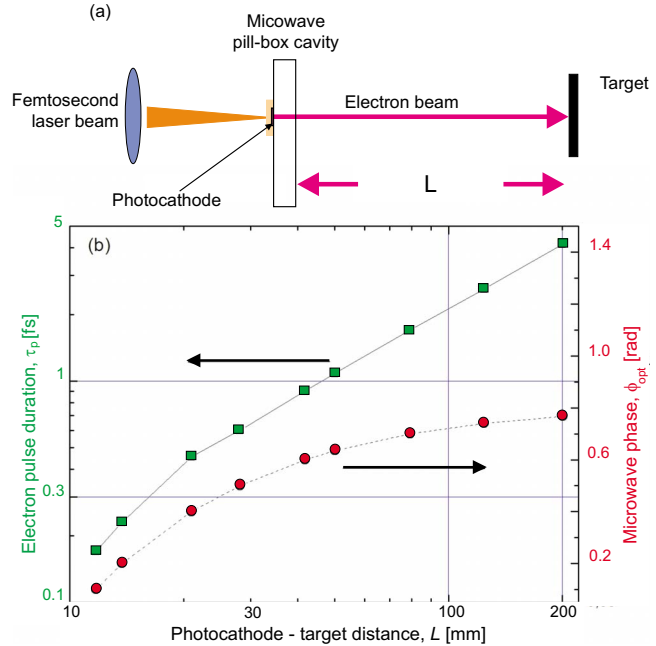


FIG. 58. (Color online) Proposal for a miniature microwave electron accelerator based on a pill-box microwave cavity. (a) The thin photocathode is illuminated from the back side. Accelerated electrons leave the cavity through a small hole on the right side. (b) Minimum electron wave-packet duration on target that can be achieved by optimizing phase focusing by the microwave field (squares); optimum microwave phase, ϕ_{opt} , at the instant of release of the electron (circles). From Fill *et al.*, 2006.

C. Electronic motion in solids and systems on surfaces

The broadest variety of electronic phenomena occurs in condensed matter. The spectrum of excitations localized in isolated particles is enriched with a number of delocalized transitions, charge-transfer processes in guest-host systems, a wealth of collective excitations such as excitons, plasmons or polaritons, charge screening on surfaces, and hot electron as well as electron-hole dynamics. These dynamics often unfold on a few-fs to sub-fs time scale. Capturing them in real time and controlling them on the electronic time scale with the electric field of light will allow researchers to explore and approach the limits of electron-based information technologies. Here we address the first steps towards attosecond resolution becoming commonplace in solid-state and surface science and related challenges.

1. Extension of attosecond spectroscopy to condensed matter

Time-resolved (two-photon) photoemission spectroscopy has been the most widely used approach to capturing transient electron states in solids and surfaces. In its first implementations an ultrashort VIS or UV pump pulse excites electrons to states above the Fermi level and a time-delayed VIS or UV probe pulse raises the electrons' energy to positive values, resulting in photoemission. The time evolution of the transient population

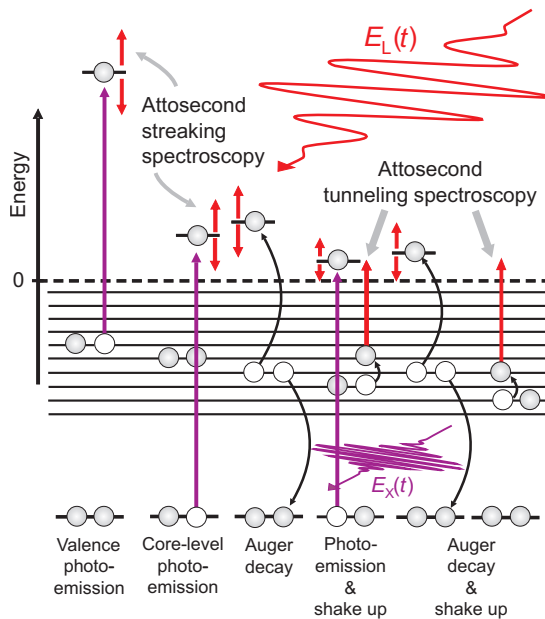


FIG. 59. (Color) Electronic excitation and relaxation processes in solids and possible ways of tracing these dynamics in real time.

of excited states can then be retrieved by analyzing the photoelectrons' energy and momentum distribution versus pump-probe delay.¹¹²

At increasing excitation intensities, a pump-pulse-induced electron emission background (Riffe *et al.*, 1993) will emerge and extend to ever higher kinetic energies. This undesirable background tends to blur the photoelectron spectrum created by a low-photon-energy probe pulse. Pioneered by Haight and co-workers, extension of time-resolved photoemission to VUV probing photon energies elegantly circumvented this problem.¹¹³ In principle, femtosecond VUV-XUV photoelectron spectroscopy can readily be extended to the attosecond domain by using a UV pump pulse with a duration of about 1 fs or less and a sub-fs XUV probe pulse (excitation, ID1; probing, IID1; detection, IIIB1-2; see Tables I–III, respectively). The former tool is not yet available but is expected to enrich the attosecond toolbox in the foreseeable future (Graf *et al.*, 2008). Alternatively, one may attempt to extend attosecond spectroscopies that have already been successfully demonstrated in the gas phase (Fig. 46) to solid matter; see Fig. 59. ATS may not

¹¹²The technique was first demonstrated in the picosecond time domain by Williams *et al.* (1982) and Yen *et al.* (1982) and with the improvement of the time resolution into the femtosecond (tens of fs) region by Schoenlein *et al.*, 1988; Bokor, 1989; Fann *et al.*, 1992; Schmuttenmaer *et al.*, 1994; Wolf *et al.*, 1996; Höfer *et al.*, 1997; Ogawa *et al.*, 1997. Phase-coherent detection has provided sub-optical-cycle resolution (Ogawa *et al.*, 1997), but retrieval of the dynamic processes from these interferometric time-resolved measurements is a nontrivial problem. For a review, see Petek and Ogawa, 1997.

¹¹³Haight and Silbermann, 1989; Haight, 1995; Bauer *et al.*, 2001; Sifalovic *et al.*, 2002. For a review, see Bauer, 2005.

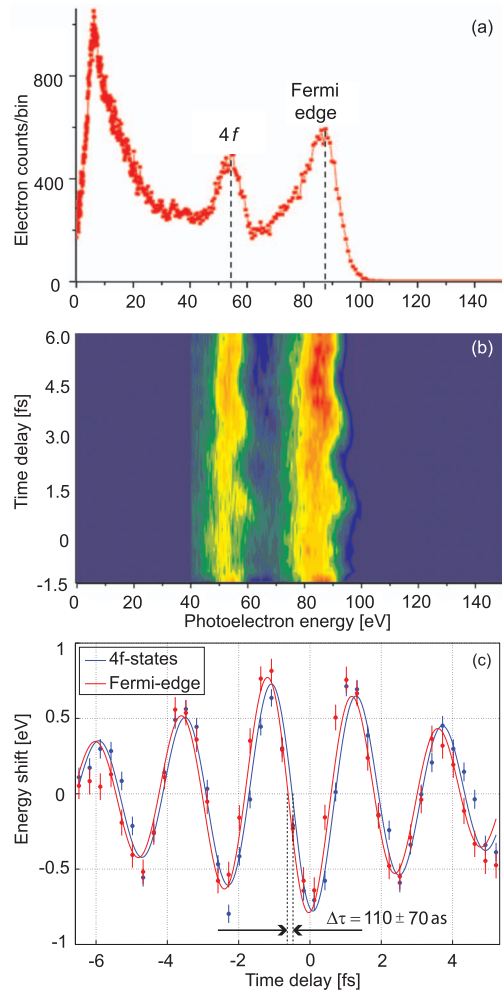


FIG. 60. (Color) Attosecond real-time observation of electronic charge transport in a solid (Cavalieri, Müller, *et al.*, 2007). Electrons were liberated by a single, 300-as, 95-eV XUV pulse in the presence of 5-fs, 750-nm, waveform-controlled pulses in a tungsten crystal. Both *p*-polarized pulses impinged on the sample at grazing incidence. (a), (b) The unperturbed XUV-induced photoelectron spectrum and the corresponding streaking spectrogram, respectively, of core-level electron emission (from the 4f level) and valence-band electron emission (from the Fermi edge) recorded with the few-cycle NIR field. (c) The center-of-mass energy shift of the recorded streaked spectra, revealing a ~110 as delay in emission of core electrons with respect to the emission of conduction band electrons. Courtesy of A. Cavalieri.

be readily applicable to solids because the intense probe tends to generate large bound-excited-state populations before and during inducing photoemission (Quéré *et al.*, 2000). AST (triggering, IE1; probing, IIC1; detection, IIIB1-2; see Tables I–III, respectively) does not suffer from this problem.

Following the first observation of the laser-assisted photoelectric effect from a solid by Miaja-Avila *et al.* (2006), Cavalieri, Müller, *et al.* (2007) performed an attosecond spectroscopic experiment in a solid; see Fig. 60. The experiment has revealed (i) a sub-fs emission time both for the delocalized conduction-band electrons re-

leased from states near the Fermi edge as well as for the localized core electrons originating from the $4f$ state, and (ii) a delay in emission of the latter by approximately 100 as. Real-time access to atomic-scale charge transport dynamics in solids is now a reality.

2. Challenges

A thorough review of electron motions unfolding within a few femtoseconds or less in solids and on surfaces is beyond the scope of this paper. Here we choose a few examples to demonstrate the tremendous potential for gaining new, in-depth insight into fundamental processes in condensed matter with the help of attosecond tools and techniques.

Charge screening in solids is one manifestation of many-body interactions (Mahan, 1993). It is predicted to establish within the inverse plasma frequency, on time scales ranging from hundreds of attoseconds in metals (Alducin *et al.*, 2004; Borisov *et al.*, 2004; Silkin *et al.*, 2007) to tens of femtoseconds in semiconductors (Huber *et al.*, 2001). One long-standing mystery in solid-state physics has been the high-energy tail of metallic x-ray spectra. Screening of the hole and electron created upon x-ray absorption has been assumed to be responsible for the observed anomalous behavior (see, e.g., Yue and Doniach, 1973; Canright, 1988), but lack of reliable data on the screening time has prevented validation of theoretical models so far. Attosecond probing of screening will also clarify the existence of unscreened bare Coulomb collisions on ultrashort time scales (Kwong and Bonitz, 2000) and that of transient excitonic states in metals before the onset of screening (Cao *et al.*, 1997; Schöne and Ekardt, 2000). The dynamics of surface excitations is yet another area offering many challenges (Echenique *et al.*, 2004).

Electron transfer across interfaces plays a central role in surface chemistry. Insight into charge transfer dynamics in macromolecular assemblies (Siffalovic *et al.*, 2004) and between adsorbate and bulk (conduction-band) states will contribute to the advancement of molecular electronics (Nitzan and Ratner, 2003; Zhu, 2004; Remacle and Levine, 2006b) and benefit the development of more efficient solar cells (O'Reagan and Graetzel, 1991). So far, the core-hole-clock technique has been the only approach providing access to charge transfer dynamics on a few-femtosecond or shorter time scale.¹¹⁴ It is based on high-resolution spectroscopy of autionization following resonant core excitation. The lifetime of the core hole provides an internal reference for clocking charge transfer from the excited bound state, allowing one to determine electron transfer times with sub-fs resolution (Schnadt *et al.*, 2002; Föhlisch *et al.*, 2005), but require careful analysis of competing relaxation channels in molecular adsorbates (Kirchmann *et al.*, 2006). Direct sub-fs probing will therefore be particularly help-

ful in complex molecular architectures (Barth *et al.*, 2005).

Collective electronic motion in nanosystems. Nanoscopic materials have attracted interest because of their engineerable electrical and optical properties. Collective electron density fluctuations play a role in most of their potential applications. Of particular interest are those that can be excited at metal-vacuum or metal dielectric interfaces: surface plasmons (Raether, 1988). The prospect of nanoplasmonic devices (Barnes *et al.*, 2003; Van Duyne, 2004) and applications ranging from medical and pharmaceutical screening through environmental monitoring to subwavelength optics has stimulated efforts to gain an insight into the fundamental dynamics of plasmon excitations (Kubo *et al.*, 2005, 2007) and identify ways of controlling it. The natural time scale of collective electron dynamics in metallic nanosystems is less than 1 fs. A combination of photoelectron emission microscopy with AST will provide access to these dynamics with nanometer and sub-fs resolution (Stockman *et al.*, 2007).

D. Future prospects: Steering and imaging atomic-scale electronic motion

1. Steering electrons with the electric field of synthesized light

Here we address two questions related to extending attosecond control of electronic motion to complex systems ranging from simple (diatomic) molecules through complex (bio)molecules to nanostructures and assemblies. First, can synthesized (waveform-controlled) light fields be used for steering electron wave packets in molecules on the electronic time scale where nuclear motion is essentially frozen? Second, can such light field control on electronic to chemical time scales affect the outcome of structural re-arrangements or chemical reactions?

Barth and Manz (2006a, 2006b) suggested that the former question may be answered affirmatively. In their numerical experiment, a circularly polarized few-cycle UV laser pulse was applied to a Mg-porphyrin model system. This pulse induced a giant unidirectional ring current, with its strength and direction controlled by the instantaneous amplitude and the direction of rotation of the UV electric field; see Fig. 61. Beyond demonstrating the control of electronic motion in a molecule, this study also revealed a route to generating—for a period of a few femtoseconds—a unipolar (nonoscillating) magnetic field of unprecedented strength. Barth and Manz predicted that a UV pulse of moderate intensity ($\sim 10^{12} \text{ W/cm}^2$) would be able to generate a giant ring current on the order of 0.1 mA within a molecule. A magnetic field on the order of 10^4 T would be required to induce the same ring current (Steiner *et al.*, 2005).

We begin our discussion of the second question by reviewing a recent experiment on sub-fs control of electron localization during breakup of a D_2^+ molecule

¹¹⁴For reviews, see Wurth and Menzel, 2000; Brühwiler *et al.*, 2002; Föhlisch, 2006.

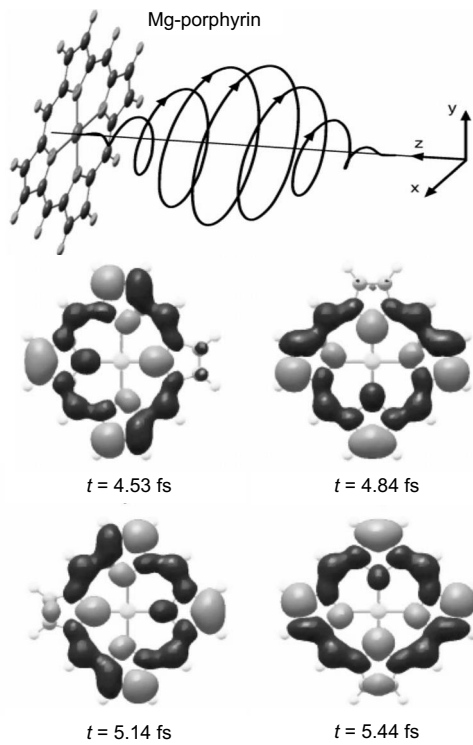


FIG. 61. Induction of unidirectional electronic ring currents in molecules. The upper panel shows an eight-cycle circularly polarized UV pulse propagating along the z axis to impinge upon a Mg-porphyrin molecule, with its plane aligned perpendicular to the z axis. The arrows indicate the time evolution of the field acting on the molecule. The lower panel shows several snapshots of instantaneous electron density distribution during the central part of the driver pulse, revealing a ring current driven by the rotating electric field. From Barth and Manz, 2006a, 2006b.

(Kling *et al.*, 2006).¹¹⁵ Ionization of D_2 was followed by electron recollision with the molecular ion D_2^+ , exciting the remaining bound electron into the dissociative $|\sigma_u\rangle$ state, still in the presence of the ionizing few-cycle laser pulse, which creates a coherent superposition of the ground $|\sigma_g\rangle$ and first excited $|\sigma_u\rangle$ state. This implies electron oscillation between the left and right nuclei as the nuclei move apart. Beyond some critical internuclear distance, the electron can no longer tunnel through the potential barrier emerging between the two nuclei. Which of the two nuclei will catch the electron is determined by the phase of the oscillatory electron motion relative to the dissociation. This phase, in turn, is controlled with attosecond precision by the carrier-envelope phase of the waveform;¹¹⁶ see Fig. 62. The experiment reveals that (i) attosecond electron motion does affect chemical changes and (ii) attosecond shaping of the light

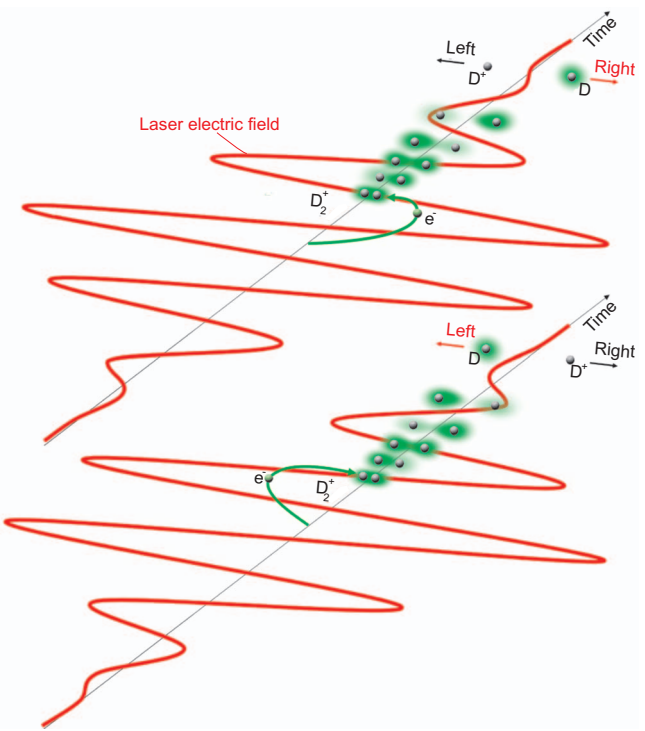


FIG. 62. (Color) Controlling electron localization during molecular dissociation with the electric field of light (Kling *et al.*, 2006). Laser-induced ionization and subsequent recollision of the freed electron triggers dissociation of the molecular ion (D_2^+). Controlling the electric field evolution in the ionizing few-cycle NIR laser field allows one to control the motion of the remaining electron (with its probability distribution shown in green) around the nuclei (spheres) while they move apart. A cosine-shaped waveform with its peak field pointing to the left or to the right forces the electron to stick—with a high probability—to the atom leaving the molecule to the right or left directions, respectively.

field in a femtosecond pulse can be used to control it (Weitzel, 2007).

Nevertheless, an electron wave packet composed of many stationary states means population of many potential energy surfaces (PESs). Different PESs often lead to different products. That is, exciting a large number of electronic states will create multiple multidimensional rovibrational wave packets which will evolve along their potential energy surfaces towards different outcomes. However, this does not necessarily mean that attosecond waveform engineering and sub-fs electron wave packet formation and steering has no future in controlling molecular dynamics.

One may speculate on a new approach: creating an electron wave packet with a sub-fs UV pulse and subsequently steering it with the shaped waveform of a light field that is strong enough to induce substantial dynamic shifts of the potential surfaces. Under these circumstances stationary PESs lose their meaning and the light-field-steered electron wave-packet motion may possibly have a dominant influence on the outcome of reactions

¹¹⁵For theoretical research, see Haljan *et al.*, 1997; Bandrauk *et al.*, 2004; Roudnev *et al.*, 2004; Hu *et al.*, 2006; Roudnev and Esry, 2007; Tong and Lin, 2007a, 2007b.

¹¹⁶He *et al.* (2007) proposed that electron localization can be made more efficient by independent start using a two-pulse control scheme.

in complex systems.¹¹⁷ This approach, if it were to work, would be new in that synthesized light fields (Fig. 14) would shape the density of bonding electrons in a molecule¹¹⁸ in a desired way on the electronic, i.e., attosecond, time scale while maintaining this control over molecular, i.e., femtosecond, time scales, allowing the desired unimolecular reaction to be completed. Only experiments will tell us whether reality lives up to these visions.

An important question for the development of science and technology is whether electron-based information processing and storage can possibly be down-scaled to atomic dimensions and sped up to the atomic time scale, i.e., to optical frequencies. Can these ultimate limits be approached, or reached and implemented in practical devices by exploiting electric interactions (electronics), magnetic interactions (spintronics), or collective electron motion (plasmonics)? Can the electric field of infrared or visible light be used to control electric signals in future atomic-scale chips,¹¹⁹ just as microwave fields do in current state-of-the-art nanoscale circuits, realizing the ultimate electron-based information technology: (solid-state) lightwave electronics? Answering these questions may be one of the central missions of attosecond science.

2. 4D imaging of electrons with subatomic resolution in space and time

In the experiments discussed in this section, tracing of electronic motion meant real-time observation of transitions of electrons between quantum states of different energies. No explicit information about changes of the probability distribution of the electrons' position has been acquired. Angle-resolved attosecond photoelectron spectra may provide access to dynamic changes in the electron distribution in simple systems, but this approach may encounter difficulties in more complex structures. Only microscopy and diffraction allows acquisition of direct information on the electron density distribution irrespective of the complexity of the system.

First, consider possibilities in microscopy. The availability of light pulses with characteristics controlled on a sub-fs scale offers several ways of furnishing well-established microscopic techniques with attosecond resolution. In photoemission electron microscopy (PEEM) the continuous-wave UV or XUV light source must simply be replaced with one emitting this radiation in the

¹¹⁷The concept of relating site-selective reactivity to charge transfer, i.e., the existence of nonstationary electronic states, in large molecules (Weinkauf *et al.*, 1997), based on the assumption: “reactivity follows charge,” is a first push in this direction.

¹¹⁸By superimposing many orbitals and adjusting this superposition during the pulse.

¹¹⁹Note that this light-field control of electric current is different from earlier demonstrations, where quantum interference governed by the cycle-averaged intensity (rather than the electric field) of light has controlled injection of electric current in semiconductors (see Costa *et al.*, 2007, and references therein).

form of attosecond bursts (Stockman *et al.*, 2007). In scanning tunneling microscopy (STM), on the other hand, electron emission from the nanometer-sized tip may be confined to several hundred attoseconds by launching electrons with a cosine-shaped few-cycle light pulse via optical field ionization (Hommelhoff *et al.*, 2006). Last but not least, ultrafast electron microscopy (UEM, Shorokhov and Zewail, 2008) may be advanced into the few-fs and possibly sub-fs regime by microwave (Fill *et al.*, 2006; Veisz *et al.*, 2007) and optical (Plettner *et al.*, 2006) acceleration. In this way several-nanometer (PEEM) and angstrom (STM, UEM) resolution in space can be combined with attosecond resolution in time.

The extension of diffraction imaging from the three spatial dimensions to the fourth, temporal, dimension is conceptually even more straightforward. Again, the electron or x-ray beam used for mapping the electron density in molecules or crystals must be replaced with a short pulse. The high (multi-keV) particle energy reconciles the apparently conflicting requirements of narrow relative energy distribution ($\leq 1\%$) and ultrashort pulse duration. The ultrashort electron or x-ray pulse allows recording snapshots of the dynamic evolution of the electron density distribution following excitation by a short pump pulse. Dynamic changes in the electron distribution may occur due to (i) the motion of the nuclei; the electron cloud virtually instantly adjusts to this motion; or (ii) electronic excitation. The former process evolves on a multi-fs time scale and mirrors atomic rearrangement in molecules or solids. It has already been imaged with sub-ps time resolution.¹²⁰ Electronic rearrangements may unfold within attoseconds. An example is shown in Fig. 63. The above-discussed techniques for sub-fs x-ray (Sec. VI) and electron (Sec. VII.B.3) pulse generation will open the way to 4D imaging of electronic as well as nuclear motion with picometer resolution in space and attosecond resolution in time.

VIII. CONCLUSIONS AND OUTLOOK

The emerging experimental and theoretical tools of attoseconds physics provide, for the first time, real-time access to the motion of electrons on atomic and subatomic scales. Access means both capture and steering with a speed matched to the rapidity of the fastest electronic phenomena. Microscopic motion of electrons plays a key role in advancing the technology of compact x-ray sources, or pushing electronics and magnetic storage to ever smaller dimensions and ever higher speeds; in triggering chemical reactions; in biological signal transduction and the damage and repair mechanisms of DNA; and in the undesirable and desired radiation-

¹²⁰For reviews, see Pfeifer, Spielmann, *et al.*, 2006; Zewail, 2006.

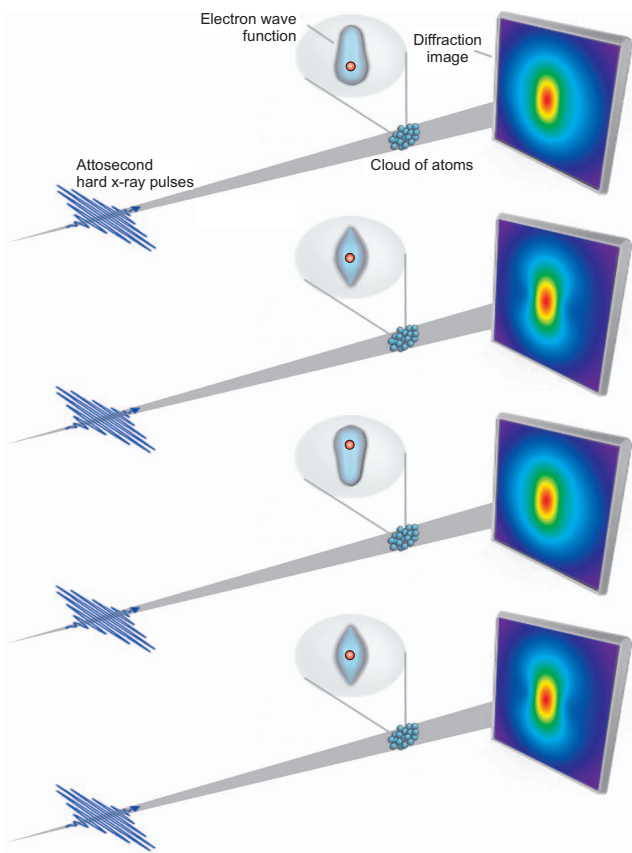


FIG. 63. (Color) Schematic of attosecond diffraction imaging of dynamic changes of atomic-scale electron distribution. As an example, hydrogen atoms excited into the $1S\text{-}2P$ coherent superposition state have been exposed to 100-as, 1-Å x-ray pulses in a numerical experiment (Yakovlev, 2007). From the recorded freeze-frame diffraction images shown on the screens, the instantaneous electron density distribution can be determined. From a series of such images electronic motion can be reconstructed with attosecond resolution in time and picometer resolution in space. Courtesy of V. Yakovlev.

induced damage to biological matter in cancer diagnostics and therapy, respectively.¹²¹

The emergence and expected future evolution of attosecond science demonstrate how different scientific disciplines and technologies, several of which have been recognized with the Nobel Prize, build upon each other to push the frontiers of science and technology. Lasers (Nobel Prize: Basov, Prokhorov, Townes) and perturbative nonlinear optics (Nobel Prize: N. Bloembergen) have permitted the generation and metrology of femtosecond laser pulses with well-controlled amplitude, opening the way to controlling and tracking chemical dynamics (Nobel Prize: A. H. Zewail). Chirped-pulse amplification and chirped multilayer mirrors have permitted routine generation of intense light pulses and pushing—with the generation of quasi-single-cycle laser

¹²¹For questions that may serve as a compass for the possible future evolution of attosecond physics, see www.attoworld.de

light—the frontiers of ultrafast optics to its ultimate limit set by the oscillation cycle of the light field. Adding the frequency-comb technique (Nobel Prize: T. W. Hänsch) to these technologies has permitted control over the attosecond evolution of ultrastrong light fields, which along with photoelectron spectroscopy (Nobel Prize: K. M. Siegbahn) has opened the door to controlling and measuring the atomic-scale motion of electrons.

With the advent of lightwave electronics (Fig. 5), sub-fs tools have become available for direct attosecond real-time observation of the motion of electrons in atoms, molecules, and solids. Based on strong-field interactions, current sub-fs electron and photon pulses are delivered with particle energies limited to \sim 100 eV. Future expansion of attosecond science to relativistic light-electron interactions affords promise of a dramatic increase in energy and further decrease in duration of the probing particles. The capability of recording movies of any microscopic motion outside the atomic core will be the consequence of these advances.

GLOSSARY OF ABBREVIATIONS

AAS	Attosecond absorption spectroscopy
AHI	Attosecond harmonic imaging
APS	Attosecond photoelectron spectroscopy
AST	Attosecond streaking spectroscopy
ATI	Above-threshold ionization
ATS	Attosecond tunneling spectroscopy
CE	Carrier envelope (phase of ultrashort pulses)
COLTRIMS	Cold-target recoil-ion-momentum spectroscopy
CRAB	Complete reconstruction of attosecond bursts
FROG	Frequency-resolved optical gating
FWHM	Full width at half maximum (e.g., of a pulse intensity profile)
HHG	High-order harmonic (radiation)
IFEL	Inverse free electron laser
IR	Infrared (radiation)
NSDI	Nonsequential double ionization
NIR	Near-infrared (radiation)
PES	Potential energy surface
QPM	Quasi-phase-matching (of high-order harmonic generation)
RABBITT	Reconstruction of attosecond beating by interference of two-photon transitions
SAE	Single active electron (model)
SFA	Strong-field approximation
SPM	Self-phase modulation
S/N	Signal-to-noise (ratio)
SPIDER	Spectral phase interferometry for direct electric field reconstruction
UEM	Ultrafast electron microscopy
VIS	Visible (radiation)
VUV	Vacuum ultraviolet (radiation)
XUV	Extreme ultraviolet (radiation)

ACKNOWLEDGMENTS

We are grateful to Andre Bandrauk, Joachim Burgdörfer, Paul Corkum, Lorenz Cederbaum, Raphy Levine, and Albert Stolow for illuminating discussions and Adrian Cavalieri, Reinhard Kienberger, and Anne L'Huillier for careful reading of the manuscript and making numerous valuable comments. We thank Adrian Cavalieri, Eleftherios Goulielmakis, Ulrich Heinzmann, Raphy Levine, Anne L'Huillier, Katsumi Midorikawa, Gerhard Paulus, Valer Tosa, Matthias Uiberacker, and Dave Villeneuve for making artwork and/or results prior to publication available for this work. We gratefully acknowledge several calculations and simulations of Vlad Yakovlev for this review. Last but not least, we are indebted to Barbara Ferus for drawing and editing the artwork and to Bettina Schütz for her support in making the manuscript ready for submission. F.K. acknowledges support of the Munich Centre for Advanced Photonics (www.munich-photonics.de). M.I. acknowledges support of the Bessel prize of the A. v. Humboldt Foundation and the NSERC Special Research Opportunity fund.

REFERENCES

- Abbamonte, P., K. D. Finkelstein, M. D. Collins, and S. M. Gruner, 2004, Phys. Rev. Lett. **92**, 237401.
- Abraham, H., and T. Lemoine, 1899, Compt. Rend. **129**, 206.
- Adair, R., C. Bockelman, and R. Peterson, 1949, Phys. Rev. **76**, 308.
- Agostini, P., and L. F. DiMauro, 2004, Rep. Prog. Phys. **67**, 813.
- Agostini, P., F. Fabre, G. Mainfray, G. Petite, and N. K. Rahman, 1979, Phys. Rev. Lett. **42**, 1127.
- Akhmanov, S. A., V. A. Vysloukh, and A. S. Chirkin, 1992, *Optics of Femtosecond Laser Pulses* (AIP, New York).
- Alducin, M., J. I. Juaristi, and P. M. Echenique, 2004, Surf. Sci. **559**, 233.
- Alfano, R. R., and S. L. Shapiro, 1970, Phys. Rev. Lett. **24**, 584.
- Alnaser, A. S., X. M. Tong, T. Osipov, S. Voss, C. M. Maharjan, P. Ranitovic, B. Ulrich, B. Shan, Z. Chang, C. D. Lin, and C. L. Cocke, 2004, Phys. Rev. Lett. **93**, 183202.
- Alnaser, A. S., S. Voss, X.-M. Tong, C. M. Maharjan, P. Ranitovic, B. Ulrich, T. Osipov, B. Shan, Z. Chang, and C. L. Cocke, 2004, Phys. Rev. Lett. **93**, 113003.
- Altucci, C., Ch. Delfin, L. Roos, M. B. Gaarde, A. L'Huillier, I. Mercer, T. Starczewski, and C.-G. Wahlström, 1998, Phys. Rev. A **58**, 3934.
- Altucci, C., V. Tosa, and R. Velotta, 2007, Phys. Rev. A **75**, 061401(R).
- Amano, M., and K. Takatsuka, 2005, J. Chem. Phys. **122**, 084113.
- Antoine, Ph., A. L'Huillier, and M. Lewenstein, 1996, Phys. Rev. Lett. **77**, 1234.
- Antoine, Ph., D. B. Milosevic, A. L'Huillier, M. B. Gaarde, P. Salieres, and M. Lewenstein, 1997, Phys. Rev. A **56**, 4960.
- Apolonski, A., P. Dombi, G. G. Paulus, M. Kakehata, R. Holzwarth, T. Udem, Ch. Lemell, K. Torizuka, J. Burgdörfer, T. W. Hänsch, and F. Krausz, 2004, Phys. Rev. Lett. **92**, 073902.
- Apolonski, A., A. Poppe, G. Tempea, C. Spielmann, T. Udem, R. Holzwarth, T. Hänsch, and F. Krausz, 2000, Phys. Rev. Lett. **85**, 740.
- Aseyev, S. A. Y. Ni, L. J. Frasinski, H. G. Muller, and M. J. J. Vrakking, 2003, Phys. Rev. Lett. **91**, 223902.
- Assion A., T. Baumert, M. Bergt, T. Brixner, B. Kiefer, V. Seyfried, M. Strehle, and G. Gerber, 1998, Science **282**, 919.
- Assion A., T. Baumert, U. Weichmann, and G. Gerber, 2001, Phys. Rev. Lett. **86**, 5695.
- Assion, A., M. Geisler, J. Helbing, and V. Seyfried, T. Baumert, 1996, Phys. Rev. A **54**, R4605.
- Averbukh, V., 2004, Phys. Rev. A **69**, 043406.
- Averbukh, V., and L. S. Cederbaum, 2006, Phys. Rev. Lett. **96**, 053401.
- Averbukh, V., I. B. Müller, and L. S. Cederbaum, 2004, Phys. Rev. Lett. **93**, 263002.
- Awasthi, M., Y. V. Vanne, and A. Saenz, 2005, J. Phys. B **38**, 3973.
- Baeva, T., S. Gordienko, and A. Pukhov, 2006a, Phys. Rev. E **74**, 046404.
- Baeva, T., S. Gordienko, and A. Pukhov, 2006b, Phys. Rev. E **74**, 065401(R).
- Baker, S., J. S. Robinson, C. A. Haworth, C. C. Chirila, M. Lein, J. W. G. Tisch, and J. P. Marangos, 2007, J. Mod. Opt. **54**, 1011.
- Baker, S., J. S. Robinson, C. A. Haworth, H. Teng, R. A. Smith, C. C. Chirila, M. Lein, J. W. G. Tisch, and J. P. Marangos, 2006, Science **312**, 424.
- Baker, S., J. S. Robinson, M. Lein, C. C. Chirilă, R. Torres, H. C. Bandulet, D. Comtois, J. C. Kieffer, D. U. Villeneneve, J. W. Tisch, and J. P. Marangos, 2008, Phys. Rev. Lett. **101**, 053901.
- Balcou, P., C. Cornaggia, A. S. L. Gomes, L. A. Lompre, and A. L'Huillier, 1992, J. Phys. B **25**, 4467.
- Baltuška, A., T. Fuji, and T. Kobayashi, 2002a, Opt. Lett. **27**, 306.
- Baltuška, A., T. Fuji, and T. Kobayashi, 2002b, Opt. Lett. **27**, 1241.
- Baltuška, A., T. Fuji, and T. Kobayashi, 2002c, Phys. Rev. Lett. **88**, 133901.
- Baltuška, A., T. Udem, M. Uiberacker, M. Hentschel, E. Goulielmakis, C. Gohle, R. Holzwarth, V. S. Yakovlev, A. Scrinzi, T. W. Hänsch, and F. Krausz, 2003, Nature (London) **421**, 611.
- Baltuška, A., M. Uiberacker, E. Goulielmakis, R. Kienberger, V. S. Yakovlev, T. Udem, T. W. Hänsch, and F. Krausz, 2003, IEEE J. Sel. Top. Quantum Electron. **9**, 972.
- Bandrauk, A. D., E. Aubanel, and J. M. Gauthier, 1994, *Molecules in Laser Fields* (Dekker, New York).
- Bandrauk, A. D., S. Barmaki, S. Chelkowski, and G. Lafmago Kamta, 2007, in *Progress in Ultrafast Laser Science Volume III*, edited by K. Yamanouchi (Kluwer, Amsterdam), p. 1.
- Bandrauk, A. D., S. Chelkowski, and H. S. Nguyen, 2004, Int. J. Quantum Chem. **100**, 834.
- Bandrauk, A. D., and N. H. Shon, 2002, Phys. Rev. A **66**, 031401.
- Barnes, W. L., A. Dereux, and T. W. Ebbesen, 2003, Nature (London) **424**, 824.
- Bartels, R., S. Backus, E. Zeek, L. Misoguti, G. Vdovin, I. P. Christov, M. M. Murnane, and H. C. Kapteyn, 2000, Nature (London) **406**, 164.
- Bartels, R., H. C. Kapteyn, M. M. Murnane, I. P. Christov, and H. Rabitz, 2004, Phys. Rev. A **70**, 043404.
- Barth, I., and J. Manz, 2006a, J. Am. Chem. Soc. **128**, 7043.
- Barth, I., and J. Manz, 2006b, Angew. Chem., Int. Ed. **45**, 2962.
- Barth, J. V., G. Costantini, and K. Kern, 2005, Nature (London) **437**, 671.

- Barth, S., S. Marburger, S. Joshi, V. Ulrich, O. Kugeler, and U. Hergenhahn, 2006, Phys. Chem. Chem. Phys. **8**, 3218.
- Bauer, M., 2005, J. Phys. D **38**, R253.
- Bauer, M., C. Lei, K. Read, R. Tobey, J. Gland, M. M. Murnane, and H. Kapteyn, 2001, Phys. Rev. Lett. **87**, 025501.
- Baum, P., and A. H. Zewail, 2006, Proc. Natl. Acad. Sci. U.S.A. **103**, 16105.
- Baumert, T., R. Thalweiser, and G. Gerber, 1993, Chem. Phys. Lett. **209**, 29.
- Beck, M., M. G. Raymer, I. A. Walmsley, and V. Wong, 1993, Opt. Lett. **18**, 2041.
- Becker, A., and F. H. M. Faisal, 1994, Phys. Rev. A **50**, 3256.
- Becker A., and F. H. M. Faisal, 2000, Phys. Rev. Lett. **84**, 3546.
- Becker A., and F. H. M. Faisal, 2002, Phys. Rev. Lett. **89**, 193003.
- Becker, A., and F. H. M. Faisal, 2005, J. Phys. B **38**, R1.
- Becker, A., F. H. M. Faisal, Y. Liang, S. Augst, Y. Beaudoin, M. Chaker, and S. L. Chin, 2000, J. Phys. B **33**, L547.
- Becker, A., L. Plaja, P. Moreno, M. Nurhuda, and F. H. M. Faisal, 2001, Phys. Rev. A **64**, 023408.
- Becker, U., and D. Shirley, 1996, Eds., *Vuv and Soft X-Ray Photoionization* (Plenum, New York).
- Becker, W., F. Grasbon, R. Kopold, D. B. Milosevic, G. G. Paulus, and H. Walther, 2002, Adv. At., Mol., Opt. Phys. **48**, 35.
- Becker, W., A. Lohr, M. Kleber, and M. Lewenstein, 1997, Phys. Rev. A **56**, 645.
- Bellini, M., 2000, Appl. Phys. B: Lasers Opt. **70**, 773.
- Beutler, H., 1935, Z. Phys. **93**, 177.
- Biegert, J., A. Heinrich, C. P. Hauri, W. Kornelis, P. Schlup, M. P. Anscombe, M. B. Gaarde, K. J. Schafer, and U. Keller, 2006, J. Mod. Opt. **53**, 87.
- Binhammer, T., E. Rittweger, R. Ell, F. X. Kärntner, and U. Morgner, 2005, IEEE J. Quantum Electron. **41**, 1552.
- Binhammer, T., E. Rittweger, U. Morgner, R. Ell, and F. X. Kärntner, 2006, Opt. Lett. **31**, 1552.
- Blanchet, V., M. Z. Zgierski, T. Seideman, and A. Stolow, 1999, Nature (London) **401**, 52.
- Bokor, J., 1989, Science **246**, 1130.
- Borisov, A. D. Sánchez-Portal, R. Díez Muino, and P. M. Echenique, 2004, Chem. Phys. Lett. **387**, 95.
- Bouhal, A., R. Evans, G. Grillon, A. Mysyrowicz, P. Breger, P. Agostini, R. C. Constantinescu, H. G. Muller, and D. von der Linde, 1997, J. Opt. Soc. Am. B **14**, 950.
- Bouhal, A., P. Salières, P. Breger, P. Agostini, G. Hamoniaux, A. Mysyrowicz, A. Antonetti, R. Constantinescu, and H. G. Muller, 1998, Phys. Rev. A **58**, 389.
- Boyd, R., 2003, *Nonlinear Optics*, 2nd ed. (Academic, New York).
- Brabec, T., M. Yu. Ivanov, and P. B. Corkum, 1996, Phys. Rev. A **54**, R2551.
- Brabec, T., and F. Krausz, 1997, Phys. Rev. Lett. **78**, 3282.
- Brabec, T., and F. Krausz, 2000, Rev. Mod. Phys. **72**, 545.
- Bradley, D. J., B. Liddy, and W. E. Sleat, 1971, Opt. Commun. **2**, 391.
- Bradley, D. J., and G. H. C. New, 1974, Proc. IEEE **62**, 313.
- Breidbach, J., and L. S. Cederbaum, 2003, J. Chem. Phys. **118**, 3983.
- Breidbach, J., and L. S. Cederbaum, 2005, Phys. Rev. Lett. **94**, 033901.
- Brena, B., D. Nordlund, M. Odelius, H. Ogasawara, A. Nilsson, and L. G. M. Pettersson, 2004, Phys. Rev. Lett. **93**, 148302.
- Bressler, C., and M. Chergui, 2004, Chem. Rev. (Washington, D.C.) **104**, 1781.
- Brixner, T., N. H. Damrauer, and G. Gerber, 2001, Adv. At., Mol., Opt. Phys. **46**, 1.
- Brixner, T., N. H. Damrauer, G. Krampert, P. Niklaus, and G. Gerber, 2003, J. Mod. Opt. **50**, 539.
- Brixner, T., N. H. Damrauer, P. Niklaus, and G. Gerber, 2001, Nature (London) **414**, 57.
- Brixner, T., and G. Gerber, 2001, Opt. Lett. **26**, 557.
- Brixner, T., G. Krampert, T. Pfeifer, R. Selle, G. Gerber, M. Wollenhaupt, O. Graefe, C. Horn, D. Liese, and T. Baumert, 2004, Phys. Rev. Lett. **92**, 208301.
- Brühlwiler, P. A., O. Karis, and N. Martensson, 2002, Rev. Mod. Phys. **74**, 703.
- Brumer, P. W., and M. Shapiro, 2003, *Principles of the Quantum Control of Molecular Processes* (Wiley, New York).
- Bryan, W. A., S. L. Stebbings, J. McKenna, E. M. L. English, M. Suresh, J. Wood, B. Srigengan, I. C. E. Turcu, J. M. Smith, E. J. Divall, C. J. Hooker, A. J. Langley, J. L. Collier, I. D. Williams, and W. R. Newell, 2006, Nat. Phys. **2**, 379.
- Budil, K. S., P. Salieres, M. D. Perry, and A. L'Huillier, 1993, Phys. Rev. A **48**, R3437.
- Bulanov, S. V., N. M. Naumova, and F. Pegoraro, 1994, Phys. Plasmas **1**, 745.
- Caillat, J., J. Zanghellini, M. Kitzler, O. Koch, W. Kreuzer, and A. Scrinzi, 2005, Phys. Rev. A **71**, 012712.
- Canright, G. S., 1988, Phys. Rev. B **38**, 1647.
- Cao, J., Y. Gao, R. J. D. Miller, and D. A. Mantell, 1997, Phys. Rev. B **56**, 1099.
- Cao, W., P. Lu, P. Lan, W. Hong, and X. Wang, 2007, J. Phys. B **40**, 869.
- Cao, W., P. Lu, P. Lan, X. Wang, and Y. Li, 2007, Phys. Rev. A **75**, 063423.
- Cao, W., P. Lu, P. Lan, X. Wang, and G. Yang, 2006, Phys. Rev. A **74**, 063821.
- Cao, W., P. Lu, P. Lan, X. Wang, and G. Yang, 2007, Opt. Express **15**, 530.
- Carrera, J. J., and S. Chu, 2007, Phys. Rev. A **75**, 033807.
- Carrera, J. J., X. M. Tong, and S. Chu, 2006, Phys. Rev. A **74**, 023404.
- Cavalieri, A. L., E. Goulielmakis, B. Horvath, W. Helml, M. Schultze, M. Fiess, V. Pervak, L. Veisz, V. S. Yakovlev, M. Uiberacker, A. Apolonski, F. Krausz, and R. Kienberger, 2007, New J. Phys. **9**, 242.
- Cavalieri, A. L., N. Müller, Th. Uphues, V. S. Yakovlev, A. Baltuška, B. Horvath, B. Schmidt, L. Blümel, R. Holzwarth, S. Hendel, M. Drescher, U. Kleineberg, P. M. Echenique, R. Kienberger, F. Krausz, and U. Heinzmann, 2007, Nature (London) **449**, 1029.
- Cederbaum, L., and J. Zobeley, 1999, Chem. Phys. Lett. **307**, 205.
- Cederbaum, L. S., J. Zobeley, and F. Tarantelli, 1997, Phys. Rev. Lett. **79**, 4778.
- Cerdeira, F., T. Fjeldly, and M. Cardona, 1973, Phys. Rev. B **8**, 4734.
- Cerullo, G., M. Nisoli, and S. De Silvestri, 1997, Appl. Phys. Lett. **71**, 3616.
- Cerullo, G., M. Nisoli, S. Stagira, and S. De Silvestri, 1998, Opt. Lett. **23**, 1283.
- Cerullo, G., M. Nisoli, S. Stagira, S. De Silvestri, G. Tempea, F. Krausz, and K. Ferencz, 1999, Opt. Lett. **24**, 1529.
- Chakraborty, H. S., M. B. Gaarde, and A. Couairon, 2006, Opt. Lett. **31**, 3662.

- Chan, K. W., C. K. Law, and J. H. Eberly, 2002, Phys. Rev. Lett. **88**, 100402.
- Chan, K. W., C. K. Law, and J. H. Eberly, 2003, Phys. Rev. A **68**, 022110.
- Chan, K. W., C. K. Law, M. V. Fedorov, and J. H. Eberly, 2004, J. Mod. Opt. **51**, 1779.
- Chang, B. Y., H. Rabitz, and I. Sola, 2003, Phys. Rev. A **68**, 031402.
- Chang, Z., 2004, Phys. Rev. A **70**, 043802.
- Chatzidimitriou-Dreismann, C. A., M. Vos, C. Kleiner, and T. Abdul-Redah, 2003, Phys. Rev. Lett. **91**, 057403.
- Chelkowski, S., A. D. Bandrauk, and P. B. Corkum, 2004, Phys. Rev. Lett. **93**, 083602.
- Chelkowski, S., G. L. Yudin, and A. D. Bandrauk, 2006, J. Phys. B **39**, S409.
- Chen, J. G., C. Li, F. P. Chi, and Y. J. Yang, 2007, Chin. Phys. Lett. **24**, 86.
- Chen, X., X. Li, J. Liu, P. Wei, X. Ge, R. Li, and Z. Xu, 2007, Opt. Lett. **32**, 2402.
- Chipperfield, L. E., L. N. Gaier, P. L. Knight, J. P. Marangos, and J. W. G. Tisch, 2005, J. Mod. Opt. **52**, 243.
- Chirilă C. C., and M. Lein, 2006a, J. Mod. Opt. **53**, 113.
- Chirilă C. C., and M. Lein, 2006b, Phys. Rev. A **73**, 023410.
- Christov, I. P., H. C. Kapteyn, and M. M. Murnane, 2000, Opt. Express **7**, 362.
- Christov, I. P., M. M. Murnane, and H. C. Kapteyn, 1997, Phys. Rev. Lett. **78**, 1251.
- Chu, X., and S.-I. Chu, 2001, Phys. Rev. A **64**, 063404.
- Cocke, C. L., and R. E. Olson, 1991, Phys. Rep. **205**, 153.
- Constant, E., D. Garzella, P. Breger, E. Mevel, C. Dorrer, C. Le Blanc, F. Salin, and P. Agostini, 1999, Phys. Rev. Lett. **82**, 1668.
- Constant, E., V. D. Taranukhin, A. Stolow, and P. B. Corkum, 1997, Phys. Rev. A **56**, 3870.
- Corkum, P. B., 1993, Phys. Rev. Lett. **71**, 1994.
- Corkum, P. B., N. Burnett, and F. Brunel, 1989, Phys. Rev. Lett. **62**, 1259.
- Corkum, P. B., N. H. Burnett, and M. Yu. Ivanov, 1994, Opt. Lett. **19**, 1870.
- Corkum, P. B., M. Yu. Ivanov, and J. Wright, 1997, Annu. Rev. Phys. Chem. **48**, 387.
- Corkum, P. B., and F. Krausz, 2007, Nat. Phys. **3**, 381.
- Cormier, E., and P. Lambropoulos, 1998, Eur. Phys. J. D **2**, 15.
- Cormier, E., I. Walmsley, E. M. Kosik, A. S. Wyatt, L. Corner, and L. F. DiMauro, 2005, Phys. Rev. Lett. **94**, 033905.
- Corsi, C., A. Pirri, E. Sali, A. Tortora, and M. Bellini, 2006, Phys. Rev. Lett. **97**, 023901.
- Costa, L., M. Betz, M. Spasenovic, A. D. Bristow, and H. M. Van Driel, 2007, Nat. Phys. **3**, 632.
- Couairon, A., J. Biegert, C. P. Hauri, W. Kornelis, F. W. Helbing, U. Keller, and A. Mysyrowicz, 2006, J. Mod. Opt. **53**, 75.
- Courant, E. D., C. Pellegrini, and W. Zakowicz, 1985, Phys. Rev. A **32**, 2813.
- Cundiff, S. T., 2002, J. Phys. D **35**, R43.
- Cundiff, S. T., and J. Ye, 2003, Rev. Mod. Phys. **75**, 325.
- Cyr, D. R., and C. C. Hayden, 1996, J. Chem. Phys. **104**, 771.
- Daniel, C., J. Full, L. González, C. Lupulescu, J. Manz, A. Merli, Š. Vajda, and L. Wöste, 2003, Science **299**, 536.
- de Boeij, W. P., M. Pshenichnikov, and D. Wiersma, 1998, Annu. Rev. Phys. Chem. **49**, 99.
- de Bohan, A., Ph. Antoine, D. B. Milosevic, and B. Piraux, 1998, Phys. Rev. Lett. **81**, 1837.
- de Bohan, A., B. Piraux, L. Ponce, R. Taieb, V. Veniard, and A. Maquet, 2002, Phys. Rev. Lett. **89**, 113002.
- De Jesus, V. L. B., B. Feuerstein, K. Zrost, D. Fischer, A. Rudenko, F. Afaneh, C. D. Schröter, R. Moshammer, and J. Ullrich, 2004, J. Phys. B **37**, L161.
- Delone, N. B., and V. P. Krainov, 1985, *Atoms in Strong Light Fields* (Springer, Berlin).
- DeMaria, A. J., W. H. Glenn, M. J. Brienza, and M. E. Mack, 1969, Proc. IEEE **57**, 2.
- Diels, J. C., and W. Rudolph, 1996, *Ultrashort Laser Pulse Phenomena* (Academic, New York).
- Dietrich, P., N. H. Burnett, M. Yu. Ivanov, and P. B. Corkum, 1994, Phys. Rev. A **50**, R3585.
- Dietrich, P., F. Krausz, and P. Corkum, 2000, Opt. Lett. **25**, 16.
- Dimitrovski, D., E. A. Solov'ev, and J. S. Briggs, 2004, Phys. Rev. Lett. **93**, 083003.
- Dinu, L. C., H. G. Muller, S. Kazamias, G. Mullot, F. Augé, Ph. Balcou, P. M. Paul, M. Kovacev, P. Breger, and P. Agostini, 2003, Phys. Rev. Lett. **91**, 063901.
- Dombi, P., A. Apolonski, Ch. Lemell, G. G. Paulus, M. Kakehata, R. Holzwarth, T. Udem, K. Torizuka, J. Burgdörfer, T. W. Hänsch, and F. Krausz, 2004, New J. Phys. **6**, 39.
- Dörner, R., V. Mergel, O. Jagutzki, L. Spielberger, J. Ullrich, R. Moshammer, and H. Schmidt-Böcking, 2000, Phys. Rep. **330**, 95.
- Drescher, M., M. Hentschel, R. Kienberger, G. Tempea, Ch. Spielmann, G. A. Reider, P. B. Corkum, and F. Krausz, 2001, Science **291**, 1923.
- Drescher, M., M. Hentschel, R. Kienberger, M. Uiberacker, V. Yakovlev, A. Scrinzi, Th. Westerwalbesloh, U. Kleineberg, U. Heinzmann, and F. Krausz, 2002, Nature (London) **419**, 803.
- Drescher, M., and F. Krausz, 2005, J. Phys. B **38**, S727.
- Dromey, B., S. Kar, C. Bellei, D. C. Carroll, R. J. Clarke, J. S. Green, S. Kneip, K. Markey, S. R. Nagel, P. T. Simpson, L. Willengale, P. McKenna, D. Neely, Z. Najmudin, K. Krushelnick, P. A. Norreys, and M. Zepf, 2007, Phys. Rev. Lett. **99**, 085001.
- Dromey, B., M. Zepf, A. Gopal, K. Lancaster, M. S. Wei, K. Krushelnick, M. Tatarakis, N. Vakakis, S. Moustazis, R. Kodama, M. Tampo, C. Stoeckl, R. Clarke, H. Habara, D. Neely, S. Karsch, and P. Norreys, 2006, Nat. Phys. **2**, 456.
- Dubietis, A., R. Butkus, and A. P. Piskarskas, 2006, IEEE J. Sel. Top. Quantum Electron. **12**, 163.
- Dudovich, N., J. Levesque, O. Smirnova, D. Zeidler, D. Comtois, M. Yu. Ivanov, D. M. Villeneuve, and P. B. Corkum, 2006, Phys. Rev. Lett. **97**, 253903.
- Dudovich, N., O. Smirnova, J. Levesque, M. Yu. Ivanov, Y. Mairesse, D. M. Villeneuve, and P. B. Corkum, 2006, Nat. Phys. **2**, 781.
- Durfee, C. G., A. R. Rundquist, S. Backus, C. Herne, M. M. Murnane, and H. C. Kapteyn, 1999, Phys. Rev. Lett. **83**, 2187.
- Dwyer, J. R., R. E. Jordan, C. T. Hebeisen, M. Harb, R. Ernststorfer, T. Dartigalongue, and R. J. D. Miller, 2007a, J. Mod. Opt. **54**, 905.
- Dwyer, J. R., R. E. Jordan, C. T. Hebeisen, M. Harb, R. Ernststorfer, T. Dartigalongue, and R. J. D. Miller, 2007b, J. Mod. Opt. **54**, 923.
- Echenique, P. M., R. Berndt, E. V. Chulkov, T. Fauster, A. Goldmann, and U. Höfer, 2004, Surf. Sci. Rep. **52**, 219.
- Eden, J. G., 2004, Prog. Quantum Electron. **28**, 197.
- Eichmann, U., M. Dörr, H. Maeda, W. Becher, and W. Sandner, 2000, Phys. Rev. Lett. **84**, 3550.
- Eigen, M., 1954, Discuss. Faraday Soc. **17**, 194.
- Elsayed-Ali, H. E., and G. Mourou, 1988, Appl. Phys. Lett. **52**,

- 103.
- Emmanouilidou, A., and J. M. Rost, 2007, Phys. Rev. A **75**, 022712.
- Eremina, E., X. Liu, H. Rottke, W. Sandner, A. Dreischuh, F. Lindner, F. Grasbon, G. G. Paulus, H. Walther, R. Moshammer, B. Feuerstein, and J. Ullrich, 2003, J. Phys. B **36**, 3269.
- Eremina, E., X. Liu, H. Rottke, W. Sandner, M. G. Schätzel, A. Dreischuh, G. G. Paulus, H. Walther, R. Moshammer, and J. Ullrich, 2004, Phys. Rev. Lett. **92**, 173001.
- Faisal, F. H. M., 1973, J. Phys. B **6**, L89.
- Faisal, F. H. M., 1987, *Theory of Multiphoton Processes* (Plenum, New York).
- Fann, W. S., R. Storz, H. W. K. Tom, and J. Bokor, 1992, Phys. Rev. Lett. **68**, 2834.
- Fano, U., 1935, Nuovo Cimento **12**, 154.
- Fano, U., 1961, Phys. Rev. **124**, 1866.
- Farkas, Gy., and Cs. Tóth, 1992, Phys. Lett. A **168**, 447.
- Faure, J., Y. Glinec, A. Pukhov, S. Kiselev, S. Gordienko, E. Lefebvre, J.-P. Rousseau, F. Burgy, and V. Malka, 2004, Nature (London) **431**, 541.
- Fedorov M. V., M. A. Efremov, A. E. Kazakov, K. W. Chan, C. K. Law, and J. H. Eberly, 2004, Phys. Rev. A **69**, 052117.
- Fedorov M. V., M. A. Efremov, A. E. Kazakov, K. W. Chan, C. K. Law, and J. H. Eberly, 2005, Phys. Rev. A **72**, 032110.
- Feldhaus, J., J. Arthur, and J. B. Hastings, 2005, J. Phys. B **38**, S799.
- Fennel, T., L. Ramunno, and T. Brabec, 2007, Phys. Rev. Lett. **99**, 233401.
- Feringa, B. L., 2001, Ed., *Molecular Switches* (Wiley-VCH, Weinheim).
- Ferry, M., A. L'Huillier, X. F. Li, L. A. Lompré, G. Mainfray, and C. Manus, 1988, J. Phys. B **21**, L31.
- Figueira de Morisson Faria, C., X. Liu, W. Becker, and H. Schomerus, 2004, Phys. Rev. A **69**, 021402.
- Figueira de Morisson Faria, C., and P. Salieres, 2007, Laser Phys. **17**, 390.
- Figueira de Morisson Faria, C., P. Salieres, P. Villain, and M. Lewenstein, 2006, Phys. Rev. A **74**, 053416.
- Figueira de Morisson Faria, C., H. Schomerus, and W. Becker, 2002, Phys. Rev. A **66**, 043413.
- Figueira de Morisson Faria, C., H. Schomerus, X. Liu, and W. Becker, 2004, Phys. Rev. A **69**, 043405.
- Fill, E. E., F. Krausz, and M. G. Raizen, 2008, New J. Phys. **10**, 093015.
- Fill, E., L. Veisz, A. Apolonski, and F. Krausz, 2006, New J. Phys. **8**, 272.
- Fittinghoff, D., P. R. Bolton, B. Chang, and K. C. Kulander, 1992, Phys. Rev. Lett. **69**, 2642.
- Fleischer, A., and N. Moiseyev, 2006, Phys. Rev. A **74**, 053806.
- Föhlisch, A., 2006, Appl. Phys. A: Mater. Sci. Process. **85**, 351.
- Föhlisch, A., P. Feulner, F. Hennies, A. Fink, D. Menzel, D. Sanchez-Portal, P. M. Echenique, and W. Wurth, 2005, Nature (London) **436**, 373.
- Fortier, T. M., P. A. Roos, D. J. Jones, S. T. Cundiff, R. D. R. Bhat, and J. E. Sipe, 2004, Phys. Rev. Lett. **92**, 147403.
- Franco, I., and P. Brumer, 2006, Phys. Rev. Lett. **97**, 040402.
- Frolov, M. V., A. V. Flegel, N. L. Manakov, and A. F. Starace, 2007a, Phys. Rev. A **75**, 063407.
- Frolov, M. V., A. V. Flegel, N. L. Manakov, and A. F. Starace, 2007b, Phys. Rev. A **75**, 063408.
- Fuji, T., N. Ishii, C. Y. Teisset, X. Gu, Th. Metzger, A. Baltuška, N. Forget, D. Kaplan, A. Galvanauskas, and F. Krausz, 2006, Opt. Lett. **31**, 1103.
- Fuji, T., J. Rauschenberger, Ch. Gohle, A. Apolonski, T. Udem, V. S. Yakovlev, G. Tempea, T. W. Hänsch, and F. Krausz, 2005, New J. Phys. **7**, 116.
- Gaarde, M. B., M. Murakami, and R. Kienberger, 2006, Phys. Rev. A **74**, 053401.
- Gaarde, M. B., and K. J. Schafer, 2002, Phys. Rev. Lett. **89**, 213901.
- Gaarde, M. B., and K. J. Schafer, 2006, Opt. Lett. **31**, 3188.
- Gaarde, M. B., K. J. Schafer, K. C. Kulander, B. Sheehy, D. Kim, and L. F. DiMauro, 2000, Phys. Rev. Lett. **84**, 2822.
- Gagnon, E., P. Ranitovic, X-M. Tong, C. L. Cocke, M. Murnane, H. Kapteyn, and A. Sandhu, 2007, Science **317**, 1374.
- Gagnon, E., I. Thomann, A. Paul, A. Lytle, S. Backus, M. Murnane, H. Kapteyn, and A. Sandhu, 2006, Opt. Lett. **31**, 1866.
- Gale, G. M., M. Cavallari, T. J. Driscoll, and F. Hache, 1995, Opt. Lett. **20**, 1562.
- Ge, Y., 2006, Phys. Rev. A **74**, 015803.
- Geddes, C. G. R., Cs. Toth, J. van Tilborg, E. Esarey, C. B. Schroeder, D. Bruhwiler, C. Nieter, J. Cary, and W. P. Lee-mans, 2004, Nature (London) **431**, 538.
- Geissler, M., and J. Meyer-ter-Vehn, 2006, private communication.
- Geissler, M., S. Rykovanov, J. Schreiber, J. Meyer-ter-Vehn, and G. D. Tsakiris, 2007, New J. Phys. **9**, 218.
- Georgescu, I., U. Saalmann, and J. M. Rost, 2007, Phys. Rev. Lett. **99**, 183002.
- Gessner, O., Y. Hikosaka, B. Zimmermann, A. Hempelmann, R. R. Lucchese, J. H. D. Eland, P.-M. Guyon, and U. Becker, 2002, Phys. Rev. Lett. **88**, 193002.
- Gessner, O., A. M. D. Lee, J. P. Shaffer, H. Reisler, S. V. Levchenko, A. I. Krylov, J. G. Underwood, H. Shi, A. L. L. East, D. M. Wardlaw, E. t. H. Chrysostom, C. C. Hayden, and A. Stolow, 2006, Science **311**, 219.
- Gibson, E. A., A. Paul, N. Wagner, R. Tobey, S. Backus, I. P. Christov, A. Aquila, E. M. Gullikson, D. T. Attwood, M. M. Murnane, and H. C. Kapteyn, 2003, Science **302**, 95.
- Gibson, E. A., A. Paul, N. Wagner, R. Tobey, D. Gaudiosi, S. Backus, I. P. Christov, M. M. Murnane, and H. C. Kapteyn, 2004, Phys. Rev. Lett. **92**, 033001.
- Gildenburg, V. B., and N. V. Vvedenskii, 2007, Phys. Rev. Lett. **98**, 245002.
- Glover, T. E., R. W. Schoenlein, A. H. Chin, and C. V. Shank, 1996, Phys. Rev. Lett. **76**, 2468.
- Göres, J., D. Goldhaber-Gordon, S. Heemeyer, M. A. Kastner, Hadas Shtrikman, D. Mahalu, and U. Meirav, 2000, Phys. Rev. B **62**, 2188.
- Goldsmith, R. H., L. E. Sinks, R. F. Kelley, L. J. Betzen, W. Liu, E. A. Weiss, M. A. Ratner, and M. R. Wasielewski, 2005, Proc. Natl. Acad. Sci. U.S.A. **102**, 3540.
- Gordienko, S., A. Pukhov, O. Shorokhov, and T. Baeva, 2004, Phys. Rev. Lett. **93**, 115002.
- Gordienko, S., A. Pukhov, O. Shorokhov, and T. Baeva, 2005, Phys. Rev. Lett. **94**, 103903.
- Gordon, A., F. Kaertner, N. Rohringer, and R. Santra, 2006, Phys. Rev. Lett. **96**, 223902.
- Goreslavskii S. P., and S. V. Popruzhenko, 1999, J. Phys. B **32**, L531.
- Goreslavskii S. P., S. V. Popruzhenko, R. Kopold, and W. Becker, 2001, Phys. Rev. A **64**, 053402.
- Goulielmakis, E., S. Koehler, B. Reiter, M. Schultze, A. J. Verhoeft, E. E. Serebryannikov, A. M. Zheltikov, and F. Krausz, 2008, Opt. Lett. **33**, 1407.

- Goulielmakis, E., E. M. Schultze, M. Hofstetter, V. S. Yakovlev, J. Gagnon, M. Uiberacker, A. L. Aquila, E. M. Gullikson, D. T. Attwood, R. Kienberger, F. Krausz, and U. Kleineberg, 2008, *Science* **320**, 1614.
- Goulielmakis, E., M. Uiberacker, R. Kienberger, A. Baltuška, V. Yakovlev, A. Scrinzi, Th. Westerwalbesloh, U. Kleineberg, U. Heinzmann, M. Drescher, and F. Krausz, 2004, *Science* **305**, 1267.
- Goulielmakis, E., V. Yakovlev, A. L. Cavalieri, M. Uiberacker, V. Pervak, A. Apolonskiy, R. Kienberger, U. Kleineberg, and F. Krausz, 2007, *Science* **317**, 769.
- Gouy, C. R., 1890, *Acad. Sci., Paris, C. R.* **110**, 1251.
- Graf, U., M. Fiess, M. Schultze, R. Kienberger, F. Krausz, and E. Goulielmakis, 2008, *Opt. Express* **16**, 18956.
- Gräfe, S., and M. Yu. Ivanov, 2007, *Phys. Rev. Lett.* **99**, 163603.
- Gray, H. B., and J. R. Winkler, 2005, *Proc. Natl. Acad. Sci. U.S.A.* **102**, 3534.
- Greenblatt, B. J., M. T. Zanni, and D. M. Neumark, 1997, *Science* **276**, 1675.
- Greenhow, R. C., and A. J. Schmidt, 1974, in *Advances in Quantum Electronics*, edited by D. W. Goodwin (Academic, London), Vol. 2, p. 158.
- Guandalini, A., P. Eckle, M. Anscombe, P. Schlup, J. Biegert, and U. Keller, 2006, *J. Phys. B* **39**, S257.
- Haan, S. L., L. Breen, A. Karim, and J. H. Eberly, 2006, *Phys. Rev. Lett.* **97**, 103008.
- Haan, S. L., L. Breen, A. Karim, and J. H. Eberly, 2007, *Opt. Express* **15**, 767.
- Haan, S. L., and Z. S. Smith, 2007, *Phys. Rev. A* **76**, 053412.
- Haan, S. L., P. S. Wheeler, R. Panfili, and J. H. Eberly, 2002, *Phys. Rev. A* **66**, 061402.
- Haight, R., 1995, *Surf. Sci. Rep.* **21**, 275.
- Haight, R., and J. A. Silbermann, 1989, *Phys. Rev. Lett.* **62**, 815.
- Haljan, P., M. Yu. Ivanov, and P. B. Corkum, 1997, *Laser Phys.* **7**, 839.
- Hänsch, T. W., 1990, *Opt. Commun.* **80**, 71.
- Hänsch, T. W., 1997, private communication.
- Harris, S. E., J. J. Macklin, and T. W. Hänsch, 1993, *Opt. Commun.* **100**, 487.
- Harris, S. E., and A. V. Sokolov, 1997, *Phys. Rev. A* **55**, R4019.
- Harris, S. E., and A. V. Sokolov, 1998, *Phys. Rev. Lett.* **81**, 2894.
- Harumiya, K., H. Kono, Y. Fujimura, I. Kawata, and A. D. Bandrauk, 2002, *Phys. Rev. A* **66**, 043403.
- Hasegawa, H., E. J. Takahashi, Y. Nabekawa, K. L. Ishikawa, and K. Midorikawa, 2005, *Phys. Rev. A* **71**, 023407.
- Hauri, C. P., W. Kornelis, F. W. Helbing, A. Heinrich, A. Couairon, A. Mysyrowicz, J. Biegert, and U. Keller, 2004, *Appl. Phys. B: Lasers Opt.* **79**, 673.
- Hauri, C. P., et al., 2007, *Opt. Lett.* **32**, 868.
- Haworth, C. A., L. E. Chipperfield, J. S. Robinson, P. L. Knight, J. P. Marangos, and J. W. G. Tisch, 2007, *Nat. Phys.* **3**, 52.
- He, F., C. Ruiz, and A. Becker, 2007, *Phys. Rev. Lett.* **99**, 083002.
- Heinrich, A., W. Kornelis, M. P. Anscombe, C. P. Hauri, P. Schlup, J. Biegert, and U. Keller, 2006, *J. Phys. B* **39**, S275.
- Hennig, H., J. Breidbach, and L. S. Cederbaum, 2005, *J. Chem. Phys.* **122**, 134104.
- Hentschel, M., R. Kienberger, Ch. Spielmann, G. A. Reider, N. Milosevic, T. Brabec, P. Corkum, U. Heinzmann, M. Drescher, and F. Krausz, 2001, *Nature (London)* **414**, 509.
- Hergott, J.-F., M. Kovacev, H. Merdji, C. Hubert, Y. Mairesse, E. Jean, P. Breger, P. Agostini, B. Carré, and P. Salières, 2002, *Phys. Rev. A* **66**, 021801(R).
- Ho, P. J., and J. H. Eberly, 2007, *Opt. Express* **15**, 1845.
- Ho, P. J., R. Panfili, S. L. Heen, and J. H. Eberly, 2005, *Phys. Rev. Lett.* **94**, 093002.
- Höfer, U., I. L. Shumay, Ch. Reuß, U. Thomann, W. Wallauer, and T. Fauster, 1997, *Science* **277**, 1480.
- Holzwarth, R., T. Udem, T. W. Hänsch, J. C. Knight, W. J. Wadsworth, P. St. J. Russell, 2000, *Phys. Rev. Lett.* **85**, 2264.
- Hommelhoff, P., Y. Sortais, A. Aghajani-Talesh, and M. A. Kasevich, 2006, *Phys. Rev. Lett.* **96**, 077401.
- Hong, K. H., J. Lee, B. Hou, J. A. Nees, E. Power, and G. A. Mourou, 2006, *Appl. Phys. Lett.* **89**, 031113.
- Hu, J., K.-L. Han, and G.-Z. He, 2005, *Phys. Rev. Lett.* **95**, 123001.
- Hu, J., M.-S. Wang, K.-L. Han, and G.-Z. He, 2006, *Phys. Rev. A* **74**, 063417.
- Hu, S. X., and L. A. Collins, 2005, *Phys. Rev. Lett.* **94**, 073004.
- Hu, S. X., and L. A. Collins, 2006, *Phys. Rev. Lett.* **96**, 073004.
- Hu, S. X., and L. A. Collins, 2007, *J. Mod. Opt.* **54**, 943.
- Hu, S. X., D. B. Milošević, W. Becker, and W. Sandner, 2001, *Phys. Rev. A* **64**, 013410.
- Huang, Y. C., D. Zheng, W. M. Tullock, and R. L. Byer, 1996, *Appl. Phys. Lett.* **68**, 753.
- Huber, R., F. Tauser, A. Brodschelm, M. Bichler, G. Abstreiter, and A. Leitenstorfer, 2001, *Nature (London)* **414**, 286.
- Huebener, R., 2005, *Electrons in Action: Roads to Modern Computers and Electronics* (Wiley-VCH Verlag, Weinheim).
- Huo, Y., Z. Zeng, Y. Leng, R. Li, Z. Xu, C. Guo, Z. Sun, and Y. Rhee, 2005, *Opt. Lett.* **30**, 564.
- Huo, Y., Z. Zeng, R. Li, and Z. Xu, 2005, *Opt. Express* **13**, 9897.
- Iaconis, C., and I. Walmsley, 1998, *Opt. Lett.* **23**, 792.
- Iaconis, C., and I. Walmsley, 1999, *IEEE J. Quantum Electron.* **35**, 501.
- Ihee, H., V. A. Lobastov, U. M. Gomez, B. M. Goodson, R. Srinivasan, C.-Y. Ruan, and A. H. Zewail, 2001, *Science* **291**, 458.
- Imran, T., Y. S. Lee, C. H. Nam, K. H. Hong, T. J. Yu, and J. H. Sung, 2007, *Opt. Express* **15**, 104.
- Irvine, S. E., P. Dombi, Gy. Farkas, and A. Y. Elezzabi, 2006, *Phys. Rev. Lett.* **97**, 146801.
- Ishikawa, K. L., 2006, *Phys. Rev. A* **74**, 023806.
- Ishikawa, K. L., E. J. Takahashi, and K. Midorikawa, 2007, *Phys. Rev. A* **75**, 021801(R).
- Itakura, R., 2007, *Phys. Rev. A* **76**, 033810.
- Itatani, J., J. Levesque, D. Zeidler, H. Niikura, H. Pepin, J. C. Kieffer, P. B. Corkum, and D. M. Villeneuve, 2004, *Nature (London)* **432**, 867.
- Itatani, J., F. Quéré, G. L. Yudin, M. Yu. Ivanov, F. Krausz, and P. Corkum, 2002, *Phys. Rev. Lett.* **88**, 173903.
- Ivanov, M. Yu., T. Brabec, and N. Burnett, 1996, *Phys. Rev. A* **54**, 742.
- Ivanov, M. Yu., P. B. Corkum, T. Zuo, and A. Bandrauk, 1995, *Phys. Rev. Lett.* **74**, 2933.
- Ivanov, M. Yu., D. Matusek, and J. Wright, 1996, *Phys. Rev. A* **54**, 5159.
- Ivanov, M. Yu., M. Spanner, and O. Smirnova, 2005, *J. Mod. Opt.* **52**, 165.
- Ivanov, M. Yu., V. Yakovlev, and F. Krausz, 2008, in *Mid-Infrared Coherent Sources and Applications*, edited by M.

- Ebrahim-Zade and I. Sorokina (Springer, Dordrecht, The Netherlands), p. 589.
- Jahnke, T., A. Czasch, M. S. Schöffler, S. Schössler, A. Knapp, M. Käss, J. Titze, C. Wimmer, K. Kreidi, R. E. Grisenti, A. Staudte, O. Jagutzki, U. Hergenhahn, H. Schmidt-Böcking, and R. Dörner, 2004, Phys. Rev. Lett. **93**, 163401.
- Jaroň-Becker, A., A. Becker, and F. H. M. Faisal, 2004, Phys. Rev. A **69**, 023410.
- Jaroň-Becker, A., A. Becker, and F. H. M. Faisal, 2006, Phys. Rev. Lett. **96**, 143006.
- Joachain, C. J., M. Dörr, and N. Klystra, 2000, Adv. At., Mol., Opt. Phys. **42**, 225.
- Johnsson, P., R. López-Martens, S. Kazamias, J. Mauritsson, C. Valentin, T. Remetter, K. Varjú, M. B. Gaarde, Y. Mairesse, H. Wabnitz, P. Salières, Ph. Balcou, K. J. Schafer, and A. L'Huillier, 2005, Phys. Rev. Lett. **95**, 013001.
- Johnsson, P., K. Varjú, T. Remetter, E. Gustafsson, J. Mauritsson, R. López-Martens, S. Kazamias, C. Valentin, Ph. Balcou, M. B. Gaarde, K. J. Schafer, and A. L'Huillier, 2006, J. Mod. Opt. **53**, 233.
- Jones, D. J., S. A. Diddams, J. K. Ranka, A. Stentz, R. S. Windeler, J. L. Hall, and S. T. Cundiff, 2000, Science **288**, 635.
- Jordan, G., J. Caillat, C. Ede, and A. Scrinzi, 2006, J. Phys. B **39**, S341.
- Jortner, J., and M. Ratner, 1997, Eds., *Molecular Electronics* (Blackwell, Oxford).
- Judson, R. S., and H. Rabitz, 1992, Phys. Rev. Lett. **68**, 1500.
- Jung, J. D., F. X. Kärnter, N. Matuschek, D. H. Sutter, F. Morier-Genoud, G. Zhang, U. Keller, V. Scheuer, M. Tilsch, and T. Tschudi, 1997, Opt. Lett. **22**, 1009.
- Jurvansuu, M., A. Kivimäki, and S. Aksela, 2001, Phys. Rev. A **64**, 012502.
- Kakehata, M., H. Takada, Y. Kobayashi, and K. Torizuka, 2004, Opt. Express **12**, 2070.
- Kakehata, M., H. Takada, Y. Kobayashi, and K. Torizuka, 2006, J. Photochem. Photobiol., A **182**, 220.
- Kakehata, M., H. Takada, Y. Kobayashi, K. Torizuka, Y. Fujihira, T. Homma, and H. Takahashi, 2001, Opt. Lett. **26**, 1436.
- Kan, C., N. H. Burnett, C. E. Capjack, and R. Rankin, 1997, Phys. Rev. Lett. **79**, 2971.
- Kane, D. J., 1999, IEEE J. Quantum Electron. **35**, 421.
- Kane, D. J., and R. Trebino, 1993, Opt. Lett. **18**, 823.
- Kanai, T., S. Minemoto, and H. Sakai, 2005, Nature (London) **435**, 470.
- Kanai, T., E. J. Takahashi, Y. Nabekawa, and K. Midorikawa, 2007, Phys. Rev. Lett. **98**, 153904.
- Kaplan, A. E., 1994, Phys. Rev. Lett. **73**, 1243.
- Kaplan, A. E., and P. Shkolnikov, 1995, Phys. Rev. Lett. **75**, 2316.
- Kaplan, D., and P. Tournois, 2004, *Ultrafast Optics IV*, edited by F. Krausz, G. Korn, P. B. Corkum, and I. A. Walmsley (Springer-Verlag, New York), p. 105.
- Karsch, S., 2004, private communication.
- Kato, H. S., M. Furukawa, M. Kawai, M. Taniguchi, T. Kawai, T. Hatsui, and N. Kosugi, 2004, Phys. Rev. Lett. **93**, 086403.
- Kawata, I., H. Kono, and Y. Fujimura, 1999, J. Chem. Phys. **110**, 11152.
- Kazansky, A. K., and N. M. Kabachnik, 2006, J. Phys. B **39**, 5173.
- Kazansky, A. K., and N. M. Kabachnik, 2007a, J. Phys. B **40**, 2163.
- Kazansky, A. K., and N. M. Kabachnik, 2007b, J. Phys. B **40**, 3413.
- Kazansky, A. K., and N. M. Kabachnik, 2007c, J. Phys. B **40**, F299.
- Keldysh, L. V., 1964, Zh. Eksp. Teor. Fiz. **47**, 1945 [Sov. Phys. JETP **20**, 1307 (1965)].
- Keller, U., 2003, Nature (London) **424**, 831.
- Kienberger, R., E. Goulielmakis, M. Uiberacker, A. Baltuška, V. Yakovlev, F. Hammer, A. Scrinzi, Th. Westerwalbesloh, U. Kleineberg, U. Heinzmann, M. Drescher, and F. Krausz, 2004, Nature (London) **427**, 817.
- Kim, C. M., I. J. Kim, and C. H. Nam, 2005, Phys. Rev. A **72**, 033817.
- Kim, H. T., V. Tosa, and C. H. Nam, 2006, J. Phys. B **39**, S265.
- Kim, I. J., C. M. Kim, H. T. Kim, G. H. Lee, Y. S. Lee, J. Y. Park, D. J. Cho, and C. H. Nam, 2004, Phys. Rev. Lett. **94**, 243901.
- Kim, J.-H., D. G. Lee, H. J. Shin, and C. H. Nam, 2001, Phys. Rev. A **63**, 063403.
- Kim, T. K., C. M. Kim, M. G. Baik, G. Umesh, and C. H. Nam, 2004, Phys. Rev. A **69**, 051805(R).
- Kimura, W., M. Babzien, I. Ben-Zvi, L. P. Campbell, D. B. Cline, C. E. Dilley, J. C. Gallardo, S. C. Gottschalk, K. P. Kusche, R. H. Pantell, I. V. Pogorelsky, D. C. Quimby, J. Skaritka, L. C. Steinhauer, V. Yakimenko, and F. Zhou, 2004, Phys. Rev. Lett. **92**, 054801.
- Kimura, W., A. van Steenbergen, M. Babzien, I. Ben-Zvi, L. P. Campbell, D. B. Cline, C. E. Dilley, J. C. Gallardo, S. C. Gottschalk, P. He, K. P. Kusche, Y. Liu, R. H. Pantell, I. V. Pogorelsky, C. C. Quimby, J. Skaritka, L. C. Steinhauer, and V. Yakimenko, 2001, Phys. Rev. Lett. **86**, 4041.
- Kinoshita, K., M. Ito, and Y. Suzuki, 1987, Rev. Sci. Instrum. **58**, 932.
- Kirchmann, P. S., P. A. Loukakos, U. Bovensiepen, M. Wolf, S. Vijayalakshmi, F. Hennies, A. Pietsch, M. Nagasono, A. Föhlisch, and W. Wurth, 2007, in *Ultrafast Phenomena XV, Proceedings of the 15th International Conference*, edited by P. Corkum *et al.*, Springer Series in Chemical Physics Vol. 88 (Springer, Berlin), p. 612.
- Kitzler, M., and M. Lezius, 2005, Phys. Rev. Lett. **95**, 253001.
- Kitzler, M., N. Milosevic, A. Scrinzi, F. Krausz, and T. Brabec, 2002, Phys. Rev. Lett. **88**, 173904.
- Kitzler, M., K. O'Keeffe, and M. Lezius, 2006, J. Mod. Opt. **53**, 57.
- Kitzler, M., X. Xie, A. Scrinzi, and A. Baltuška, 2007, Phys. Rev. A **76**, 011801(R).
- Klamroth, T., 2006, J. Chem. Phys. **124**, 144310.
- Kling, M. F., Ch. Siedschlag, A. J. Verhoeft, J. I. Khan, M. Schultze, Th. Uphues, Y. Ni, M. Uiberacker, M. Drescher, F. Krausz, and M. J. J. Vrakking, 2006, Science **312**, 246.
- Kobayashi, T., A. Shirakawa, and T. Fuji, 2001, IEEE J. Sel. Top. Quantum Electron. **7**, 525.
- Kobayashi, Y., T. Sekikawa, Y. Nabekawa, and S. Watanabe, 1998, Opt. Lett. **23**, 64.
- Kobayashi, Y., D. Yoshitomi, K. Iwata, H. Takada, and K. Torizuka, 2007, Opt. Express **15**, 9748.
- Kofman, A. G., and G. Kurizki, 2000, Nature (London) **405**, 546.
- Kono, H., Y. Sato, M. Kanno, K. Nakai, and T. Kato, 2006, Bull. Chem. Soc. Jpn. **79**, 196.
- Kono, H., Y. Sato, N. Tanaka, T. Kato, K. Nakai, S. Koseki, and Y. Fujimura, 2004, Chem. Phys. **304**, 203.
- Kopold, R., D. B. Milošević, and W. Becker, 2000, Phys. Rev. Lett. **84**, 3831.
- Kosik, E. M., L. Corner, A. S. Wyatt, E. Cormier, I. A. Walms-

- ley, and L. F. DiMauro, 2005, *J. Mod. Opt.* **52**, 361.
- Kosuge, A., T. Sekikawa, X. Zhou, T. Kanai, S. Adachi, and S. Watanabe, 2006, *Phys. Rev. Lett.* **97**, 263901.
- Kovacev, M., Y. Maïresse, E. Priori, H. Merdji, O. Tcherbakoff, P. Monchicourt, P. Breger, E. Mevel, E. Constant, P. Salieres, B. Carré, and P. Agostini, 2003, *Eur. Phys. J. D* **26**, 79.
- Krause, J., K. Schafer, and K. Kulander, 1992, *Phys. Rev. Lett.* **68**, 3535.
- Krause, P., T. Klamroth, and P. Saalfrank, 2005, *J. Chem. Phys.* **123**, 074105.
- Krehl, P., and S. Engemann, 1995, *Shock Waves* **5**, 1.
- Kress, M., T. Löffler, M. D. Thomson, R. Dörner, H. Gimpel, K. Zrost, T. Ergler, R. Moshammer, U. Morgner, J. Ullrich, and H. G. Roskos, 2006, *Nat. Phys.* **2**, 327.
- Kroll, N. M., P. L. Morton, M. N. Rosenbluth, 1981, *IEEE J. Quantum Electron.* **QE-17**, 1436.
- Kruer, W. L., 2003, *The Physics of Laser-Plasma Interactions* (Westview, Boulder).
- Kubo, A., Y. S. Jung, H. K. Kim, and H. Petek, 2007, *J. Phys. B* **40**, S259.
- Kubo, A., K. Onda, H. Petek, Z. Sun, Y. S. Jung, and H. K. Kim, 2005, *Nano Lett.* **5**, 1123.
- Kuchiev, M. Yu, 1987, *Pis'ma Zh. Eksp. Teor. Fiz.* **45**, 404 [*JETP Lett.* **45**, 319 (1987)].
- Kugeler, O., G. Prümper, R. Hentges, J. Viefhaus, D. Rolles, U. Becker, S. Marburger, and U. Hergenhahn, 2004, *Phys. Rev. Lett.* **93**, 033002.
- Kulander, K. C., K. J. Schafer, and J. L. Krause, 1992, *Atoms in Intense Laser Fields*, edited by M. Gavrila (Academic, New York), p. 247.
- Kulander, K. C., K. J. Schafer, and J. L. Krause, 1993, in *Super-Intense Laser-Atom Physics*, edited by B. Piraux, A. L'Huillier, and K. Rzazewski, Vol. 316 of NATO Advanced Study Institute Series B: Physics (Plenum, New York), p. 95.
- Kuleff, A. I., J. Breidbach, and L. S. Cederbaum, 2005, *J. Chem. Phys.* **123**, 044111.
- Kuleff, A. I., and L. S. Cederbaum, 2007, *Phys. Rev. Lett.* **98**, 083201.
- Kwong, N.-H., and M. Bonitz, 2000, *Phys. Rev. Lett.* **84**, 1768.
- Lambropoulos, P., 1985, *Phys. Rev. Lett.* **55**, 2141.
- Lambropoulos, P., and P. Zoller, 1981, *Phys. Rev. A* **24**, 379.
- Lan, P., P. Lu, W. Cao, Y. Li, and X. Wang, 2007, *Phys. Rev. A* **76**, 021801(R).
- Lan, P., P. Lu, W. Cao, X. Wang, and W. Hong, 2007, *Opt. Lett.* **32**, 1186.
- Lan, P., P. Lu, W. Cao, X. Wang, and G. Yang, 2006, *Phys. Rev. A* **74**, 063411.
- Lappas, D. G., and A. L'Huillier, 1998, *Phys. Rev. A* **58**, 4140.
- Le, A.-T., T. Morishita, and C. D. Lin, 2008, *Phys. Rev. A* **78**, 023814.
- Le, Anh-Thu, X.-M. Tong, and C. D. Lin, 2006, *Phys. Rev. A* **73**, 041402.
- Lee, D. G., H. J. Shin, Y. H. Cha, K. H. Hong, J.-H. Kim, and C. H. Nam, 2001, *Phys. Rev. A* **63**, 021801(R).
- Lee, Y. S., J. H. Sung, C. H. Nam, T. J. Yu, and K. H. Hong, 2005, *Opt. Express* **13**, 2969.
- Lehr, L., M. T. Zanni, C. Frischkorn, R. Weinkauf, and D. M. Neumark, 1999, *Science* **284**, 635.
- Lein, M., 2005, *Phys. Rev. Lett.* **94**, 053004.
- Lein, M., 2007, *J. Phys. B* **40**, R135.
- Lein, M., P. P. Corso, J. P. Marangos, and P. L. Knight, 2003, *Phys. Rev. A* **67**, 023819.
- Lein, M., V. Engel, and E. K. U. Gross, 2001, *Opt. Express* **8**, 411.
- Lein, M., E. K. U. Gross, and V. Engel, 2001, *Phys. Rev. A* **64**, 023406.
- Lein, M., E. K. U. Gross, and V. Engel, 2002, *Laser Phys.* **12**, 487.
- Lein, M., N. Hay, R. Velotta, J. P. Marangos, and P. L. Knight, 2002, *Phys. Rev. Lett.* **88**, 183903.
- Lein, M., T. Kreibich, E. K. U. Gross, and V. Engel, 2002, *Phys. Rev. A* **65**, 033403.
- Lein, M., J. P. Marangos, and P. L. Knight, 2002, *Phys. Rev. A* **66**, 051404(R).
- Levine, R. D., 2005, *Molecular Reaction Dynamics* (Cambridge University Press, Cambridge, England).
- Levine, R. D., and F. Remacle, 2006, private communication.
- Levis, R. J., G. Menkir, and H. Rabitz, 2001, *Science* **292**, 709.
- Lewenstein, M., Ph. Balcou, M. Yu. Ivanov, A. L'Huillier, and P. B. Corkum, 1994, *Phys. Rev. A* **49**, 2117.
- Lewenstein, M., P. Salieres, and A. L'Huillier, 1995, *Phys. Rev. A* **52**, 4747.
- Lezius, M., V. Blanchet, D. M. Rayner, D. M. Villeneuve, A. Stolow, and M. Yu. Ivanov, 2001, *Phys. Rev. Lett.* **86**, 51.
- L'Huillier, A., and P. Balcou, 1993, *Phys. Rev. Lett.* **70**, 774.
- L'Huillier, A., L. A. Lompre, G. Mainfray, and C. Manus, 1983, *Phys. Rev. A* **27**, 2503.
- Li, C., E. Moon, H. Mashiko, C. M. Nakamura, P. Ranitovic, C. M. Mahajan, C. L. Cocke, and Z. Chang, 2006, *Opt. Express* **14**, 11468.
- Li, C., E. Moon, H. Wang, H. Mashiko, C. M. Nakamura, J. Tackett, and Z. Chang, 2007, *Opt. Lett.* **32**, 796.
- Lichters, R., J. Meyer-ter-Vehn, and A. Pukhov, 1996, *Phys. Plasmas* **3**, 3425.
- Lin, C. D., X. M. Tong, and T. Morishita, 2006, *J. Phys. B* **39**, S419.
- Lindner, F., G. G. Paulus, H. Walther, A. Baltuška, E. Goulielmakis, M. Lezius, and F. Krausz, 2004, *Phys. Rev. Lett.* **92**, 113001.
- Lindner, F., M. G. Schätzel, H. Walther, A. Baltuška, E. Goulielmakis, F. Krausz, D. B. Milosevic, D. Bauer, W. Becker, and G. G. Paulus, 2005, *Phys. Rev. Lett.* **95**, 040401.
- Liu, X., C. Figueira de Morisson Faria, W. Becker, and P. B. Corkum, 2006, *J. Phys. B* **39**, L305.
- Liu, X., H. Rottke, E. Eremina, W. Sandner, E. Goulielmakis, K. O. Keeffe, M. Lezius, F. Krausz, F. Lindner, M. G. Schätzel, G. G. Paulus, and H. Walther, 2004, *Phys. Rev. Lett.* **93**, 263001.
- Liu, Y., X. J. Wang, D. B. Cline, M. Babzien, J. M. Fang, J. Gallardo, K. Kusche, I. Pogorelsky, J. Skaritka, and A. van Steenbergen, 1998, *Phys. Rev. Lett.* **80**, 4418.
- Lobastov, V. A., R. Srinivasan, and A. H. Zewail, 2005, *Proc. Natl. Acad. Sci. U.S.A.* **102**, 7069.
- Loh, Z.-H., C. H. Greene, and S. R. Leone, 2008, *Chem. Phys.* **350**, 7.
- Loh, Z.-H., M. Khalil, R. E. Correa, R. Santra, C. Buth, and S. R. Leone, 2007, *Phys. Rev. Lett.* **98**, 143601.
- Lohr, A., M. Kleber, R. Kopold, and W. Becker, 1997, *Phys. Rev. A* **55**, R4003.
- López-Martens, R., J. Mauritsson, P. Johnsson, and A. L'Huillier, 2004, *Phys. Rev. A* **69**, 053811.
- López-Martens, R., K. Varjú, P. Johnsson, J. Mauritsson, Y. Maïresse, P. Salieres, M. B. Gaarde, K. J. Schafer, A. Persson, S. Svanberg, C.-G. Wahlström, and A. L'Huillier, 2005, *Phys. Rev. Lett.* **94**, 033001.
- Ma, L.-S., R. K. Shelton, H. C. Kapteyn, M. M. Murnane, and

- J. Ye, 2001, Phys. Rev. A **64**, 021802.
- Ma, Y.-Y., Z.-M. Sheng, Y.-T. Li, W.-W. Chang, X.-H. Yuan, M. Chen, H.-C. Wu, J. Zheng, and J. Zhang, 2006, Phys. Plasmas **13**, 110702.
- Macklin, J., J. D. Kmetec, and C. L. Gordon III, 1993, Phys. Rev. Lett. **70**, 766.
- Madhavan, V., W. Chen, T. Jamneala, M. F. Crommie, and N. S. Wingreen, 1998, Science **280**, 567.
- Maeda, H., M. Dammasch, U. Eichmann, W. Sandner, A. Becker, and F. H. M. Faisal, 2000, Phys. Rev. A **62**, 035402.
- Mahan, G. D., 1993, *Many-Particle Physics*, 2nd ed. (Plenum, New York).
- Mairesse, Y., A. De Bohan, L. J. Frasinski, H. Merdji, L. C. Dinu, P. Monchicourt, P. Bréger, M. Kovacev, T. Auguste, B. Carré, H. G. Muller, P. Agostini, and P. Salieres, 2004, Phys. Rev. Lett. **93**, 163901.
- Mairesse, Y., A. De Bohan, L. J. Frasinski, H. Merdji, L. C. Dinu, P. Monchicourt, P. Bréger, M. Kovacev, R. Taieb, B. Carré, H. G. Muller, P. Agostini, and P. Salieres, 2003, Science **302**, 1540.
- Mairesse, Y., and F. Quéré, 2005, Phys. Rev. A **71**, 011401(R).
- Mangles, S. P. D., C. D. Murphy, Z. Najmudin, A. G. R. Thomas, J. L. Collier, A. E. Dangor, E. J. Divall, P. S. Foster, J. G. Gallacher, C. J. Hooker, D. A. Jaroszynski, A. J. Langley, W. B. Mori, P. A. Norreys, F. S. Tsung, R. Viskup, B. R. Walton, and K. Krushelnick, 2004, Nature (London) **431**, 535.
- Manzoni, C., C. Vozzi, E. Benedetti, G. Sansone, S. Stagira, O. Svelto, S. De Silvestri, M. Nisoli, and G. Cerullo, 2006, Opt. Lett. **31**, 963.
- Marburger, S., O. Kugeler, U. Hergenhahn, and T. Möller, 2003, Phys. Rev. Lett. **90**, 203401.
- Markevitch, A. N., S. M. Smith, D. A. Romanov, H. B. Schlegel, M. Yu. Ivanov, and R. J. Levis, 2003, Phys. Rev. A **68**, 011402(R).
- Martinez, T. J., M. Ben-Nun, and R. D. Levine, 1996, J. Phys. Chem. **100**, 7884.
- Martinez, T. J., M. Ben-Nun, and R. D. Levine, 1997, J. Phys. Chem. **101**, 6389.
- Mashiko, H., C. M. Nakamura, C. Li, E. Moon, H. Wang, J. Tackett, and Z. Chang, 2007, Appl. Phys. Lett. **90**, 161114.
- Matsubara, E., K. Yamane, T. Sekikawa, and M. Yamashita, 2007, J. Opt. Soc. Am. B **24**, 985.
- Matuschek, N., F. X. Kärtner, and U. Keller, 1998, IEEE J. Sel. Top. Quantum Electron. **4**, 197.
- Mauritsson, J., P. Johnsson, E. Gustafsson, A. L'Huillier, K. J. Schafer, and M. B. Gaarde, 2006, Phys. Rev. Lett. **97**, 013001.
- McPherson, A., G. Gibson, H. Jara, U. Johann, T. S. Luk, I. A. McIntyre, K. Boyer, C. K. Rhodes, 1987, J. Opt. Soc. Am. B **4**, 595.
- Meckel, M., D. Comtois, D. Zeidler, A. Staudte, D. Pavicic, H. C. Bandulet, H. Pépin, J. C. Kieffer, R. Dörner, D. M. Villeneuve, and P. B. Corkum, 2008, Science **320**, 1478.
- Mercouris, T., Y. Komninos, and C. A. Nicolaides, 2004, Phys. Rev. A **69**, 032502.
- Mercouris, T., Y. Komninos, and C. A. Nicolaides, 2007a, Phys. Rev. A **75**, 013407.
- Mercouris, T., Y. Komninos, and C. A. Nicolaides, 2007b, Phys. Rev. A **76**, 033417.
- Merdji, H., M. Kovacev, W. Boutu, P. Salieres, F. Vernay, and B. Carré, 2006, Phys. Rev. A **74**, 043804.
- Miaja-Avila, L., C. Lei, M. Aeschlimann, J. L. Gland, M. M. Murnane, H. C. Kapteyn, and G. Saathoff, 2006, Phys. Rev. Lett. **97**, 113604.
- Mikhailova, Yu. M., V. T. Platonenko, and S. G. Rykovanov, 2005, JETP Lett. **81**, 571.
- Milošević D., and W. Becker, 2002, Phys. Rev. A **66**, 063417.
- Milošević D., G. G. Paulus, D. Bauer, and W. Becker, 2006, J. Phys. B **39**, R203.
- Mineo, H., K. Nagaya, M. Hayashi, and S. H. Lin, 2007, J. Phys. B **40**, 2435.
- Mirkin, C. A., and M. A. Ratner, 1992, Annu. Rev. Phys. Chem. **43**, 719.
- Miyamoto, N., M. Kamei, D. Yoshitomi, T. Kanai, T. Sekikawa, T. Nakajima, and S. Watanabe, 2004, Phys. Rev. Lett. **93**, 083903.
- Miyashita, O., M. Y. Okamura, and J. N. Onuchic, 2005, Proc. Natl. Acad. Sci. U.S.A. **102**, 3558.
- Monastyrskiy, M., S. Andreev, D. Greenfield, G. Bryukhnevich, V. Tarasov, and M. Yu Schelev, 2005, in *High-Speed Photography and Photonics*, edited by B. J. Thompson (SPIE, Bellingham, WA), Vol. 5580 p. 324.
- Morishita, T., A.-T. Le, Z. Chen, and C. D. Lin, 2008, Phys. Rev. Lett. **100**, 013903.
- Morishita, T., S. Watanabe, and C. D. Lin, 2007, Phys. Rev. Lett. **98**, 083003.
- Morishita, Y., X.-J. Liu, N. Saito, T. Lischke, M. Kato, G. Prümper, M. Oura, H. Yamaoka, Y. Tamenori, I. H. Suzuki, and K. Ueda, 2006, Phys. Rev. Lett. **96**, 243402.
- Morlens, A.-S., P. Balcou, P. Zeitoun, C. Valentin, V. Laude, and S. Kazamias, 2005, Opt. Lett. **30**, 1554.
- Moshammer, R., B. Feuerstein, W. Schmitt, A. Dorn, C. D. Schröter, J. Ullrich, H. Rottke, C. Trump, M. Wittmann, G. Korn, K. Hoffmann, and W. Sandner, 2000, Phys. Rev. Lett. **84**, 447.
- Moshammer, R., W. Schmitt, J. Ullrich, H. Kollmus, A. Cassimi, R. Dörner, O. Jagutzki, R. Mann, R. E. Olson, H. T. Prinz, H. Schmidt-Böcking, and L. Spielberger, 1997, Phys. Rev. Lett. **79**, 3621.
- Mourou, G., T. Tajima, and S. V. Bulanov, 2006, Rev. Mod. Phys. **78**, 309.
- Mourou, G., and S. Williamson, 1982, Appl. Phys. Lett. **41**, 44.
- Mücke, O. D., T. Tritschler, M. Wegener, U. Morgner, F. X. Kärtner, G. Khitrova, H. M. Gibbs, 2004, Opt. Lett. **29**, 2160.
- Muller, H. G., and F. C. Kooiman, 1998, Phys. Rev. Lett. **81**, 1207.
- Murray, R., and M. Ivanov, 2008, J. Mod. Opt. **55**, 2513.
- Musumeci, P., S. Ya. Tochitsky, S. Boucher, C. E. Clayton, A. Doyuran, R. J. England, C. Joshi, C. Pellegrini, J. E. Ralph, J. B. Rosenzweig, C. Sung, S. Tolmachev, G. Travish, A. A. Varfolomeev, A. A. Varfolomeev, Jr., T. Yarovoi, and R. B. Yoder, 2005, Phys. Rev. Lett. **94**, 154801.
- Nabekawa, Y., H. Hasegawa, E. J. Takahashi, and K. Midorikawa, 2005, Phys. Rev. Lett. **94**, 043001.
- Nabekawa, Y., T. Shimizu, T. Okino, K. Furusawa, H. Hasegawa, K. Yamanouchi, and K. Midorikawa, 2006, Phys. Rev. Lett. **97**, 153904.
- Nakajima, T., and S. Watanabe, 2006, Opt. Lett. **31**, 1920.
- Naumov, S., A. Fernandez, R. Graf, P. Dombi, F. Krausz, and A. Apolonskiy, 2005, New J. Phys. **7**, 216.
- Naumova, N. M., J. A. Nees, I. V. Sokolov, B. Hou, and G. Mourou, 2004, Phys. Rev. Lett. **92**, 063902.
- Naumova, N., I. Sokolov, J. Nees, A. Maksimchuk, V. Yanovsky, and G. Mourou, 2004, Phys. Rev. Lett. **93**, 195003.
- Nest, M., R. Padmanaban, and P. Saalfrank, 2007, J. Chem. Phys. **126**, 214106.
- Neumark, D. M., 2001, Annu. Rev. Phys. Chem. **52**, 255.

- Neutze, R., R. Wouts, D. van der Spoel, E. Weckert, and J. Hajdu, 2000, *Nature (London)* **406**, 752.
- Nicolaides, C. A., T. Mercouris, and Y. Komninos, 2002, *J. Phys. B* **35**, L271.
- Niikura, H., P. B. Corkum, and D. M. Villeneuve, 2003, *Phys. Rev. Lett.* **90**, 203601.
- Niikura, H., F. Légaré, R. Hasbani, A. D. Bandrauk, M. Y. Ivanov, D. M. Villeneuve, and P. B. Corkum, 2002, *Nature (London)* **417**, 917.
- Niikura, H., F. Légaré, R. Hasbani, M. Y. Ivanov, D. M. Villeneuve, and P. B. Corkum, 2003, *Nature (London)* **421**, 826.
- Niikura, H., D. M. Villeneuve, and P. B. Corkum, 2005, *Phys. Rev. Lett.* **94**, 083003.
- Nikolopoulos, L. A. A., E. P. Benis, P. Tzallas, D. Charalambidis, K. Witte, and G. D. Tsakiris, 2005, *Phys. Rev. Lett.* **94**, 113905.
- Nikolopoulos, L. A. A., and P. Lambropoulos, 2001, *J. Phys. B* **34**, 545.
- Nishioka, H., W. Odajima, K. Ueda, and H. Takuma, 1995, *Opt. Lett.* **20**, 2505.
- Nisoli, M., S. De Silvestri, and O. Svelto, 1996, *Appl. Phys. Lett.* **68**, 2793.
- Nisoli, M., S. De Silvestri, O. Svelto, R. Szipöcs, K. Ferencz, C. Spielmann, S. Sartania, and F. Krausz, 1997, *Opt. Lett.* **22**, 522.
- Nitzan, A., 2001, *Annu. Rev. Phys. Chem.* **52**, 681.
- Nitzan, A., and M. A. Ratner, 2003, *Science* **300**, 1384.
- Nguyen, N. A., and A. D. Bandrauk, 2006, *Phys. Rev. A* **73**, 032708.
- Nomura, Y., R. Hörlein, P. Tzallas, B. Dromey, S. Rykovanov, Zs. Major, J. Osterhoff, S. Karsch, L. Veisz, M. Zepf, D. Charalambidis, F. Krausz, and G. D. Tsakiris, 2009, *Nat. Phys. (to be published)*.
- Nordlund, D., H. Ogasawara, H. Bluhm, O. Takahashi, M. Odelius, M. Nagasono, L. G. M. Pettersson, and A. Nilsson, 2007, *Phys. Rev. Lett.* **99**, 217406.
- Norrish, R. G. W., and G. Porter, 1949, *Nature (London)* **164**, 658.
- Ogawa, S., H. Nagano, H. Petek, and A. Heberle, 1997, *Phys. Rev. Lett.* **78**, 1339.
- Öhrwall, G., M. Tchaplyguine, M. Lundwall, R. Feifel, H. Bergersen, T. Rander, A. Lindblad, J. Schulz, S. Peredkov, S. Barth, S. Marburger, U. Hergenhahn, S. Svensson, and O. Björneholm, 2004, *Phys. Rev. Lett.* **93**, 173401.
- Oishi, Y., M. Kaku, A. Suda, F. Kannari, and K. Midorikawa, 2006, *Opt. Express* **14**, 7230.
- Oishi, Y., A. Suda, F. Kannari, and K. Midorikawa, 2005, *Rev. Sci. Instrum.* **76**, 093114.
- O'Keeffe, K., P. Jöckl, H. Drexel, V. Grill, F. Krausz, and M. Lezius, 2004, *Appl. Phys. B: Lasers Opt.* **78**, 583.
- Okunishi, M., T. Morishita, G. Prümper, K. Shimada, C. D. Lin, S. Watanabe, and K. Ueda, 2008, *Phys. Rev. Lett.* **100**, 143001.
- O'Reagan, B., and M. Grätzel, 1991, *Nature (London)* **353**, 737.
- Palmer, R., 1972, *J. Appl. Phys.* **43**, 3014.
- Panfili, R., S. L. Haan, and J. H. Eberly, 2002, *Phys. Rev. Lett.* **89**, 113001.
- Patchkovskii, S., Z. X. Zhao, T. Brabec, and D. Villeneuve, 2006, *Phys. Rev. Lett.* **97**, 123003.
- Paul, A., R. Bartels, I. P. Christov, H. C. Kapteyn, M. M. Murnane, and S. Backus, 2003, *Nature (London)* **421**, 51.
- Paul, A., E. A. Gibson, X. Zhang, A. Lytle, T. Popmintchev, X. Zhou, M. M. Murnane, I. P. Christov, and H. C. Kapteyn, 2006, *IEEE J. Quantum Electron.* **42**, 14.
- Paul, P. M., E. S. Toma, P. Berger, G. Mullot, F. Auge, Ph. Balcou, H. G. Muller, and P. Agostini, 2001, *Science* **292**, 1689.
- Paulus, G. G., F. Grasbon, H. Walther, P. Villoresi, M. Nisoli, S. Stagira, E. Priori, and S. De Silvestri, 2001, *Nature (London)* **414**, 182.
- Paulus, G. G., F. Lindner, H. Walther, A. Baltuška, E. Goulielmakis, M. Lezius, and F. Krausz, 2003, *Phys. Rev. Lett.* **91**, 253004.
- Paulus, G. G., F. Lindner, H. Walther, A. Baltuška, and F. Krausz, 2005, *J. Mod. Opt.* **52**, 221.
- Penent, F., J. Paladoux, J. P. Lablanquie, L. Andric, R. Feitel, and J. H. D. Eland, 2005, *Phys. Rev. Lett.* **95**, 083002.
- Perelomov, A. M., and V. S. Popov, 1967, *Zh. Eksp. Teor. Fiz.* **52**, 514 [Sov. Phys. JETP **25**, 336 (1967)].
- Perelomov, A. M., V. S. Popov, and M. V. Terent'ev, 1966a, *Zh. Eksp. Teor. Fiz.* **50**, 1393 [Sov. Phys. JETP **23**, 924 (1966)].
- Perelomov, A. M., V. S. Popov, and M. V. Terent'ev, 1966b, *Zh. Eksp. Teor. Fiz.* **51**, 309 [Sov. Phys. JETP **24**, 207 (1967)].
- Pérez-Hernández, J. A., and L. Plaja, 2007, *Phys. Rev. A* **76**, 023829.
- Petek, H., and S. Ogawa, 1997, *Prog. Surf. Sci.* **56**, 239.
- Pfeifer, T., L. Gallmann, M. J. Abel, D. M. Neumark, and S. R. Leone, 2006a, *Opt. Lett.* **31**, 975.
- Pfeifer, T., L. Gallmann, M. J. Abel, D. M. Neumark, and S. R. Leone, 2006b, *Phys. Rev. Lett.* **97**, 163901.
- Pfeifer, T., A. Jullien, M. J. Abel, P. M. Nagel, L. Gallmann, D. M. Neumark, and S. R. Leone, 2007, *Opt. Express* **15**, 17120.
- Pfeifer, T., C. Spielmann, and G. Gerber, 2006, *Rep. Prog. Phys.* **69**, 443.
- Pirozhkov, A. S., S. V. Bulanov, T. Zh. Esirkepov, M. Mori, A. Sagisaka, and H. Daido, 2006, *Phys. Plasmas* **13**, 013107.
- Platonenko, V. T., and V. Strelkov, 1999, *J. Opt. Soc. Am. B* **16**, 435.
- Plettner, T., R. L. Byer, E. Colby, B. Cowan, C. M. S. Sears, J. E. Spencer, and R. H. Siemann, 2005, *Phys. Rev. Lett.* **95**, 134801.
- Plettner, T., P. P. Lu, and R. L. Byer, 2006, *Phys. Rev. ST Accel. Beams* **9**, 111301.
- Poater, J., M. Duran, M. Solá, and B. Silvi, 2005, *Chem. Rev. (Washington, D.C.)* **105**, 3911.
- Popov, A. M., O. V. Tikhonova, and E. A. Volkova, 2007, *Laser Phys.* **17**, 103.
- Popov, V. S., 2004, *Phys. Usp.* **47**, 855.
- Popruzhenko, S. V., Ph. A. Korreev, S. P. Goreslavski, and W. Becker, 2002, *Phys. Rev. Lett.* **89**, 023001.
- Popruzhenko, S. V., N. I. Shvetsov-Shilovski, S. P. Goreslavski, W. Becker, and G. G. Paulus, 2007, *Opt. Lett.* **32**, 1372.
- Pozar, D. M., 2004, *Microwave Engineering*, 3rd ed. (Wiley, New York).
- Prauzner-Bechcicki, J. S., K. Sacha, B. Eckhardt, and J. J. Zakrzewski, 2005, *Phys. Rev. A* **71**, 033407.
- Protopapas, M., D. G. Lappas, C. H. Keitel, and P. L. Knight, 1996, *Phys. Rev. A* **53**, R2933.
- Pukhov, A., and S. Gordienko, 2006, *Philos. Trans. R. Soc. London, Ser. A* **364**, 623.
- Pukhov, A., S. Gordienko, and T. Baeva, 2003, *Phys. Rev. Lett.* **91**, 173002.
- Pukhov, A., and J. Meyer-ter-Vehn, 2002, *Appl. Phys. B* **74**, 355.
- Quéré, F., S. Guizard, Ph. Martin, G. Petite, H. Merdji, B.

- Carré, J.-F. Hergott, and L. Le Déroff, 2000, Phys. Rev. B **61**, 9883.
- Quéré, F., J. Itatani, G. L. Yudin, and P. B. Corkum, 2003, Phys. Rev. Lett. **90**, 073902.
- Quéré, F., Y. Mairesse, and J. Itatani, 2005, J. Mod. Opt. **52**, 339.
- Raether, H., 1988, Ed., *Surface Plasmons* (Springer, Berlin).
- Ray, D., B. Ulrich, I. Bocharova, C. Maharjan, P. Ranitovic, B. Gramkow, M. Magrakvelidze, S. De, I. V. Litvinyuk, A.-T. Le, T. Morishita, C. D. Lin, G. G. Paulus, and C. L. Cocke, 2008, Phys. Rev. Lett. **100**, 143002.
- Reckenthäler, P., M. Centurion, V. S. Yakovlev, M. Lezius, F. Krausz, and E. E. Fill, 2008, Phys. Rev. A **77**, 042902.
- Reichert, J., R. Holzwarth, T. Udem, and T. W. Hänsch, 1999, Opt. Commun. **172**, 59.
- Reid, K. L., 2003, Annu. Rev. Phys. Chem. **54**, 397.
- Reiss, H. R., 1980a, Phys. Rev. A **22**, 1786.
- Reiss, H. R., 1980b, J. Opt. Soc. Am. **7**, 574.
- Reiss, H. R., 1992, Prog. Quantum Electron. **16**, 1.
- Remacle, F., R. Kienberger, F. Krausz, and R. D. Levine, 2007, Chem. Phys. **338**, 342.
- Remacle, F., and R. D. Levine, 1997, J. Chem. Phys. **107**, 3382.
- Remacle, F., and R. D. Levine, 1999, J. Chem. Phys. **110**, 5089.
- Remacle, F., and R. D. Levine, 2006a, Proc. Natl. Acad. Sci. U.S.A. **103**, 6793.
- Remacle, F., and R. D. Levine, 2006b, Faraday Discuss. **131**, 45.
- Remacle, F., and R. D. Levine, 2007, Z. Phys. Chem. (Munich) **221**, 647.
- Remacle, F., R. D. Levine, and M. A. Ratner, 1998, Chem. Phys. Lett. **285**, 25.
- Remacle, F., R. D. Levine, E. W. Schlag, and R. Weinkauf, 1999, J. Phys. Chem. A **103**, 10149.
- Remetter, T., P. Johnsson, J. Mauritsson, K. Varjú, Y. Ni, F. Lépine, E. Gustafsson, M. Kling, J. Kahn, R. López-Martens, K. J. Schafer, M. J. J. Vrakking, and A. L'Huillier, 2006, Nat. Phys. **2**, 323.
- Renault, A., D. Z. Kandula, S. Witte, A. L. Wolf, R. Th. Zinkstok, W. Hogervorst, and K. S. E. Eikema, 2007, Opt. Lett. **32**, 2363.
- Rice, S., and M. Zhao, 2000, *Optical Control of Molecular Dynamics* (Wiley, New York).
- Riedle, E., M. Beutter, S. Lochbrunner, J. Piel, S. Schenkl, S. Sporlein, and W. Zinth, 2000, Appl. Phys. B: Lasers Opt. **71**, 457.
- Riffe, D. M., X. Y. Wang, M. C. Downer, D. L. Fisher, T. Tajima, J. L. Erskine, and R. M. More, 1993, J. Opt. Soc. Am. B **10**, 1424.
- Rohringer, N., A. Gordon, and R. Santra, 2006, Phys. Rev. A **74**, 043420.
- Rolles, D., M. Braune, S. Cvejanović, O. Geßner, R. Hentges, S. Korica, B. Langer, T. Lischke, G. Prümper, A. Reinköster, J. Viehaus, B. Zimmermann, V. McKoy, and U. Becker, 2005, Nature (London) **437**, 711.
- Rottke, H., C. Trump, M. Wittmann, G. Korn, W. Sandner, R. Moshammer, A. Dorn, C. D. Schröter, D. Fischer, J. P. Crespo Lopez-Urrutia, P. Neumayer, J. Diepenwisch, C. Höhr, B. Feuerstein, and J. Ullrich, 2002, Phys. Rev. Lett. **89**, 013001.
- Roudnev, V., and B. D. Esry, 2007, Phys. Rev. A **76**, 023403.
- Roudnev, V., B. D. Esry, and I. Ben-Itzhak, 2004, Phys. Rev. Lett. **93**, 163601.
- Rousse, A., C. Rischel, and J.-C. Gauthier, 2001, Rev. Mod. Phys. **73**, 17.
- Rudenko, A., K. Zrost, B. Feuerstein, V. L. B. de Jesus, C. D. Schröter, R. Moshammer, and J. Ullrich, 2004, Phys. Rev. Lett. **93**, 253001.
- Ruiz, C., L. Plaja, L. Roso, and A. Becker, 2006, Phys. Rev. Lett. **96**, 053001.
- Rundquist, A., C. G. Durfee, III, S. Backus, C. Herne, Z. Chang, M. M. Murnane, and H. C. Kapteyn, 1998, Science **280**, 1412.
- Rzazewski, K., and J. H. Eberly, 1981, Phys. Rev. Lett. **47**, 408.
- Sakai, K., S. Miyazaki, S. Kawata, S. Hasumi, and T. Kikuchi, 2006, Laser Part. Beams **24**, 321.
- Salamin, Y. I., and C. H. Keitel, 2000, Appl. Phys. Lett. **77**, 1082.
- Saldin, E. L., E. A. Schneidmiller, and M. V. Yurkov, 2004, Opt. Commun. **239**, 161.
- Salieres, P., B. Carre, L. Le Deroff, F. Grasbon, G. G. Paulus, H. Walther, R. Kopold, W. Becker, D. B. Milosevic, A. Sanpera, and M. Lewenstein, 2001, Science **292**, 902.
- Salieres, P., A. L'Huillier, P. Antoine, and M. Lewenstein, 1999, Adv. At., Mol., Opt. Phys. **41**, 83.
- Sansone, G., E. Benedetti, F. Calegari, C. Vozzi, L. Avaldi, R. Flammini, L. Poletto, P. Villoresi, C. Altucci, R. Velotta, S. Stagira, S. De Silvestri, and M. Nisoli, 2006, Science **314**, 443.
- Santra, R., and R. W. Dunford, and L. Young, 2006, Phys. Rev. A **74**, 043403.
- Santra, R., and A. Gordon, 2006, Phys. Rev. Lett. **96**, 073906.
- Sartania, S., Z. Cheng, M. Lenzer, G. Tempea, C. Spielmann, and F. Krausz, 1997, Opt. Lett. **22**, 1562.
- Schafer, K. J., M. B. Gaarde, A. Heinrich, J. Biegert, and U. Keller, 2004, Phys. Rev. Lett. **92**, 023003.
- Schafer, K. J., and K. C. Kulander, 1990, Phys. Rev. A **42**, 5794.
- Schafer, K. J., and K. C. Kulander, 1997, Phys. Rev. Lett. **78**, 638.
- Schafer, K. J., B. Yang, L. F. DiMauro, and K. C. Kulander, 1993, Phys. Rev. Lett. **70**, 1599.
- Schelev, M. Ya., M. C. Richardson, and A. J. Alcock, 1971, Appl. Phys. Lett. **18**, 354.
- Schins, J. M., P. Breger, P. Agostini, R. C. Constantinescu, H. G. Müller, A. Bouhal, G. Grillon, A. Antonetti, and A. Mysyrowicz, 1996, J. Opt. Soc. Am. B **13**, 197.
- Schins, J. M., P. Breger, P. Agostini, R. C. Constantinescu, H. G. Müller, G. Grillon, A. Antonetti, and A. Mysyrowicz, 1994, Phys. Rev. Lett. **73**, 2180.
- Schmuttenmaer, C. A., M. Aeschlimann, H. E. Elsayed-Ali, R. J. D. Miller, D. A. Mantel, J. Cao, and Y. Gao, 1994, Phys. Rev. B **50**, 8957.
- Schnadt, J., P. A. Brühwiler, L. Patthey, J. N. O'Shea, S. Södergren, M. Odellus, R. Ahuja, O. Karis, M. Bässler, P. Persson, H. Siegbahn, S. Lunell, and N. Martensson, 2002, Nature (London) **418**, 620.
- Schneider, T., P. L. Chocian, and J.-M. Rost, 2002, Phys. Rev. Lett. **89**, 073002.
- Schnürer, M., Z. Cheng, M. Hentschel, G. Tempea, P. Kálmán, T. Brabec, and F. Krausz, 1999, Phys. Rev. Lett. **83**, 722.
- Schoenlein, R. W., J. G. Fujimoto, G. L. Eesley, and T. W. Capehart, 1988, Phys. Rev. Lett. **61**, 2596.
- Schöne, W.-D., and W. Ekardt, 2000, Phys. Rev. B **62**, 13464.
- Schultz, K. D., C. I. Blaga, R. Chirla, P. Colosimo, J. Cryan, A. M. March, C. Roedig, E. Sistrunk, J. Tate, J. Wheeler, P. Agostini, and L. F. DiMauro, 2007, J. Mod. Opt. **54**, 1075.
- Schultze, M., E. Goulielmakis, M. Uiberacker, M. Hofstetter, J. Kim, D. Kim, F. Krausz, and U. Kleineberg, 2007, New J. Phys. **9**, 243.

- Schweigert, I. V., and S. Mukamel, 2007, Phys. Rev. A **76**, 012504.
- Scrinzi, A., M. Geissler, and T. Brabec, 2001a, Phys. Rev. Lett. **86**, 412.
- Scrinzi, A., M. Geissler, and T. Brabec, 2001b, Laser Phys. **11**, 169.
- Scrinzi, A., M. Yu. Ivanov, R. Kienberger, and D. M. Villeneuve, 2005, J. Phys. B **39**, R1.
- Sears, C. M. S., E. R. Colby, B. M. Cowan, R. H. Siemann, J. E. Spencer, R. L. Byer, and T. Plettner, 2005, Phys. Rev. Lett. **95**, 194801.
- Seel, M., and W. Domcke, 1991, J. Chem. Phys. **95**, 7806.
- Sekikawa, T., T. Kanai, and S. Watanabe, 2003, Phys. Rev. Lett. **91**, 103902.
- Sekikawa, T., T. Katsura, S. Miura, and S. Watanabe, 2002, Phys. Rev. Lett. **88**, 193902.
- Sekikawa, T., A. Kosuge, T. Kanai, and S. Watanabe, 2004, Nature (London) **432**, 605.
- Seres, J., E. Seres, A. J. Verhoef, G. Tempea, C. Strelci, P. Wobrauscheck, V. Yakovlev, A. Scrinzi, C. Spielmann, and F. Krausz, 2005, Nature (London) **433**, 596.
- Seres, J., V. S. Yakovlev, E. Seres, Ch. Strelci, P. Wobrauscheck, C. Spielmann, and F. Krausz, 2007, Nat. Phys. **3**, 878.
- Shan, B., and Z. Chang, 2001, Phys. Rev. A **65**, 011804(R).
- Shan, B., S. Ghimire, and Z. Chang, 2005, J. Mod. Opt. **52**, 277.
- Shapiro, M., and Y. Zeiri, 1986, J. Chem. Phys. **85**, 6449.
- Sheehy, B., J. D. D. Martin, L. F. DiMauro, P. Agostini, K. J. Schafer, M. B. Gaarde, and K. C. Kulander, 1999, Phys. Rev. Lett. **83**, 5270.
- Shirakawa, A., and T. Kobayashi, 1998, Appl. Phys. Lett. **72**, 147.
- Shirakawa, A., I. Sakane, and T. Kobayashi, 1998, Opt. Lett. **23**, 1292.
- Shirakawa, A., I. Sakane, M. Takasaka, and T. Kobayashi, 1999, Appl. Phys. Lett. **74**, 2268.
- Shorokov, D., and A. H. Zewail, 2008, Phys. Chem. Chem. Phys. **10**, 2879.
- Shverdin, M. Y., D. R. Walker, D. D. Yavuz, G. Y. Yin, and S. E. Harris, 2005, Phys. Rev. Lett. **94**, 033904.
- Shvetsov-Shilovski, N. I., S. P. Goreslavski, S. V. Popruzhenko, W. Becker, and G. G. Paulus, 2007, Laser Phys. Lett. **4**, 726.
- Siegman, A., 1986, *Lasers* (University Science Books, Mill Valley).
- Siffalovic, P., M. Drescher, and U. Heinzmann, 2002, Europhys. Lett. **60**, 924.
- Siffalovic, P., M. Michelwirth, P. Bartz, B. Decker, C. Agena, C. Schäfer, S. Molter, R. Ros, M. Bach, M. Neumann, D. Andelmetti, J. Mattay, U. Heinzmann, and M. Drescher, 2004, J. Biotechnol. **112**, 139.
- Silkin, V. M., M. Quijada, R. Díez Muino, E. V. Chulkov, and P. M. Echenique, 2007, Surf. Sci. **601**, 4546.
- Simpson, J., and U. Fano, 1963, Phys. Rev. Lett. **11**, 158.
- Siwick, B. J., J. R. Dwyer, R. E. Jordan, and R. J. D. Miller, 2003, Science **302**, 1382.
- Smirnova, O., S. Patchkovskii, and M. Spanner, 2007, Phys. Rev. Lett. **98**, 123001.
- Smirnova, O., M. Spanner, and M. Ivanov, 2006, J. Phys. B **39**, S323.
- Smirnova, O., V. S. Yakovlev, and M. Ivanov, 2005, Phys. Rev. Lett. **94**, 213001.
- Smirnova, O., V. S. Yakovlev, and A. Scrinzi, 2003, Phys. Rev. Lett. **91**, 253001.
- Smith, P. W., M. A. Duguay, and E. P. Ippen, 1974, Prog. Quantum Electron. **3**, 107.
- Sokolov, A., M. Y. Shverdin, D. R. Walker, D. D. Yavuz, A. M. Burzo, G. Y. Yin, and S. E. Harris, 2005, J. Mod. Opt. **52**, 285.
- Sokolov, A., D. R. Walker, D. D. Yavuz, G. Y. Yin, and S. E. Harris, 2001, Phys. Rev. Lett. **87**, 033402.
- Sola, I., 2004, Phys. Rev. A **69**, 033401.
- Sola, I. J., E. Mével, L. Elouga, E. Constant, V. Strelkov, L. Poletto, P. Villoresi, E. Benedetti, J-P. Caumes, S. Stagira, C. Vozzi, G. Sansone, and M. Nisoli, 2006, Nat. Phys. **2**, 319.
- Sola, I. J., A. Zair, R. López-Martens, P. Johnsson, K. Varjú, E. Cormier, J. Mauritsson, A. L'Huillier, V. Strelkov, E. Mével, and E. Constant, 2006, Phys. Rev. A **74**, 013810.
- Spanner, M., O. Smirnova, and M. Yu. Ivanov, 2004, J. Phys. B **37**, L243.
- Spielmann, C., C. Kan, N. H. Burnett, T. Brabec, M. Geissler, A. Scrinzi, M. Schnürer, and F. Krausz, 1998, IEEE J. Sel. Top. Quantum Electron. **4**, 249.
- Srinivasan, R., V. A. Lobastov, C.-Y. Ruan, and A. H. Zewail, 2003, Helv. Chim. Acta **86**, 1761.
- Stapelfeldt, H., E. Constant, H. Sakai, and P. B. Corkum, 1998, Phys. Rev. A **58**, 426.
- Steiner, E., A. Soncini, and P. W. Fowler, 2005, Org. Biomol. Chem. **3**, 4053.
- Steinmeyer, G., D. H. Sutter, L. Gallmann, N. Matuschek, and U. Keller, 1999, Science **286**, 1507.
- Stingl, A., M. Lenzner, C. Spielmann, and F. Krausz, 1995, Opt. Lett. **20**, 602.
- Stockman, M., M. Kling, U. Kleineberg, and F. Krausz, 2007, Nat. Photonics **1**, 539.
- Stolow, A., 2003a, Annu. Rev. Phys. Chem. **54**, 89.
- Stolow, A., 2003b, Int. Rev. Phys. Chem. **22**, 377.
- Stolow, A., A. E. Bragg, and D. M. Neumark, 2004, Chem. Rev. (Washington, D.C.) **104**, 1719.
- Strasser, D., F. Goulay, and S. R. Leone, 2007, J. Chem. Phys. **127**, 184305.
- Strelkov, V. V., 2006, Phys. Rev. A **74**, 013405.
- Strelkov, V., A. Zair, O. Tcherbakoff, R. López-Martens, E. Cormier, E. Mével, and E. Constant, 2004, Appl. Phys. B: Lasers Opt. **78**, 879.
- Strelkov, V., A. Zair, O. Tcherbakoff, R. López-Martens, E. Cormier, E. Mevel, and E. Constant, 2005, J. Phys. B **38**, L161.
- Strickland, A. D., and G. Mourou, 1985, Opt. Commun. **56**, 219.
- Suda, A., M. Hatayama, K. Nagasaka, and K. Midorikawa, 2005, Appl. Phys. Lett. **86**, 111116.
- Sung, C., S. Ya. Tochitsky, S. Reiche, J. B. Rosenzweig, C. Pellegrini, and C. Joshi, 2006, Phys. Rev. ST Accel. Beams **9**, 120703.
- Sussman, B. J., M. Yu. Ivanov, and A. Stolow, 2005, Phys. Rev. A **71**, 051401.
- Sussman, B. J., D. Townsend, M. Yu. Ivanov, and A. Stolow, 2006, Science **314**, 278.
- Suzuki, T., 2006, Annu. Rev. Phys. Chem. **57**, 555.
- Szent-Györgyi, A., 1941, Science **93**, 609.
- Szipöcs, R., K. Ferencz, C. Spielmann, and F. Krausz, 1994, Opt. Lett. **19**, 201.
- Takahashi, E., Y. Nabekawa, and K. Midorikawa, 2004, Appl. Phys. Lett. **84**, 4.
- Takahashi, E., Y. Nabekawa, T. Otsuka, M. Obara, and K. Midorikawa, 2002, Phys. Rev. A **66**, 021802(R).
- Takahashi, S., and K. Takatsuka, 2006, J. Chem. Phys. **124**, 144101.

- Takatsuka, K., 2006, J. Chem. Phys. **124**, 064111.
- Takatsuka, K., 2007, J. Phys. Chem. A **111**, 10196.
- Takeuchi, S., and T. Kobayashi, 1994, J. Appl. Phys. **75**, 2757.
- Taranukhin, V. D., 2004, J. Opt. Soc. Am. B **21**, 419.
- Tarasevitsch, A., K. Lobov, C. Wünsche, and D. von der Linde, 2007, Phys. Rev. Lett. **98**, 103902.
- Tate, J., T. Auguste, H. G. Muller, P. Salieres, P. Agostini, and L. F. DiMauro, 2007, Phys. Rev. Lett. **98**, 013901.
- Tavella, F., A. Marcinkevicius, and F. Krausz, 2006, Opt. Express **14**, 12822.
- Tavella, F., Y. Nomura, L. Veisz, V. Pervak, A. Marcinkevicius, and F. Krausz, 2007, Opt. Lett. **32**, 2227.
- Tcherbakoff, O., E. Mevel, D. Descamps, J. Plumridge, and E. Constant, 2003, Phys. Rev. A **68**, 043804.
- Telle, H. R., G. Steinmeyer, A. E. Dunlop, J. Stenger, D. H. Sutter, and U. Keller, 1999, Appl. Phys. B: Lasers Opt. **69**, 327.
- Tempea, G., M. Geissler, and T. Brabec, 1999, J. Opt. Soc. Am. B **16**, 669.
- Tempea, G., F. Krausz, Ch. Spielmann, and K. Ferencz, 1998, IEEE J. Sel. Top. Quantum Electron. **4**, 193.
- Thaury, C., F. Quéré, J.-P. Geindre, A. Levy, T. Ceccotti, P. Monot, M. Bougeard, F. Réau, P. d'Oliveira, P. Audebert, R. Marjoribanks, and Ph. Martin, 2007, Nat. Phys. **3**, 424.
- Toma, E. S., H. G. Muller, P. M. Paul, P. Breger, M. Cheret, P. Agostini, C. Le Blanc, G. Mullot, and G. Cheriaux, 2000, Phys. Rev. A **62**, 061801(R).
- Tong, X. M., and S.-I. Chu, 1998, Phys. Rev. A **57**, 452.
- Tong, X. M., and C. D. Lin, 2006, Phys. Rev. A **73**, 042716.
- Tong, X. M., and C. D. Lin, 2007a, Phys. Rev. Lett. **98**, 123002.
- Tong, X. M., and C. D. Lin, 2007b, J. Phys. B **40**, 641.
- Torres, R., N. Kajumba, J. G. Underwood, J. S. Robinson, S. Baker, J. W. G. Tisch, R. de Nalda, W. A. Bryan, R. Velotta, C. Altucci, I. C. E. Turcu, and J. P. Marangos, 2007, Phys. Rev. Lett. **98**, 203007.
- Tournois, P., 1997, Opt. Commun. **140**, 245.
- Trebino, R., 2000, *Frequency-Resolved Optical Gating: The Measurement of Ultrashort Laser Pulses* (Kluwer Academic, Norwell, MA).
- Trebino, R., K. W. DeLong, D. N. Fittinghoff, J. N. Sweetser, M. A. Krumbügel, B. A. Richman, and D. J. Kane, 1997, Rev. Sci. Instrum. **68**, 3277.
- Trebino, R., and D. J. Kane, 1993, J. Opt. Soc. Am. A **10**, 1101.
- Tsakiris, G. D., K. Eidmann, J. Meyer-ter-Vehn, and F. Krausz, 2006, New J. Phys. **8**, 19.
- Tzallas, P., D. Charalambidis, N. A. Papadogiannis, K. Witte, and G. Tsakiris, 2003, Nature (London) **426**, 267.
- Tzallas, P., D. Charalambidis, N. A. Papadogiannis, K. Witte, and G. D. Tsakiris, 2005, J. Mod. Opt. **52**, 321.
- Udem, T., R. Holzwarth, and T. W. Hänsch, 2002, Nature (London) **416**, 233.
- Überacker, M., T. Uphues, M. Schultze, A. J. Verhoef, V. Yakovlev, M. F. Kling, J. Rauschenberger, N. M. Kabachnik, H. Schröder, M. Lezius, K. L. Kompa, H.-G. Muller, M. J. J. Vrakking, S. Hendel, U. Kleineberg, U. Heinemann, M. Drescher, and F. Krausz, 2007, Nature (London) **446**, 627.
- Ullrich, J., R. Moshammer, R. Doerner, O. Jagutzki, V. Mergel, H. Schmidt-Böcking, and L. Spielberger, 1997, J. Phys. B **30**, 2917.
- Van Duyne, R. P., 2004, Science **306**, 985.
- Van Slack, C., and S. Hughes, 2007, Phys. Rev. Lett. **98**, 167404.
- Varin, C., and M. Piché, 2006, Phys. Rev. E **74**, 045602(R).
- Varjú, K., P. Johnsson, R. López-Martens, T. Remetter, E. Gustafsson, J. Mauritsson, M. B. Gaarde, K. J. Schafer, Ch. Erny, I. Sola, A. Zaïr, E. Constant, E. Cormier, E. Mével, and A. L'Huillier, 2005, Laser Phys. **15**, 888.
- Varjú, K., Y. Mairesse, P. Agostini, P. Breger, B. Carré, L. J. Frasinski, E. Gustafsson, P. Johnsson, J. Mauritsson, H. Merdji, P. Monchicourt, A. L'Huillier, and P. Salieres, 2005, Phys. Rev. Lett. **95**, 243901.
- Vaval, N., and L. S. Cederbaum, 2007, J. Chem. Phys. **126**, 164110.
- Veisz, L., G. Kurkin, K. Chernov, V. Tarnetsky, A. Apolonski, F. Krausz, and E. Fill, 2007, New J. Phys. **9**, 451.
- Volkov, D. M., 1935, Z. Phys. **94**, 250.
- Volkova, E. A., A. M. Popov, and O. V. Tikhonova, 2007, Opt. Spectrosc. **102**, 159.
- Vogt, G., G. Krampert, P. Niklaus, P. Nuernberger, and G. Gerber, 2005, Phys. Rev. Lett. **94**, 068305.
- Vozzi, C., F. Calegari, E. Benedetti, J.-P. Caumes, G. Sansone, S. Stagira, M. Nisoli, R. Torres, E. Heesel, N. Kajumba, J. P. Marangos, C. Altucci, and R. Velotta, 2005, Phys. Rev. Lett. **95**, 153902.
- Wagner, N., A. Wuest, I. Christov, T. Popmintchev, X. Zhou, M. Murnane, and H. Kapteyn, 2006, Proc. Natl. Acad. Sci. U.S.A. **103**, 13279.
- Walker, B., E. Mevel, B. Yang, P. Breger, J. P. Chambaret, A. Antonetti, L. F. DiMauro, and P. Agostini, 1993, Phys. Rev. A **48**, R894.
- Walker, B., B. Sheehy, L. F. DiMauro, P. Agostini, K. J. Schafer, and K. C. Kulander, 1994, Phys. Rev. Lett. **73**, 1227.
- Walker, B., B. Sheehy, K. C. Kulander, and L. F. DiMauro, 1996, Phys. Rev. Lett. **77**, 5031.
- Walmsley, I. A., and V. Wong, 1996, J. Opt. Soc. Am. B **13**, 2453.
- Walters, Z. B., S. Tonzani, and C. Greene, 2007, J. Phys. B **40**, F277.
- Wang, P. X., Y. K. Ho, X. Q. Yuan, Q. Kong, N. Cao, A. M. Sessler, E. Esarey, and Y. Nishida, 2001, Appl. Phys. Lett. **78**, 2253.
- Wang, W., P. X. Wang, Y. K. Ho, Q. Kong, Y. Gu, and S. J. Wang, 2007, Rev. Sci. Instrum. **78**, 093103.
- Watanabe, S., K. Kondo, Y. Nabekawa, A. Sagisaka, and Y. Kobayashi, 1994, Phys. Rev. Lett. **73**, 2692.
- Watson, J. B., A. Sanpera, D. G. Lappas, P. L. Knight, and K. Burnett, 1997, Phys. Rev. Lett. **78**, 1884.
- Weber, T., A. O. Czasch, O. Jagutzki, A. K. Müller, V. Mergel, A. Khieftets, E. Rotenberg, G. Meigs, M. H. Prior, S. Daveau, A. Landers, C. L. Cocke, T. Osipov, R. Díez Muiño, H. Schmidt-Böcking, and R. Dörner, 2004, Nature (London) **431**, 437.
- Weber, T., M. Weckenbrock, A. Staudte, L. Spielberger, O. Jagutzki, V. Mergel, F. Afaneh, G. Urbasch, M. Vollmer, H. Giessen, and R. Dörner, 2000a, Phys. Rev. Lett. **84**, 443.
- Weber, T., M. Weckenbrock, A. Staudte, L. Spielberger, O. Jagutzki, V. Mergel, F. Afaneh, G. Urbasch, M. Vollmer, H. Giessen, and R. Dörner, 2000b, J. Phys. B **33**, L127.
- Weckenbrock, M., A. Becker, A. Staudte, S. Kammer, M. Smolarski, V. R. Bhardwaj, D. M. Rayner, D. M. Villeneuve, P. B. Corkum, and R. Dörner, 2003, Phys. Rev. Lett. **91**, 123004.
- Weckenbrock, M., D. Zeidler, A. Staudte, Th. Weber, M. Schoeffler, M. Meckel, S. Kammer, M. Smolarski, O. Jagutzki, V. R. Bhardwaj, D. M. Rayner, D. M. Villeneuve, P. B. Corkum, and R. Dörner, 2004, Phys. Rev. Lett. **92**, 213002.

- Weiner, A. M., 1995, *Prog. Quantum Electron.* **19**, 161.
- Weiner, A. M., J. P. Heritage, and E. M. Kirschner, 1988, *J. Opt. Soc. Am. B* **5**, 1563.
- Weinkauf, R., P. Schanen, A. Metsala, E. W. Schlag, M. Bürgle, and H. Kessler, 1996, *J. Chem. Phys.* **100**, 18567.
- Weinkauf, R., P. Schanen, D. Yang, S. Soukara, and E. W. Schlag, 1995, *J. Chem. Phys.* **99**, 11255.
- Weinkauf, R., E. W. Schlag, T. J. Martinez, and R. D. Levine, 1997, *J. Chem. Phys.* **99**, 11255.
- Weitzel, K.-M., 2007, *ChemPhysChem* **8**, 213.
- Wernet, Ph., D. Nordlund, U. Bergmann, M. Cavalleri, M. Odelius, H. Ogasawara, L. A. Näslund, T. K. Hirsch, L. Ojamäe, P. Glatzel, L. G. M. Pettersson, and A. Nilsson, 2004, *Science* **304**, 995.
- Wickenhauser, M., J. Burgdörfer, F. Krausz, and M. Drescher, 2005, *Phys. Rev. Lett.* **94**, 023002.
- Wickenhauser, M., J. Burgdörfer, F. Krausz, and M. Drescher, 2006, *J. Mod. Opt.* **53**, 247.
- Wilhelm, T., J. Piel, and E. Riedle, 1997, *Opt. Lett.* **22**, 1494.
- Wille, K., 2000, *The Physics of Particle Accelerators* (Oxford University Press, Oxford).
- Williams, I. D., J. McKenna, J. Wood, M. Suresh, W. A. Bryan, S. L. Stebbings, E. M. L. English, C. R. Calvert, B. Srigengan, E. J. Divall, C. J. Hooker, A. J. Langley, and W. R. Newell, 2007, *Phys. Rev. Lett.* **99**, 173002.
- Williams, R. T., R. R. Royt, J. C. Rife, J. P. Long, and M. N. Kabler, 1982, *J. Vac. Sci. Technol.* **21**, 509.
- Williamson, J. C., J. Cao, H. Ihée, H. Frey, and A. H. Zewail, 1997, *Nature (London)* **386**, 159.
- Williamson, J. C., M. Dantus, S. B. Kim, and A. H. Zewail, 1992, *Chem. Phys. Lett.* **196**, 529.
- Williamson, J. C., and A. H. Zewail, 1991, *Proc. Natl. Acad. Sci. U.S.A.* **88**, 5021.
- Williamson, S., G. Mourou, and J. C. M. Li, 1984, *Phys. Rev. Lett.* **52**, 2364.
- Witte, S., R. Th. Zinkstok, A. L. Wolf, W. Hogervorst, W. Ubachs, and K. S. E. Eikema, 2006, *Opt. Express* **14**, 8168.
- Wittmann, T., B. Horvath, W. Helml, M. G. Schätzel, X. Gu, A. L. Cavalieri, G. G. Paulus, and R. Kienberger, 2008, unpublished.
- Wohllben, W., T. Buckup, J. L. Herek, R. J. Cogdell, and M. Motzkus, 2003, *Biophys. J.* **85**, 442.
- Wohllben, W., T. Buckup, J. L. Herek, H. Hashimoto, R. J. Cogdell, and M. Motzkus, 2004, in *Femtochemistry and Femtobiology: Ultrafast Events in Molecular Science*, edited by J. L. Hynes and M. Martin (Elsevier, Burlington MA), p. 91.
- Wohllben, W., T. Buckup, J. L. Herek, and M. Motzkus, 2005, *ChemPhysChem* **6**, 850.
- Wolf, M., E. Knoesel, and T. Hertel, 1996, *Phys. Rev. B* **54**, R5295.
- Wonisch, A., U. Neuhausler, N. M. Kabachnik, T. Uphues, M. Uiberacker, V. Yakovlev, F. Krausz, M. Drescher, U. Kleineberg, and U. Heinzmann, 2006, *Appl. Opt.* **45**, 4147.
- Wonisch, A., Th. Westerwalbesloh, W. Hachmann, N. Kabachnik, U. Kleineberg, and U. Heinzmann, 2004, *Thin Solid Films* **464-465**, 473.
- Wu, K., X. Yang, and H. Zeng, 2007, *Appl. Phys. B: Lasers Opt.* **88**, 189.
- Wu, Y., and X. Yang, 2007, *Phys. Rev. A* **76**, 013832.
- Wurth, W., and D. Menzel, 2000, *Chem. Phys.* **251**, 141.
- Xie, X., G. Jordan, M. Wickenhauser, and A. Scrinzi, 2007, *J. Mod. Opt.* **54**, 999.
- Xu, J., and X.-C. Zhang, 2006, *THz Science and Technology* (Peking University Press, Beijing, China).
- Xu, L., C. Spielmann, A. Poppe, T. Brabec, F. Krausz, and T. W. Hänsch, 1996, *Opt. Lett.* **21**, 2008.
- Yakovlev, V., 2007, private communication.
- Yakovlev, V. S., F. Bammer, and A. Scrinzi, 2005, *J. Mod. Opt.* **52**, 395.
- Yakovlev, V. S., M. Ivanov, and F. Krausz, 2007, *Opt. Express* **15**, 15351.
- Yakovlev, V. S., and A. Scrinzi, 2003, *Phys. Rev. Lett.* **91**, 153901.
- Yamane, K., Z. Zhang, K. Oka, R. Morita, M. Yamashita, and A. Suguro, 2003, *Opt. Lett.* **28**, 2258.
- Yamashita, M., K. Yamane, and R. Morita, 2006, *IEEE J. Sel. Top. Quantum Electron.* **12**, 213.
- Yang, B., K. J. Schafer, B. Walker, K. C. Kulander, P. Agostini, and L. F. DiMauro, 1993, *Phys. Rev. Lett.* **71**, 3770.
- Yavin, E., A. K. Boal, E. D. A. Stemp, E. M. Boon, A. L. Livingston, V. L. O'Shea, S. S. David, and J. K. Barton, 2005, *Proc. Natl. Acad. Sci. U.S.A.* **102**, 3546.
- Ye, J., and S. T. Cundiff, 2005, in *Femtosecond Optical Frequency Comb Technology*, edited by J. Ye and S. T. Cundiff (Springer Science + Business Media, New York), p. 12.
- Yen, R., J. M. Liu, N. Bloembergen, T. K. Yee, J. G. Fujimoto, and M. M. Salour, 1982, *Appl. Phys. Lett.* **40**, 185.
- Yu, T. J., K.-H. Hong, H.-G. Choi, J. H. Sung, I. W. Choi, D.-K. Ko, J. Lee, J. Kim, D. E. Kim, C. H. Nam, 2007, *Opt. Express* **15**, 8203.
- Yudin, G. L., A. D. Bandrauk, and P. Corkum, 2006, *Phys. Rev. Lett.* **96**, 063002.
- Yudin, G. L., S. Chelkowski, J. Itatani, A. D. Bandrauk, and P. Corkum, 2005, *Phys. Rev. A* **72**, 051401(R).
- Yudin, G. L., and M. Ivanov, 2001a, *Phys. Rev. A* **64**, 013409.
- Yudin, G. L., and M. Y. Ivanov, 2001b, *Phys. Rev. A* **63**, 033404.
- Yudin, G. L., S. Patchkovskii, P. B. Corkum, and A. D. Bandrauk, 2007, *J. Phys. B* **40**, F93.
- Yue, J. T., and Doniach, 1973, *Phys. Rev. B* **8**, 4578.
- Yurchenko, S. N., S. Patchkovskii, I. Litvinuk, P. Corkum, and G. Yudin, 2004, *Phys. Rev. Lett.* **93**, 223003.
- Zair, A., O. Tcherbakoff, E. Mével, E. Constant, R. López-Martens, J. Mauritsson, P. Johnsson, and A. L'Huillier, 2004, *Appl. Phys. B: Lasers Opt.* **78**, 869.
- Zamith, S., Y. Ni, A. Gürler, L. D. Noordam, H. G. Muller, and M. J. J. Vrakking, 2004, *Opt. Lett.* **29**, 2303.
- Zavelani-Rossi, M., G. Cerullo, S. De Silvestri, L. Gallmann, N. Matuschek, G. Steinmeyer, U. Keller, G. Angelow, V. Scheuer, and T. Tschudi, 2001, *Opt. Lett.* **26**, 1155.
- Zeek, E., K. Maginnis, S. Backus, U. Russek, M. Murnane, G. Mourou, and H. Kapteyn, 1999, *Opt. Lett.* **12**, 1540.
- Zeidler, D., A. Staudte, A. B. Bardon, D. M. Villeneuve, R. Doerner, and P. B. Corkum, 2005, *Phys. Rev. Lett.* **95**, 203003.
- Zeng, Z., Y. Cheng, X. Song, R. Li, and Z. Xu, 2007, *Phys. Rev. Lett.* **98**, 203901.
- Zepf, M., B. Dromey, M. Landreman, P. Foster, and S. M. Hooker, 2007, *Phys. Rev. Lett.* **99**, 143901.
- Zewail, A., 2000, *J. Phys. Chem. A* **104**, 5660.
- Zewail, A. H., 2006, *Annu. Rev. Phys. Chem.* **57**, 65.
- Zewail, A. H., 1994, *Femtochemistry Volume I and II* (World Scientific, Singapore).
- Zhang, J., L. Bai, S. Gong, Z. Xu, and D.-S. Guo, 2007, *Opt. Express* **15**, 7261.
- Zhang, P., Y. R. Song, and Z. G. Zhang, 2006, *Acta Phys. Sin.*

- 55**, 6208.
- Zhang, X., A. R. Libertun, A. Paul, E. Gagnon, S. Backus, I. P. Christov, M. M. Murnane, and H. C. Kapteyn, R. A. Bartels, Y. Liu, and D. T. Attwood, 2004, Opt. Lett. **29**, 1357.
- Zhang, X., A. Lytle, T. Popmintchev, A. Paul, N. Wagner, M. Murnane, H. C. Kapteyn, and I. P. Christov, 2005, Opt. Lett. **30**, 1971.
- Zhao, Z. X., and C. D. Lin, 2005, Phys. Rev. A **71**, 060702(R).
- Zhou, X., Z. Chen, T. Morishita, A.-T. Le, and C. D. Lin, 2008, Phys. Rev. A **77**, 053410.
- Zhou, XiaoXin, X. M. Tong, Z. X. Zhao, and C. D. Lin, 2005a, Phys. Rev. A **72**, 033412.
- Zhou, XiaoXin, X. M. Tong, Z. X. Zhao, and C. D. Lin, 2005b, Phys. Rev. A **71**, 061801.
- Zheltikov, A. M., 2006a, Phys. Usp. **49**, 605.
- Zheltikov, A. M., 2006b, Phys. Rev. A **74**, 053403.
- Zholents, A. A., and W. M. Fawley, 2004, Phys. Rev. Lett. **92**, 224801.
- Zhu, X.-Y., 2004, Surf. Sci. Rep. **56**, 1.
- Zhu, C., S. Nangia, A. W. Jasper, and D. G. Truhlar, 2004, J. Chem. Phys. **121**, 7658.
- Zimmermann, B., M. Lein, and J. M. Rost, 2005, Phys. Rev. A **71**, 033401.
- Zon, B. A., 2000, J. Exp. Theor. Phys. **91**, 899.
- Zrost, K., A. Rudenko, T. Ergler, B. Feuerstein, V. L. B. de Jesus, C. D. Schröter, R. Moshammer, and J. Ullrich, 2006, J. Phys. B **39**, S371.